The National Carbon Capture Center at the Power Systems Development Facility

Final Report

October 1, 2008 – December 30, 2014

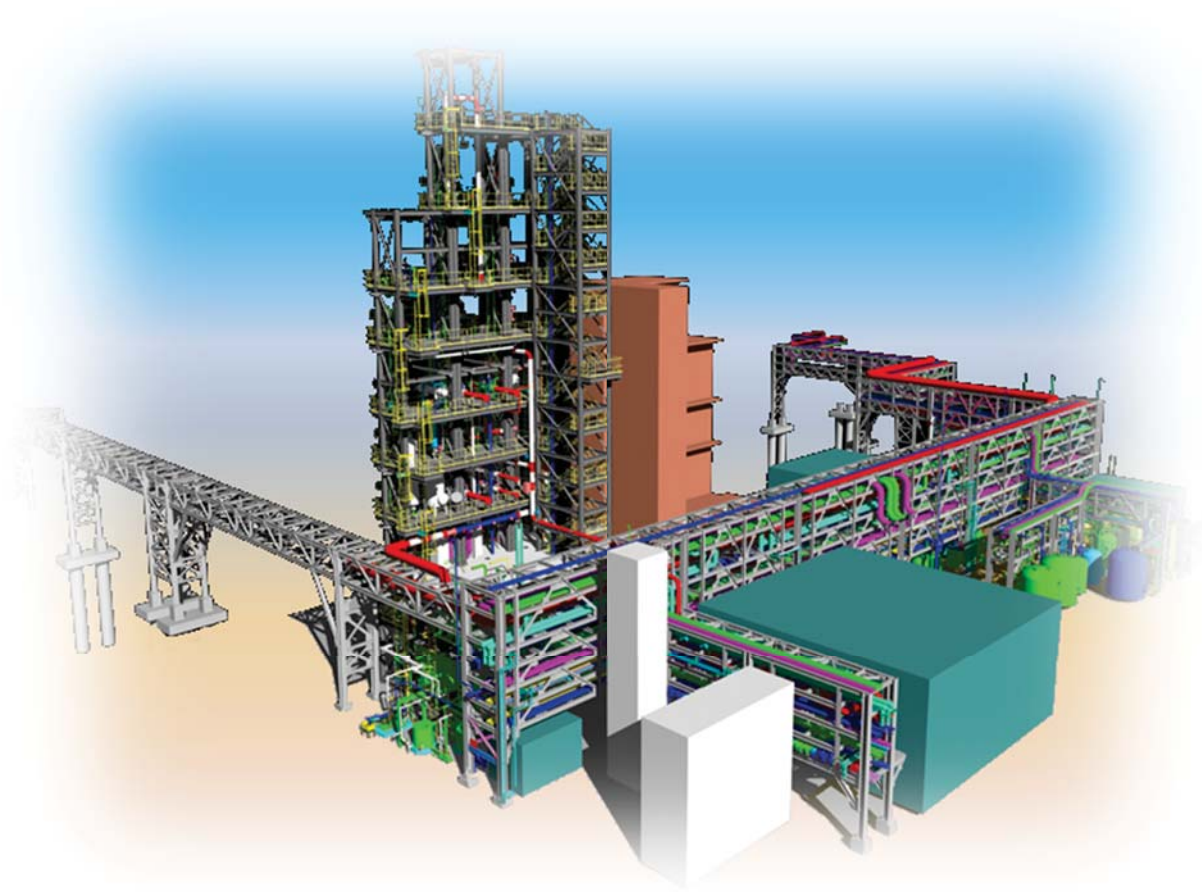

DOE Cooperative Agreement
DE-NT0000749

The National Carbon Capture Center at the Power Systems Development Facility

Final Report

October 1, 2008 – December 30, 2014

DOE Cooperative Agreement DE-NT0000749

Prepared by:
Southern Company Services, Inc.
Power Systems Development Facility
P.O. Box 1069, Wilsonville, AL 35186
Phone: 205-670-5840
Fax: 205-670-5843
E-mail: nccc@southernco.com
http://www.NationalCarbonCaptureCenter.com

Disclaimer

This report was prepared as an account of work sponsored by an agency of the United States Government. Neither the United States Government nor any agency thereof, nor any of their employees, nor Southern Company Services, Inc., nor any of its employees, nor any of its subcontractors, nor any of its sponsors or co-funders, makes any warranty, expressed or implied, or assumes any legal liability or responsibility for the accuracy, completeness, or usefulness of any information, apparatus, product, or process disclosed, or represents that its use would not infringe privately owned rights. Reference herein to any specific commercial product, process, or service by trade name, trademark, manufacturer or otherwise, does not necessarily constitute or imply its endorsement, recommendation, or favoring by the United States Government or any agency thereof. The views and opinions of authors expressed herein do not necessarily state or reflect those of the United States Government or any agency thereof.

This report is available to the public from the National Technical Information Service, U.S. Department of Commerce, 5285 Port Royal Road, Springfield, VA 22161. Phone orders are accepted at (703) 487-4650.

Abstract

The National Carbon Capture Center (NCCC) at the Power Systems Development Facility supports the Department of Energy (DOE) goal of promoting the United States' energy security through reliable, clean, and affordable energy produced from coal. Work at the NCCC supports the development of new power technologies and the continued operation of conventional power plants under CO_2 emission constraints. The NCCC includes adaptable slipstreams that allow technology development of CO_2 capture concepts using coal-derived syngas and flue gas in industrial settings. Because of the ability to operate under a wide range of flow rates and process conditions, research at the NCCC can effectively evaluate technologies at various levels of maturity and accelerate their development path to commercialization.

During its first contract period, from October 1, 2008, through December 30, 2014, the NCCC designed, constructed, and began operation of the Post-Combustion Carbon Capture Center (PC4). Testing of CO_2 capture technologies commenced in 2011, and through the end of the contract period, more than 25,000 hours of testing had been achieved, supporting a variety of technology developers. Technologies tested included advanced solvents, enzymes, membranes, sorbents, and associated systems.

The NCCC continued operation of the existing gasification facilities, which have been in operation since 1996, to support the advancement of technologies for next-generation gasification processes and pre-combustion CO_2 capture. The gasification process operated for 13 test runs, supporting over 30,000 hours combined of both gasification and pre-combustion technology developer testing.

Throughout the contract period, the NCCC incorporated numerous modifications to the facilities to accommodate technology developers and increase test capabilities. Preparations for further testing were ongoing to continue advancement of the most promising technologies for future power generation processes.

Acknowledgement

The authors wish to acknowledge the contributions and support provided by DOE project manager Morgan “Mike” Mosser. We would also like to thank our co-funding partners: the Electric Power Research Institute, American Electric Power, Duke Energy, Luminant, NRG Energy, Arch Coal, Cloud Peak Energy, Peabody Energy, and Rio Tinto. The material in this report is based upon work supported by the DOE under award DE-NT0000749. However, any opinions, findings, conclusions, or recommendations expressed herein are those of the authors and do not necessarily reflect the views of the DOE.

Table of Contents

List of Figures

List of Tables

List of Abbreviations and Acronyms

A-E	Anion Exchange
B&W	Babcock & Wilcox
C-E	Cation-Exchange
CCAT	Connecticut Center for Advanced Technologies
CGE	Cold Gas Efficiency
CH_4	Methane
CMR	Catalytic Membrane Reactor
CMS	Carbon Molecular Sieve
CO	Carbon Monoxide
COE	Cost of Electricity
COS	Carbonyl Sulfide
DEPG	Dimethyl Ether of Polyethylene Glycol
DMI	Dimethylimadizole
DOE	Department of Energy
EERC	Energy and Environmental Research Center
EPA	Environmental Protection Agency
FGD	Flue Gas Desulfurization
FT	Fischer-Tropsch
FTIR	Fourier Transform Infrared
G	Gas
GC	Gas Chromatograph or Gas Chromatographs
GC-ICPMS	Gas Chromatography Inductively Coupled Plasma Mass Spectrometer
GTA	Glycerol Triacetate
H_2S	Hydrogen Sulfide
H_2SO_4	Sulfuric Acid
HPL	High-Performance Liquid
HSS	Heat Stable Salt
HSX	Hybrid Siloxane
ICP-MS	Inductively Coupled Plasma Mass Spectrometry
IGCC	Integrated Gasification Combined Cycle
JM	Johnson Matthey
L	Liquid
L/G	Liquid-to-Gas Ratio
LHV	Lower Heating Value
LOI	Loss on Ignition
MDEA	Methyl Diethanolamine
MEA	Monoethanolamine
MEI	Methylimidazole
MM5	Modified Method 5
MPT	Media & Process Technology
MS	Mass Spectroscopy
MTR	Membrane Technology & Research
NCCC	National Carbon Capture Center
NDIR	Non-Dispersive Infrared
NETL	National Energy Technology Laboratory
NIOSH	National Institute of Occupational Safety and Health
NO	Nitrogen Oxide
NO_2	Nitrogen Dioxide
NOx	Nitrogen Oxides
OSHA	Occupational Safety and Health Administration
OSU	Ohio State University
PC	Pulverized Coal
PC4	Post-Combustion Carbon Capture Center
PCC	Post-Combustion CO_2 Capture
PCD	Particulate Control Device
PDMS	Polydimethyl Siloxane
PEL	Permissible Exposure Limit
PRB	Powder River Basin
PSDF	Power Systems Development Facility
PSTU	Pilot Solvent Test Unit
RCRA	Resource Conservation and Recovery Act
S/L	Steam-to-Liquid Ratio
SCL	Syngas Chemical Looping
SCR	Selective Catalytic Reduction
SCU	Syngas Conditioning Unit
SDA	Spray Dryer Absorber
SO_3	Sulfur Trioxide
SOFC	Solid Oxide Fuel Cell
SRD	Specific Reboiler Duty
SRI	Southern Research Institute
SRII	SRI International
SSTU	Slipstream Solvent Test Unit
TCLP	Toxicity Characteristic Leaching Procedure
TDL	Tunable Diode Laser
TPD	Ton per Day
UA	University of Alabama
UT-Austin	University of Texas at Austin
WGS	Water-Gas Shift
WPI	Worcester Polytechnic Institute
ZVI	Zero-Valent Iron

1.0 EXECUTIVE SUMMARY

The National Carbon Capture Center (NCCC) at the Power Systems Development Facility (PSDF) is a key component of the Department of Energy's (DOE's) strategy in promoting the United States' economic, environmental, and energy security through reliable, clean, and affordable power produced from coal. Located in Wilsonville, Alabama, the NCCC is a cost-effective, flexible test center for evaluating the critical components of advanced CO_2 capture and power generation technologies. The center was established in 2008 to build on the experience, expertise, and infrastructure in place at the PSDF, which has been in operation since 1996. The PSDF history boasts the evaluation of a multitude of advanced technologies under the highest engineering standards with zero lost-time accidents.

Project Partnership with DOE

The DOE conceived the PSDF as the premier advanced coal power generation research and development facility of the world, to "serve as the proving ground for many new advanced power systems." Since operations began, the PSDF has been a center for national efforts to develop clean, high efficiency coal-based power generation technologies. Two significant achievements–in addition to many secondary goals that were met–were the development of hot gas filtration to improve energy efficiency and the development of a gasifier suitable for use with low-rank coals, which comprise over half of the total coal reserves in the U.S. and the world. These two technologies have progressed to commercialization with an Integrated Gasification Combined Cycle (IGCC) power plant in Kemper County, Mississippi.

Project Mission and Approach

Offering a world-class neutral test facility and a highly specialized staff, the NCCC accelerates the commercialization of advanced technologies to enable fossil fuel-based power plants to achieve near-zero emissions. Work at the NCCC supports the development of new power technologies and the continued operation of conventional power plants under CO_2 emission constraints.

In undertaking its mission, the NCCC is involved in a range of activities in the areas of post-combustion CO_2 capture, gasification, and pre-combustion CO_2 capture to develop the most promising technologies for future commercial deployment. The test facilities, shown in Figure 1, include the original PSDF site, which houses the gasification and pre-combustion CO_2 capture processes, and the Post-Combustion Carbon Capture Center (PC4), located at the adjacent Alabama Power E.C. Gaston power plant.

Figure 1. NCCC Facilities

Reporting Period

This report covers the work performed under DOE contract DE-NT0000749, which initially spanned the five-year period from October 1, 2008, through September 30, 2013. The original contract was amended with a no-cost extension through December 30, 2014. In early 2014, the NCCC was awarded a new DOE contract, DE-FE0022596, through a competitive bidding process. The new contract period began on June 6, 2014, to be completed on May 31, 2019. Work accomplished with funding under the new contract will be covered in subsequent reports.

1.1 Post-Combustion CO_2 Capture

1.1.1 PC4 Facilities

The PC4 utilizes flue gas from Plant Gaston Unit 5, a base-loaded, 880-MW gross supercritical pulverized coal boiler fired with Alabama medium-sulfur bituminous coal. The unit meets all environmental requirements utilizing state-of-the-art controls; thus, the flue gas extracted for testing is fully representative of commercial conditions. As shown in Figure 2, the center provides sites for technology developers' bench-scale and pilot-scale test units. The Pilot Solvent Test Unit (PSTU) and the Slipstream Solvent Test Unit (SSTU) are fully integrated systems for comprehensive solvent characterization at pilot-scale and at bench-scale, respectively. An air dilution system is also available for CO_2 capture testing under simulated natural gas flue gas conditions.

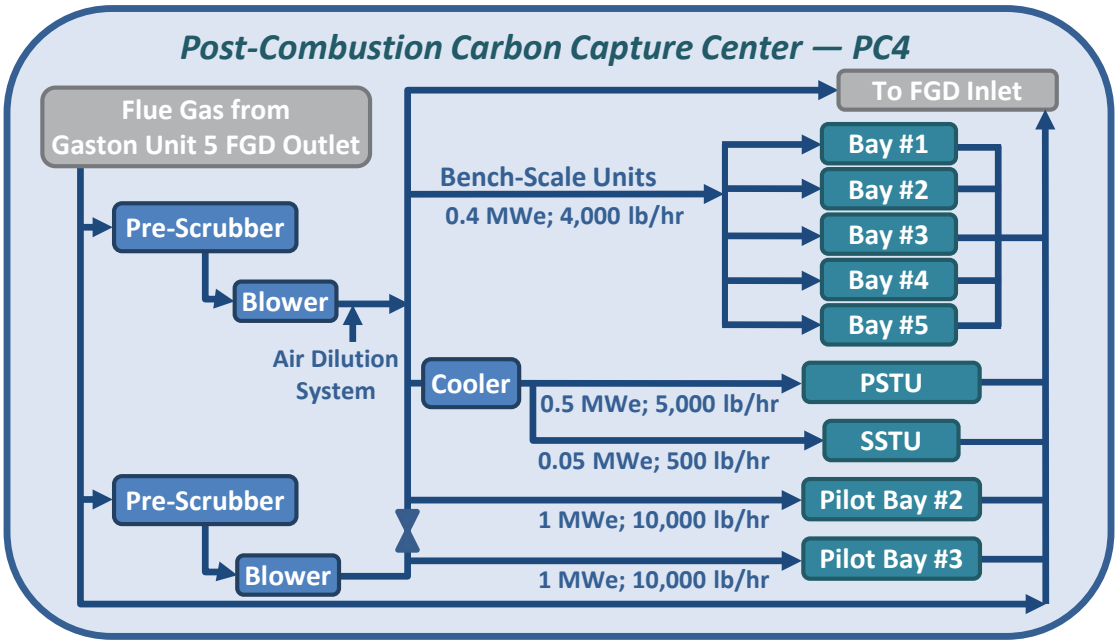

Figure 2. Schematic of PC4 Test Facilities

1.1.2 Post-Combustion CO_2 Capture Accomplishments

In less than three years, the NCCC engineered and constructed the PC4, now a world-wide focal point for development of advanced CO_2 capture technologies for conventional and advanced coal- and natural gas-fired power generation. During the contract period, PC4 operation supported more than 25,000 hours of testing, which involved advanced solvents, enzymes, membranes, sorbents, and associated systems. Operation of the PSTU encompassed more than 9,500 hours, validating high quality data acquisition and supporting the commercial development of several advanced amine solvents. In addition to the technology testing, a number of modifications were incorporated to increase plant capacity and flexibility. Table 1 summarizes the technology testing completed, and highlights of progress and testing are discussed below.

Table 1. Summary of Post-Combustion CO_2 Capture Testing Completed

Developer Name/Technology Tested	Test Dates	Hours
PSTU Operation		
NCCC/Monoethanolamine (MEA) Solvent Baseline	3/11 - 5/11	1,140
Babcock & Wilcox/OptiCap™ Solvent	9/11 - 12/11	2,000
NCCC/MEA Solvent Baseline	3/12	400
Hitachi/H3-1 Solvent	4/12 - 7/12	1,300
Cansolv/DC-201 Solvent	7/12 - 10/12	1,725
Chiyoda/T-3 Solvent	12/12 - 6/13	1,500
Cansolv/DC-201 Solvent with Natural Gas Flue Gas Simulation	7/13 - 10/13	1,500
Technology Developer Units		
Aker Clean Carbon/Mobile Test Unit	6/11 - 12/11	2,592
Membrane Technology & Research/Polaris™ CO_2 Membrane	11/11 - 8/14	9,119
Codexis/Carbonic Anhydrase Enzymes	5/12	336
Akermin/Immobilized Carbonic Anhydrase Enzymes	1/13 - 10/13	3,500
SRI International/Sorbent	10/13 - 8/14	250
DOE/Sorbent	2/14 - 8/14	672

PC4 Modifications

Plant upgrades completed in 2014 increased the total PC4 capacity from 12,000 lb/hr of flue gas to about 30,000 lb/hr, allowing simultaneous operation of pilot units. Several other modifications were made to accommodate the objectives of technology developers utilizing the PSTU. One of these modifications was the implementation of an air dilution system to simulate natural gas flue gas operations, under which the PC4 operated for 2,500 hours. The NCCC also added the SSTU to allow testing of solvents, such as those in early stages of development, available only in amounts smaller than the 4,000 gallons required for the PSTU.

Monoethanolamine (MEA) Solvent Baseline Testing

The NCCC conducted two baseline solvent test campaigns with MEA in the PSTU. The first campaign was performed while commissioning the PSTU in 2011. The mass and energy balance closures achieved during commissioning were all close to 100 percent, which was exceptional for such a large pilot plant and validated the accuracy of the flow and composition measurements. The system proved easily capable of greater than 90 percent CO_2 capture with the MEA solvent. Test equipment for sampling MEA degradation products was established, and analytical procedures were identified for determining their concentrations in the CO_2-depleted flue gas streams.

A second MEA baseline campaign was conducted to further investigate two areas identified from the first campaign: higher than expected solvent carryover in the CO_2-depleted flue gas from the wash tower, and significant accumulation of heavy metals (most notably selenium) in the solvent. Testing suggested that SO_3 aerosols present in the flue gas can cause high solvent carryover rates, and investigations began to identify methods of improving the capture of these aerosols and thus lowering solvent carryover. Work was performed to fully characterize the

metals present in the flue gas and to determine how total selenium and its species varied with time. A laboratory program was developed to assess procedures to precipitate heavy metals from the solvent. Initial results with the addition of zero-valent iron powder indicated that over 75 percent of the selenium can be precipitated out.

During 2014, another MEA campaign was underway on behalf of the DOE's Carbon Capture Simulation Initiative for computer process modeling of solvent systems. This work was undertaken to collect process information that was previously unavailable, including data for wide-ranging steady state conditions and for dynamic conditions. Results of the campaign will be published in subsequent reports.

Babcock & Wilcox (B&W) OptiCap Solvent

B&W conducted a three-month test program of its OptiCap solvent in the PSTU in 2011. Regeneration energy values in the range of 1,100 to 1,125 BTU/lb CO_2 were achieved on multiple occasions at a CO_2 removal efficiency of 90 percent, representing a 30 percent reduction over 30-wt% MEA. These results are consistent with lab- and pilot-scale measurements, as well as B&W process simulations, which indicate that further energy savings are possible when using a cross-flow heat exchanger optimized for the OptiCap solvent.

Hitachi H3-1 Solvent

Hitachi conducted extensive testing of over 1,300 hours with its H3-1 solvent in the PSTU in 2012. The CO_2 capture performance of the H3-1 solvent during the test campaign averaged around 90 percent over a range of boiler loads, flue gas compositions, and test conditions. With H3-1, about 37 percent lower solvent flow rate was needed compared with 30-wt% MEA to achieve greater than 90 percent CO_2 capture. For a new CO_2 capture system, this would translate to savings in capital cost and operating cost since smaller equipment would be sufficient to achieve high removal efficiencies and a smaller amount of solvent would be pumped through the process loop. At 1,034 Btu/lb CO_2, the regeneration energy required for H3-1 was about 34 percent lower than that for MEA.

Cansolv Solvent

Cansolv Technologies conducted two tests with DC-201 solvent in the PSTU. The first test in 2012 demonstrated that the DC-201 solvent required 40 percent less energy than MEA to achieve the same capture rate using three packing sections in the absorber. The solvent also required 50 percent less circulation, the solvent-to-flue gas (liquid-to-gas or L/G) ratio being 4 kg/Nm^3 for MEA and 2 kg/Nm^3 for DC-201. Parametric tests varying the amine concentration in the solvent showed that when reducing amine concentration from 53 to 40 wt%, CO_2 capture efficiency decreased from about 90 to 84 percent. The optimum operation with respect to energy consumption was between 45 to 55 wt% solvent concentration. After three months of testing, the total amount of organic acids in the DC-201 solvent was 500 ppmw in solution, indicating a very low degradation rate of the solvent under these conditions.

Testing of the Cansolv DC-201 solvent under natural gas flue gas simulated conditions was completed in 2013. Throughout the campaign, CO_2 capture was maintained near 90 percent. The overall capture performance did not deteriorate significantly as transformation products increased in concentration, since the DC-201 solvent transformation products maintain a capacity

for capturing CO_2. Testing demonstrated a maximum increase in overall energy consumption (stripping factor) of about 10 percent without intercooling or energy integration. Solvent emissions testing showed 33 times greater emissions with natural gas simulated flue gas and 77 times greater emissions with typical coal flue gas over emissions with ambient air. Two additional tests with Cansolv solvents were completed in 2014 under the new contract.

Chiyoda T-3 Solvent

Testing of the Chiyoda T-3 solvent for 1,500 hours of operation included 24 test conditions, and mass balances were completed for each condition with 97 percent or higher closures. Parametric testing showed that the optimum solvent-to-flue gas ratio was around 2.4 L/ Nm^3, about 50 percent lower than for MEA. For 90 percent capture, the regeneration energy for T-3 was 2.6 GJ/tonne (1,110 BTU/lb), around 30 percent lower than for MEA. The results also showed that the T-3 solvent was significantly less corrosive than MEA.

Aker Clean Carbon Mobile Test Unit (MTU)

Aker Clean Carbon demonstrated its pilot-scale solvent system, the MTU, in 2011. During the more than 2,500 hours of operation with CO_2 capture, Aker completed its original test matrix, which included parametric tests performed to investigate the factors influencing the specific reboiler duty, solvent CO_2 loading, and emissions. Testing with 30-wt% MEA was also completed to develop a baseline for comparison of results. Test results reported by Aker included a significant reduction in emissions of solvent components when using Aker's low emissions design and reduced energy consumption (about 20 percent lower specific reboiler duty) using the Aker CCAmine solvent compared to 30-wt% MEA solvent.

Codexis Enzymes

Codexis performed testing of a bench-scale system using carbonic anhydrase enzymes to accelerate the rate of CO_2 capture for low-energy solvents that have desirably low heats of reaction such as methyl diethanolamine (MDEA). The testing confirmed the stability of the enzyme in the presence of trace contaminants and demonstrated robust system operation, with CO_2 capture averaging around 65 percent at a rate of capture over 25 times greater than for MDEA alone.

Akermin Enzymes

With more than 3,500 hours of operation, Akermin successfully confirmed proof-of-concept of its pilot-scale process featuring immobilized carbonic anhydrase enzymes using a potassium carbonate solvent and an amine solvent. Operation with the low-cost, non-volatile potassium carbonate produced a regenerated CO_2 stream with 99.9 percent purity, and average steady performance showed about 80 percent CO_2 capture, with values up to 90 percent CO_2 capture achieved. Unlike operation with amine-based solvents, solvent carryover was below detection limits, with less than 1.6 percent per year capacity loss due to heat stable salts. Data demonstrated that the enzyme operation resulted in a seven-fold increase in flue gas flow rate while maintaining 90 percent CO_2 capture in the same column and a six-fold increase in the mass transfer coefficient. Subsequent operation with Akermin's AKM-24 solvent showed 80 to 90 percent capture at design conditions with continued enzyme stability. The PC4 test data provided a well-defined path for Akermin to further optimize system performance to achieve as much as 15-fold acceleration of CO_2 capture.

Membrane Technology & Research (MTR) CO_2 Membrane

Membrane Technology & Research operated its 1-ton CO_2/day membrane process for over 9,100 hours on flue gas. Long-term operation demonstrated CO_2 capture rates of better than 90 percent and stable Polaris membrane module performance with real flue gas. Full-scale spiral-wound cross-flow and sweep modules were developed for this project and were shown to operate effectively. Important for multi-year operations, the modules also demonstrated stable performance over numerous shutdowns and restarts. Based on the operational experience, MTR refined the process by incorporating new designs for membrane modules and optimizing operation with a new compressor. The test data were used to support a 20-fold scale-up. In 2014, the new 20-ton/day system was installed, and commissioning was completed in preparation for a six-month field test in 2015.

SRI International (SRII) Sorbent

The SRI International 40-kWe sorbent skid was tested in 2014. Continuous operation was achieved by using a combination of indirect and direct steam heating of the sorbent in the CO_2 stripper. The indirect heating demonstrated the potential for heat recovery from the hot dehydrator exhaust. The performance indicators were lower than expected based on previous testing of SRII's smaller unit at the University of Toledo. While the target CO_2 capture efficiency was 90 percent, the test results showed that only 70 percent capture was reached. The concentration of CO_2 in the stripper outlet was 93 percent, also lower than seen previously. Design modifications and process optimization are expected to improve performance and increase the capture rate to the targeted value of 90 percent. SRII will use the operational data for future testing at a 0.5-MWe scale.

DOE Sorbent Unit

The DOE tested its Carbon Capture Unit (C2U) to evaluate CO_2 sorbents composed of amines on a solid substrate. The focus of these tests was exploring the accumulation of heavy metals from flue gas, such as selenium, on the 32D sorbent. Analysis of sorbent samples taken following the circulation tests and the batch tests showed no permanent loss of CO_2 capture capacity with 400 hours of flue gas exposure. Trace metals analysis was underway.

Linde-BASF Pilot Solvent Process

A 1-MWe CO_2 capture pilot plant processing up to 30 tons CO_2 /day was constructed and made ready for long-term testing in 2015. The unit incorporates BASF's novel amine-based process along with Linde's process and engineering innovations such as a dry bed for emission control, high capacity structured packing in the absorber, gravity driven intercooler, and location of the blower downstream of the absorber.

1.2 Gasification Technology

1.2.1 Gasification Facilities

The NCCC gasification process, represented in Figure 3, features the Transport Gasifier, a pressurized, advanced circulating fluidized bed reactor. The process includes dry feed systems, syngas coolers, the Particulate Control Device (PCD) for hot gas particulate filtration, continuous ash depressurization systems for ash cooling and removal, and a syngas recycle system.

Gasification operation provides syngas for testing of gasification-related technologies in addition to testing of pre-combustion CO_2 capture technologies. Test runs are generally conducted for 750 hours two or three times per year.

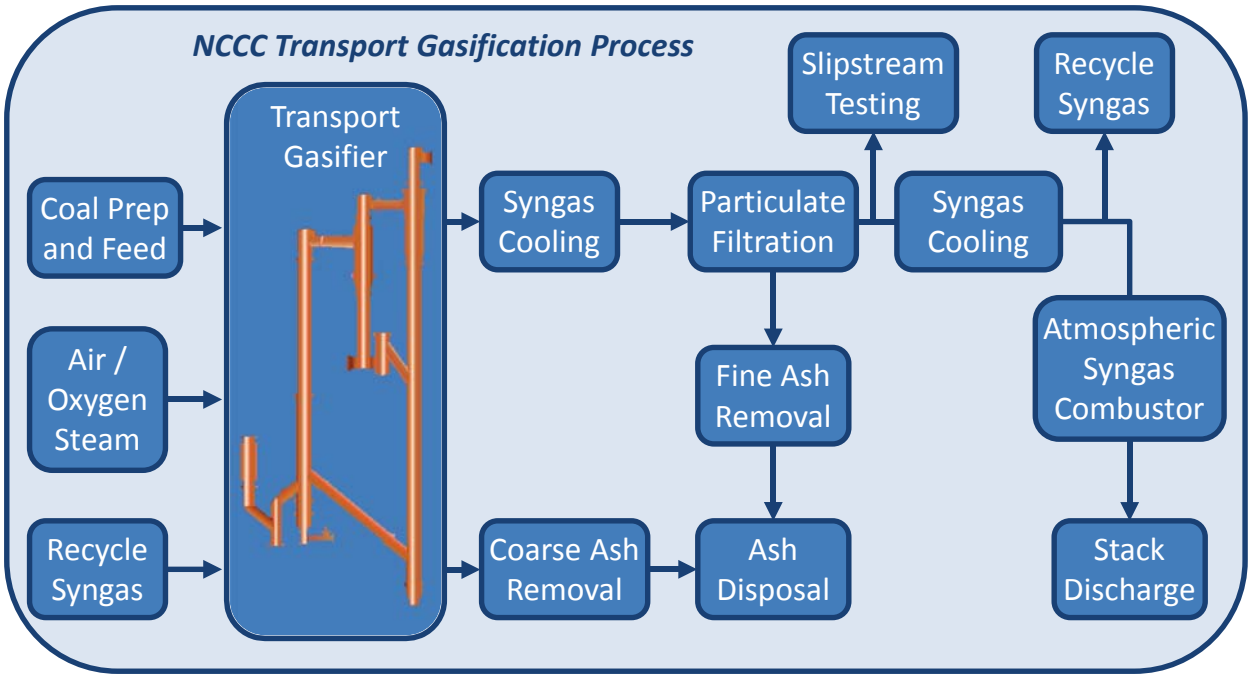

Figure 3. Schematic of NCCC Gasification Process

1.2.2 Gasification Technology Accomplishments

The gasification process operated in 13 different test runs, R01 through R13, for about 9,500 hours, bringing the total operational hours to over 21,000 since gasification operations commenced in 1999. In addition to supporting pre-combustion CO_2 capture processes, gasification operation enabled development of several in-house gasification support processes, and more than 12,500 hours combined of testing of gasification-related technologies by outside developers. Table 2 lists the developer technologies tested during the reporting period. Accomplishments in the area of gasification follow.

Table 2. Summary of Gasification Technology Developer Testing Completed

Developer Name/Technology Tested	Test Dates	Hours
Connecticut Center for Advanced Technologies/Biomass Gasification	6/12	219
Undisclosed Developers/Water-Gas Shift Catalysts	2/09 - 3/14	5,529
Undisclosed Developer/Carbonyl Sulfide Hydrolysis Catalyst	11/13 - 3/14	950
Johnson Matthey/Mercury Sorbent	2/09 - 3/14	3,760
National Energy Technology Laboratory (NETL)/Mass Spectrometer	7/10	--
NETL/Solid Oxide Fuel Cell	8/09	450
Stanford University/Tunable Diode Laser	11/12 - 8/13	1,560
Southern Research Institute/Fischer-Tropsch Catalyst	3/14	84

Biomass Co-Gasification

In support of the development of biomass as a low-carbon, renewable energy source, the NCCC operated with biomass co-gasification during three test runs. To address potential operability concerns with biomass, NCCC staff conducted off-line feeder testing and laboratory agglomeration tests prior to the first biomass gasification in 2009. By adjusting the process parameters according to the off-line and lab test data, the gasification process operated with reliable feeding and with no evidence of ash agglomeration, corrosion, or excessive tar formation. For all three runs with biomass, average steady state carbon conversions were greater than 98 percent.

Biomass operation, summarized in Table 3, was conducted under various conditions using Powder River Basin (PRB) subbituminous coal and Mississippi lignite. The third biomass test was performed on behalf of the Connecticut Center for Advanced Technologies (CCAT) in support of the Department of Defense goal of the development of domestic, renewable feedstock for liquid fuel production.

Table 3. Summary of Biomass Operation

Run Number	Gasifier Fuels	Biomass Percent of Total Feed Rate	Gasifier Oxidant	Hours
R03	PRB/Raw Biomass	20 wt%	Air	200
R04	Mississippi Lignite/Raw Biomass	20 wt%	Air	109
R08	PRB/Raw and Torrefied Biomass	10 to 30 wt%	Oxygen	219

Coal Feeder Development

Significant improvements were achieved in the feed rate stability of the developmental Pressure Decoupled Advanced Coal (PDAC) feeder, which was designed at the NCCC. The improvements were accomplished through incremental changes to the physical configuration, control logic, and instrumentation. The increased feeder reliability resulted in higher availability of the gasifier and allowed the implementation of automatic gasifier controls.

Sensor Development

Dynatrol vibration level probes installed in the PDAC feeder showed excellent reliability and allowed more responsive control of the coal fill cycles. A Drexelbrook point sensitive level probe installed in the top of the feeder dispense vessel permitted control at a higher fill level and thus improved feed rate stability by preventing funneling in the vessel. A new Densflow coal feed rate measuring device was also installed on the PDAC feeder, although results showed the need for improvements in accuracy.

Testing was conducted with a sapphire thermowell in gasifier service, which was modified by the supplier, Emerson Process Management, based on early operational results. The ongoing collaboration of the vendor and NCCC staff resulted in significantly improved performance without the degradation of the sapphire thermowell-housed thermocouple seen in early operation. During recent operation, the sapphire thermowell-housed thermocouple consistently read within 1 percent of the reference thermocouple.

Hot Gas Filtration

The NCCC continued the development of hot gas filter elements with efficiency evaluations and syngas operation. Operation with six different element types, consisting of either sintered metal powder or sintered metal fiber, demonstrated stable operation and resulted in near particulate-free outlet syngas. Long-term evaluations demonstrated excellent filtration performance (>99.9999) over an expected two-year commercial service for the most extensively tested elements.

Water-Gas Shift (WGS) Catalysts

Studies to optimize WGS catalyst operation showed that CO conversions adequate to facilitate high CO_2 capture rates can be achieved at lower steam-to-CO molar ratios than those traditionally recommended. Evaluation of the impact of these test results for a commercial 500-MW IGCC power plant showed that the acceptable reduction in steam-to-CO molar ratio (from 2.6 to 1.6) corresponds to a substantial 40-MW increase in net electrical output.

In addition to this study, more than 3,500 hours of testing was achieved with one developmental catalyst to evaluate long-term stability, and results showed no significant degradation of the catalyst. Conversion of CO was typically around 70 percent with syngas produced from PRB coal. Higher conversions up to 90 percent were achieved while the gasifier operated with lignite, as the higher moisture fuel increased the syngas steam-to-CO ratio.

Carbonyl Sulfide (COS) Hydrolysis Catalysts

Testing began with a developmental COS hydrolysis catalyst. About 950 hours of testing was achieved, and test data will be used to guide future catalyst designs.

Johnson Matthey (JM) Mercury Sorbent

A high temperature palladium-based mercury sorbent from Johnson Matthey was tested as a method to remove mercury while retaining the high efficiency of warm gas conditions. Two levels of palladium loading were evaluated, 2- and 5-wt%, and the sorbent achieved greater than 99 percent capture of mercury, selenium, and arsenic in both sweet and sour syngas conditions.

NETL Solid Oxide Fuel Cell (SOFC)

Operation of the NETL's solid oxide fuel cell multi-cell array demonstrated over 450 hours of continuous operation on partially cleaned syngas. Over 4,500 cell-hours of data were collected, and more than 1 kilowatt of total power was produced. Performance showed remarkable robustness of SOFC materials to trace material exposure as well as acceptable power density given the modest heating value of the supplied syngas. The test represented the longest duration continuous SOFC test conducted using direct coal syngas as fuel.

NETL Mass Spectrometer

NETL's gas chromatography inductively coupled plasma mass spectrometer (GC-ICPMS) was used for the first time in the field to measure mercury concentrations directly during testing of the Johnson Matthey mercury sorbent. Although measured mercury levels from the GC-ICPMS were higher than those determined by Environmental Protection Agency (EPA) Method 29, the

results demonstrated the potential to gather real-time data and to facilitate control over key parameters.

Ohio State University (OSU) Syngas Chemical Looping (SCL)

The SCL pilot-scale process was constructed and installed, and initial commissioning was conducted. During off-line operations, solids circulation was successfully performed at operating pressures up to 132 psig for 184 hours. The results indicated reliable reactor system operation with the expected syngas conversion capacity and hydrogen generation. Further, the results showed that the solid circulation rate is controllable within the full range of design conditions. During the R13 gasification run, planned start-up of the SCL was precluded by issues with the burner. OSU will incorporate burner modifications for future syngas operation of the SCL process.

Stanford University Tunable Diode Laser (TDL)

In 2012, Stanford University first tested the TDL technology with syngas downstream of the PCD for real-time in-situ monitoring of H_2O, CO_2, and gas temperature in a gasification process. Operation was conducted throughout the gasification run, from start-up to shutdown. The TDL data showed excellent agreement with the existing analyzers and with in-situ measurements, and the rapid time resolution of the TDL allowed it to capture variations in syngas conditions that were previously not evident. The TDL data was about 30 minutes ahead of the existing gas chromatographs (GCs).

For testing in 2014, the TDL was modified to additionally detect syngas CO and CH_4 and thus extend the utility of laser-absorption sensing for gasification processes. The testing validated the earlier results, with meaningful data obtained for the four syngas species. During the gasifier start-up, the laser transmission was attenuated by more than 99.9 percent by the scattering from particulate in the syngas. Even at the low laser transmission conditions, the sensor was able to simultaneously monitor all four species with sub-second time resolution with signal-to-noise ratios better than 10 on all four syngas species. The success of the TDL sensor campaigns at the NCCC showed that laser absorption sensing is not only possible in engineering-scale gasifiers, but could be an important new diagnostic tool with the potential for new control strategies in future gasifier utilization and development.

Southern Research Institute (SRI) Fischer-Tropsch (FT) Catalyst

SRI tested a 5-lb/hr bench-scale FT synthesis reactor system to produce liquid transportation fuels using a selective, wax-free, cobalt FT catalyst. Activities completed included system commissioning, catalyst testing with bottle gas, and syngas cleanup testing. The catalyst testing demonstrated efficient heat removal and nearly isothermal conditions in the two-inch fixed-bed reactor. A hydrogen-to-CO ratio of 1.95 to 2.01 was maintained, and operation achieved design conversions and production rates of more than 2 liter/day. SRI will complete system modifications for future catalyst testing with syngas.

Gasifier Process Modifications

Several modifications were made to the gasification process during the contract period to address equipment-related issues. The most significant modification made was the replacement of the gasifier standpipe to address refractory damage.

1.3 Pre-Combustion CO_2 Capture

1.3.1 Pre-Combustion CO2 Capture Facilities

The NCCC's pre-combustion CO_2 capture program allows evaluation of solvents, sorbents, catalysts, membranes, and other emerging technologies with coal-derived, particulate-free syngas produced during gasification runs. Test areas for pre-combustion are located adjacent to the gasifier structure and include the Syngas Conditioning Unit (SCU) and a test bay for pilot-scale projects. These slipstreams offer developers an opportunity to test technologies at commercially relevant conditions, obtaining real-time data to assess the effectiveness of the technologies with variations in syngas quality during normal operation. Figure 4 provides a simplified schematic of the pre-combustion facilities.

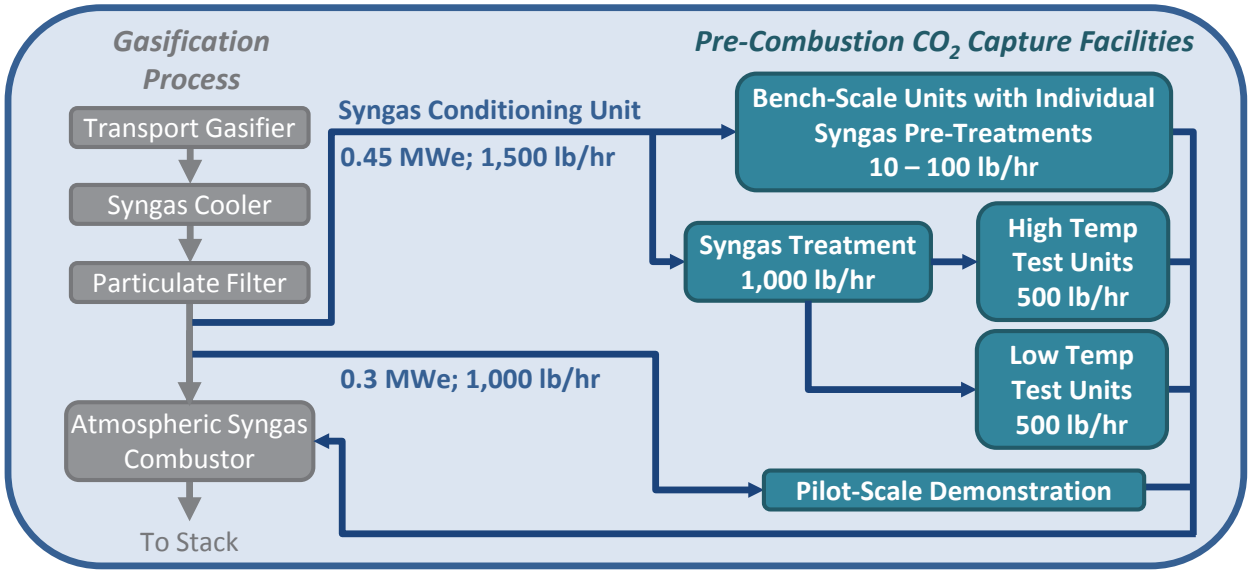

Figure 4. Schematic of Pre-Combustion CO_2 Capture Facilities

Technologies are tested over a wide range of operating conditions, with syngas conditioning tailored to meet the needs of each process. Syngas treatments include heating, cooling, hydrocarbon and sulfur removal, water-gas shift, and syngas augmentation with bottle gases. Off-line testing with bottle gases is also conducted in some cases.

1.3.2 Pre-Combustion CO_2 Capture Accomplishments

Pre-combustion CO_2 capture testing included 17,680 hours of membrane and sorbent operation in the SCU. In most cases, initial testing resulted in scale-ups and expanded testing of the technologies, such as:

- Hydrogen membranes from Media & Process Technology (MPT) and MTR underwent scale-ups of at least 10 to 1, with MPT further integrating WGS catalyst with the membrane tube bundle.

- MTR's CO_2 membranes were scaled-up 10-fold, and were the basis for another 10-fold scale-up to a CO_2 liquefaction process.
- A seven-fold scale-up of the Worcester Polytechnic Institute (WPI) hydrogen membranes was underway.
- TDA Research's initial CO_2 sorbent testing was expanded to include WGS functionality.

SCU operation also included characterization of chemical and physical solvents with syngas during gasification runs and with bottle gas in off-line operation. Solvent testing progressed from establishing operating and sampling protocols to developing a database of solvent characteristics to use as a basis of comparison. The facilities allowed the first syngas operation for new solvents which had previously been tested only in lab settings with bottle gases.

Table 4 summarizes the pre-combustion CO_2 capture technologies tested, and highlights of accomplishments follow in the discussion below.

Table 4. Summary of Pre-Combustion CO_2 Capture Testing Completed

Developer Name/Technology Tested	Test Dates	Hours
Media & Process Technology/Carbon Molecular Sieve Hydrogen Membranes	2/09 - 8/13	2,009
Membrane Technology & Research/Polaris CO_2 Membranes	11/09 - 3/13	4,412
Membrane Technology & Research/Membrane-Assisted CO_2 Liquefaction	11/12 - 8/13	818
Membrane Technology & Research/Proteus™ Hydrogen Membranes	11/09 - 3/14	5,270
Worcester Polytechnic Institute/Palladium-Based Hydrogen Membranes	5/11 - 3/14	4,275
Eltron Research & Development/Hydrogen Transport Membranes	11/12	204
TDA Research/CO_2 Sorbent	10/11 - 3/13	692
Various Developers including NETL and University of Alabama/Solvents	2/09 - 11/13	--

Facility Upgrades

To accommodate new projects, the SCU capacity was increased from 200 to 1,500 lb/hr of syngas, and a new gas analyzer building, control room, and motor control center were installed to upgrade the existing facilities. Another major addition to the SCU was the syngas cleaning system with 1,000-lb/hr syngas capacity providing pre-treatments for sulfur and hydrocarbon removal, WGS, and COS hydrolysis. Additional instrumentation, gas analyzers, superheated steam supply, syngas treatment equipment, and a hydrogen and CO bottle gas supply system with a firewall were installed. A new pilot-scale area was added with a 1,000-lb/hr syngas supply and utilities.

Media & Process Technology Carbon Molecular Sieve (CMS)

Media & Process Technology first tested its hydrogen-selective membrane, the Carbon Molecular Sieve, with single tubes. Testing progressed to a pilot bundle containing up to 17 tubes before developing a full-scale 86-tube bundle with a total surface area of 8.2 ft^2 processing up to 50 lb/hr of syngas. After successfully demonstrating the full-scale CMS in 2012, MPT incorporated WGS functionality into the CMS bundle to produce a catalytic membrane reactor (CMR), providing separation of hydrogen simultaneously with its formation.

Test results validated the membrane's high stability in the presence of aggressive gas-phase contaminants such as sulfur and nitrogen species, allowing it to operate with untreated syngas. Testing demonstrated that the selectivity of the membrane is sufficient to deliver hydrogen purity between 90 and 95 percent for syngas with 12 percent hydrogen; treatment of the desulfurized permeate stream with a polishing palladium/copper alloy membrane developed by MPT can achieve 99 percent purity. Testing of the CMS consistently showed stable operation with no apparent performance degradation. Operation with the CMR achieved CO conversions up to 50 percent without steam addition, and with no reduction in membrane permeance. MPT will continue to develop the CMS and the CMR technology.

MTR Polaris CO_2 Membrane and Membrane-Assisted CO_2 Liquefaction

MTR initially tested its Polaris CO_2 membrane at 10 lb/hr, and then scaled it up to 50 lb/hr. Testing of the CO_2 membranes demonstrated CO_2 enrichment from 10 percent in the feed to 40 to 60 percent in the permeate. Testing with syngas without sulfur pre-treatment showed that the membrane modules were stable in the presence of H_2S. The membranes showed H_2S/CO_2 selectivity of around 3; thus, the Polaris membranes also provide an option for co-capture of H_2S and CO_2.

Based on the successful operation of the Polaris membrane, MTR designed an integrated membrane-assisted liquefaction process at a 500-lb/hr scale that was first operated in late 2012. Operation demonstrated high purity liquid CO_2 production, and operational stability improved over three test runs. The membrane system continuously produced a liquid CO_2 stream containing more than 95 percent CO_2 at sub-zero temperatures (-27°F) and high pressure (about 400 psi). The liquid CO_2 production rate improved significantly in the final run, at 35 to 40 lb/hr (compared to 15 lb/hr in the first run), which corresponded to about 60 to 70 percent of the feed CO_2. Operation of the liquefaction unit demonstrated stable performance and reliable liquid CO_2 production.

MTR Proteus Hydrogen Membranes

MTR scaled up the hydrogen membrane from a 1-lb/hr stamp cell to spiral-wound modules, first at 10 lb/hr, and later at a 50-lb/hr scale. The hydrogen membranes demonstrated stable operation at temperatures up to 300°F for extended periods and in the presence of sulfur and other contaminants. Testing typically resulted in permeate hydrogen concentrations over 80 percent, which represents a seven-fold hydrogen enrichment of the feed for temperatures between 212 and 302°F. MTR also began development of second-generation (Gen-2) Proteus membranes for operation up to about 400°F. The successful results of the Gen-2 Proteus membrane stamps provided a baseline for future optimization and membrane performance improvement.

Worcester Polytechnic Institute/Palladium-Based Hydrogen Membranes

WPI conducted testing to optimize the composition of its palladium-based membranes. Thirteen palladium and palladium alloy membranes were tested individually at 842°F under syngas conditions in a single membrane module. The total testing time for all membranes was 4,275 hours, representing about half a year of commercial operation. The testing demonstrated about 1.4 lb/day of hydrogen production and 99.9 percent hydrogen purity. Based on the testing, WPI began preparations for scaled-up testing in future runs.

Eltron Research & Development/Hydrogen Transport Membranes

Eltron's hydrogen transport membranes were tested at about 640°F for a total of 204 hours during R09, including 183 hours of syngas operation with hydrogen enrichment and 21 hours with bottle hydrogen/nitrogen gases. The system operated with 10 lb/hr shifted and sweetened syngas (less than 1 ppmv sulfur). With hydrogen enrichment, the hydrogen concentration of the syngas reached about 38 to 40 vol% (dry basis). Hydrogen purity in the permeate stream was greater than 99.87 percent during the entire testing period, which indicated excellent membrane integrity without leakage. Post-run inspection showed the membranes to be in good condition.

CO_2 Sorbent Testing

TDA tested a CO_2 sorbent system in 2011 for 308 hours and over 1,200 adsorption and regeneration cycles, utilizing about 5 lb/hr sweet, shifted syngas. The results showed the sorbent technology to be fully capable of removing more than 90 percent of CO_2 from the syngas generated by an air-blown Transport Gasifier. The sorbent maintained consistent performance in the field, which closely matched the results in the laboratory using a simulated syngas mixture, suggesting that the potential impurities in the coal-derived syngas gas did not lead to sorbent degradation.

TDA modified the process to combine the WGS reaction and sorbent CO_2 capture in the same reactor for testing in 2013, during which the system operated for 384 hours using 3.5 lb/hr of untreated syngas. The average overall CO_2 capture rate for the run was over 96 percent with an average overall CO conversion of 96.4 percent at an average steam-to-CO ratio of 1.1. The CO conversion at the 1.1 steam-to-CO ratio was more than 5 percent greater than that predicted by the WGS reaction equilibrium at the operating conditions (a temperature of 450°F and pressure of 200 psig). This shift in equilibrium was attributed to the closely coupled removal of the CO_2 product gas, which enabled the reaction to more closely approach completion.

CO_2 Solvent Testing

Operation with CO_2 capture solvents led to the development of accurate sampling methods and the understanding of process chemistry. In establishing a database of solvent characteristics, NCCC researchers evaluated chemical solvents including ammonia (used to define solvent testing and sampling techniques), the well-established solvent potassium carbonate, and the potentially commercial solvent potassium prolinate. Physical solvents tested include polydimethyl siloxane (PDMS), the well-documented solvent dimethyl ether of polyethylene glycol (DEPG), glycerol triacetate (GTA), alkylimidazoles, and hybrid siloxane. In addition to CO_2 absorption characteristics, solvents were evaluated and compared for co-absorption of hydrogen sulfide (H_2S), regeneration characteristics and performance with water addition. The solvent testing supported DOE/NETL studies and research at the University of Alabama.

1.4 Technology Assessment

Technology Screening

In collaboration with the DOE, the NCCC developed a technology screening process for identifying technologies to be included in the NCCC test plan. The NCCC maintains a candidate technologies inventory that includes all major developers of relevant technology. Candidate

technologies are evaluated using both quantitative screening criteria and qualitative screening criteria related to shared DOE and NCCC objectives and budget considerations.

Evaluation of Transport Oxy-Combustion (TROC™) Technology

Studies were completed to evaluate the technical and economic aspects of TROC technology. These efforts allowed refinement of the process flow sheet and investigation of potential applications of this technology. The studies conclude that in both retrofit and greenfield applications, TROC is a scalable, economically competitive, near-zero emissions option for generating coal-fired power where CO_2 capture is required. A comparison of TROC with pulverized coal plants with CO_2 capture indicated that the TROC greenfield case had the lowest levelized cost of electricity. A comparison of TROC with natural gas combined cycle showed that TROC offers a viable economic alternative at capacity factors above 40 percent and an economic benefit at capacity factors above 70 percent.

Evaluation of Solvent-Based Post-Combustion CO_2 Capture

To assess the progress made in post-combustion CO_2 capture solvent development, an engineering and economic evaluation of post-combustion CO_2 capture (PCC) plant designs was completed using the solvent tested at the NCCC with the lowest heat of regeneration (referred to as the advanced solvent). Compared to MEA, the increase in the cost of electricity was 30 percent lower for the advanced solvent. Despite this significant improvement, the cost of electricity was still 50 percent higher than for the reference plant without CO_2 capture. Ways in which this cost increase can be lowered include reducing fuel costs, increasing net power, and incorporating alternative equipment designs. The alternative designs could lower capital cost and also consume less energy. Two of the designs discussed are to be tested at the PC4 in the next few years: a membrane contactor to replace absorber and stripper equipment, and flash regeneration in place of a stripper.

2.0 POST-COMBUSTION CO_2 CAPTURE

The PC4 provides for testing of flue gas CO_2 capture processes at a range of operating conditions and technology development stages. As illustrated in Figure 5, the PC4 features five bays for bench-scale units up to 0.1 MWe each; the PSTU for solvent testing at up to 0.5 MWe; the SSTU for solvent testing at up to 0.05 MWe; and test bays for larger units up to 1.0 MWe. An air dilution system is available for CO_2 capture testing under simulated natural gas flue gas conditions. The site also includes an independent control room, electrical infrastructure, and a balance of plant area containing utilities and chemical storage/handling facilities.

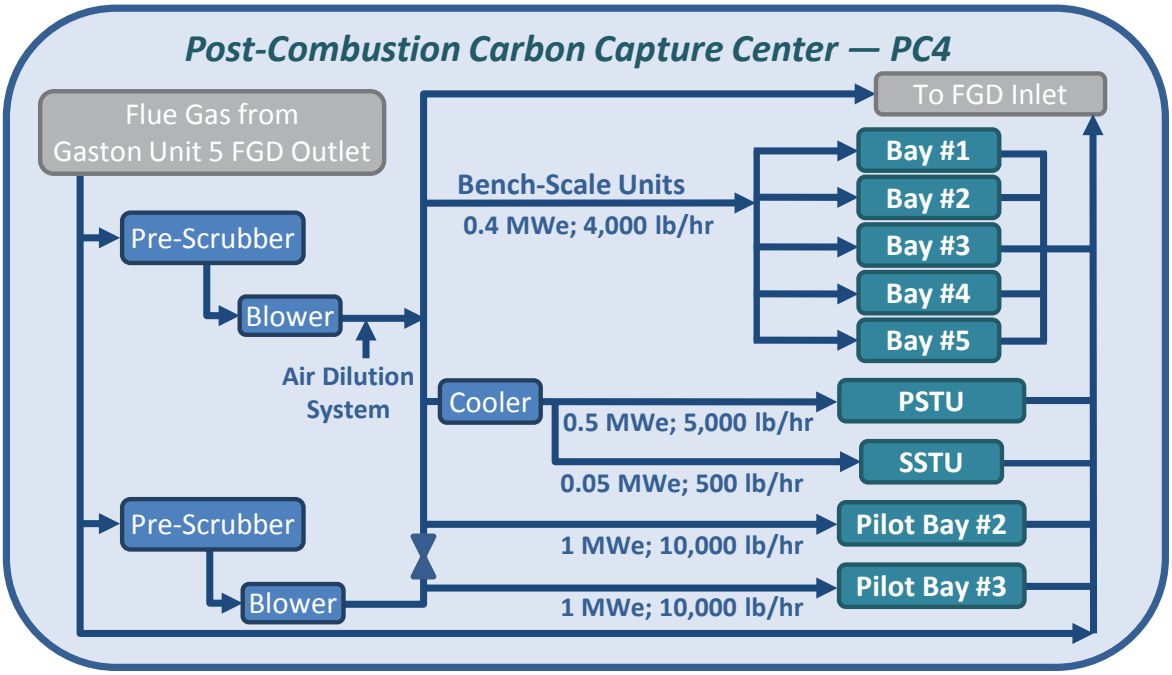

Figure 5. Schematic of PC4 Test Facilities

The PC4 utilizes up to 35,000 lb/hr of flue gas from Plant Gaston Unit 5, a base-loaded, 880-MW gross supercritical pulverized coal boiler fired with Alabama medium-sulfur bituminous coal. The unit meets all environmental requirements, utilizing a selective catalytic reduction unit for control of nitrogen oxides (NOx), sodium bicarbonate injection at strategic locations to control SO_3 emissions, hot-side electrostatic precipitators, and a wet flue gas desulfurization (FGD) unit to control SO_2 emissions. Hence, the flue gas extracted for PC4 testing is entirely representative of the gas that would be processed by a CO_2 post-combustion capture system. Table 5 provides the flue gas composition, temperature, and pressure with typical coal-fired operation and with air dilution for simulated natural gas flue gas operations.

Table 5. Average Values of Flue Gas Components and Conditions

	Coal-Derived Flue Gas	Simulated Natural Gas Flue Gas
CO_2, vol%	12.1	4.2
Oxygen, vol%	7.1	16.1
H_2O, vol%	7.6	5.4
Nitrogen Oxide (NO), ppm	41.0	13.0
Nitrogen Dioxide (NO_2), ppm	6.5	2.0
Temperature, ^oF	155	155
Pressure, inH_2O	20	20

2.1 PC4 Design and Construction

In late 2008, design of the PC4 began, and site preparation was underway with recovery of an area from the Plant Gaston coal pile run-off pond (see Figure 6). Design and procurement of major equipment also began.

Figure 6. Initial PC4 Site Preparation

By mid-2010, underground supports and foundations had been installed. By the end of the year, installation of major equipment, including a utility bridge, the PSTU, administration/control room and motor control center buildings, as well as major balance-of-plant systems, was completed. Figure 7 provides photographs of the installation of the utility bridge and the PSTU.

Figure 7. Installation of Utility Bridge and PSTU

Final construction activities were completed in early 2011, as shown in Figure 8. Commissioning of the PSTU was accomplished in March, and testing by technology developers began in mid-year.

Figure 8. Final Construction of the PC4

2.1.1 PC4 Modifications

To accommodate simultaneous testing of pilot-scale projects, several upgrades were completed in 2014. The total flue gas capacity of the PC4 was increased from 12,000 lb/hr to about 35,000 lb/hr. This project involved the following:

- A forced draft fan delivering 20,000 lb/hr with a higher delivery head replaced the original fan with a delivery rate of 12,000 lb/hr to the PSTU. The original fan was re-located to the inlet of Pilot Bay 3.
- A new pre-scrubber was added at the Pilot Bay 3 inlet.
- The random packing in the PSTU pre-scrubber was replaced with structured packing to maintain high SO_2 collection efficiency at the higher flue gas flow rate.
- To meet the higher cooling duty requirements, a second cooling tower cell was added along with larger water circulation pumps.
- Electrical infrastructure additions included a new 2,500 KVA transformer and switchgear.

2.1.2 PSTU Modifications

In addition to the upgrades described above that increased the PSTU throughput, several modifications were made to accommodate specific technology developer tests.

- New instrumentation and equipment were installed for testing the B&W solvent. The added instrumentation (such as temperature and viscosity measurements) and associated equipment have been used in all subsequent PSTU tests.
- A rich solvent circulation loop and a rich solvent line to the regenerator were installed at the request of Chiyoda. These additions can be used by future developers to further investigate capital costs of a regeneration system, or to further load the solvent with the absorber recycle loop.
- A flue gas dilution system was added to simulate conditions of natural gas combined cycle flue gas to accommodate solvent testing by Cansolv. Piping was added to introduce air into the flue gas leaving the pre-scrubber to lower the CO_2 from about 12 vol% to as low as 4 vol%. This system has since been used by multiple developers.

2.1.3 Slipstream Solvent Test Unit

The NCCC installed the SSTU (shown in Figure 9) to increase the flexibility of the PC4 by allowing testing of solvents, such as those in early stages of development, available only in amounts smaller than the 4,000 gallons required for the PSTU. The SSTU comprises a pre-scrubber, condenser, absorber, regenerator, and associated equipment along with analytical instrumentation. Engineering work was completed to identify and incorporate needed modifications, and operation of the unit is planned for 2015.

Figure 9. View of PC4 Bench-Scale Area with Installed SSTU

2.2 PSTU Description

The PSTU was designed to achieve 90 percent CO_2 capture using a 30 percent aqueous MEA solution. MEA is used as the baseline, or reference, solvent against which other solvents tested can be compared. To accommodate the range of solvent properties, the PSTU design is very flexible operationally. Figure 10 provides a schematic of the PSTU.

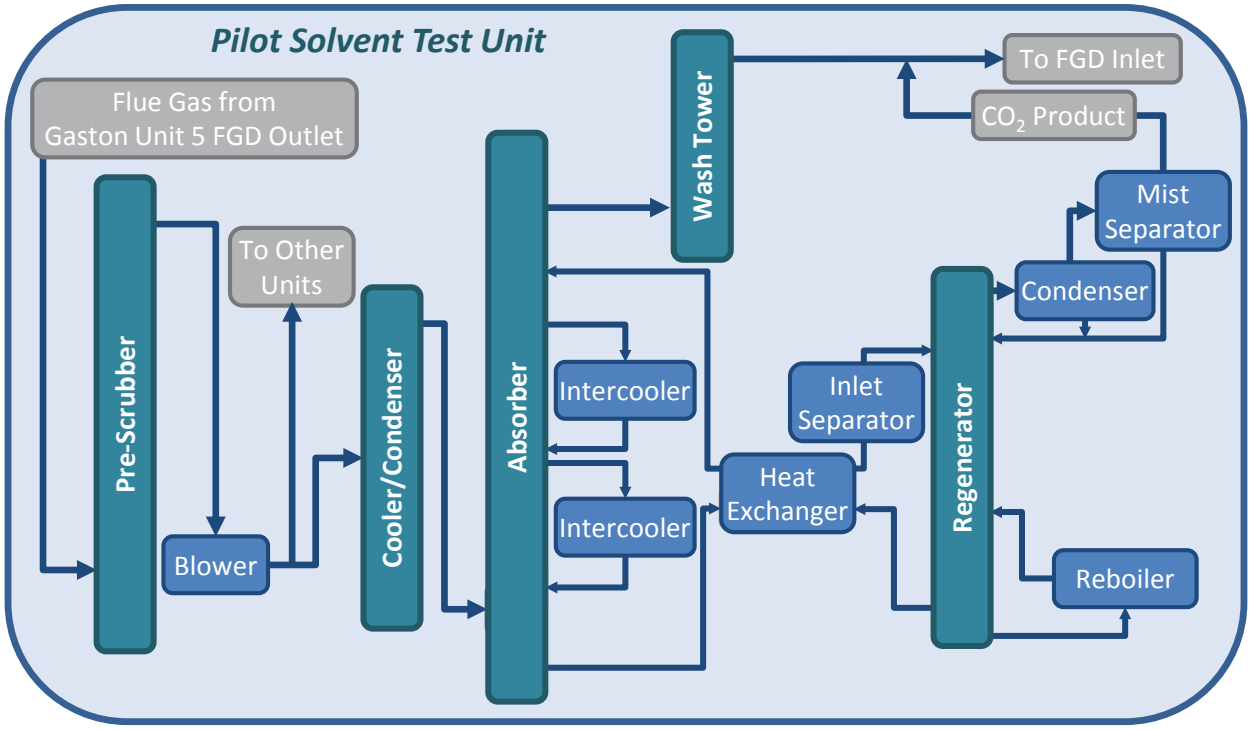

Figure 10. Schematic of PSTU

The five major sub-systems of the PSTU are:

- A pre-scrubber which removes the small amount of SO_2 remaining in the flue gas
- A cooler/condenser unit that cools the flue gas to appropriate reaction temperatures and removes flue gas moisture
- An absorber to promote efficient gas-liquid contacting to remove CO_2 from the flue gas
- A wash tower that cools the CO_2-depleted flue gas, removing trace amounts of entrained solvent
- A regenerator that provides heat to release the CO_2 from the solvent

Major design features are listed below.

- The vessels are spaced to allow for modifications and additional equipment to be installed to investigate alternative flow schemes.

- The regenerator is designed to operate at up to 215 psia as some solvents can be regenerated at pressure, offering the advantage of a reduced CO_2 compression ratio.
- The absorber and regenerator are designed to allow alternative packing and other gas-liquid contacting arrangements to be readily installed.
- The absorber and regenerator are designed with numerous process nozzles to allow for different flow schemes and with sufficient instrumentation nozzles for comprehensive data collection.
- The system is designed to cover a wide range of flue gas and solvent flow turndown to accommodate process variations arising from the use of solvents with different properties. The turndown ratios are 2:1 for gas and from 3:1 to 5:1 for liquid.
- As a range of solvents is to be used, the equipment is easily drained and cleaned.
- As the corrosivity of the different solvents is not known, for experimental convenience the vessels are made from 316L stainless steel.
- All vessels use structured packing (Sulzer Mellapak Plus M252-Y).

The process requirements for the major columns are specified in Table 6.

Table 6. PSTU Column Characteristics

Equipment	Pre-Scrubber	Cooler/ Condenser	Absorber	Wash Tower	Regen-erator
Outside Diameter, in	30	24	26	24	24
Number of Beds	1	1	3*	1	2*
Bed Height, ft	20	10	20; 10	10	20; 7
Maximum Operating Temperature, °F	200	200	300	200	400
Maximum Operating Pressure, psig	15	15	15	15	200
Sump Volume	No	No	Yes	No	Yes
Mist Eliminator	Yes	Yes	Yes	Yes	Yes
Viewing Ports	Yes	Yes	Yes	Yes	Yes
Addt'l Nozzles for Multistage Feed/Takeoff	No	No	Yes	No	Yes

*+1 for future use

2.2.1 Instrumentation and Control Scheme

V-cone differential pressure flow meters are used to measure the untreated flue gas entering the pre-scrubber, the treated flue gas entering and the CO_2-depleted flue gas exiting the absorber, and the CO_2 stream exiting the regenerator. Coriolis meters are used to measure the flow of cool-lean solvent entering the absorber and cool-rich solvent exiting. These meters can also determine the liquid density, and so also serve to monitor solvent composition.

The overall process was designed to operate automatically. Several major control strategies were established for the overall process as detailed below. Local temperature and level controls were also implemented for individual equipment operation.

The temperatures at two gas exit points from the wash tower and the separator downstream of the regenerator are controlled as closely as possible to the flue gas inlet temperature. This way, the net water gain or loss is minimized for overall water balance management and preservation of the solvent concentration.

The solvent flow rate in the circulation loop is controlled based on the inlet flue gas flow rate and the overall CO_2 removal efficiency. The performance data can be evaluated based on the CO_2 flow rate and treated flue gas flow rate as well as on-line sampling.

Pressure controls are included for the gas outlets and solvent loop. The two gas exit points have different pressure controls for the required absorption and regeneration processes, which can differ depending on the solvent tested.

2.2.2 Gas Analysis Methods

Table 7 lists the gas sampling locations in the PSTU and analysis methods used as of 2014.

Table 7. PSTU Gas Analyzers

Stream	Species	Technique
Absorber Inlet	CO_2	NDIR
	Oxygen	Paramagnetic
	SO_2	Ultraviolet
Absorber Outlet	Oxygen	Paramagnetic
	CO_2	NDIR
	NO	NDIR
	NO_2	NDIR
Regenerator Outlet	CO_2	By difference

In addition to the commercially established techniques listed in Table 7, the NCCC developed an impinger train for analysis of amine and degradation products in the flue gas exiting the absorber. The sample train, shown in Figure 11, processes gas that is extracted isokinetically to obtain a representative sample. An ice bath removes both droplets and condensable liquids in an EPA Modified Method 5 (MM5) sample system. Contact between liquid and gas is minimized, and gas is never bubbled through liquid. One of the impingers has an impaction plate to help collect small droplets. Downstream of the ice bath is a manifold section where smaller gas flows can be drawn through sample systems.

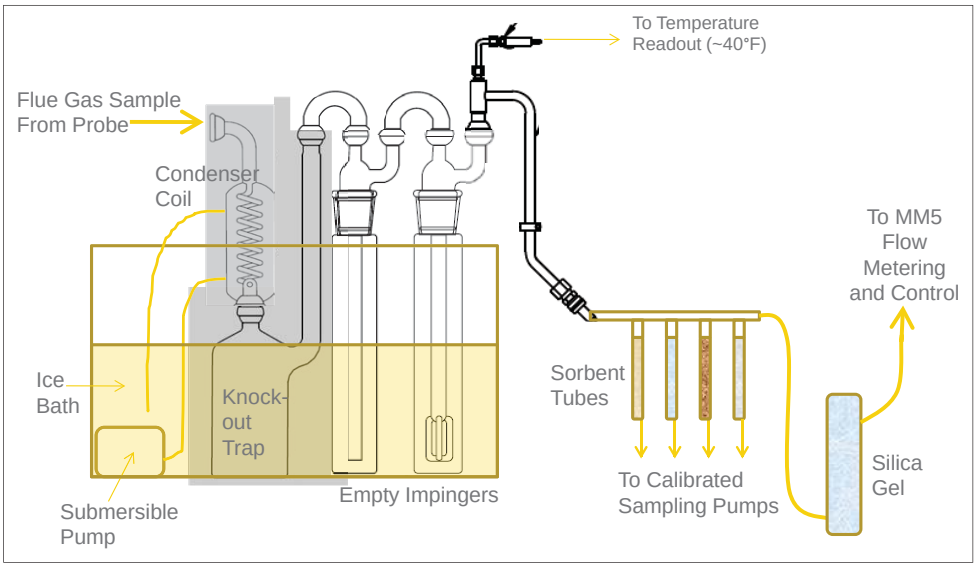

Figure 11. NCCC Gas Sampling Train Used to Measure Carryover of Amine and Degradation Products

Since startup of the PSTU in 2011, a number of analyzer changes have been made, which are described below.

Zirconia Probe for Oxygen Measurements

Initially, a zirconia probe was used to determine the oxygen content of the absorber inlet flue gas. This technology had been used successfully for monitoring oxygen in the drying gas for the PSDF coal mills. The ceramic sensing element in the probe operates at around 1,450ºF, and because of this was not selected for the absorber outlet, where the high temperature could be an ignition source for the solvent vapor present. Instead, a paramagnetic probe was selected for this location. The zirconia probe performance deteriorated with time more rapidly than expected and had to be replaced more frequently than planned. This deterioration occurred because of the impact with fine water droplets carried over from the direct-contact cooler. Thus, the zirconia probe was replaced with a paramagnetic probe, which performed reliably without replacement at the absorber outlet.

Capacitance Probes for Moisture Measurements

Initially, capacitance probes were installed to determine the moisture content of the absorber inlet and outlet flue gas streams and the regenerator CO_2 outlet stream. The data collected were inaccurate, so the probes were removed from service. As the gas streams at these three locations are saturated, the moisture content can be calculated using temperature, pressure, and the molecular weight of the gas.

Fourier Transform Infrared (FTIR) Instrument for Measurements of Nitrogen Compounds and Moisture

An FTIR was initially installed at the absorber outlet to monitor ammonia, NO, NO_2, moisture, and amine content of the flue gas. Samples were taken from the wash tower outlet on the eighth floor of the PSTU structure and fed through a 170-foot long heated sample line to the analyzer unit in the on-site laboratory located on the ground floor. The exit flue gas contained a

significant number of water droplets that rapidly destroyed the sensor, which operated at around 400ºF (formation of the droplets is promoted by sulfur trioxide (SO_3) present in the flue gas from Plant Gaston). Measures taken to eliminate the droplets were: extracting the sample from the duct using a heated probe and operating the heated line at the maximum temperature to evaporate them; and installing a demister at the inlet to the heated line. These measures were not successful in protecting the sensor, and so the FTIR was removed from service.

Non-Dispersive Infrared (NDIR) Instrument for Measurements of Nitrogen Oxides

NO_2 is a precursor in the formation of nitrosamines and also reacts with the amine solvent. To support the investigation of their H3-1 solvent, Hitachi requested that NO_2 meters be installed at the inlet to the absorber. The initial instrument, installed in March 2012, was an NDIR instrument with a catalytic converter. The instrument measures NO, but not NO_2, for a fixed time interval before the sample stream is redirected over the catalyst for a similar time interval to convert the NO_2 to NO and measure the total NOx. The NO_2 is the difference between the two measurements, but as NO is around 95 percent of the total NOx, the calculated value of NO_2 is subject to error. As NO_2 was the most important measurement, NDIR instruments to measure NO and NO_2 specifically were installed at the beginning of 2014.

2.2.3 Liquid Analysis Methods

Liquid samples are extracted from these four locations:

- Regenerator outlet, hot-lean solution typically at 230°F
- Absorber inlet, cool-lean solution, typically 110°F, and having the same composition as the hot-lean solution
- Absorber outlet, cool-rich solution, typically 130°F
- Regenerator inlet, hot-rich solution, typically 215°F with the same composition as the cool-rich solution

An auto-titration system is used to determine the solvent concentration and CO_2 loading. The water concentration is determined by difference, although it can be determined by the Karl Fischer method if required. The auto-titrator takes a sample automatically every 30 minutes at each location. To determine the CO_2 loading, the samples are titrated with potassium hydroxide and with sulfuric acid to determine the solvent concentration. The hot samples are cooled to around 100°F to prevent CO_2 flashing from the solution and thereby altering its composition.

Auto-titration analyses of the solvent CO_2 loading are cross-checked using periodic laboratory titrations, carbon mole balance calculations, and the total CO_2 analysis procedure. The total CO_2 analysis procedure, illustrated by Figure 12, was developed at the University of Texas and refined at the NCCC, and has been shown to give accurate measurements of the CO_2 loading in various known standard solutions. The CO_2 present in the sample is liberated by adding sulfuric acid solution. A metered flow of nitrogen sweeps the CO_2 into a continuous analyzer, and the output signal is integrated to determine the total amount of CO_2 contained in the sample.

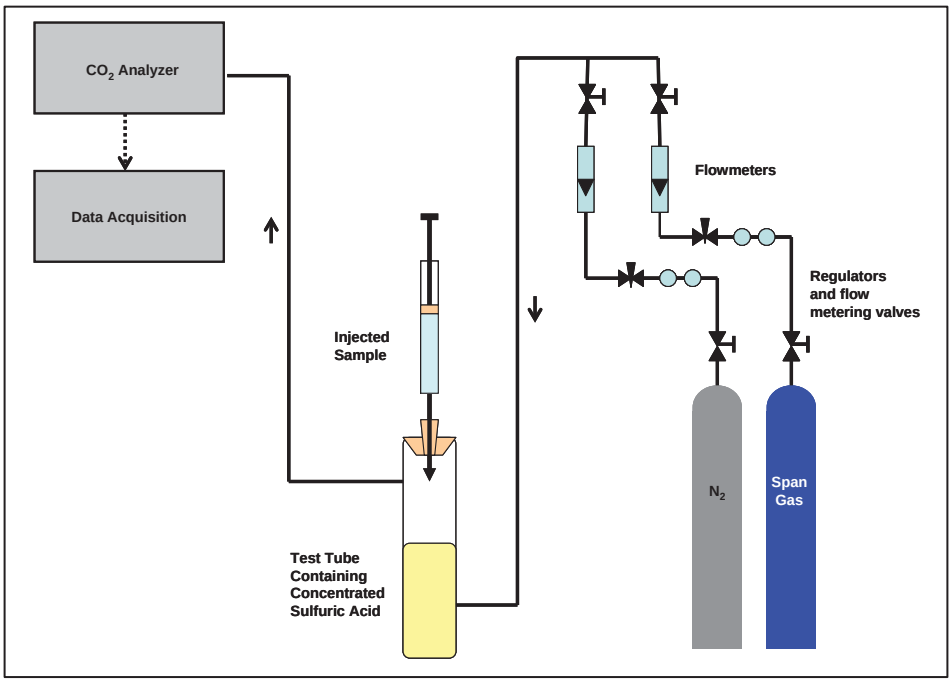

Figure 12. Total CO_2 Analysis Apparatus

2.3 MEA Baseline Testing

In early 2011, construction and pre-commissioning of the PSTU were completed, and commissioning and baseline testing with MEA were conducted from March 22 through May 17, 2011. Operation with MEA totaled 1,140 hours. Process issues were steadily resolved and control circuits tuned, allowing the plant to be operated in a controlled and safe manner at steady conditions. The process operated as designed, and flow rates and analysis procedures for the gas and liquid streams were all validated. This operational success demonstrated the readiness to support testing of developers' solvents. However, the 2011 MEA baseline campaign identified some issues that required further investigation.

- MEA carryover from the wash tower was in excess of 100 ppmv, compared to the vapor equilibrium value of 3 ppmv. These high values exceed limits for volatile organic compounds and result in excessive solvent make up rates.
- Degradation products in the regenerated CO_2 stream were not sampled. The laboratories used to measure degradation in the CO_2-depleted flue gas streams declined to measure degradation products in the solvent.
- End-of-run analysis of the used solvent revealed selenium and chromium contents, each in excess of 1 ppmw, which makes the solvent a hazardous waste if sent to disposal.

An MEA follow-up test campaign was completed from March 8 through March 25, 2012, to investigate these observations further. The majority of the 30-wt % MEA solution used for the 2012 campaign had been used in the 2011 campaign, but make-up was required to achieve the operating inventory. The 2012 campaign included just over 400 test hours.

2.3.1 2011 MEA Baseline Test Campaign

For the 2011 campaign, a total of 23 balance periods were completed, and the process data collected were carefully scrutinized to identify sources of error. No serious flaws were discovered, but a few corrections were made to calculation procedures, resulting in mass balance closures very close to 100 percent for the absorber.

Achieving good heat balances was complicated by the absence of reliable data for solvent specific heat, which is a function of temperature, MEA concentration, and CO_2 loading. MEA degradation products were measured in the CO_2-depleted flue gas stream exiting the wash tower. The degradation products were all at very low levels and, where they have been defined, well below OHSA Permissible Exposure Limits (PELs). Only two nitrosamines were detected, and these were present below the parts-per-million level. It is emphasized that these results are preliminary and that the sampling and analytical procedures are still under development.

The first mass balance period was completed on April 11 and the final one on May 17, 2011. During this 36-day period, Gaston Unit 5 took a five-day outage from April 23 to 27. The range of conditions covered is presented in Table 8. Although the intercoolers were tested, no balance periods were completed with the intercoolers in service. The reclaimer system was not tested.

Table 8. Summary of Test Conditions for 2011 MEA Baseline Test Campaign

Test Condition	Value
Total operating hours	1,140
Number of balance periods	23
Balance period durations, hours	3 to 8
Absorber CO_2 mass balance closure, %	96.6 to 104.6*
CO_2 removal rates, %	58.5 to 98.9
Total CO_2 captured, tons	400
MEA concentration, wt. %	17.5 to 39.3 (nominally 20, 30 and 40)
Absorber inlet flue gas flow rates (G), lb/hr (kg/hr)	3,120 to 5,040 (1,410 to 2,290)
Absorber inlet liquid flow rates (L), lb/hr (kg/hr)	12,000 to 27,500 (5,440 to 12,500)
L/G mass ratio	2.78 to 5.69
Reboiler steam flow rates (S), lb/hr (kg/hr)	680 to 2,460 (310 to 1,120)
S/L mass ratio (steam/liquid)	0.044 to 0.121
CO_2 loading of absorber inlet MEA, mol/mol	0.123 to 0.343
CO_2 loading of absorber outlet MEA, mol/mol	0.409 to 0.551
Absorber inlet flue gas composition, vol% wet	
CO_2	11.4 to 12.9 **
Oxygen	4.6 to 7.1
Moisture	6.3 to 7.3
SO_2	Less than 1 ppmv

*(CO_2 in inlet flue gas)/(CO_2 in CO_2-depleted flue gas + CO_2 removed by solvent)
**No CO_2 removed by caustic in pre-scrubber

In completing the mass balances, some adjustments were made to the process data where appropriate. These are discussed below.

Gas Mass Flow Rate Measurement

The flow from the differential pressure V-cone meters are determined by the following simplified equation:

$$M_g = k \times (dP \times \rho_g)^{0.5} \times Y$$

where:

Mg = mass flow rate of gas in lb/s
k = a constant incorporating gc, meter dimensional parameters, and meter discharge coefficient
dP = differential pressure, inches of water
ρ_g = gas density at conditions upstream of meter, lb/ft^3
Y = gas expansion factor

The flow from the transmitter was pressure- and temperature-compensated, but the density was a fixed value regardless of gas composition. To gain a more accurate flow measurement, the variation in gas compensation and its effect on density must be accounted for. This is especially true for the CO_2-depleted flue gas stream leaving the absorber, where the CO_2 content varies inversely with capture efficiency. As part of the data analysis, the density was adjusted for gas composition. This is not required for operational control, where a representative fixed value for density will suffice. Also, linking the flow rate to the gas composition could be problematic during gas analyzer malfunctions. Gas composition also affects the gas expansion factor, but the effect is too small to warrant correction.

The absorber inlet and outlet gas flows are considered reliable, but the CO_2 flow from the regenerator did not always match the CO_2 removed in the absorber. For the first ten runs, the CO_2 regenerator flow showed reasonable agreement, although the impulse lines had been connected the wrong way and the signal was reversed to compensate. During the five-day outage, the impulse lines were installed correctly, but thereafter the CO_2 regenerator flow rates were lower than those projected from the absorber data. This was likely due to a low spot in one of the impulse lines biasing the pressure differential over the meter. Having validated the meter, this fault was not detected until close to the end of the run. As there was good agreement between the CO_2 removed from the absorber gas and liquid flow streams, the average of these two values was used as the regenerator outlet flow.

For two of the periods, the absorber inlet oxygen analyzer was reading low, resulting in a poor oxygen balance closure. These errors occurred following calibration, so the values were changed to those immediately prior to calibration. The cause of the problem was rectified.

For the majority of the runs, the values for MEA and CO_2 determined by automatic titration gave satisfactory mass balance closures. Some of the values for the 40 wt% MEA runs resulted in poor MEA and CO_2 closures and were replaced by values from analysis of the manual samples.

2.3.1.1 Mass Balance Closures Achieved for Absorber

The mass and heat balance envelope was originally drawn around the absorber and wash tower. This produced acceptable mass balance closures but resulted in some errors in the heat balances. The wash tower includes a cooling circuit and is instrumented to allow the heat removed from

the CO_2-depleted flue gas to be estimated. For freeze protection, the cooling circuit is heat traced and insulated, and some of the heat removed by the cooler was introduced by the heat tracing. This was noted during a period when the flue gas flow was off but the cooling water temperature was still increasing. To avoid this error, the envelope was drawn around only the absorber. The flue gas composition was unchanged, and there was sufficient information to determine the moisture content at the wash tower inlet. The MEA content at the inlet was not estimated, but this flow is considered to be sufficiently low as to not introduce significant error.

Following a change in test conditions, process parameters were closely monitored to identify when steady conditions were re-established and the next test condition could proceed. In addition to temperatures and pressures throughout the absorber and regenerator, parameters monitored included:

- Liquid levels in vessels
- Flow rate of flue gas entering and CO_2-depleted flue gas exiting the absorber
- CO_2 content of flue gas entering and CO_2-depleted flue gas exiting the absorber
- Flow rate of CO_2 leaving the regenerator
- Flow rate of steam to the reboiler
- Flow rate and CO_2 content of lean amine entering the absorber and rich amine leaving

Once these parameters were steady, the solvent contained within the absorber and regenerator was allowed to be displaced one more time (for about 2 hours), after which the next test period could proceed. Figure 13 plots key data trends used in selecting the balance periods. The liquid solvent flow was increased to increase the liquid-to-gas (L/G) ratio and the steam flow to increase the steam-to-liquid (S/L) ratio, with the flue gas flow remaining constant. Once the solvent CO_2 loadings had stabilized, the balance period was selected.

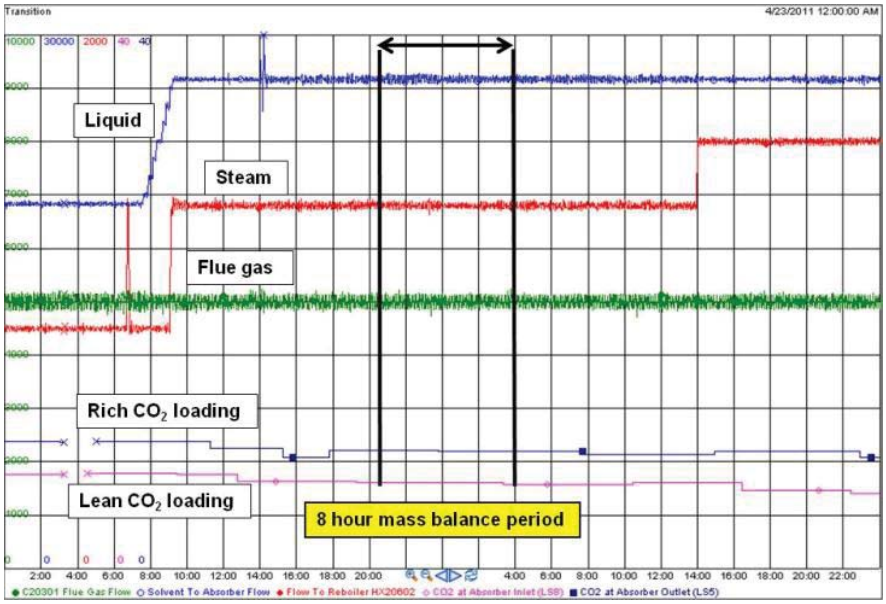

Figure 13. Typical Approach to Mass Balance Period

Figure 14 compares the total flows (gas plus liquid) entering and leaving the absorber. This is primarily a comparison of the liquid flows, as the liquid represents 75 to 85 percent of the total. A slight bias in the data indicated the exit flow was on average 0.8 percent higher than the inlet flow.

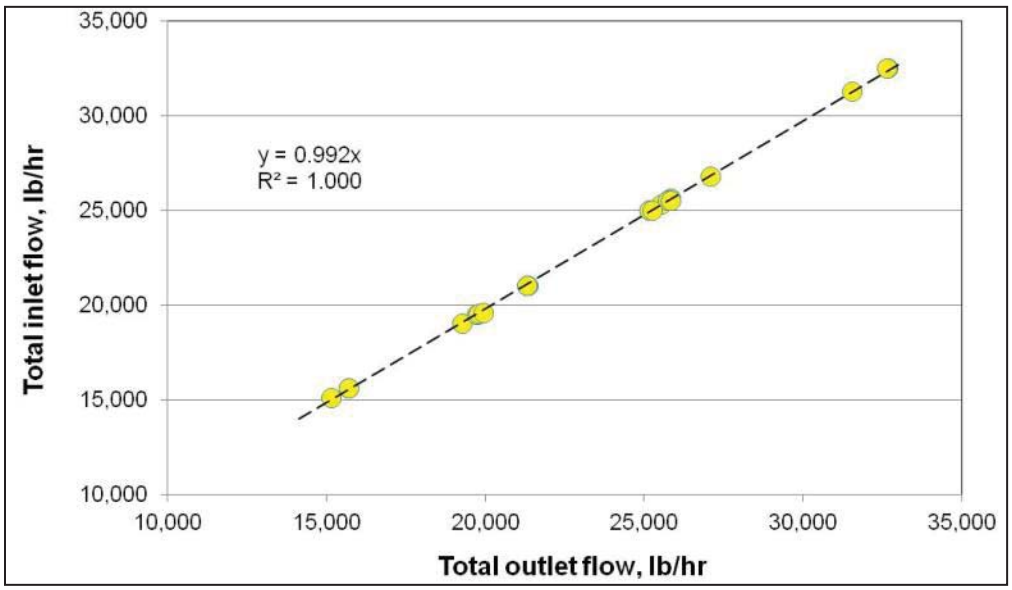

Figure 14. Comparison of Total Flows Entering and Leaving the Absorber

Figure 15 plots the water flow (gas plus liquid) entering and exiting the absorber. Water represents 60 to 80 percent of the solvent flow. There was almost perfect agreement between the inlet and outlet flows.

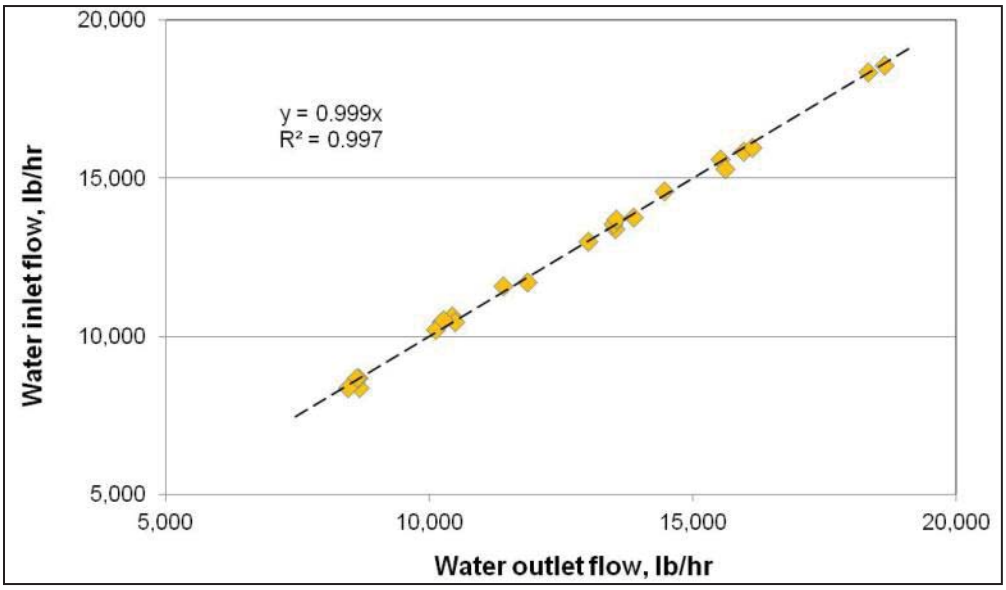

Figure 15. Comparison of Water Flows Entering and Exiting the Absorber

Figure 16 compares the MEA flow entering and exiting the absorber. MEA represents 20 to 40 percent of the solvent flow. There was a slight bias in the data, with the exit flow on average 0.7 percent higher than the inlet flow.

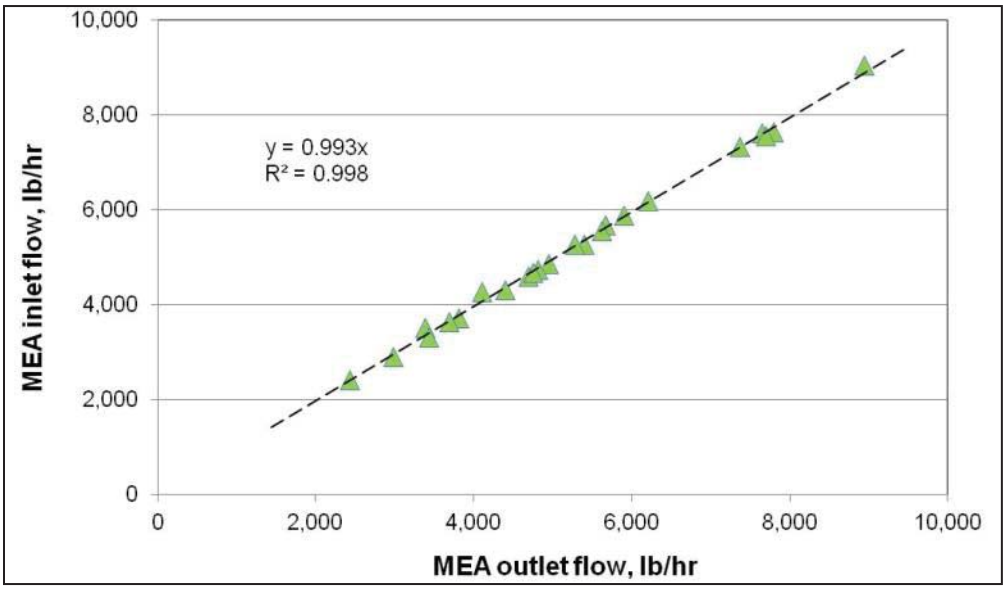

Figure 16. Comparison of MEA Flows Entering and Exiting the Absorber

Figure 17 provides a plot of the total CO_2 flow (gas and liquid) entering and leaving the absorber. CO_2 represents 5.2 to 9.1 percent of the total flow. There was a slight bias in the data, with the exit flow being on average 0.2 percent higher than the inlet flow.

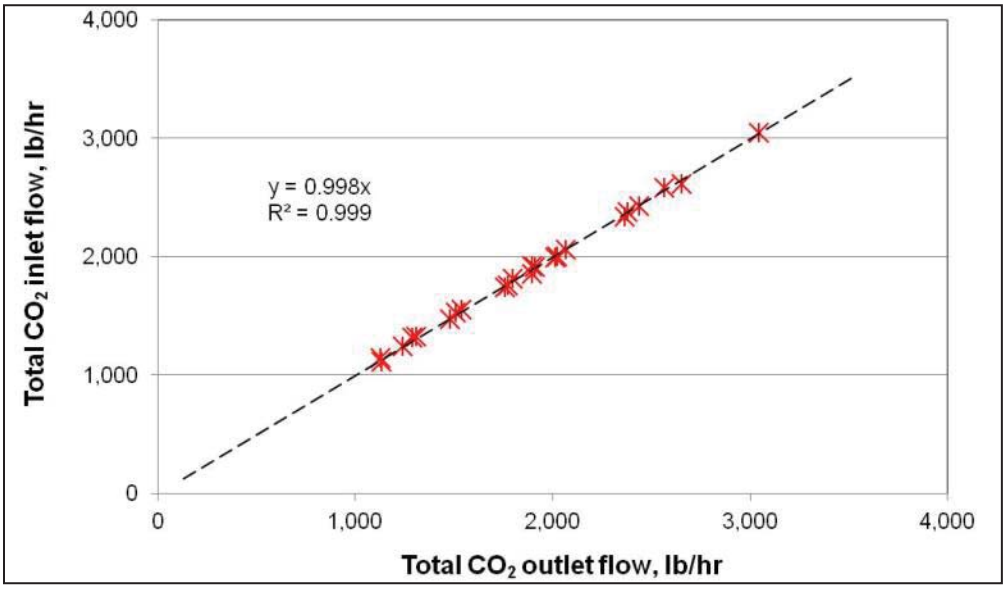

Figure 17. Comparison of CO_2 Flows Entering and Exiting the Absorber

Figure 18 compares the CO_2 removed from the flue gas in the absorber to the CO_2 absorbed by the solvent. The two flows agreed well.

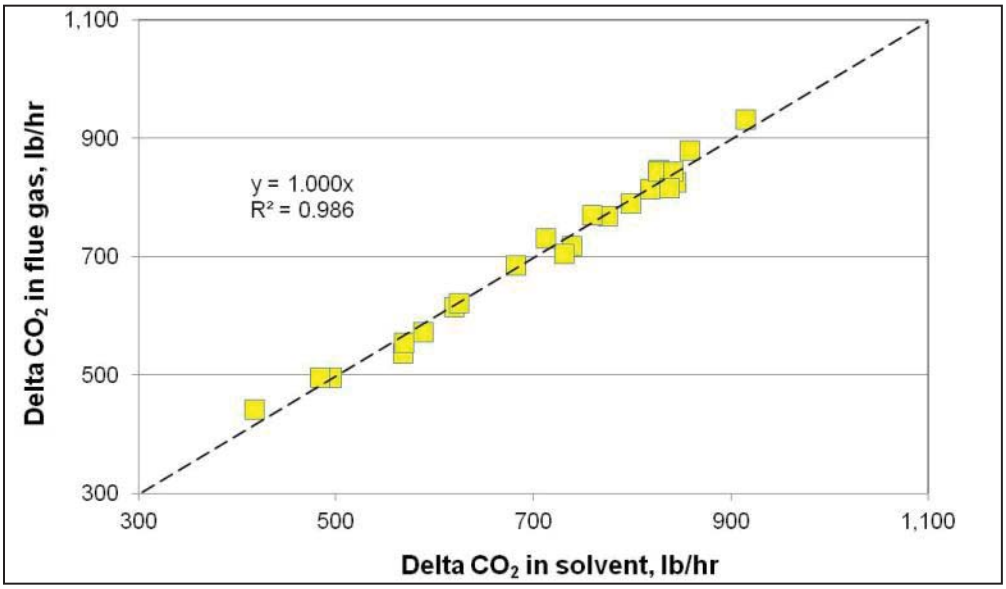

Figure 18. Comparison of Changes in CO_2 Content of Solvent and Flue Gas in Absorber

Figure 19 compares the oxygen in the flue gas entering and exiting the absorber. There was a slight bias in the data with the exit flow being on average 0.3 percent higher than the inlet flow.

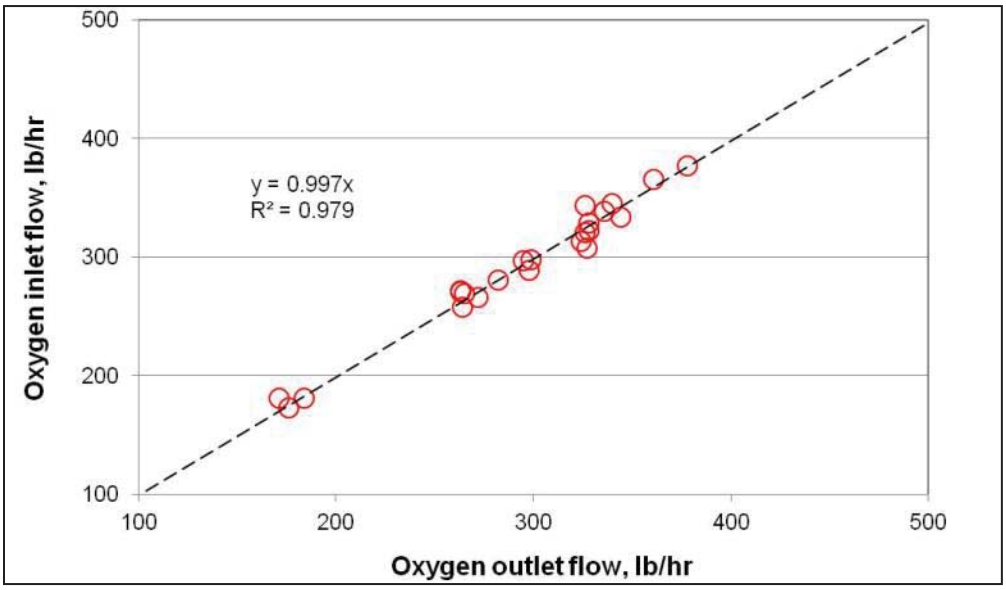

Figure 19. Comparison of Oxygen Flows in Flue Gas Entering and Exiting the Absorber

Figure 20 compares the nitrogen in the flue gas entering and exiting the absorber. This is determined by difference, and the fit emphasizes the accuracy of the measured values of moisture, oxygen, and CO_2. There is a slight bias in the data with the exit flow being on average 0.1 percent lower than the inlet flow.

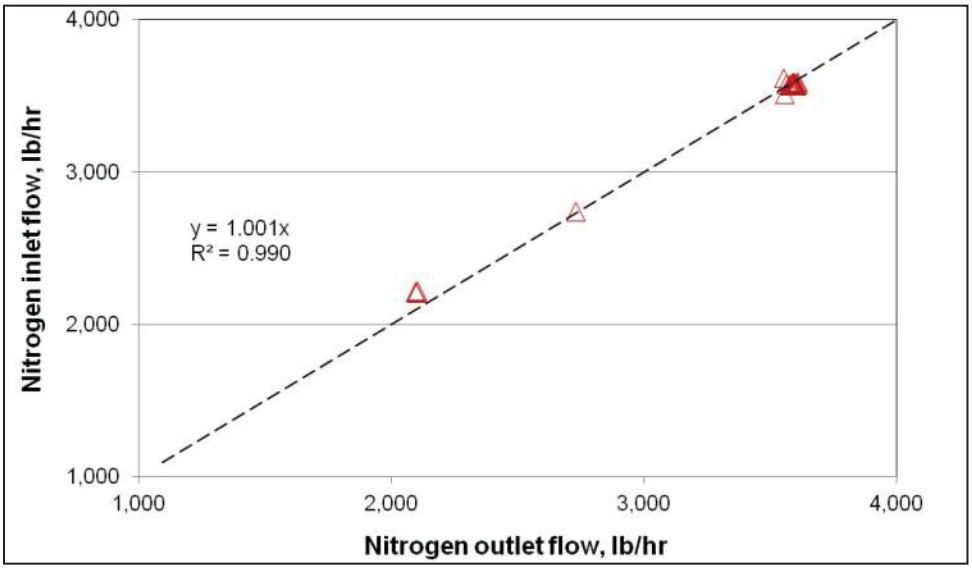

Figure 20. Comparison of Nitrogen Flows in Flue Gas Entering and Leaving the Absorber

The data have an underlying bias with the outlet flows on average being slightly higher than the inlet flows. This slight bias is considered to arise from the small difference in liquid flow rate measurements discussed earlier. Nevertheless, the closures achieved on all species are excellent for such a large pilot plant and validate the accuracy of the flow and composition measurements. The only measurement found to be invalid was the CO_2 exit flow from the regenerator. This most likely arose from a blocked impulse line, which was subsequently rerouted. The data are plotted in Figure 21 for the two periods, prior to April 28 and after April 28 (before and after the Gaston Unit 5 outage). The initial data showed good agreement, but the later data were in less agreement.

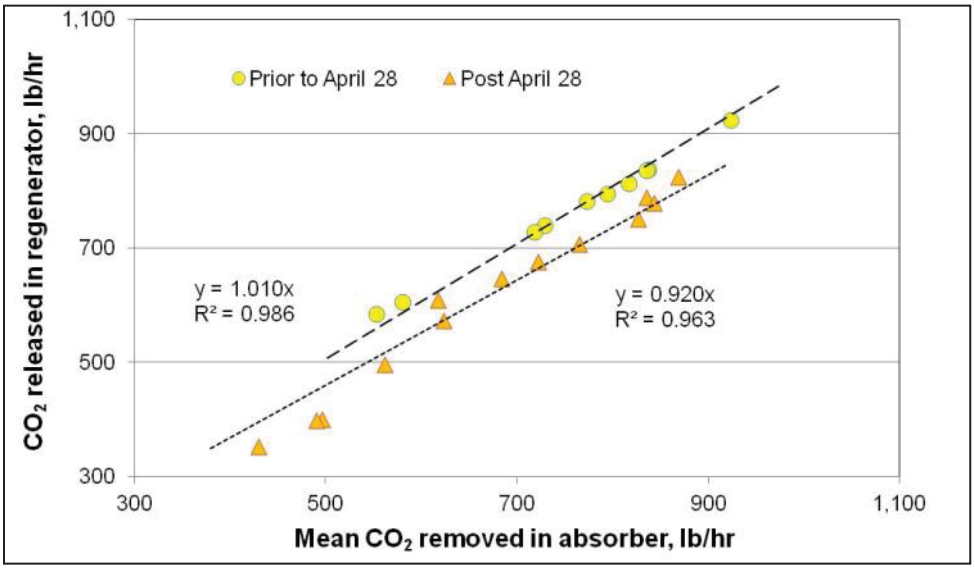

Figure 21. Comparison of CO_2 Released in Regenerator with that Removed in Absorber

2.3.1.2 Heat Balance Closures Achieved for Absorber

The liquid streams account for a large proportion of the absorber heat balance. For example, about 80 percent of the heat entering the absorber is in the liquid stream. Hence, the heat balance is very sensitive to the specific heat of the liquid, which varies with temperature, MEA concentration, and CO_2 loading. Values calculated from a commercial modeling software routine are presented in Figure 22 and Figure 23. The figures show, respectively, how specific heat varied with temperature and CO_2 loading for 30 percent MEA and how it varied with temperature and MEA concentration for 0.2 molar CO_2 loading. At higher temperatures, the values fell as vapor formed and contributed to the specific heat.

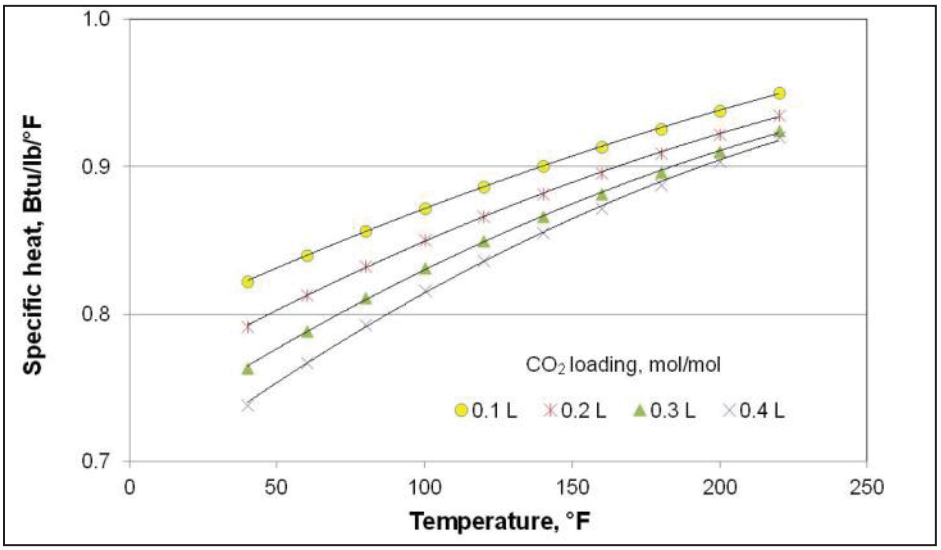

Figure 22. Variation of Solvent Specific Heat with CO_2 Loading and Temperature for 30 wt% MEA Solution

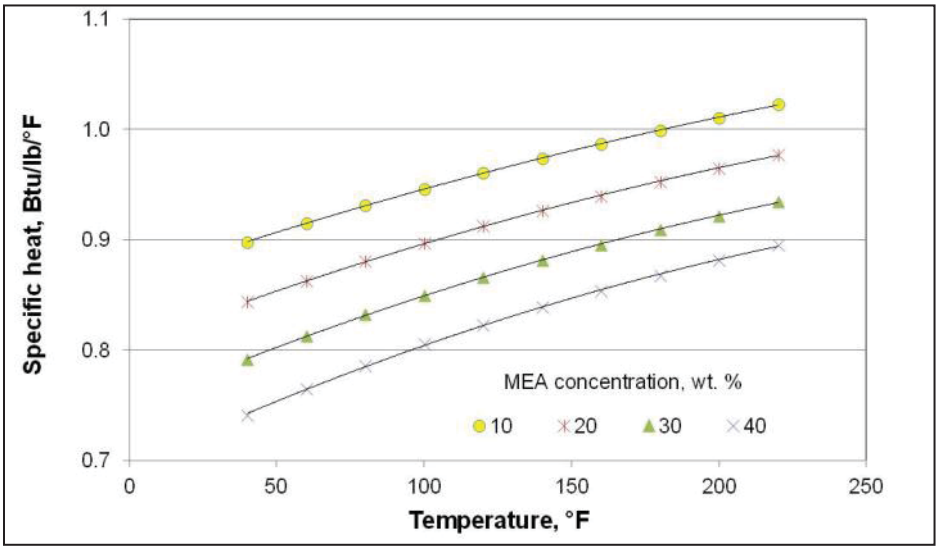

Figure 23. Variation of Solvent Specific Heat with MEA Concentration and Temperature for 0.2 Molar CO_2 Loading

Values from the software were used in the formulation of the heat balances. Closures in the range of 93 to 100 percent were achieved, which were acceptable but not as good as those for the mass balances. Given that the mass balance closures were so good, it was concluded that either the predicted values for specific heat or the heat of reaction used were inaccurate. The literature revealed enthalpies from 870 to 930 Btu/lb for the heat of reaction of CO_2 with MEA, and a value of 900 Btu/lb was used. Information presented by the University of Texas at Austin (UT-Austin) indicated that a more appropriate value was 820 Btu/lb. When this value was used, the closures improved, averaging close to 100 percent for the test periods.

2.3.1.3 Measurement of Amine Degradation Products

The flue gas leaving the absorber of a commercial post-combustion CO_2 capture process discharges to atmosphere, so it is important to determine the amine and amine byproducts carried over in this stream. SRI developed the sampling and analytical procedures required to characterize the flue gas stream leaving the PSTU absorber.

To determine whether the vapor of the MEA-based materials could be collected by condensation, vapor pressure data were determined for some of the critical species expected to be present. Figure 24 presents the temperature dependence of vapor pressure for various species.

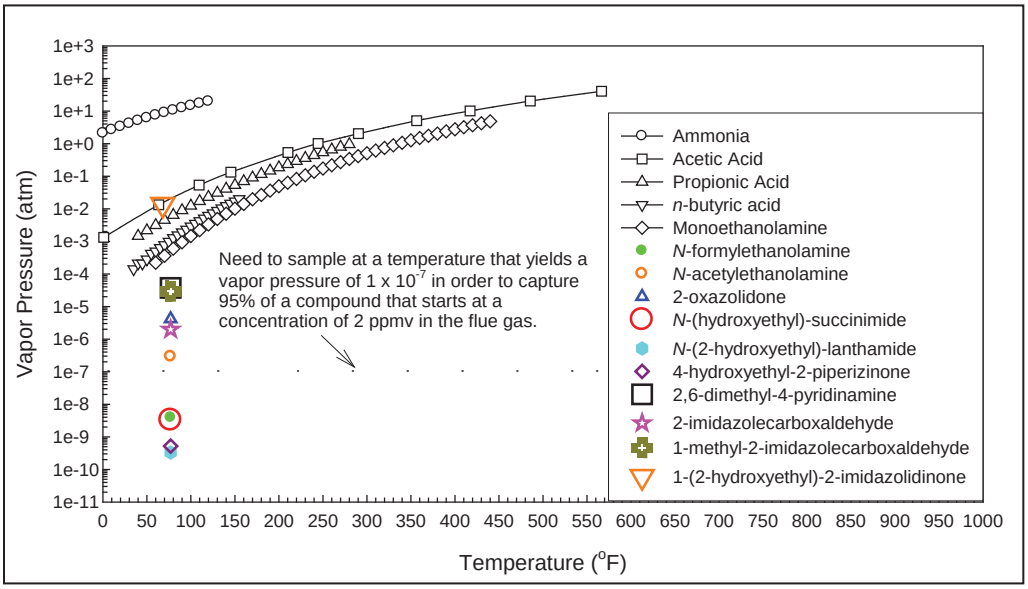

Figure 24. Vapor Pressure as a Function of Temperature for Various Amine Degradation Products

Based on thermodynamic modeling and the assumption that the concentration of the species of interest in the flue gas exiting the wash tower is around 2 ppmv, to capture 95 percent of the species, the vapor pressure would have to be below 10^{-7} atmospheres. From Figure 24, very few of the degradation products have vapor pressures below this vapor pressure at 32ºF, indicating that condensation in an ice bath alone would not be effective at collecting all the degradation products. Therefore, the sampling system would need to include provisions for capturing the portion of the species that remains in the vapor phase after the ice bath. Because of heat transfer limitations, the ice bath typically only cools the sampled flue gas sample to 40°F, increasing the vapor-phase concentrations of the species present.

Based on the above discussion points, the selected analysis method employed the EPA MM5 extractive sampling train coupled with the use of sorbent tubes (see Figure 11) to capture the species that remain as vapor. The CO_2-depleted flue gas stream exits the wash tower at around 125°F and 15.1 psia and is saturated with water vapor with some droplet carryover. As the degradation products could be present in the flue gas as either vapor or droplets, the sampling is completed isokinetically to ensure that representative amounts of the various components are collected. To yield reliable data, saturating the resins in the sorbent tubes with moisture must be avoided. As so much moisture is present (saturated vapor plus droplets) in the gas stream, it is essential to collect all water droplets and reduce the dew point as much as possible. This approach collects almost all the moisture present in the sample, droplets and vapor, and the condensable portion of the degradation products present. The vast majority of the condensed material is water, resulting in very dilute solutions of the degradation products. Fortunately, there are analytical techniques that can measure the expected degradation products in the microgram-per-liter range. The vapors present in the stream leaving the cooler are collected in the sorbent tubes.

The exiting gas flow at around 40°F is drawn through separate sorbent tubes arranged in parallel that contain specially treated resins to capture the degradation products present as vapor. These tubes were developed for industrial hygiene applications to monitor exposure to contaminants in the work environment. The techniques for using and analyzing these tubes have been developed by the National Institute of Occupational Safety and Health (NIOSH) and the Occupational Safety and Health Administration (OSHA). Both organizations have conducted extensive testing of the tubes and the associated analytical procedures to demonstrate that they are accurate for the specified components.

The liquid samples and the sorbent tubes were analyzed for degradation products at outside laboratories in accordance with the appropriate NIOSH and OSHA analytical protocols. Table 9 provides the analytical methods used. For one run, the gas stream was bubbled through 0.02-N sulfuric acid to determine if this treatment stage reduced the amount of the degradation products present.

As nitrosamines are decomposed by ultraviolet light, the sample train shown in Figure 11 was shielded from daylight. After completion of sampling, the condensate was transferred to amber glass containers and the sorbent tubes were wrapped in foil. All liquid samples and sorbent tubes were refrigerated before being sent for analysis.

Table 9. Analytical Methods Used for Condensates and Sorbent Tubes

Chemical Species in Condensate	Analytical Procedure	Technique
Volatile Organics incl. Ketones	EPA 8260C	Gas Chromatograph/Mass Spectroscopy (MS)
Non-Halogenated Organics incl. Amines	EPA 8015B	Direct Injection Gas Chromatograph
Carbonyl Compounds incl. Aldehydes	EPA 8315A	High-Performance Liquid Chromatography
Nitrosamines	RJ Lee Int'l Method	Thermal Energy Analyzer
Chemical Species in Vapor	**Analytical Procedure**	**Sorbent Tube Description**
Ketones	NIOSH 1550	Coconut Shell Carbon
Ketones	OHSA 31	Coconut Shell Charcoal for Total Hydrocarbons
Amines	OSHA 60	Naphthylisothiocyanate on XAD-2 Resin
Aldehydes	NIOSH 2532M	2,4-Dinitrophenylhydrazine on Silica Gel
Formaldehyde	NIOSH 2539, OHSA 52	Hydroxymethyl Piperadine on XAD-2 Resin
Nitrosamines	NIOSH 2522	Thermosorb/N
Nitrosamines	OHSA 31	Glass Fiber for Nitrosodiethanolamine

Preliminary results for the vapor measurements are summarized in Table 10. For the liquid phase concentrations, the compounds were present in water removed by the knock-out trap and are expressed as the equivalent vapor concentration in flue gas. Vapor phase concentrations indicate compounds present as vapor downstream of the knock-out trap and measured by sorbent tubes.

Table 10. Degradation Products Identified in Flue Gas Exiting Absorber Wash Tower

Species/Phase	Phase	Concentration, ppmv		OSHA PEL, ppmv
		Without Acid Wash	With Acid Wash	
Formaldehyde	Liquid Vapor	0.057-0.112 0.0047	<0.0023	0.75
Acetaldehyde	Liquid Vapor	0.015-0.179 0.562	0.093	200
Butylaldehyde	Vapor	<0.0045	0.0049	None
Ethylamine	Vapor	0.128	<0.0279	10
Dimethylamine	Vapor	0.043	<0.0279	10
Nitrosomorpholine	Liquid Vapor	0.0287 0.000025	<0.000014	None
Nitrosodiethanolamine	Vapor	0.00213	Not detected	None

The following observations were made from the available data with respect to the vapor phase:

- Only two nitrosamine compounds were detected above the lower detection limit of the analytical techniques employed; nitrosomorpholine and nitrosodiethanolamine were both detected well below the parts-per-million level in the vapor phase.
- Compounds detected at parts-per-billion level were formaldehyde, acetaldehyde, butylaldehyde, ethylamine, and dimethylamine.

- All compounds detected were well below OSHA PELs. These limits represent the safe weighted-average concentration for continuous exposure during an eight-hour work shift.
- Bubbling the flue gas sample through dilute sulfuric acid was effective in reducing emission levels, in some cases to below the lower detection limit. As the formaldehyde was not expected to react with dilute sulfuric acid, the reduction of all the species listed in Table 10 may have arisen simply by being bubbled through a liquid.

2.3.2 2012 MEA Baseline Test Campaign

2.3.2.1 MEA Carryover

Based on information from industry experts, the MEA carryover is thought to occur because of the presence of SO_3 aerosol in the flue gas. The aerosol acts as a nucleation site for the formation of droplets into which the MEA diffuses. Many of the droplets are too small to be collected efficiently in the wash tower and thus escape with the CO_2-depleted flue gas. It was theorized that MEA carryover could be reduced by controlling absorber temperature (higher or lower) to increase droplet size and make them more easily removable. A parametric test program was defined, the major variables of which were: operation with two and three beds, with and without intercooling; and adjustment of the wash water MEA concentration. Coincidentally, for a portion of the test period, a higher sulfur coal was burned, allowing the effect of higher SO_3 to be investigated also.

- Test 1 was a repeat of the major operating conditions in the 2011 MEA testing, using three beds without intercooling. The MEA concentration in the wash water was the intrinsic value determined by the operating conditions.
- Test 2 was similar to Test 1 but with both intercoolers in service to provide the maximum degree of cooling. The MEA concentration in the wash water was adjusted to the same value as for Test 1 to eliminate this as a variable. Solvent carryover increased 3.5 times, presumably as a consequence of lowering the absorber solvent temperature.
- Test 3 employed only two beds with one intercooling stage, and again the MEA concentration in the wash water was adjusted to the value achieved in Test 1. Solvent carryover was reduced, possibly because the unused upper bed was collecting droplets.
- Test 4 was similar to Test 3 but with the wash water flushed several times to achieve the lowest possible MEA concentration, which is considered responsible for the reduced solvent carryover.
- Test 5 was similar to Test 3 but without intercooling and with the MEA concentration in the wash water achieving its intrinsic value. The solvent carryover was the lowest of all the tests, presumably because the higher solvent temperatures resulted in the formation of larger droplets coupled with the droplet interception capability of the inactive upper bed.
- Test 6 was similar to Test 3 but allowing the wash water to achieve its intrinsic MEA concentration, which accounts for the increased solvent carryover.
- Tests 7, 8, and 9 were similar to Test 5, but conducted with flue gas from a higher sulfur coal, resulting in higher SO_3 in the flue gas entering the absorber. On average, this

resulted in 80-percent higher solvent carryover, roughly proportional to the increase in SO_3 level. The three results indicated a high level of data reproducibility.

The results are presented in Table 11.

Table 11. Parametric Tests Results for Solvent Carryover from Absorber Wash Tower

Test	Beds	Number of Intercoolers	Maximum Temperature, °F	MEA in Wash Water, wt%	Total MEA Carryover, lb/hr
Alabama Bituminous Coal (Flue Gas with 1.8 ppmv SO_3)					
1	3	0	174	1.05 (1)	2.1
2	3	2	160	0.98 (2)	7.3
3	2	1	162	1.06 (2)	4.9
4	2	1	163	0.22 (3)	3.8
5	2	0	174	0.92 (1)	1.1
6	2	1	163	5.58 (1)	5.9
Higher Sulfur Illinois Coal (Flue Gas with 3.2 ppmv SO_3)					
7	2	0	176	1.16 (1)	1.8
8	2	0	174	1.02 (1)	2.1
9	2	0	174	1.08 (1)	1.7

(1) Intrinsic Values (2) Adjusted to ~1% (3) Reduced Using Fresh Water

These data indicate that MEA carryover:

- Increased with SO_3 level—In the moist environment of the absorber, the SO_3 aerosol forms a nucleus for droplet formation, the liquid composition being determined by local water-MEA concentrations. Stack measurements performed by others indicate that 4 ppm of H_2S in flue gas corresponds to about 10^6 particles/cm^3, the majority being 0.1 microns or smaller, so there are abundant sites for droplet formation.
- Decreased with increasing solvent temperature—It is hypothesized that the higher the temperature, the larger the droplets formed and so the easier they are removed in the wash tower.
- Decreased with the upper absorber bed inactive—It is hypothesized that the liquid present on the surface of the structured packing in the upper bed intercepts some of the smaller droplets that would have otherwise passed through the wash tower.
- Decreased with wash water MEA content—The lower the MEA content of the wash water, the lower the equilibrium MEA vapor content of the gas stream.

Based on these results, NCCC communicated with suppliers of gas-liquid contactor equipment to determine how wash tower performance might be improved. One designer recommended that the structured packing be replaced with a bubble tray design, recirculating water between tray levels and feeding clean water to the upper tray. The supporting modeling work did not predict

the decreased solvent carryover, reducing confidence in the success of the proposed modification.

The NCCC contacted Sulzer, the original equipment supplier, to discuss an innovation designed to greatly reduce carryover. If the lean solvent returned to the absorber is too cool, it sub-cools the rising flue gas stream, resulting in temporary super-saturation and the formation of aerosols and giving rise to increased solvent carryover. The Sulzer innovation addresses this carryover mechanism by suppressing the formation of the aerosols, but does not address the mechanism arising from aerosols already present in the flue gas. Consequently, it was concluded that the Sulzer innovation would not be beneficial for the circumstances at the NCCC.

2.3.2.2 Total Amine and Degradation Product Carryover

To determine the composition of the vapor and liquid leaving the wash tower and the regenerator condenser, the NCCC uses the MM5 extractive sampling train described previously. The results of the analyses are presented in Table 12. The majority of the species collected were in the liquid phase. For example, the total MEA present is 135 ppmv and only 4 ppmv was present in the vapor (both concentrations are expressed as being present in the gas phase). However, this is the vapor content at 40°F (leaving the ice bath of the MM5 sampling apparatus), not the flue gas temperature (125°F). Passage through the bath results in the condensation of an unknown amount of vapor; hence, by convention, results are expressed as vapor.

Table 12. Amine and Degradation Product Carryover during MEA Testing

Analyte	Outlet Concentration, ppmv [1]	
	Wash Tower	Regenerator
MEA	135	0.061
Formaldehyde	0.32	2.09
Acetaldehyde	0.69	2.04
Ammonia	140	3.5
Ethyl amine	0.036	Not detected
Acetone	0.18	0.033
Acetonitrile	0.039	0.023
Acetic acid	0.021	0.020
Propionic acid	0.23	0.26
N-Nitrosodimethylamine [2]	0.000225	0.0000058
N-Nitrosodiethanolamine [2]	0.00106	Not detected

[1] Expressed as ppmv in the gas phase

[2] Present only in vapor samples

The conclusions from this area of testing were:

- Almost all the MEA carryover from the capture plant occurs downstream of the wash tower. As discussed previously, this is because of the SO_3 present in the flue gas. There is essentially no SO_3 present in the regenerator, and MEA carryover is almost negligible.

- Over 97 percent of ammonia produced is carried over from the wash tower, suggesting that oxidation degradation is more pronounced than thermal degradation. Adding an oxidation inhibitor will reduce solvent degradation and so lower ammonia release.
- As ammonia is a degradation by-product, the other degradation products may also be promoted by oxidation. The majority of the formaldehyde and acetaldehyde is carried over from the regenerator, likely due to their lower volatility compared to ammonia.
- Only two nitrosamines were detected: nitrosodimethylamine, which was below 1 ppb, and nitrosodiethanolamine, at about 1 ppb. Neither was detected in the liquid samples.

In the 2011 MEA baseline campaign, an additional impinger was added to the sampling train to allow the CO_2-depleted flue gas to bubble through 0.02-N sulfuric acid (H_2SO_4). It was anticipated that this would react with the MEA and lower the carryover. The MEA was indeed reduced, but so too were other species that do not react readily with sulfuric acid (e.g., acetaldehyde). Hence, it was possible that removal was as a result of bubbling the gas through a liquid not necessarily sulfuric acid.

The tests were repeated in March 2012 using water and sulfuric acid as the reagent. As only one sample train is available, three separate runs had to be completed: a baseline test with the additional impinger dry, followed on subsequent days by runs with sulfuric acid and with water. The results are presented in Table 13. The mode of testing may account for some of the variability, but both liquids appeared equally able to remove the species listed. On the basis of these results, passing the CO_2-depleted stream through an acid-wash stage would not be effective. Moreover, the solvent would be lost to the process, so if used would increase solvent makeup costs.

Table 13. Effect of Scrubber Liquid in Impingers on Vapor Emissions

Sampled Compound	Wash Tower Outlet, ppmv			Scrubbing Efficiency, %	
	No Liquid	H_2SO_4	Water	H_2SO_4	Water
MEA	4.40	3.02	2.13	31.44	51.52
Formaldehyde	0.035	0.0020	0.0031	94.34	91.19
Acetaldehyde	0.628	0.492	0.734	21.53	-16.97
Ammonia	53.7	4.75	1.74	91.14	96.75
Ethyl amine	0.0356	0.0325	0.0255	8.47	28.18
N-Nitrosodimethylamine	0.000225	0.0000371	0.0000172	83.51	92.36

2.3.2.3 Breakdown Products Detected in Solvent

The major degradation products present in the lean solvent are presented in Table 14. The values in the rich solvent were similar. The concentration of individual constituents generally increased with time. The amount of the compounds would be reduced by use of an oxidation inhibitor. As the constituents originated from breakdown of MEA, the constituents will vary with the solvent used.

Table 14. Major Degradation Products in Lean MEA

Constituent	Concentration, ppmw		
	3/9/2012	3/15/2012	3/22/2012
Formaldehyde	1.91	4.69	6.48
Acetaldehyde	0.21	0.29	0.37
Acrolein	0.15	0.30	0.39

Figure 25 shows the solvent color change over time, moving from pale yellow to a rich reddish brown. Similar color changes have been observed with other solvents. The cause of the color change has not been established, but may be degradation products or the accumulation of metals.

Figure 25. Color Change of Solvent During 2012 MEA Baseline Test Campaign

2.3.2.4 Metal Accumulation in Solvent

According to the EPA, a waste is considered hazardous if it exhibits at least one of four characteristics: ignitability, corrosivity, reactivity, and toxicity. Solvent disposal was deemed to only be influenced by toxicity criteria, so only this characteristic is discussed.

Over time, water percolates through solids in a landfill and dissolves contaminants that may pose health risks if that water enters the food chain. The Toxicity Characteristic Leaching Procedure (TCLP) simulates this leaching process and determines which of the contaminants identified by the EPA are present and in what concentration. Forty chemicals are currently listed, including heavy metals, pesticides, solvents, and some other organics. In the case of a liquid with less than 0.5-wt% solids, the liquid is considered to be the TCLP leachate.

If regulated limits of any one of the 40 chemicals are exceeded, then the waste is considered hazardous under the Resource Conservation and Recovery Act (RCRA) and must be disposed meeting strictly enforced requirements, all at increased cost to the waste producer. If sent to disposal, the landfill must include a barrier to contain groundwater with a facility to treat any run off. Before entering the landfill, some hazardous wastes may require treatment such as stabilization and/or solidification. In some instances, to reduce the volume of waste, incineration with stringent flue gas cleanup may be used.

If more than 2,200 lb of hazardous waste is produced per calendar month, then the producer is determined to be a Large Quantity Generator, and this carries additional requirements, such as reporting and accounting requirements, further adding to the cost of waste disposal. The most economical way to proceed is likely to be identifying how to avoid producing the hazardous waste, if at all possible.

At the end of the test campaign, consideration was given to disposing of the used solvent. In accordance with RCRA requirements, solvent analysis was completed for the eight metals listed in Table 15 and included the 40 regulated chemicals. These were all determined by inductively coupled plasma mass spectrometry (ICP-MS) except for mercury, which was determined by cold-vapor atomic fluorescence spectroscopy. While the RCRA limits provided in the table are in units of ppbw, the RCRA limit is actually defined in units of mg/L (1,000 ppbw is approximately equal to 1 mg/L).

Table 15. RCRA-Listed Metals in Solvent from 2012 MEA Test Campaign

Metals	Inlet Gas Concentration, ppbw	Liquid Concentrations, ppbw			RCRA Limit, ppbw	Probable Source of Buildup
		Fresh MEA	Makeup Water	Final MEA Solution		
Arsenic	1.13	< 12	0.462	219	5,000	Flue Gas
Barium	3.40	< 12	54.3	265	100,000	Flue Gas
Cadmium	< 0.14	< 12	< 0.225	< 10	1,000	
Chromium	0.315	< 12	0.927	45,090	5,000	Corrosion
Lead	0.271	< 12	2.34	< 10	5,000	
Mercury	0.009	> 0.50	> 0.50	> 0.50	200	
Selenium	9.74	44.1	< 0.225	1,950	1,000	Flue Gas
Silver	< 7.00	< 12	< 0.225	< 500	5,000	

The initial solvent for the 400-hour 2012 campaign was 50 percent fresh MEA and 50 percent from the 1,140-hour 2011 campaign, so the metals concentration is roughly equivalent to a 1,000 hour run (1140/2 + 400). Even in this short time, two metals exceeded the RCRA limit.

- Chromium was measured at 45,090 ppbw, well in excess of the 5,000-ppbw limit. The majority of the chromium originates from corrosion of the 316L stainless steel, which is composed of about 18 percent chromium. The 316L was selected for the vessel material due to its corrosion resistance, although these results indicate that a corrosion inhibitor is needed as well. The chromium would be significantly reduced by fabricating the plant from carbon steel, which is standard industrial practice.
- Selenium was measured at 1,950 ppbw, almost twice the 1,000-ppbw limit. The selenium originates mainly from the flue gas. Speciation testing using Reverse Phase, Ultra-High Pressure Liquid Chromatography, Inductively Coupled Plasma, Triple Quadrupole Mass Spectrometry (RP-UHPLC-ICP-TQMS) showed that 50 percent of the selenium was selenide, 25 percent selenite, and 25 percent elemental selenium. Selenate, the most toxic form of selenium, was below the detection limit.

- The presence of amine interfered with the RP-UHPLC-ICP-TQMS procedure when used to determine the chromium species present, but the procedure successfully determined the species of arsenic present. For arsenic, 17 percent was present as arsenite and 83 percent as arsenate. Although both are toxic, the former is the most toxic.
- The other metals present above the lower detection limits (LDLs), arsenic (219 ppbw) and barium (265 ppbw) both originate mainly from the flue gas.
- The flue gas content of RCRA metals is very low, but the high level of gas-liquid contact and the chemical environment in the absorber appears effective at removing much of it.
- The fresh MEA contained about 44 ppbw of RCRA metals (mainly selenium) but the used MEA contained 47,250 ppbw (mainly chromium).
- The solvent process includes a reclaimer to thermally separate the solvent from heat stable salts. It is likely that the metals in Table 15 will remain with the residue, and although this will reduce the quantity of waste, the concentration will be approximately 10 times higher.

The ICP-MS analysis revealed the presence of a range of other metals not included in the RCRA limit. Table 16 presents these additional metals that originate either from corrosion of the materials of construction or from the flue gas. Discussion on some of the metals follows.

- Cobalt was above 1,000 ppbw and is considered to be a corrosion product. The cobalt present in the solvent may have originated from metal workings from fabrication, as cobalt is used to harden and thus increase wear resistance of metal components.
- Iron, manganese, and nickel (with chromium) were present in the same proportions as are those metals in 316L stainless steel, the material used in fabricating the PSTU vessels. Iron and manganese are also present in the flue gas.
- Calcium and magnesium originate from the flue gas, probably material picked up from the FGD as fine particulate.
- Sodium originates from the flue gas, and is almost certainly material picked up from the pre-scrubber.
- The fresh MEA contained about 920 ppbw of other metals (mainly aluminum), but the used MEA contained 628,750 ppbw (mainly sodium and iron).

Table 16. Non-RCRA-Listed Metals in Solvent from 2012 MEA Test Campaign

Metal	Inlet Gas Concentration, ppbw	Liquid Concentrations, ppbw			Probable Source of Buildup
		Fresh MEA	Makeup Water	Rich MEA Solution	
Aluminum	281	< 120	272	4,060	Flue Gas
Calcium	684	< 1200	15,720	23,100	Flue Gas/FGD
Cobalt [(1)]	< 0.07	< 12	0.431	1,020	Corrosion
Iron	17.6	191	18,410	137,200	Corrosion
Magnesium	21.4	< 240	4,660	15,340	Flue Gas/FGD
Manganese	74.3	< 60	83.2	5,620	Flue Gas/Corrosion
Molybdenum [(1)]	< 0.28	< 12	0.886	5,270	Flue Gas
Nickel [(1)]	0.205	24.8	2.42	28,770	Corrosion
Potassium	38.8	< 1200	1,520	6,480	Flue Gas
Sodium	49.7	< 1200	5,110	399,100	Flue Gas/Pre-scrubber
Strontium	3.20	< 12	46.2	84.7	Flue Gas
Tungsten	< 0.70	< 12	< 0.225	1,590	Flue Gas
Vanadium	< 0.28	< 12	3.14	165	Flue Gas
Uranium	< 0.14	< 12	< 0.225	12.3	Flue Gas
Zinc	2.95	< 120	27.4	940	Flue Gas

[(1)] Regulated in California

2.3.2.5 Anion Accumulation in Solvent

The anions in the MEA and presented in Table 17 were measured using ion chromatography. Note that the concentrations were measured in ppmw, not ppbw as for the cations. The major inorganic anion detected was sulfate, the majority of which likely arises from salts of sodium (pre-scrubber), calcium and magnesium (wet FGD), and potassium and aluminum (coal ash), all cations being detected in used MEA (see Table 16). Some sulfate may also arise from the transmission of SO_2 from the caustic scrubber, but this is thought to be a minor source. The chloride, nitrate, and nitrite originate from the flue gas, and the oxalate and formate are solvent degradation products.

Table 17. Anions in Solvent from 2012 MEA Test Campaign

Anion	Rich MEA Concentration, ppmw	Probable Source of Buildup
Sulfate	1,010	Flue Gas
Chloride	21.2	Flue Gas
Nitrate	19.3	Flue Gas
Nitrite	2.3	Flue Gas
Oxalate	393	Solvent Degradation
Formate	1,820	Solvent Degradation

2.3.2.6 Solvent Metals Removal

While contaminants in the solvent must be limited to prevent operational issues such as foaming, deposition, and sludge formation, one of the greatest concerns is reducing the selenium level, as it infringes the RCRA limit. Because chromium originates from corrosion, it is assumed that its concentration can be managed by appropriate selection of materials of construction. Hence, the initial studies concentrated on the removal of selenium with the effect on the other materials present.

Metals Removal Using Established Water Treatment Methods

NCCC staff has consulted with water treatment experts to determine how selenium might be most economically removed. Based on studies of selenium chemistry for water treatment, three different waste water chemical treatment procedures were identified.

- Treatment with copper chloride solution without pH adjustment
- Treatment with ferric chloride solution with pH adjustment using sulfuric acid
- Treatment with zero-valent iron (ZVI) powder with and without pH adjustment

All three treatment techniques have been reported to remove selenium successfully from a variety of wastewater streams, but there is no known experience of their use to treat MEA solutions. The tests were carried out using a bench-scale jar tester, consisting of several stirred beakers that allowed a range of conditions to be tested simultaneously and so accelerate progress of parametric testing.

No precipitation of solids was observed with either copper or ferric chloride, even when a flocculant was added, indicating that there was no removal of selenium or any other metals. It is assumed that the MEA interfered with the precipitating reaction, possibly by chelating the metal cations. As MEA is a buffer, a large amount of acid was needed to adjust the pH, and consequently much of the MEA was consumed. From this observation, it was concluded that for a removal process to be successful, it should not require acidification.

For the ZVI tests with acidification for pH adjustment into the range 5 to 6, approximately 75 percent of the selenium in the MEA solution was removed, lowering the concentration from approximately 900 ppbw to 200 ppbw. No other metals were removed. Speciation tests revealed the following characteristics of the removal process:

- Selenide constituted 54 percent of the selenium and the ZVI removed 95 percent of it, reducing the concentration from 490 ppbw to 20 ppbw.
- Selenite constituted 44 percent of the selenium, and the ZVI removed 75 percent of it, reducing the concentration from 400 ppbw to 100 ppbw.
- The selenate constituted around 1 percent of the selenium, and the ZVI reduced the amount to below the lower detection limit.
- The elemental selenium was not detected initially, but increased to around 80 ppbw, possibly the acid promoting a conversion from one of the other species.

The selenium species in the used solvent were determined twice, first without treatment, at a pH of 10.3, and then with acidification to reach a pH of 5 to 6. Table 18 presents the results. The biggest change was the increase in selenite and corresponding reduction in elemental selenium occurring as a result of acidification. Variation of species with oxygen-reduction potential and pH has been observed by researchers investigating water treatment processes. These are the first known results for aqueous amine solutions.

Table 18. Selenium Species in MEA Solvent with and without pH Adjustment

Species	Percentage of Selenium Species	
	Without pH Treatment	With pH Treatment
Selenide	50	54
Selenite	25	45
Elemental	25	Not detected
Selenate	Not detected	1

Metals Removal Using ZVI Method at Texas A&M University

MEA samples were sent to Texas A&M University to be treated using their proprietary process based on ZVI without acidification. A bench-scale jar tester was used with the pH of the MEA at its intrinsic value of 10.3. Table 19 lists the removal efficiency of ZVI treatment for the metals that were measurable in the solvent. The difference in separation performance compared to the NCCC test results may arise from not using sulfuric acid for pH adjustment. Some of the non-listed metals (calcium, iron, and potassium) increased in concentration, presumably because they are present in the ZVI oxide mixture.

Table 19. Efficiency of Metals Removal from MEA Solvent with Texas A&M ZVI Process

	Metal	Removal Efficiency, %
RCRA-Listed Metals	Arsenic	96
	Barium	98
	Selenium	80
	Chromium	31
Non-Listed Metals	Aluminum	15
	Cobalt	80
	Magnesium	39
	Manganese	86
	Molybdenum	16
	Nickel	66
	Sodium	5
	Strontium	74
	Tungsten	63
	Vanadium	83
	Uranium	67
	Zinc	64

Metals Removal Using Sorbents

One supplier recommended three sorbents developed for water treatment, which were evaluated in the bench-scale jar tester without acidification. The sorbents are 650-micron silica matrix materials (marketed as Self Assembled Monolayers on Mesoporous Supports) licensed from Battelle. The three sorbents tested were:

- ESL-63 for removal of lead, zinc, cobalt, iron, and nickel
- FESL-63 for removal of selenium, chromium, and arsenic
- THSL-63 for removal of mercury, cadmium, lead, selenium, cobalt, iron and magnesium

None of the sorbents, individually or in combination, removed any of the metals. Again, the MEA is believed to interfere with the separation mechanism, and there are no plans to test other sorbents.

Other Methods of Metal Removal

Methods used by the petrochemical industry for removing contaminants from MEA include ion exchange and electrodialysis. Further investigation of these techniques is planned to determine their efficacy in removing metals as well as degradation products from MEA.

2.3.2.7 Oxygen Content of CO_2 from Regenerator

The CO_2 specification for pipeline transportation is that it contains less than 100 ppmv of oxygen to inhibit corrosion of carbon steel. The oxygen can be transferred into the regenerator either dissolved in the solvent or as flue gas entrained with the solvent pumped from the absorber sump. It was decided to measure this important parameter. A gas chromatograph was investigated initially but the argon peak of the carrier gas obscured the oxygen peak. Instead, a GE O2X1 fuel-cell oxygen detector probe was selected for the measurement program. Attempts to make continuous measurements were confounded by small leaks resulting in high oxygen contents. Therefore, a batch mode of sampling and analysis was used. Six samples were taken, and the average oxygen content was about 10 ppmv, indicating that the oxygen content of the CO_2 stream is well below the 100-ppmv limit.

2.4 Aker Clean Carbon Mobile Test Unit

Aker Clean Carbon tested the MTU at the PC4 in 2011, first with the CCAmine solvent, and later with MEA to establish a reference solvent. The MTU is designed to process 2,400 lb/hr of flue gas, with a CO_2 capture rate of up to 400 lb/hr. Figure 26 shows the MTU as it was being installed. Primary test objectives included examination of emissions and emission control, solvent degradation, and energy requirements. Secondary objectives were to develop and improve understanding of solvent performance, reclaiming equipment performance, methods for analysis of degradation products, and plant operation.

Figure 26. Installation of the MTU at PC4

The CCAmine campaign commenced on June 27, and long-term and parametric tests were performed until November 18, 2011. From November 19 through December 13, 2011, a short MEA campaign was performed. The hours and total CO_2 captured for these two campaigns are provided in Table 20.

Table 20. Summary of Aker Test Campaign Hours and Total CO_2 Captured

Campaign	Hours with Solvent Circulation	Hours with CO_2 Capture	Total CO_2 Captured, kg
CCAmine	3,092	2,182	228,928
MEA	542	410	40,396

Some observations on the operational experience are as follows:

- Round-the-clock operation was achieved at controlled conditions.
- The extended continuous operation increased understanding of plant and equipment performance and improved the ability to respond to upsets in power plant operation.
- The MTU was designed for northern European operation and was supplied with air-cooled heat exchangers. Summer temperatures in Alabama required the addition of water cooling to some circuits.

During this time, a series of parametric tests were completed, as listed below:

- The regeneration energy was determined for different operating conditions.
- A 30-wt% MEA test was completed to compare performance with CCAmine solvent.
- Degradation products and solvent carryover in the absorber and regenerator gas exit streams were measured.
- Results from Aker's degradation measurement technique were compared with samples taken by the NCCC sampling.

- Emission levels were reduced by adjusting demister operating conditions.
- The reclaimer operated and reduced the concentration of impurities by 80 percent with only minimal loss of solvent.

2.4.1 Environmental Results

2.4.1.1 Aker Emission Reduction Technology

An amine based CO_2 absorber is normally equipped with one or more water wash sections above the CO_2 absorption section. The main objectives of the water wash is to absorb amine vapor in order to minimize emission of amine to air and to cool the gas and condense water in order to fulfill the requirement for water balance across the entire capture plant. The condensation of water from the flue gas is a source for wash water make-up. Excess water in the water wash system is bled off and routed to the amine section below, and the effect of these make-up and bleed streams is reduced amine concentration in the water wash liquid.

One assumes close approach to equilibrium in the top of the water wash packed section with liquid recycling, meaning the gas will contain an amine concentration equivalent to the amine vapor pressure from the solution, which again is dictated by the wash liquid temperature, amine concentration, CO_2 loading and pH. Hence, a water wash operating at low temperature with high liquid replacement rate is preferred in order to minimize the amine slip to atmosphere, since lower temperature and lower amine concentration decrease corresponding vapor pressures.

Ammonia and alkyl amines produced by degradation of solvent amines in the process tend to escape the absorber via the emitted flue gas in the same rate as it is produced, since the solubility of these compounds in the solvent and water wash sections is very limited and equilibrium concentration will be quickly obtained.

The MTU contains two water wash sections, where the upper section can be utilized for additional emission control (pH controlled polishing section) in dedicated campaigns. Both sections consist of packed beds with liquid recycling. By controlling the pH in the upper wash section, the vapor pressure of ammonia and amines are eliminated. In addition to the two wash sections, the upper amine section was sometimes used as a third wash section. In this case, only the lower amine bed of 11.3 meter depth was applied for CO_2 absorption.

Aker performed three emission measurements campaigns, where off-line gas sampling from the top of the absorber was conducted. The MTU is also equipped with a Gasmet FTIR for on-line monitoring of ammonia and amine emission down to ppm levels.

2.4.1.2 Experimental

Gas sampling was performed from the top section of the absorber, above the demister at the absorber top. A 4-mm inner diameter Teflon probe was applied, the length of the sampling line from the extraction point in the center of the absorber top to the first impinger bottle was 0.5 m. The sampling was non-isokinetic, and the sampling probe was perpendicular to the gas direction. The sampling train was located on a bracket connected to the top of the tower. A mobile lift was used for access.

The sampling train consisted of three impinger bottles in series. The first two bottles were filled with 20 ml of 0.1 M sulfamic acid. The objective was to collect all relevant compounds (amines, nitrosamines, and ammonia) but at the same time avoid artifact formation of nitrosamines. Sulfamic acid is a nitrite scavenger, and previous lab tests have shown that it is less likely to form nitrosamines than is sulfuric acid.

The third bottle was an empty liquid trap, in case of carryover from the upstream bottles. The bottles were weighed before and after sampling for determination of water content in the gas. A gas tight pump and a gas meter was located downstream of the three impingers. The impingers were stored in an ice bath during sampling, and the gas meter measured the actual accumulated gas flow. Each sampling was done over a period of approximately one hour to collect sufficient amounts of analyte for subsequent liquid analysis.

Solvent (lean amine) and water wash samples were taken at the same time as the gas samples. The collected samples (impinger content, solvent, and water wash samples) were sent to an off-site lab for analysis. The samples were analyzed for amines including alkyl amines, ammonia, nitrosamines, and nitramines. The main analyses were done by mass spectrometry. By knowing the total impinger content and amount of gas sampled, the gas concentrations of the various elements in the treated flue gas are calculated.

The analyses of ammonia and alkyl amines were originally performed by GC-MS after derivatization with benzene sulfonyl chloride. This method has a very high sensitivity of about 1 ug/L for alkyl amines and 1 mg/L for ammonia. However, it was discovered that sulfamic acid was a poor choice for sampling of ammonia. After the third test campaign, it was found in the literature that sulfamic acid in water solution may hydrolyze to ammonium bisulfate. GC-MS analysis of a blank 0.1 M sulfamic acid sample prepared on-site showed indeed an ammonia concentration of 14.5 mg/L, which was comparable to the impinger analysis in this work and would correspond to an ammonia emission of a few ppmv. Hence, sulfamic acid is not applicable for sampling of ammonia; reagents like hydrochloric or sulfuric acid should be used.

2.4.1.3 Results

After starting up the plant in June, high amine emission was seen on the FTIR, even with operation of the pH-controlled wash that eliminates emission of ammonia and volatile alkyl amines. Similar emission behavior was seen in previous testing, where the amine emission could not be explained by the water wash vapor-liquid equilibrium assumption. This clearly indicated that the emission of solvent amine was mist controlled. Hydrophilic compounds such as solvent amines tend to be accumulated in the mist. Because of the tiny size of the mist particles (around 1 μm), they tend to penetrate wash sections and conventional knitted mesh demisters. For the same reason, isokinetic gas sampling is not required for mist sampling. The FTIR gas analyzer samples and evaporates the mist in the heated sampling line (working at 180°C), and hence measures the total amine content as vapor. It has been discovered that the mist precursors are ultrafine particles entering the absorber. The origin of these particles is not clear, but potential sources are sulfuric acid mist, ammonium sulfate formed in the power plant's selective catalytic reduction process, Trona powder (for SO_3 control), or combustion generated fly ash.

The fine particles are initially acting as nuclides for heterogeneous condensation of water in regions inside the absorber where water-saturated gas is rapidly cooled. When formed, the mist droplets absorb amine from the surrounding gas phase. Earlier emission measurements have proven that, in the absorber system with two proper water wash sections, the mist borne emission is the main contributor to the overall amine emission. In particular, amines that show high reaction rates with CO_2 are more likely to follow the mist out of the absorber, since the amine gets tied up as carbamate in the mist droplets, which reduces the amine vapor pressure and hence the rate of amine desorption from the mist droplets in regions where the partial pressure of amine is lower (e.g., second water wash or pH controlled wash section).

On the other hand, the observed emission of ammonia without the emission control in operation is not related to the mist emission. This is ascribed to the very limited solubility of ammonia and hence very low accumulation in the mist droplets. Any significant ammonia emission will be in vapor form, and the average ammonia emission over time will equal the ammonia production rate.

Aker has developed a mist abatement technology (Anti-Mist), which was incorporated in the MTU and was tested out at the PC4. Figure 27 shows the emission of solvent amine for periods where the MTU was operated with conventional as well as with anti-mist design, clearly demonstrating the benefits of the anti-mist design.

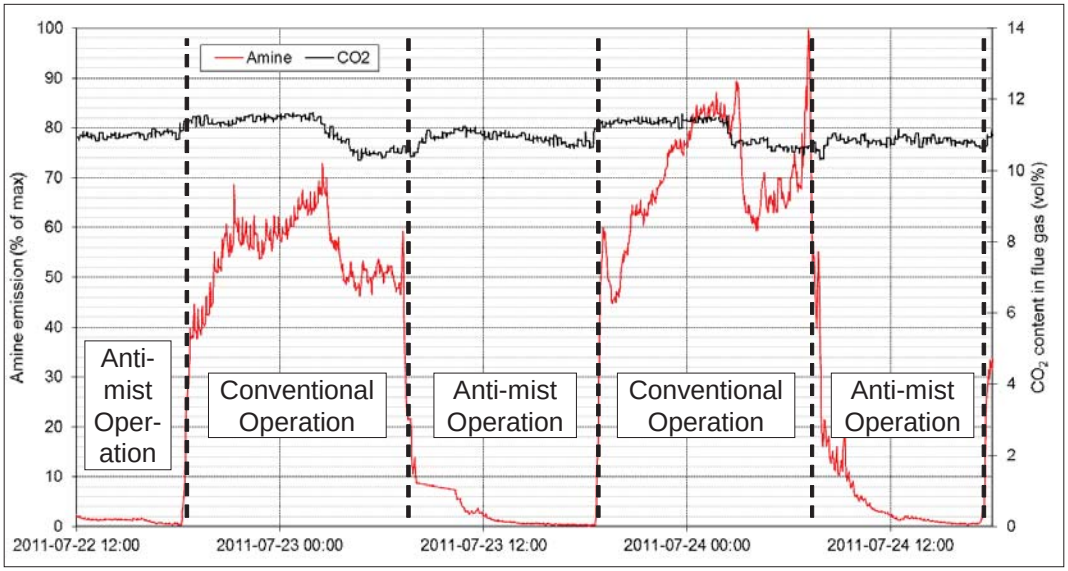

Figure 27. Solvent Emissions with Conventional and Anti-Mist Operation

Due to low concentrations, the FTIR is not able to detect alkyl amines. With the anti-mist system in operation, the solvent amines were also below detection limit of the FTIR. Manual sampling according to the procedure outlined previously were performed. Table 21 and Table 22 show results from the last emission campaign (Emission Test Campaign 3) carried out in November 2011. The emission control system was in service during Tests 4 and 5.

Table 21. Results from Gas Emission Measurement for Aker Test Campaign 3

Test	Amine 1, ppm dry	Amine 2, ppm dry	Nitros-amines, ppm dry	Dimethyl-amine, ppm dry	Methyl-amine, ppm dry	Ethyl-amine, ppm dry	Diethyl-amine, ppm dry
1: Base Case, 113°F Absorber Top	0.06	1.15	0.0028	0.0013	0.002	0.0027	0.0009
2: Base Case, 108°F Absorber Top	0.07	3.10	0.0057	0.0009	0.002	0.0025	0.0009
3: Base case, 122°F Absorber Top	0.11	4.57	0.0050	0.0012	0.004	0.0058	0.0018
4: Acid Wash	0.06	1.60	0.0021	< 0.0007*	< 0.002*	< 0.0002*	< 0.0001*
5: Acid Wash	0.04	1.48	0.0025	< 0.0006*	< 0.001*	< 0.0002*	< 0.0001*

*Samples below detection limits indicated

As explained previously, the manual measurements of ammonia failed due to artifact formation of ammonia in the sulfamic acid solution used as impinger absorbent. Reduction in ammonia emission during pH controlled wash tests was, however, seen on the FTIR readings. Table 22 compares average on-line emissions recorded by the FTIR with values from manually taken samples.

Table 22. Comparison of Gas Emission Measurement and FTIR for Aker Test Campaign 3

Test	Manual Sampling		FTIR		
	Amine 1, ppmv dry	Amine 2, ppmv dry	Amine 1, ppmv wet	Amine 2, ppmv wet	NH_3, ppmv wet
1	0.06	1.15	0.3	0.4	3
2	0.07	3.10	0	1.5	2.5
3	0.11	4.57	0	2.7	4.8
4	0.06	1.60	0	0.9	<1
5	0.04	1.48	0	0.6	<1

From the test results above it can be concluded that the pH controlled wash system was effective at capturing gaseous phase alkaline compounds, i.e. ammonia and alkyl amines. The test results also show the low amine emissions achieved with the anti-mist design; however, additional reduction may be achieved through further optimization.

The emission control (pH controlled wash) system is operated adiabatically to avoid condensation of water from the flue gas. The emission control removes only contaminants which are already at ppm or ppb levels. The circulating liquid will mainly contain ammonium salt, which is highly soluble at the relevant temperatures. A bleed maintains a steady state salt concentration. It is known that slightly acidic conditions favor nitrosamine formation if secondary amines and nitrite are present. Emission control tests performed at the MTU at the PC4 where an acidic solution containing nitrite scavenger was used for pH control showed no formation of nitrosamine in the liquid wash solution.

Some dedicated samples from Test Campaign 3 were analyzed for Nitramine 1 and Nitramine 2. No nitramines were in the solvent, water wash, wash water from emission control, or in impinger solutions used for flue gas emission sampling. The detection limits in lean solvent were 10 µg/L

and 100 µg/L for Nitramine 1 and Nitramine 2, respectively. The detection limits in wash samples and impinger solution were 0.1 µg/L and 1 µg/L for Nitramine 1 and Nitramine 2, respectively. The impinger solution detection limits correspond to gas phase emissions detection limits of 0.04 µg/Nm^3 for Nitramine 1 and 0.4 µg/Nm^3 for Nitramine 2.

2.4.1.4 MEA Campaign

A 30-wt% MEA campaign was performed from November 11 through December 13, 2011. The purpose of these runs was to collect baseline data for the MTU and to facilitate comparison of Aker's improved amine to a reference solvent.

The anti-mist mode of operation was well demonstrated during the MEA campaign. Figure 28 shows the FTIR readings of MEA concentration in the absorber outlet. From the beginning, the absorber was operated in "conventional mode", causing high MEA emissions. Then on November 28, the operation was changed to partial anti-mist mode. The emission of MEA improved, but was still around 20 ppm. The full anti-mist mode was applied on November 29, and the FTIR reading of MEA dropped to less than 1 ppm. The CO_2 capture was maintained at 90 percent throughout the period, and the plant was running with neutral water balance. The MTU remained in stable anti-mist operation until December 6, when conventional operation was resumed, and then the MEA emissions returned to previous levels.

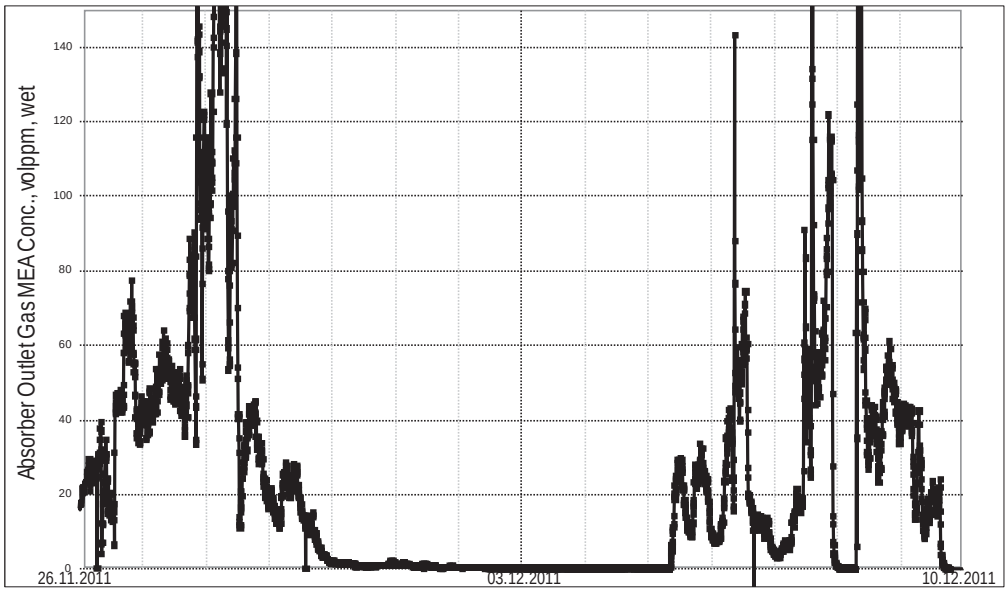

Figure 28. Trends of Emissions during the Aker MEA Campaign

The generating unit was in stable high load operation for the entire period except for a short upset on November 26, causing low CO_2 concentration in the flue gas. The MTU was down for several hours on December 8 before the campaign was stopped on December 10.

No manual emission sampling was performed during the MEA campaign, but the recorded FTIR data strongly indicates that the MEA emission is mist-borne, and that MEA behaves similarly to the Amine 2 compound in CCAmine. There was no pH control of the emission control section during this campaign.

Overall, the tests have indicated that the combination of anti-mist design and pH controlled polishing can virtually eliminate emissions of alkaline constituents from amine based post combustion capture plants. Both the anti-mist system and the emission control system are patent-pending.

2.4.2 Process Performance

2.4.2.1 CO_2 Mass Balance and CO_2 Capture

CO_2 mass balances are calculated based on three methods: a) CO_2 mass flow in CO_2 product stream, b) from CO_2 flow in and out of absorber, and c) from CO_2 lean and rich liquid loadings. Results are plotted in Figure 29. For all calculations of derived parameters based on CO_2 capture (for instance, specific reboiler duty, or SRD) the average is based on CO_2 stream and gas side only. This is due to erratic solvent flow readings on both the rich and lean sides.

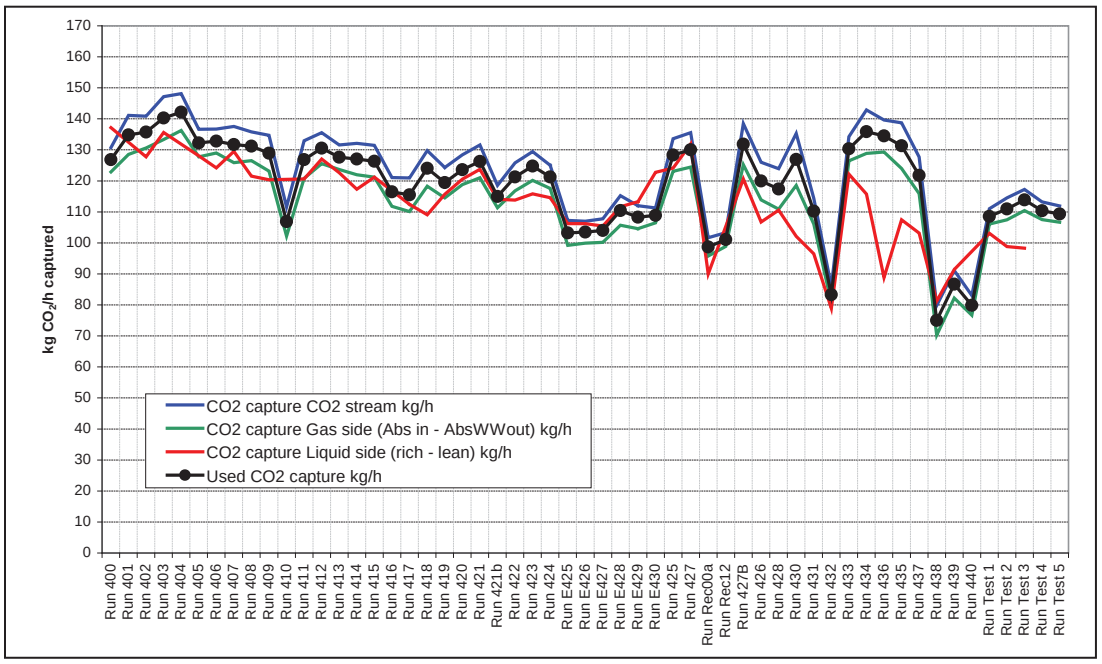

Figure 29. CO_2 Mass Balances for Aker Test Campaigns

2.4.2.2 Regeneration Energy Consumption

SRD is calculated from the reboiler duty and CO_2 mass balances. Representative optimum SRD levels were found by optimization of operating conditions for both CCAmine and MEA. SRD for the CCAmine solvent was shown to be approximately 18 to 20 percent lower than MEA. Values were obtained without the use of Energy Saver, both for MEA and CCAmine. The improved performance of CCAmine compared to MEA is due to differences in solvent characteristics. It was found that CCAmine gives lower stripper overhead temperature, which results in less steam loss to overhead. The working capacity of the solvent is also higher in CCAmine compared to MEA, resulting in less sensible heat loss.

Parameters affecting SRD were tested. Solvent total amine concentration and solvent amines blend ratio were factors found to have large effect. By varying total amine concentration by 30 percent and blend ratio by 30 percent, SRD numbers varied by 20 percent. The effect of rich-lean heat exchanger cold side temperature approach is also large; SRD varied by more than 30 percent when comparing approach temperatures below 10 K and above 25 K, explained by large sensible heat loss at high approach temperatures. The effect of direct contact cooler outlet temperature on SRD was insignificant in the range of 45 to 49°C. Reboiler temperature is important for optimization of SRD.

2.4.2.3 Degradation and Corrosion Intensity

The heat stable salt (HSS) level was analyzed by ion exchange and titration, and results are shown in Figure 30. The data is for the period from June through November 2011. The drop in HSS concentrations after capture of approximately 150,000 kg of CO_2 was due to solvent reclaiming, which removed approximately 80 percent of non-volatile compounds.

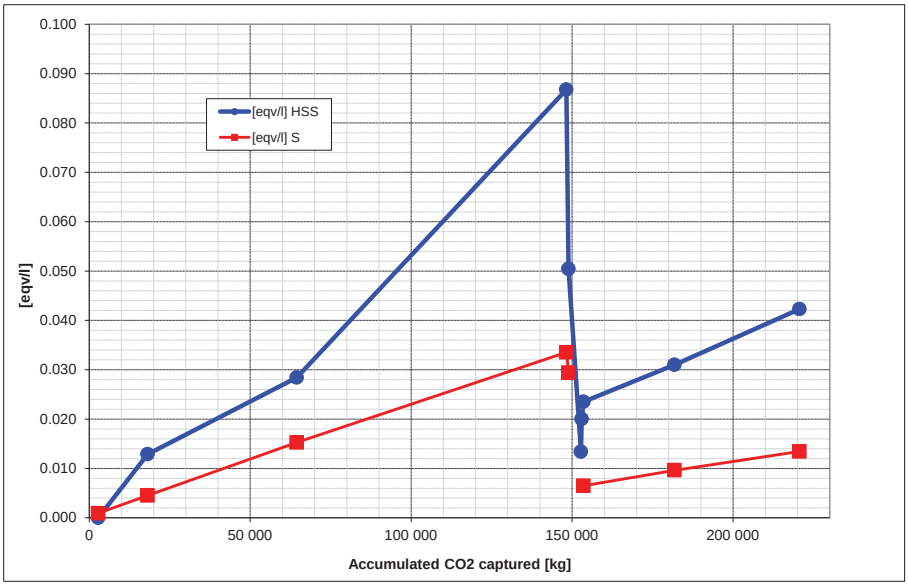

Figure 30. HSS Analysis Data from the Aker CCAmine Campaign

Metals and sulfur concentrations in the liquid solvent were analyzed by inductively coupled mass spectrometry (ICP-MS), and are plotted against the cumulative amount of captured CO_2 in Figure 31. The data covers the period from June through November 2011. The low metal ion concentrations indicated a low corrosion potential of the CCAmine solvent. Amine loss due to degradation was estimated based on inventory control, emission losses, waste logging, and sample extraction.

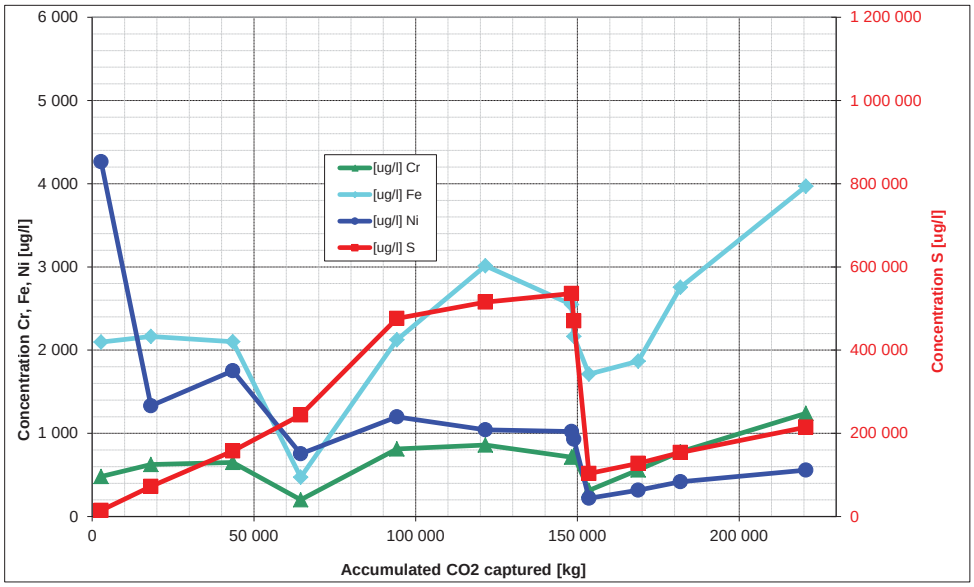

Figure 31. Solvent Analysis Data from the Aker CCAmine Campaign

2.4.2.4 Reclaimer Campaign Overview

A reclaimer campaign was carried out during week 39, from September 26 through October 1, 2011. The actual reclamation took place over 47 hours, with a total of 1,721 kg amine treated at a constant feed rate of 40 kg/hr while injecting sodium hydroxide for neutralization. Conclusions from the reclaimer campaign were:

- Approximately 84 percent of the HSS in the lean amine before beginning reclaimer operation was removed during the solvent feed period of the reclaiming process.
- There was no net loss of free amine during the reclaiming period, as the free amine concentration in the lean solvent was the same before and after reclaiming. Also, single amine levels were practically unchanged after reclaiming.
- The viscosity was decreased in the lean solvent by reclaiming, while the viscosity in the reclaimer liquid increased significantly during the reclaiming process.
- There was no significant increase in total heat duty during reclaiming.
- SRD values before and after reclaiming were equal.

2.4.2.5 Working Capacity

Net CO_2 loading defined as the difference between CO_2 rich and lean solvent loadings given in mol CO_2/L solvent was calculated for the executed runs with CCAmine. Maximum net loading obtained was 2.3 mol CO_2/L solvent, corresponding to a working capacity for the solvent of 10 wt%. The majority of results were, however, in the range of 1.6 to 2.0 mol CO_2/L solvent, corresponding to a working capacity for the solvent between 7 and 9 percent. MEA has a working capacity lower than CCAmine, typically between 5 and 7 wt%.

2.4.2.6 Total Solvent Regeneration Energy

No heat integration was included in the design of Aker's MTU tests at PC4. The only major contribution to heat supply was an electrical heater in the stripper reboiler. Regeneration energy consumption as described previously hence becomes the total solvent regeneration energy.

2.4.2.7 Kinetics

Kinetic characteristics for the solvent were assessed based on obtained CO_2 loading in the CO_2 rich solvent. Maximum CO_2 loading in rich solvent obtained in the MTU CCAmine campaign can be seen from Figure 32, which shows rich flow CO_2 loading versus CO_2 capture for experiments performed at full absorber packing height. It can be seen that CO_2 loading drops when approaching and exceeding 90 percent CO_2 capture.

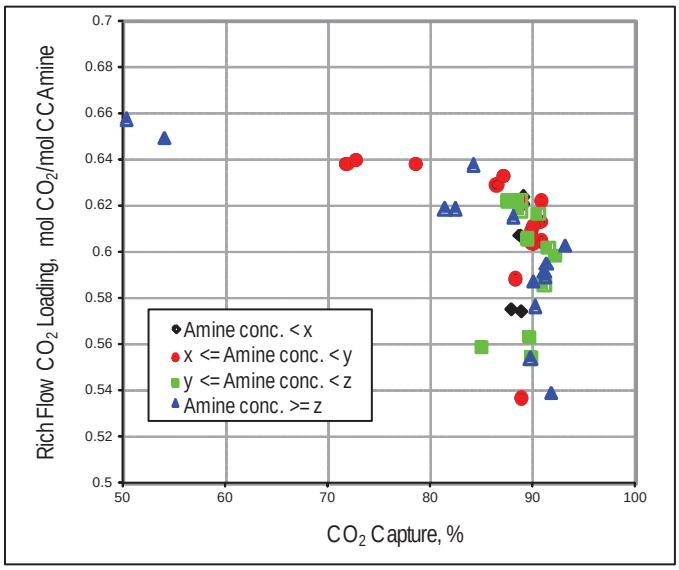

Figure 32. Rich Solvent CO_2 Loading Obtained in Aker CCAmine Campaign

The effect of changing the absorber feed point was investigated, and comparable runs with lower/upper feed points indicate that rich loading decreases by 12 percent when reducing packing height by 39 percent. SRD was not significantly increased.

2.5 Babcock & Wilcox Solvent

B&W completed a three-month test campaign using its proprietary OptiCap solvent at the PSTU from September 15, 2011, through December 7, 2011, for approximately 2,000 hours of operation. Primary test objectives were to:

- Gather data for process simulation model validation
- Characterize effluent streams, including stack emissions and liquid and solid wastes
- Gather data on the oxidative, thermal, and chemical aspects of solvent degradation and reclamation

- Perform corrosion studies to determine appropriate construction materials for a commercial plant

Below are some of the characteristics of the OptiCap solvent gathered from previous studies, which were further quantified as a result of testing at the PC4:

- Resistance to Oxidative Degradation—Preliminary testing of the OptiCap solvent indicated a relatively high level of resistance to degradation in the presence of high concentrations of oxygen, which translates into low solvent make-up rates and solid waste generation rates.
- Resistance to Thermal Degradation—The OptiCap solvent had been shown to be stable at operating temperatures up to 300°F. This attribute offers the potential for regeneration at higher operating temperatures and pressures, which could lead to significant energy savings in terms of CO_2 compression.
- Ease of Reclaiming—Results indicated that thermal reclaiming is likely the primary technology for removing degradation species formed using the OptiCap solvent. Thermal reclaiming is a well-known technology which has been used successfully for decades for solvent regeneration. Other potential technologies for solvent regeneration include systems such as carbon beds and ion exchange systems.
- Lower Volatility—Compared to 30 wt% MEA, the OptiCap solvent showed decreased volatility which results in reduced solvent losses to the stack and decreased energy requirements for cooling in the solvent wash section of the absorber.
- Increased Mass Transfer Rate—The rate of absorption of CO_2 for the OptiCap solvent is approximately twice that of 30 wt% MEA. This characteristic offers capital cost savings with reduced absorber tower height, quantity of packing, etc., as well as reduced power consumption, due to decreased pressure drop through the absorber and decreased pump power required for solvent recirculation.
- Increased CO_2 Carrying Capacity—Because the OptiCap solvent can be loaded with approximately twice the amount of CO_2 per unit of solvent, the solvent recirculation rate is decreased, saving not only the energy required to pump the solvent within the system, but also the energy required to heat and cool the solvent in the various process stages.

Testing under actual power plant flue gas conditions at the NCCC was required to confirm the research performed in both the B&W lab and pilot plant regarding the above characteristics of the OptiCap solvent. In addition, phenomena such as solvent degradation, system corrosion, and waste stream formation must be studied across time periods which exceed the duration of most lab- or bench-scale test campaigns.

2.5.1 Modifications to the PSTU

Collaboration between B&W and NCCC personnel resulted in modifications made to the PSTU both to address items arising from the risk assessment as well as items which were requested to increase the amount and quality of data which could be obtained from the pilot test campaign. These modifications are summarized below.

Piping with manual drain valves were added upstream of the pumps following the absorber, regenerator, and flash tank sumps, which terminated at a solvent storage tank. This allowed for the sumps of these vessels to drain to a single location via gravity, as the vessel sumps were elevated, and the solvent tank was located at grade. Other modifications included:

- Additions of a portable hot water heater and water nozzle connections at each pump, allowing for the injection of hot water directly to any area where precipitation might occur.
- Addition of drains to the cross-flow heat exchanger for emergency situations
- Installation of a Dewar vessel with an induction nozzle to promote mixing, for adding CO_2 when required to increase the bulk solvent loading
- Addition of some instrumentation and nozzles to facilitate data acquisition and allow installation of electrical resistance probes and weight loss coupons

2.5.2 OptiCap Solvent Testing

During the test campaign, a total of approximately 115 test conditions were run. Information regarding the variation of certain operating parameters is listed in Table 23. Throughout the campaign, mass balances were closed to within 5 percent or less (often much lower), and a significant quantity of data was gathered to compare with B&W's process simulation models.

Table 23. Range of Operating Parameters for OptiCap Solvent Test Campaign

Parameter	Range
Solvent Recirculation Rate, lb/hr	Varying
Lean Solvent Temperature, °F	Varying
Wash Temperature, °F	As required
CO_2 Removal Efficiency, %	80 to 95
Flue Gas Flow Rate, lb/hr	3,500 to 5,000
Flue Gas Temperature, °F	104 to 130
Intercooler Usage	On/Off
Intercooler Temperature, °F	Varying
Regenerator Pressure, psig	Varying
Reflux Route	Regenerator/Absorber
Reboiler Steam Flow Rate, lb/hr	As required
Thermal Reclaimer Usage	On/Off

In addition to the operating data gathered for process model validation and verification, the test campaign also yielded a great deal of data in other areas of interest, such as corrosion, solvent degradation, and effluent stream characterization. In addition to automatic samples which were continuously withdrawn from the system for purposes of auto-titration to check solvent concentration and CO_2 loading, manual samples were withdrawn at regular intervals both to serve as a check to the automatic samples as well as to further characterize the chemical composition of various process streams.

In addition to the quantitative data, a significant amount of non-quantitative information was generated during the campaign. During the three-month test period, B&W engineers experienced and successfully managed several upsets typical of those associated with operating a coal-fired power plant. Experiencing these upsets, the operator reactions, and the solvent response will be instrumental in designing a commercial system.

Throughout the range of scenarios which occurred, no major interruptions in testing were encountered. Partially by design and partially due to unplanned events, B&W was afforded the opportunity to explore the solubility window of the OptiCap solvent, on both the rich and lean sides of the operating curves. The target CO_2 removal (which was typically 90 percent), was routinely achieved with relative ease. Finally, no solvent precipitation occurred in any of the solvent circulation piping in the PSTU during the campaign.

2.5.3 Results

2.5.3.1 Regeneration Energy

During baseline MEA testing at NCCC, the lowest measured value for 30 wt% aqueous MEA was 1,507 BTU/lb CO_2, which was achieved at 86 percent CO_2 removal. During the same testing, the lowest measured value for 40 wt% aqueous MEA was 1,245 BTU/lb CO_2, which was achieved at 82 percent CO_2 removal. The lowest value achieved at 90 percent CO_2 removal (which was the typical value during OptiCap testing) was 1,300 BTU/lb CO_2, which is generally consistent with published values.

During the OptiCap test campaign, regeneration energy values in the range of 1,100 to 1,125 BTU/lb CO_2 were achieved on multiple occasions, at a CO_2 removal efficiency of 90 percent. These results are consistent with lab- and pilot-scale measurements, as well as B&W process simulations, which indicate that further energy savings are possible when using a cross-flow heat exchanger optimized for the OptiCap solvent (which was not the case with the equipment in the PSTU). Table 24 summarizes these results.

Table 24. Comparison of Performance of OptiCap and MEA Solvents

Solvent	CO_2 Removal, %	Energy Consumption, BTU/lb CO_2
30 wt% MEA	86	1,507
40 wt% MEA	90	1,300
OptiCap	90	1,110

2.5.3.2 Corrosion Studies

As described previously, B&W requested that additional nozzles be installed in various vessels and piping throughout the PSTU before the start of the OptiCap test campaign so that critical corrosion data could be gathered. Nineteen nozzles were installed at 12 different locations. Retractable weight-loss coupon holders were placed at each location, with two C1010 carbon steel and two 316L stainless steel coupons attached to each holder. Electrical resistance probes, six constructed of C1010 carbon steel and one was constructed of 316L stainless steel, were

installed at seven of these locations. Additionally, solvent samples taken weekly were analyzed for corrosion species.

Weight loss analysis gave 96 percent reproducibility in the corrosion studies at the PC4. One coupon was considered an outlier (CS-7.2) and one coupon was considered not reproducible (SS-9.2) based on non-replication of results with their respective adjacent specimens.

The highest measured corrosion rate of carbon steel, 17 mils per year (mpy), was observed in the regenerator where the highest process temperatures existed. Outside of the regenerator, the measured carbon steel corrosion rates were below 10 mpy. However, some instances of mild CO_2 pitting were observed. A detailed analysis of the stainless steel coupons indicated that the highest stainless steel corrosion rate was 5 mpy, also occurring in the regenerator.

Electrochemical Corrosion Test

Electrochemical corrosion testing was performed on solvent samples extracted weekly to explore the corrosive behavior of the OptiCap solution under different process conditions to aid in future material selection. Variables studied included: process temperatures (similar to regenerator and absorber conditions), fresh OptiCap solutions (after preparation) as well as degraded solutions (subjected to both rich and lean CO_2 loading conditions), and dissolved metals concentration.

Analyses consisted of electrochemical corrosion screening tests using carbon steel (C1010) to evaluate the possibility of utilizing this material in areas of the CO_2 capture plant. In addition, evaluating OptiCap solutions at different time intervals provided an understanding of how degradation and dissolved metal concentrations impacted the corrosivity of the material. The analyses conducted included open circuit potential, potentiostatic scans, and linear polarization resistance. The linear polarization resistance technique provided corrosion rates, allowing the evaluation of different process environments, which were characterized by solvent solution samples taken weekly for comparison.

Overall, both the degraded and non-degraded OptiCap solvent solutions provided more corrosion resistance to carbon steel than 30 wt% MEA, which resulted in a five times higher corrosion rate using the same test method and materials.

2.5.3.3 Solvent Degradation and Carryover

During operation, CO_2 capture solvents are degraded by three mechanisms resulting in degradation products accumulating in the solvent, reducing solvent efficacy and possibly fouling heat transfer surfaces causing process inefficiencies.

- Oxidative degradation occurs in the absorber when the solvent is exposed to oxygen introduced with the inlet flue gas. Work at UT-Austin shows that if oxygen dissolved or entrained in the solvent passes to the cross heat exchanger, the oxygen in combination with the elevated temperatures accelerates the degradation reactions.
- Thermal degradation occurs when the solvent is exposed to elevated temperatures such as in the regenerator, the reboiler, the rich-solvent piping from the cross-flow exchanger to regenerator, and the lean-solvent piping from the regenerator to the cross-flow exchanger.

- Degradation by contaminants occurs when the solvent is exposed to flue gas contaminants such as SO_2, NO_2, and coal ash constituents.

Some degradation products are released in the vapor phase or as droplets, the majority of which are removed in the wash tower circulating water but some are potentially released to atmosphere in the CO_2-depleted flue gas stream. The degradation of OptiCap solvent has been studied in the laboratory, but the NCCC test campaign was the first opportunity to characterize the performance of the solvent on coal-fired flue gas and to determine how its chemical composition changed throughout the test. A variety of reaction products are formed, requiring different analytical techniques for detection in the liquid solvent.

- Formates and acetates are detected using anion-exchange (A-E) chromatography.
- Amines and amides are detected using cation-exchange (C-E) chromatography.
- Nitrosamines are detected using high-performance liquid (HPL) chromatography.

Liquid samples were taken on a weekly basis, and before and after each test condition. The samples were refrigerated to minimize any further chemical reactions prior to sample analysis. Rich solvent samples from the first seven weeks of testing and the baseline solvent are shown in Figure 33. The change in solvent color from a pale yellow to a dark brown is an indication of the formation and accumulation of degradation products. In addition to liquid samples, the gas sampling train (see Figure 11) was used to sample the gas stream leaving the wash tower. Three test runs were completed at intervals throughout the campaign.

Figure 33. Solvent Color Changes during the OptiCap Solvent Testing

Discussion of Results

Figure 34 presents solvent composition data collected by A-E chromatography. The spectra for the four samples show that the species detected increased as the test campaign progressed. Two of the peaks identified are for formate and acetate. Figure 35 presents a log-linear plot for formate formation. The data for the acetate followed a similar trend.

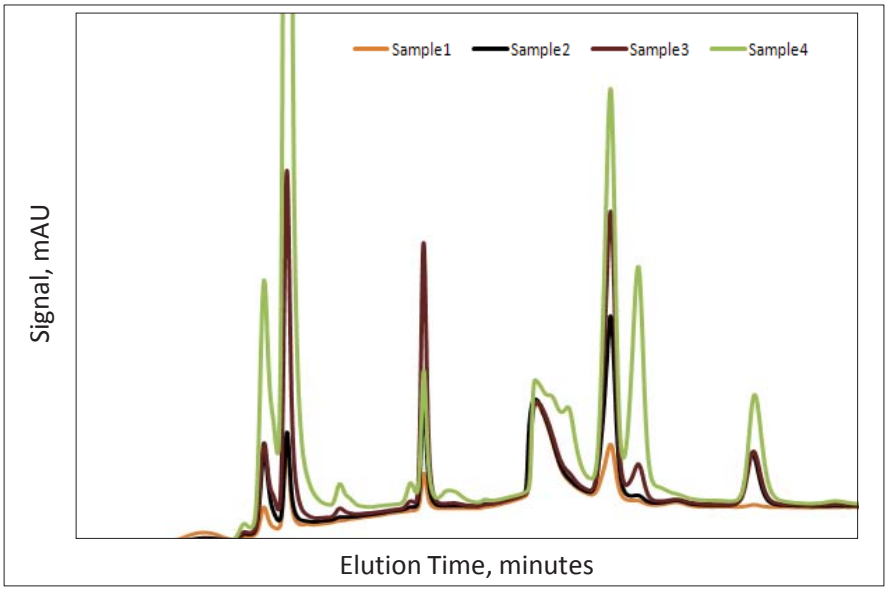

Figure 34. A-E Chromatography Spectra for Four Samples

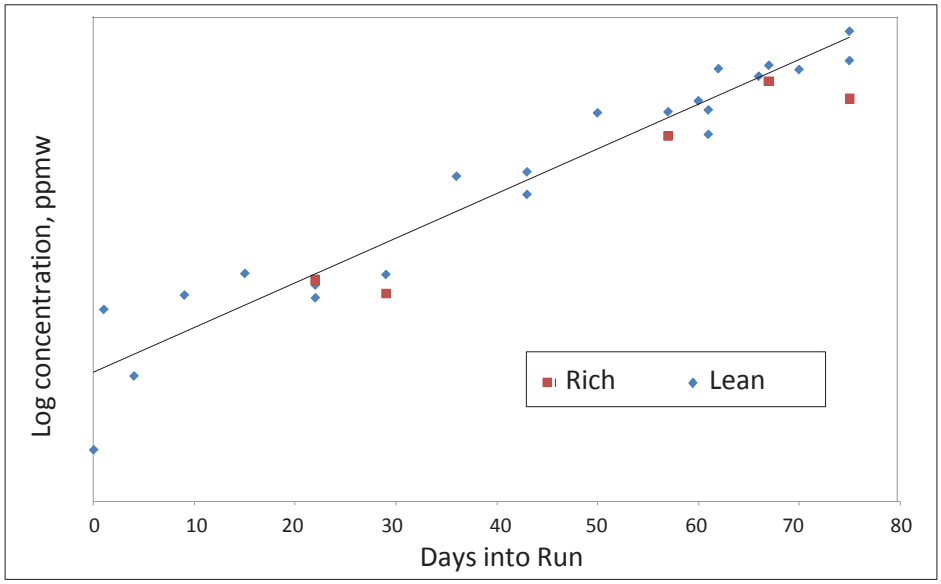

Figure 35. Rate of Formate Production from A-E Chromatography Spectra Data

The degradation product with the highest concentration detected by C-E chromatography was n-formyl-OptiCap, which followed a log-linear trend similar to that for formate as shown in Figure 35. Aminoethyl-OptiCap and hydroxyethyl-OptiCap were also formed and achieved a steady value approximately half way through the run, indicating that they were intermediate species created in the formation of other degradation products.

HPL chromatograph spectra detected several nitrosamines in the solvent but only one was clearly identified, mononitroso-OptiCap (MNOC). Like the species detected by A-E and C-E chromatography, the nitrosamine concentration increased with time with the exception of MNOC. The MNOC concentration reached a peak value after one week of operation, after

which it declined to an equilibrium value. It is hypothesized that the MNOC peak was formed because of high flue gas NO_2 at the beginning of the run and decayed progressively because of exposure to high temperatures in the regenerator. As MNOC was the only compound affected, it must be more sensitive to these two parameters than the other nitrosamines formed.

Nitrosamine data was also collected with the NCCC gas sampling train, but analytical techniques were not available to detect MNOC. Nitrosamine was detected in only one sample, as n-nitrosodimethylamine (MDMA) in the condensate of the sample taken near the end of the campaign. No MDMA was detected in the vapor phase for any of the tests. The results for the tests in which MDMA was detected are provided in Table 25.

Table 25. Nitrosamine Measurements using NCCC Gas Sampling Train

Analyte	Condensate, ppbv	Adsorbent Tube, ppbv
n-Nitrosodimethylamine	0.0116	<0.0254
n-Nitrosomethylethylamine	<0.0019	<0.0213
n-Nitrosodiethylamine	<0.0017	<0.0184
n-Nitrosodi-n-Propylamine	<0.0013	<0.0144
n-Nitrosodi-n-Butylamine	<0.0011	<0.0119
n-Nitrosopiperadine	<0.0015	<0.165
n-Nitrosopyrrolidine	<0.0017	<0.0188
n-Nitrosomorpholine	<0.0015	<0.0162
n-Nitrosodiethanolamine	<0.0013	<0.244

Emissions from the wash tower were lower for OptiCap than for MEA. Nevertheless, OptiCap solvent emissions were higher than predicted by modeling and laboratory work, and aerosols are considered to be a contributing factor to this increase. Two observations were made.

- OptiCap emissions decreased with Gaston Unit 5 operating load. Based on B&W boiler experience, as load decreases, aerosol concentration in the flue gas decreases. As the PSTU inlet flue gas flow was constant during the testing, fewer aerosols would have entered the absorber at lower boiler loads, resulting in the lower solvent emissions.
- OptiCap solvent emissions increased with lower wash tower flue gas exit temperatures, which is indicative of increased fogging, resulting in increased droplet carryover.

2.6 Hitachi H3-1 Solvent

Hitachi's H3-1 solvent test campaign at the NCCC was conducted from April 24 through July 16, 2012, including over 1,300 operating hours. Table 26 presents the range of operating conditions covered during testing.

Table 26. Operating Parameters for Hitachi Solvent Testing

Operating Parameter	Range
Absorber Flue Gas Flow Rate (G), lb/hr	4,000 to 6,000
Solvent Flow Rate (L), lb/hr	7,000 to 17,000
Reboiler Steam Flow Rate (S), lb/hr	700 to 1,100
Absorber Inlet Flue Gas Temperature, °F	96 to 122
Absorber Inlet Solvent Temperature, °F	96 to 114
Wash Tower Exit Temperature, °F	107 to 123
Regenerator Pressure, psig	3 to 22
Inlet Flue Gas CO_2 Content, vol%	11 to 13
Number of Absorber Beds	1, 2, and 3
Intercoolers	On and Off

2.6.1 CO_2 Capture Performance

Figure 36 shows the CO_2 capture performance of the H3-1 solvent during the test campaign, averaging around 90 percent over a range of boiler loads, flue gas compositions, and test conditions. The low values of CO_2 removal marked by 'A' in the figure were completed to extend the range of data collected and include tests at very low solvent flow rates and with only one absorber bed in service.

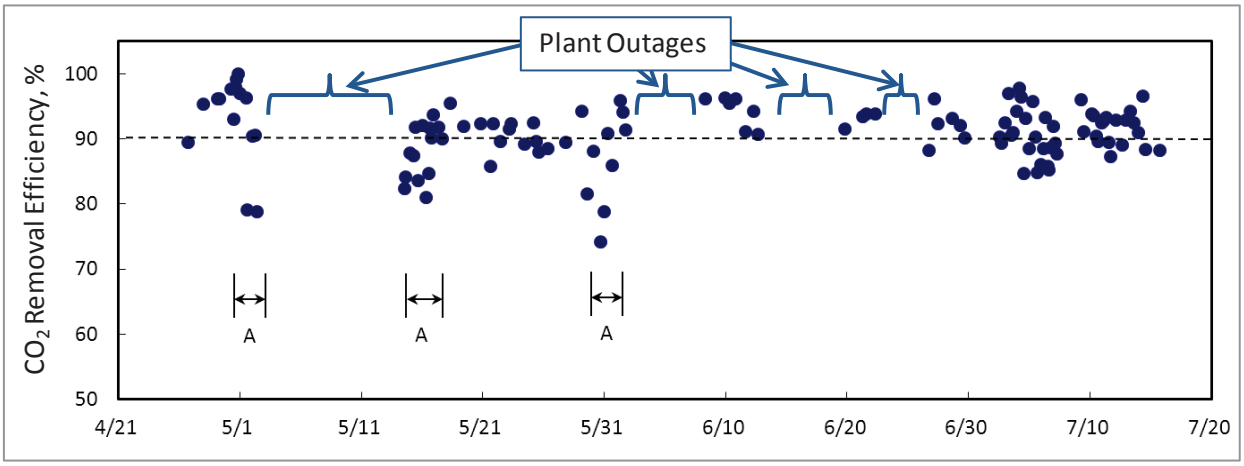

Figure 36. Overall CO_2 Capture Performance of Hitachi H3-1 Solvent

2.6.2 Parametric Test Results

2.6.2.1 Absorber Pressure Drop

During the first week of testing, baseline tests were conducted to verify the range of operability. The inlet flue gas flow to the absorber was varied between 4,000 and 6,000 lb/hr for different solvent circulation rates, and the pressure drop in the absorber was measured. The maximum superficial velocity of flue gas tested was 6 ft/sec. Figure 37 shows the effect of absorber

pressure drop at different superficial velocities. Pressure drop did not increase rapidly with increasing gas flow rate, and within this test range, flooding in the absorber was not observed.

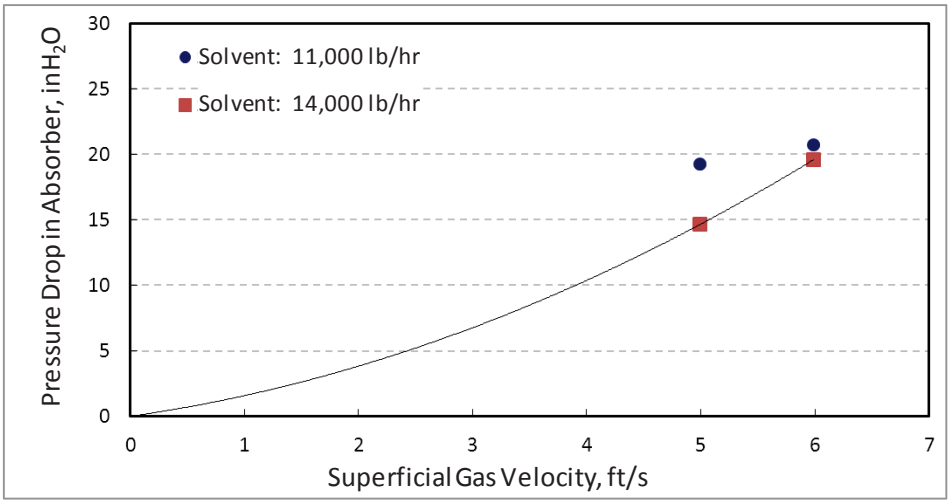

Figure 37. Effect of Absorber Pressure Drop on Changing Gas Flow Rate for H3-1 Solvent

2.6.2.2 Solvent Circulation Rate and Regeneration Energy

CO_2 removal efficiency for a particular solvent circulation rate varies with the absorber inlet CO_2 concentration, which depends on the plant boiler load. During the test campaign, the inlet CO_2 concentration was typically below 12 vol% at 700 MW, the lowest load level, above 12 vol% at 900 MW, full boiler load. Figure 38 shows the effect of solvent flow rate on CO_2 capture performance at low load conditions. As the solvent circulation rate increased to 7,000 lb/hr, the CO_2 removal efficiency increased to a maximum value of about 96 percent. As solvent flow rate increased further, CO_2 capture efficiency began to decrease.

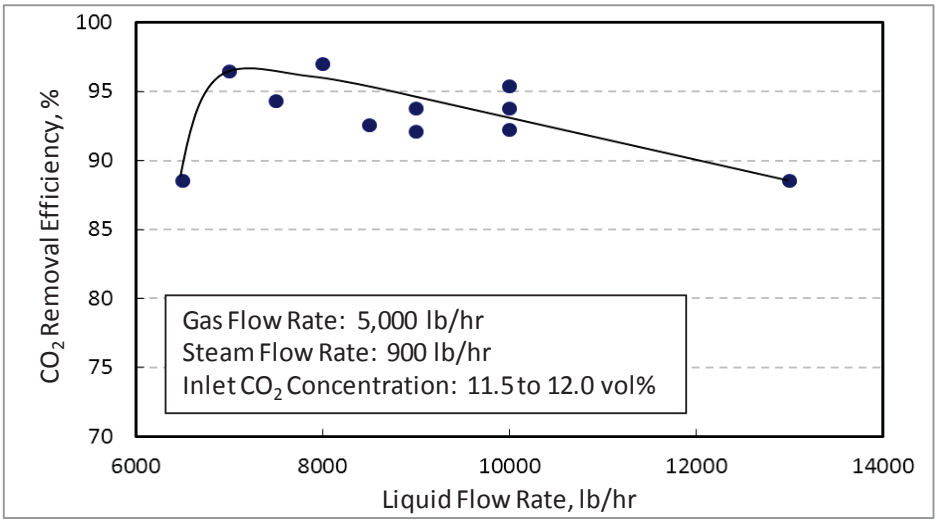

Figure 38. Liquid Flow Rate vs. CO_2 Removal for H3-1 Solvent at Low Load Conditions

This observation is explained by the trends in CO_2 loading for the rich and lean solvent shown in Figure 39. At lower solvent flows, the difference in CO_2 loading between the rich and lean

solvent was large, enabling high CO_2 removal efficiencies. As the solvent flow rate increased, the lean loading also increased because the heat provided (reboiler steam flow held constant) was insufficient to release all the CO_2 from the rich solvent. The net CO_2 loading (rich minus lean loading) at high solvent flow rates decreased significantly, thereby reducing CO_2 removal efficiency.

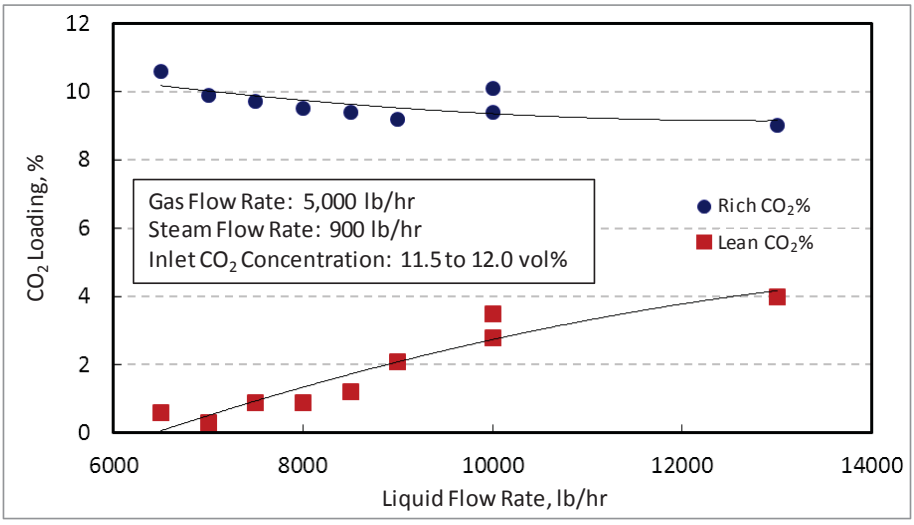

Figure 39. Liquid Flow Rate vs. CO_2 Loading for H3-1 Solvent at Low Load Conditions

As reboiler steam flow was constant and the amount of CO_2 captured decreased at solvent flow rates greater than the optimal value of 7,000 lb/hr, the regeneration energy increased correspondingly, as shown in Figure 40. For a solvent flow rate of about 7,000 lb/hr where the CO_2 capture was its maximum, the regeneration energy was at its minimum value of approximately 2.4 GJ/ton of CO_2 or 1,030 Btu/lb of CO_2.

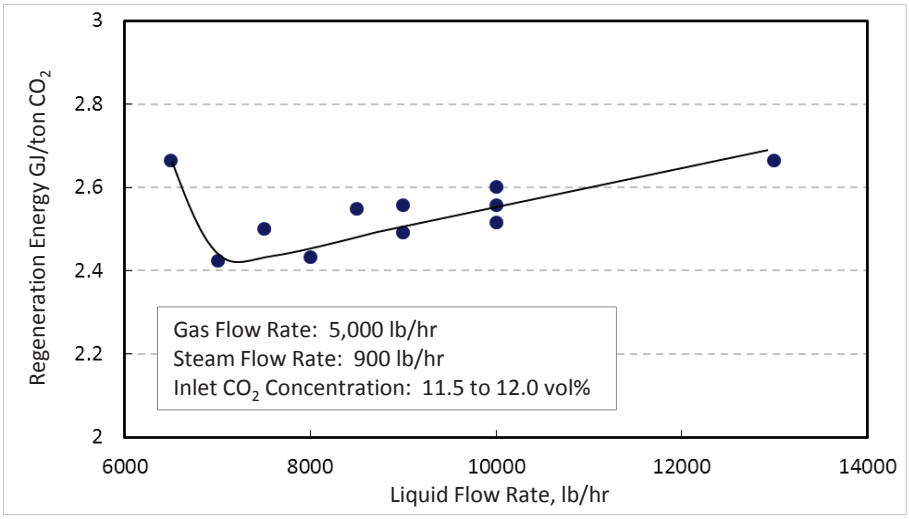

Figure 40. Liquid Flow Rate vs. Regeneration Energy for H3-1 Solvent at Low Load Conditions

Figure 41 shows the effect of solvent flow rate on CO_2 capture performance at full-load conditions. Showing a similar trend to the partial load case, the amount of CO_2 captured

increased with solvent flow rate up to an optimal value of about 10,000 lb/hr, beyond which capture efficiency decreased. The trends for the rich and lean loadings for the full-load case are shown in Figure 42.

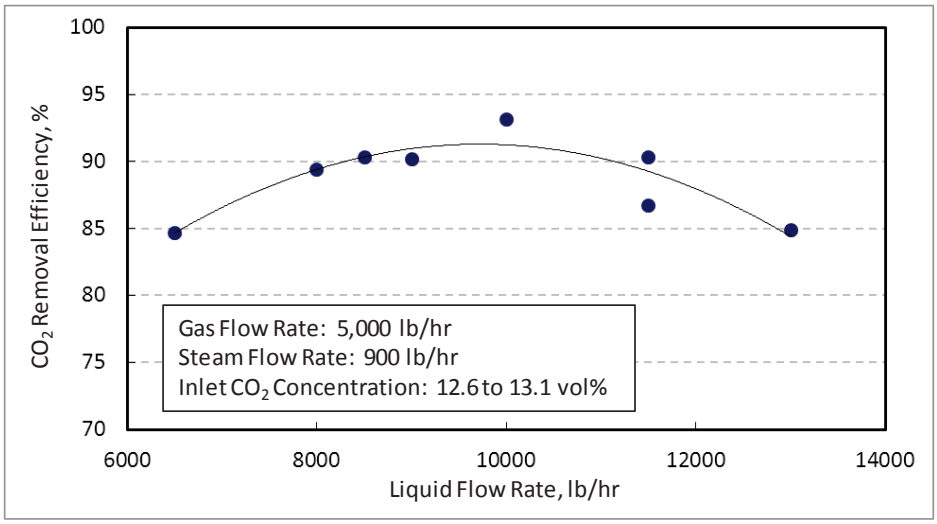

Figure 41. Liquid Flow Rate vs. CO_2 Removal for H3-1 Solvent at Full Load Conditions

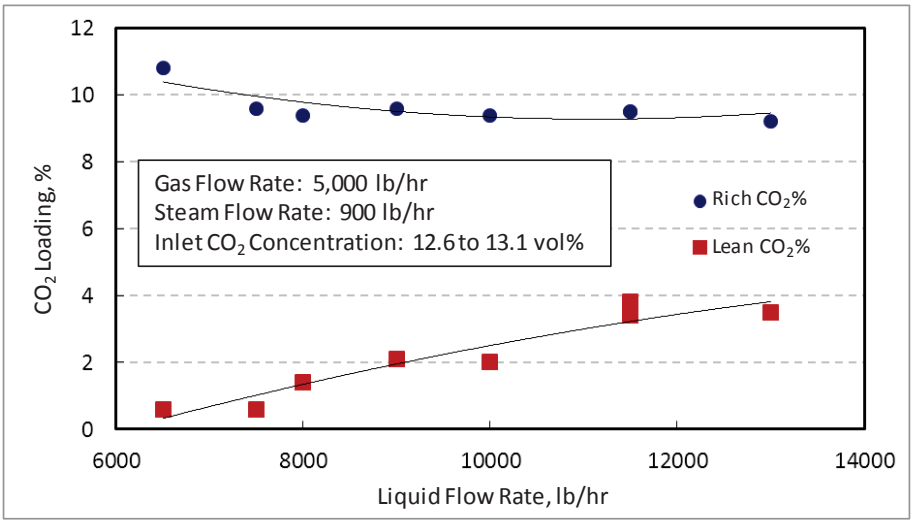

Figure 42. Liquid Flow Rate vs. CO_2 Loading for H3-1 at Full Load Conditions

As demonstrated in Figure 43, at a solvent flow rate of 10,000 lb/hr, the regeneration energy reached a minimum value of approximately 2.4 GJ/ton of CO_2 or 1,030 Btu/lb of CO_2, similar to that observed at partial load conditions.

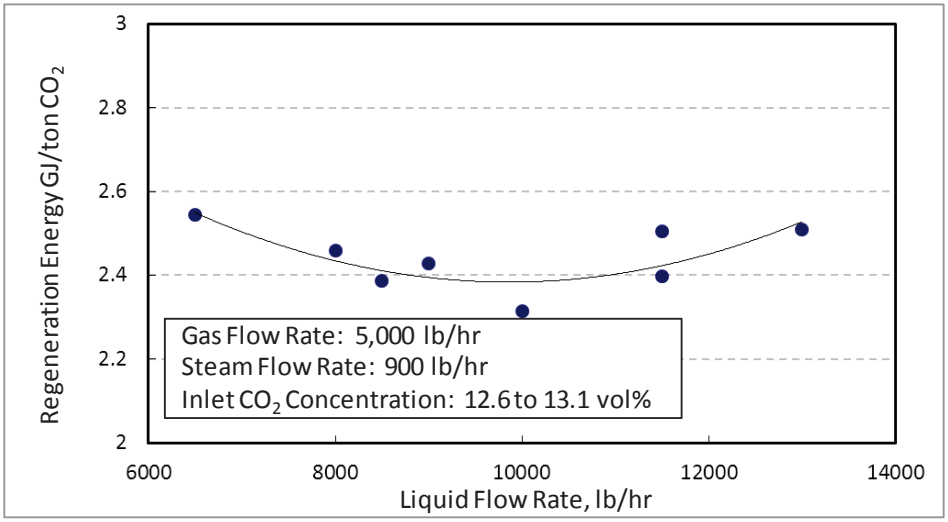

Figure 43. Liquid Flow Rate vs. Regeneration Energy for H3-1 Solvent at Full Load Conditions

2.6.2.3 CO_2 Mass Balance

The CO_2 mass balance was checked by comparing CO_2 removed from the flue gas with CO_2 produced at the regenerator. CO_2 released from the regenerator was measured at the outlet of the mist separator. Figure 44 shows that over the duration of testing, the CO_2 concentration in the gas phase between the absorber and regenerator correlate reasonably well. Due to the relative lack of consistency of CO_2 concentration in the liquid side and the reliable measurements in the gas-phase, regeneration energy for the H3-1 testing was determined using the gas-phase CO_2 concentrations.

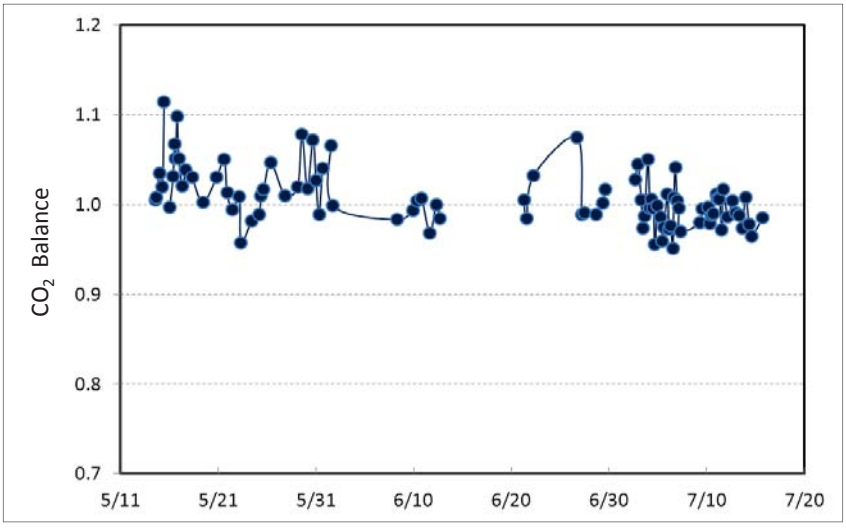

Figure 44. CO_2 Balance on the Gas-side for H-3 Solvent Testing

2.6.2.4 Reboiler Steam Flow Rate

Figure 45 gives results from testing the influence of steam flow rate on CO_2 removal efficiency. The inlet flue gas flow and solvent circulation rates were kept constant at 5,000 lb/hr and

10,000 lb/hr, respectively. Generally, the CO_2 removal efficiency increased with the reboiler steam flow rate. At the partial load condition when the inlet CO_2 concentration was low, the CO_2 removal efficiency was higher than that of the full load condition.

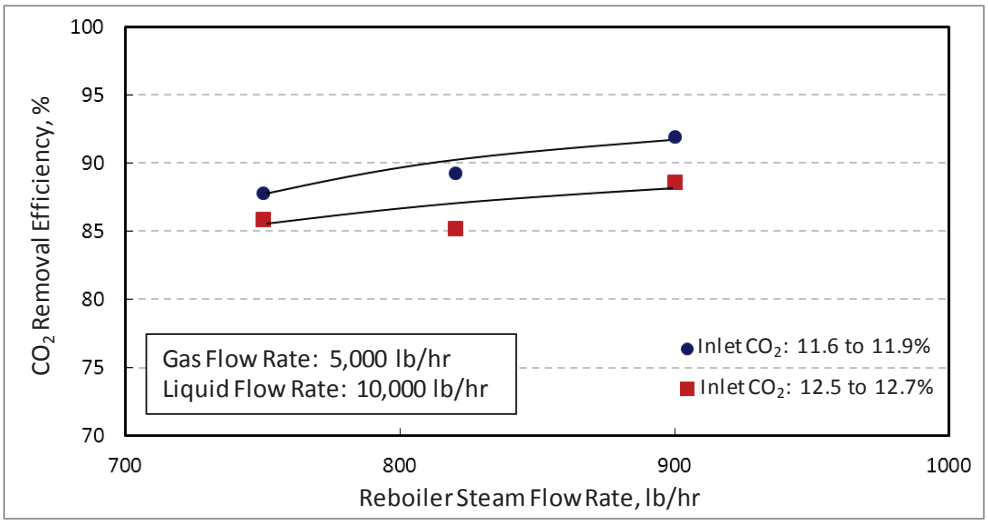

Figure 45. Reboiler Steam Flow Rate vs. CO_2 Removal Efficiency for H3-1 Solvent

Figure 46 plots the rich and lean loading of the solvent for the tests shown in Figure 45. CO_2 loading in the rich solvent was not affected by reboiler steam flow rate, but the lean solvent loading decreased slightly with increasing steam flow rate. Leaner solvent in the absorber and correspondingly, higher net working capacity, resulted in higher CO_2 removal efficiency at a steam flow rate of 900 lb/hr.

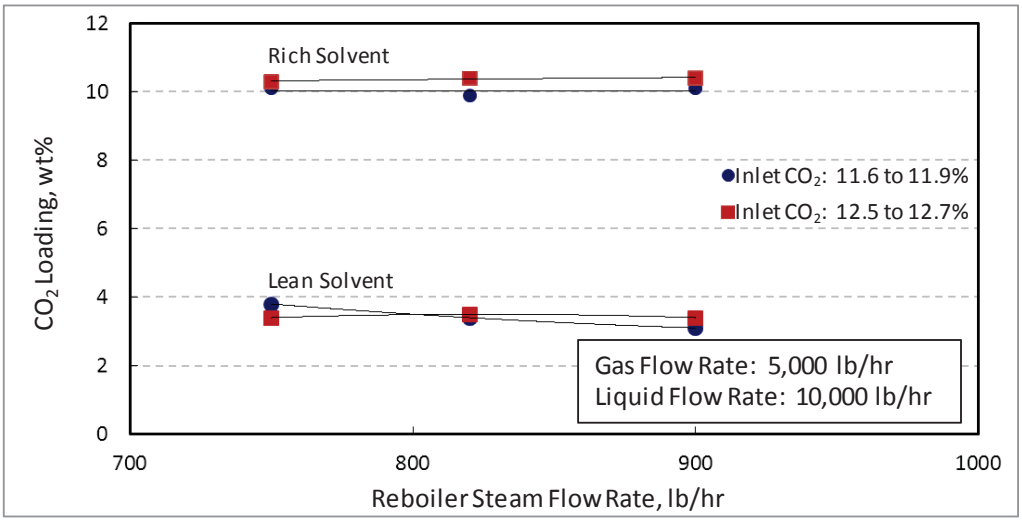

Figure 46. Reboiler Steam Flow Rate vs. CO_2 Loading for H3-1 Solvent

2.6.2.5 Temperature of Flue Gas and Solvent at Absorber Inlet

The effect of temperature of the lean solvent and flue gas at the absorber inlet were verified during the parametric tests. Inlet solvent temperature was controlled using the lean solvent

cooler located upstream of the lean solvent storage tank. From the lean solvent storage tank, solvent is fed to the absorber. A wide range of temperatures was tested, but the lower end of the range was limited by the cooling water temperature, which could not be reduced below 96°F (even during night) due to warm ambient conditions.

Figure 47 shows the CO_2 removal efficiencies for the tests performed by changing the absorber inlet temperature of the solvent, at both partial load and full load conditions. Inlet flue gas temperature was maintained by controlling the cooling water flow to the cooler/condenser located upstream of the absorber. As shown in Figure 48, CO_2 removal efficiency decreased slightly with increasing temperature at the temperatures below 104°F. As the temperature of the inlet gas increased beyond this value, there was no appreciable effect on the CO_2 removal efficiency. The impact of temperatures of both solvent and flue gas at the absorber inlet on CO_2 capture was small for the ranges tested.

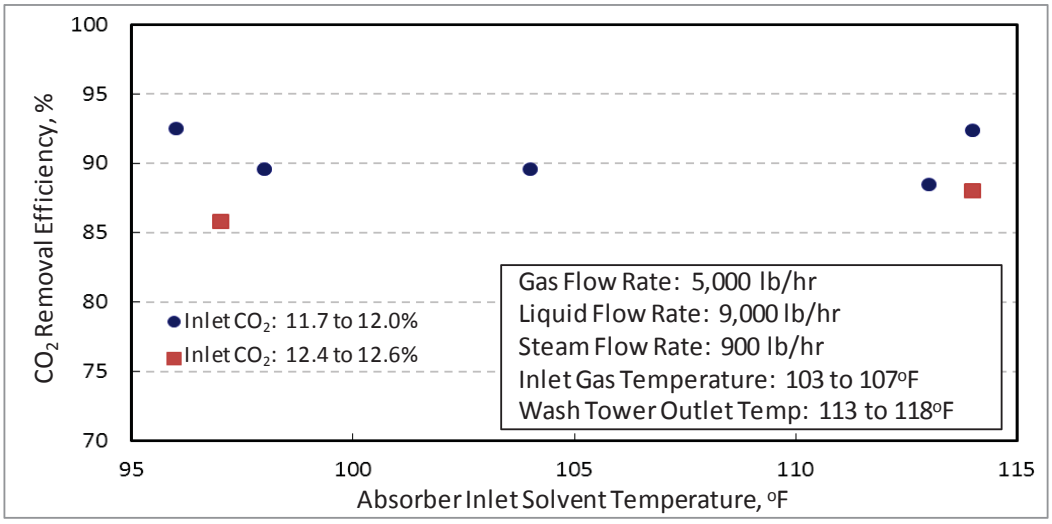

Figure 47. Effect of Solvent Temperature at the Absorber Inlet on CO_2 Removal Efficiency

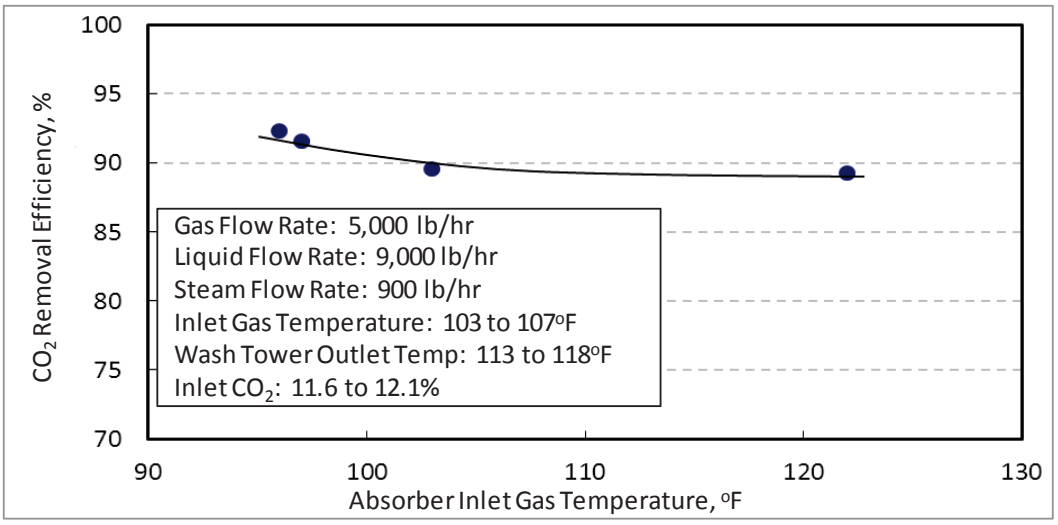

Figure 48. Effect of Flue Gas Temperature at the Absorber Inlet on CO_2 Removal Efficiency

2.6.2.6 Number of Absorber Beds

The PSTU absorber contains three stages of packed beds with structured packing. The effect of the number of absorber beds was investigated during the H3-1 testing, and the results are given in Figure 49. During one-bed operation, the bottom bed was in service, and during two-bed operation, the bottom two beds were in service. As expected, with an increasing number of packed beds, greater CO_2 removal efficiency was achieved. At the operating test conditions with only two packing stages in service, close to 90 percent of the CO_2 was captured. With all three packing stages in operation, CO_2 removal efficiency increased further but with a smaller increment.

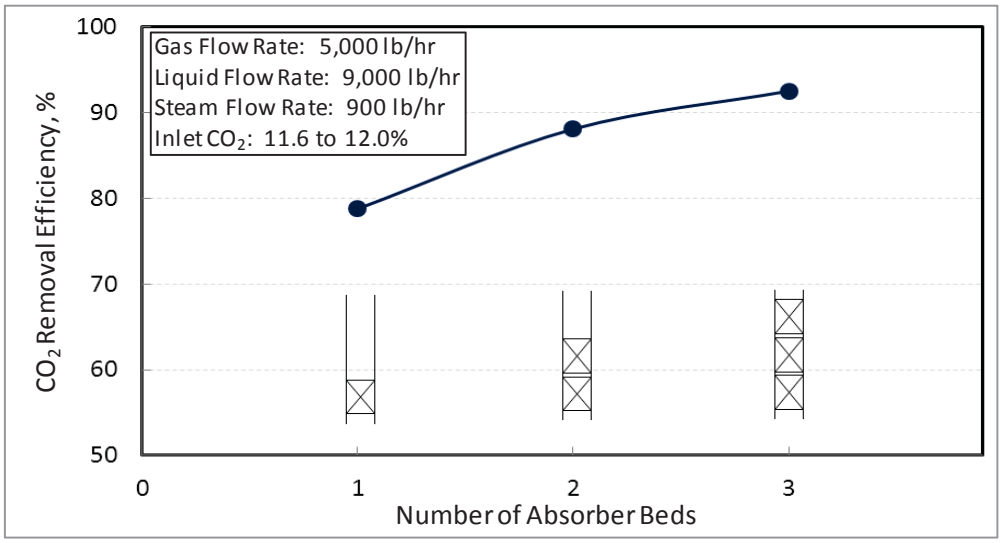

Figure 49. Effect of Number of Absorber Beds on CO_2 Removal Efficiency

2.6.2.7 Intercoolers

CO_2 absorption in amine is an exothermic reaction, resulting in increased temperature along the flue gas path. Therefore, the influence of solvent cooling in the absorber on the CO_2 capture efficiency was examined by operating with the intercoolers. The absorber includes two intercoolers located between the three packed beds. Both intercoolers were used when the intercooler was in service, and the entire solvent flow was routed through each intercooler before being re-distributed over the next packed bed in the absorber. Figure 50 shows the results of the tests with and without the intercoolers in service. For these tests, flue gas flow rate was 5,000 lb/hr, solvent circulation rate was 9,000 lb/hr, and the reboiler steam flow rate was 900 lb/hr. Without the use of intercoolers, about 90 percent CO_2 removal was achieved. With the intercoolers in service, a 6 percent improvement in the CO_2 removal efficiency was achieved at the same test conditions. This is because at low temperatures, the CO_2 carrying capacity of the solvent is greater than at higher temperatures.

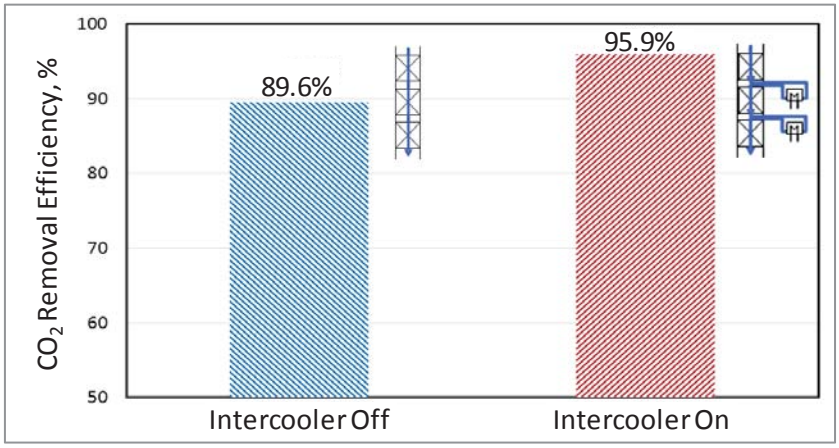

Figure 50. Effect of Intercoolers on CO_2 Removal Efficiency

Figure 51 provides the temperature profiles along the height of the absorber for the two tests with and without intercoolers. With the intercooler in service, the absorber internal temperature was lower by 10 to 20°F within the packing stages. By lowering the temperature within the absorber, the amount of CO_2 absorbed can be increased without changing the solvent circulation rate or reboiler duty.

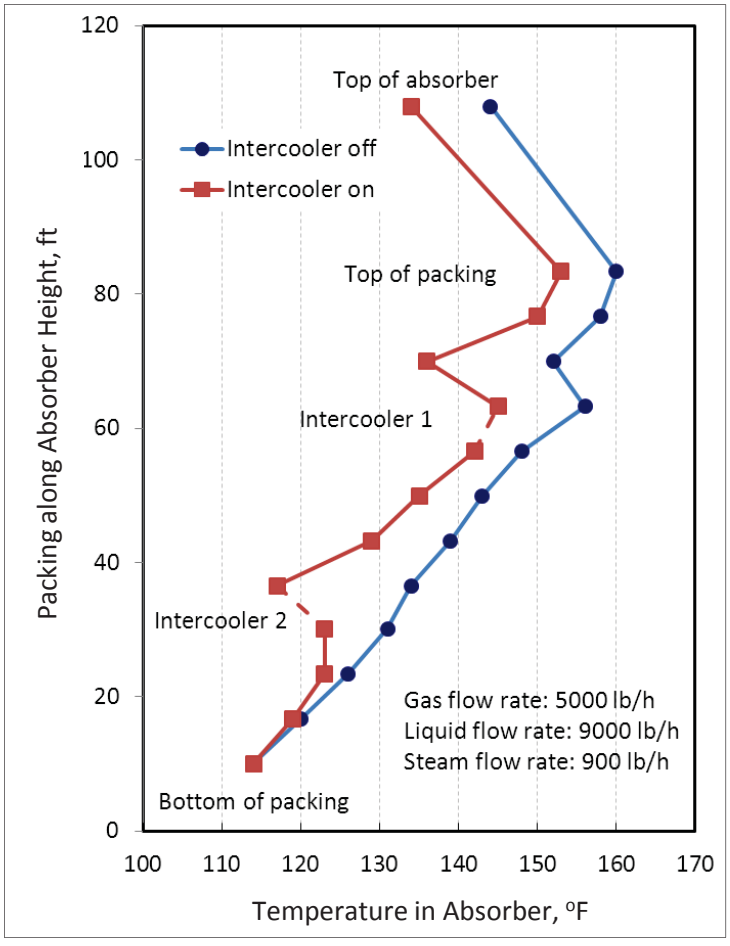

Figure 51. Temperature Profile within the Absorber with and without Intercoolers in Service

2.6.3 Comparison of H3-1 Performance with MEA

Table 27 summarizes the performance of H3-1 compared with NCCC test results for MEA under similar operating conditions such as flue gas flow rate (5,000 lb/hr) and inlet CO_2 concentrations (12.5 to 13 percent). All three absorber beds were in service, and intercoolers were not used. With H3-1, about 37 percent lower solvent flow rate is needed compared with 30 wt% MEA to achieve greater than 90 percent CO_2 capture. For a new CO_2 capture system, this would translate to savings in capital cost and operating cost since smaller equipment would be sufficient to achieve high removal efficiencies and a smaller amount of solvent would be pumped through the process loop. At 2.4 GJ/ton CO_2 or 1,034 Btu/lb CO_2, the regeneration energy required for H3-1 is about 34 percent lower than that for MEA.

Table 27. Comparison of H3-1 Performance with MEA

Solvent	Liquid-Gas Ratio, lb/lb	CO_2 Removal Efficiency, %	Inlet CO_2 Concentration, %	Regeneration Energy, GJ/ton CO_2
30 wt% MEA	3.2	92	12.5 - 13.0	3.6
H3-1	2	93	12.8	2.4

2.6.4 Amine Carryover and Secondary Products

Amine carryover was measured by collecting gas samples at the outlet of the wash tower. The same sampling set-up and location have been used to measure amine carryover during the MEA tests. Three samples were collected during parametric tests in May and July 2012. The amine carryover from these tests was estimated to be 66, 55, and 68 ppm with an average of 63 ppm. This is about half the value of amine carryover measured when operating with MEA, which was about 135 ppm.

Although the extent of carryover was less for H3-1 compared to 30 wt% MEA, the amount of amine carryover for both the solvents was much higher than expected values. This indicates that amine carryover is not only contingent upon the type of solvent, but strongly depends on the design and operation of the absorber and the wash tower. It is understood that amine diffuses into fine droplets that are formed due partly to the presence of SO_3 aerosol in the flue gas, and this mist escapes from the absorber and wash tower along with the CO_2-depleted flue gas. By improving the design of the mist eliminators in the absorber and wash tower, for example, the amount of amine-entrained in the mist can be reduced. Reducing the temperature of the wash water and increasing the wash water circulation rate would also considerably reduce the amount of amine mist and vapor leaving the wash tower.

As discussed in Section 2.3, amine carryover is also dependent on factors such as solvent temperature in the absorber, amine concentration in the wash water, and whether the top most bed is active or not. In the absorber, as the MEA solvent temperature increased, carryover decreased. It is thought that at higher temperatures the droplets formed are larger and hence can be removed easily by the wash tower. Also, by reducing the concentration of amine in the wash water, the equilibrium vapor pressure of amine can be reduced, thereby decreasing the amine carryover leaving the wash tower. NCCC has shown that when operating with the two lower beds instead of all three beds in the absorber and without intercooling, amine carryover was

lower. The upper inactive bed was thought to be knocking out the smaller droplets that would have otherwise passed through to the wash tower. By adjusting one or more of the operating parameters, amine carryover from the wash tower can be reduced.

Gas samples at the outlet of the wash tower were also collected using a different method, which is shown in Figure 52. This sampling set-up mainly consisted of a heated Teflon sampling line; two impingers in an ice bath, one containing water and the other, an organic solvent (xylene), and a rotameter. Amine carryover measured by this method was higher than that measured by the knock-out trap method. This difference in the concentrations between the two methods could be due to the sampling technique. In the knock-out trap method, when the sample gas was rapidly chilled, amine mist may have been generated that passed through the empty impinger. Due to the absence of a water impinger, any mist that may have formed was not collected.

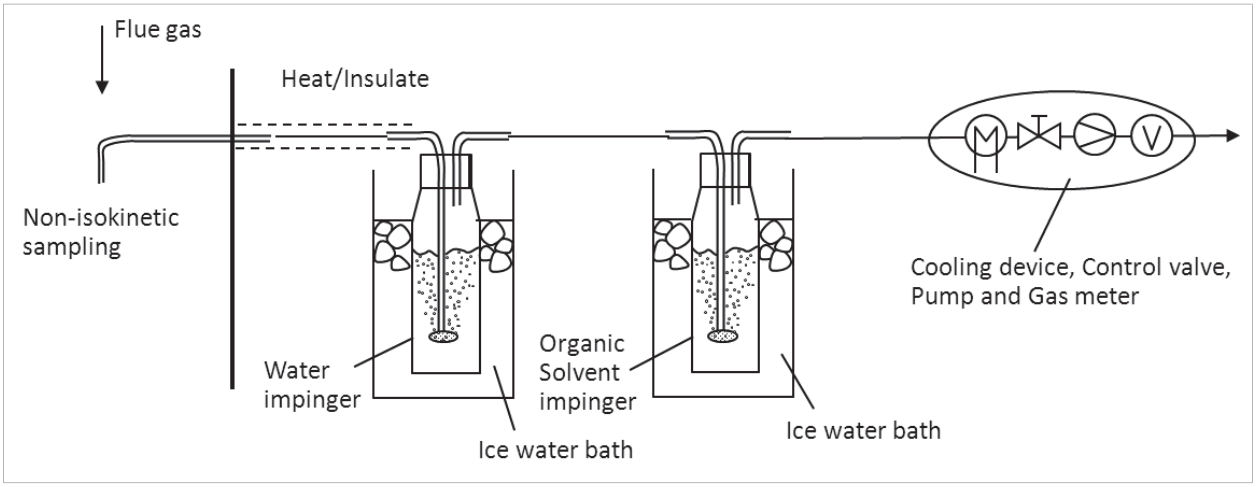

Figure 52. Gas Sampling Method for Amine Carryover using Organic Solvent

Furthermore, the amine carryover measured by the method shown in Figure 52 exceeded the expected value determined based on the outlet temperature of the wash tower. This is most likely due to the presence of amine mist in the sample gas. Even though sampling was done in a non-isokinetic manner, amine mist can still be carried along in the sample stream and collected in the water impinger. The difference in amine carryover concentrations determined by the two sampling methods and the comparison to expected values suggests that the sampling methods may need to be further improved to get accurate measurements. High amine carryover with both H3-1 and MEA indicate that improvements are necessary in the absorber and wash tower in order to reduce amine slip. The design and operation of the wash tower have a significant impact on the release of amine both as fine mist and as vapor.

Gas samples were also collected at the outlet of the wash tower to analyze for nitrosamine emissions. The sampling method for nitrosamine emissions included a heated Teflon sample line, an acid impinger to suppress further reactions of NO_2, and amine in the sampling train before it is adsorbed on the Thermosorb/N sorbent cartridge to capture the nitrosamine in the gas. Three samples were collected at different times during the test campaign and the temperature at the outlet of the wash tower was different for each of these tests. Analysis by an external lab

showed that nitrosamine was not detected in these gas samples. The detection limit was 0.05 μg/cartridge, or about 0.25 μg/m^3.

2.6.5 Solvent Degradation

Solvent samples from the outlet of the absorber (CO_2-rich) and inlet to the absorber (CO_2-lean) were collected regularly (roughly one set per test) to perform manual titration for verification of the amine and CO_2 concentrations measured by the auto-titrator. Some of the samples were analyzed for degradation products, and the results are plotted for formic acid and oxalic acid formation over operating time in Figure 53. As expected, the concentration of the degradation products was very low, in the range of 10 to 15 ppmw, after 1,000 hours of testing. Over a similar duration of NCCC's testing with MEA, the concentration of oxalates and formates measured from MEA solvent samples were much higher, at 393 ppmw and 1,820 ppmw, respectively. Figure 53 also shows that as H3-1 testing progressed with time, the concentration of formic acid and oxalic acid in the solvent slightly increased. The reduction in acid concentration at about 950 hours was due to the introduction of fresh solvent to the process loop at about 750 hours. This was done to maintain sufficient liquid level in the process solvent tank for the lean solvent pump to work effectively.

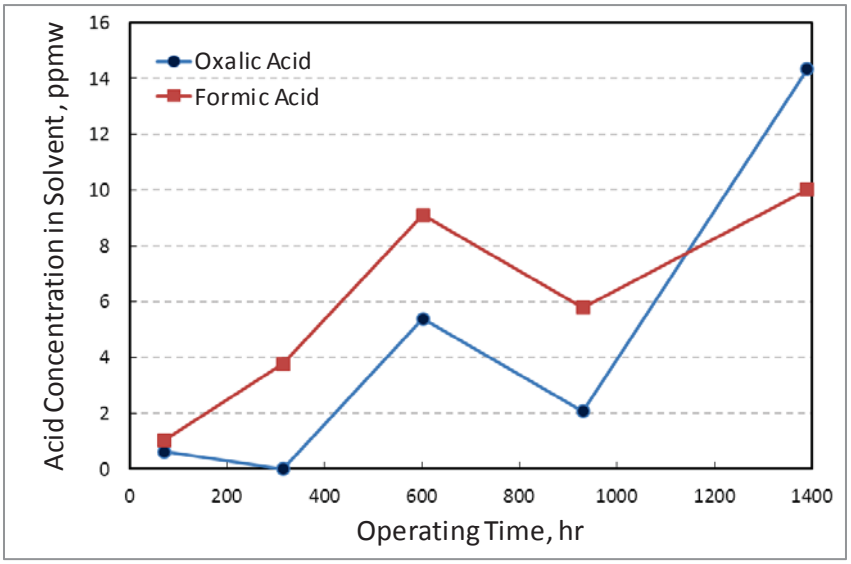

Figure 53. Degradation Products in H3-1 Solvent

The formation of heat stable salts as sulfates in the solvent was also measured by analyzing lean solvent samples taken at various intervals of testing. Sulfate compounds are formed due to the reaction of the amine and SO_2 in the flue gas. During the H3-1 testing, the inlet SO_2 concentration was controlled in the pre-scrubber and maintained between 1 and 2 ppm for most of the testing, increasing to 3 to 4 ppm during the latter part of the test campaign. Figure 54 is a plot of the concentration of sulfates in the solvent at different test durations. The formation of degradation products increased with time, and after 1,200 hours, the sulfate concentration was around 900 ppmw. After about 1,000 hours of MEA baseline testing, the sulfate concentration in the rich MEA solvent as reported by NCCC was 1,010 ppmw. The presence of sodium, calcium,

and magnesium in the solvent indicates that at least in part the sulfate detected originates from carryover from the PSTU caustic scrubber and Plant Gaston's limestone-based FGD.

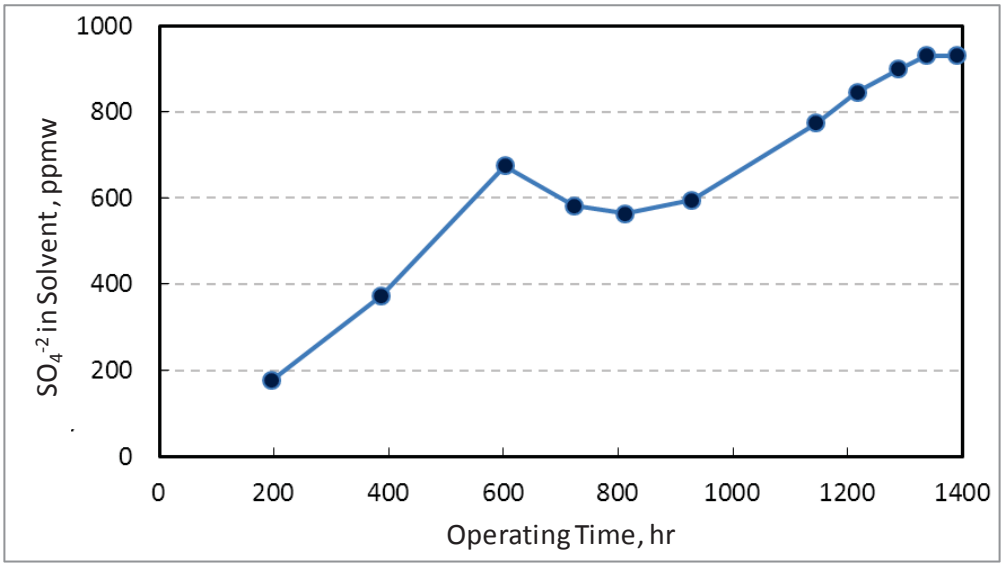

Figure 54. Sulfate Concentration in H3-1 Solvent

2.6.6 Corrosion

Three electrical resistance probes were located in the absorber and one each in the wash tower, inlet separator, regenerator, and mist separator. The three probes within the absorber were located at different elevations, which are at different temperature regions due to the exothermic nature of the absorption reaction of CO_2 in the amine. The probe readings at all three locations in the absorber were similar, showing that from top to bottom there was no significant difference in corrosion. For all locations in the PSTU, the probe measurements were nearly constant throughout testing, indicating no significant corrosion.

2.6.7 Metals in Solvent

The concentration of metals in the H3-1 solvent was analyzed for accumulation of metals that are present in the flue gas and to verify corrosion effects. Table 28 lists the results of the analysis of H3-1 and MEA. The H3-1 samples were analyzed by two labs—an independent laboratory in Japan that analyzed samples at two operating time intervals, 900 hours and 1,350 hours of testing, and Alabama Power's General Test Laboratory that analyzed samples after the completion of testing. NCCC provided the data for MEA samples that were analyzed after 1,000 hours of testing. The RCRA limits for some of the metals are also listed in the table.

Table 28. Concentration of Metals in H3-1 Solvent

Metal	H3-1, Lab Analysis, mg/L		H3-1, TCLP Analysis, mg/L	MEA, mg/L	RCRA Limit, mg/L
	900 hr	1,350 hr	1,350 hr	1,000 hr	
Ba	<0.01	<0.01	<1	0.27	100
Cr	0.63	0.84	<1	45.09	5
Se	3.3	5.4	2.9	1.95	1
As	0.42	0.68	2.3	0.22	5
Cd	0.05	0.01	<1	<0.01	1
Pb	<0.01	<0.01	<1	<0.01	5
Hg	<0.1	<0.1	<0.05	<0.005	0.2
Ag	0.01	<0.01	<0.2	<0.5	5
Fe	0.61	0.58	--	137.20	--
Ni	0.10	0.17	--	28.77	--
Mn	0.01	0.01	--	5.62	--
Co	<0.01	<0.01	--	1.02	--

Metals such as barium, selenium, arsenic, cadmium, lead, mercury, and silver are typically present in the flue gas, but do not affect the CO_2 capture performance of the solvent or energy requirement for the process. Except for selenium, the concentration of these metals in the H3-1 solvent was much lower than the RCRA limits.

Chromium, iron, nickel, manganese, and cobalt are metals that are present in the stainless steel material used in absorber and regenerator construction and are generally not likely to be present in the flue gas in significant quantities. The presence of these metals in the solvent indicates corrosion in the process equipment. As shown in Table 28, the concentration of these metals in H3-1 was insignificant and orders of magnitude lower than that measured in MEA. Such low concentrations confirm results from the electrical resistance probe measurements and Hitachi's previous test results that the H3-1 solvent has very low corrosivity.

2.7 Codexis Enzymes

In May 2010, Codexis received $4.7 million from ARPA-E to investigate the use of carbonic anhydrase enzymes to accelerate the rate of CO_2 capture for solvents that have desirably low heats of reaction such as methyldiethanolamine (MDEA), ammonia, and potassium carbonate. The enzyme is mixed with the solvent and so must be resistant to decomposition at regeneration temperatures. Thus, a major objective of this ARPA-E funded research was to demonstrate the stability of the enzyme under operating conditions.

Previous testing on the enzyme technology was conducted with synthetic flue gas in bench-scale stirred cell reactors and a wetted wall column and in a pilot-scale with the Codexis Test Unit (shown in Figure 55). The tests at the PC4 were the first using coal-derived flue gas to determine the stability of the enzyme in the presence of trace contaminants.

Figure 55. Codexis Enzyme Test Unit Installed at the PC4

The Codexis Test Unit consists of absorber columns and a desorber tank. Both absorber columns are over 20 feet tall with a 4-inch internal diameter. The absorber contains loose packing while the desorber is an open vessel without packing. The unit was designed for a flue gas flow of 850 standard ft^3/hr, a solvent flow rate of 260 lb/hr, and a CO_2 removal rate of 14 lb/hr.

NCCC staff completed the design and construction necessary to accommodate the Codexis Test Unit for initial exposure of the solvent and enzymes to flue gas. Commissioning and testing were completed in a two-week period at the end of May using MDEA. Figure 56 provides trends of the operation over a six-day period with CO_2 capture averaging around 65 percent at a rate of capture over 25 times greater than for MDEA alone with 0.2 g/L of enzyme loading. No apparent effect of trace metals or elevated process temperatures on enzyme performance was seen.

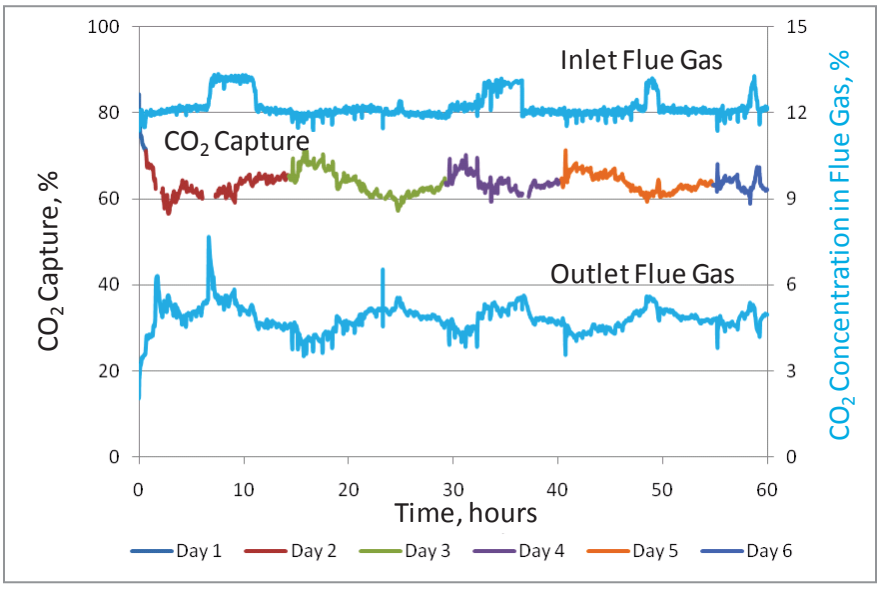

Figure 56. Results of Codexis Enzyme Testing

2.8 Akermin Enzymes

Akermin has been developing immobilization/stabilization systems to deploy carbonic anhydrase enzyme into the absorber of commercial gas-liquid contactor systems to accelerate the capture of CO_2 in widely available low-cost commodity base chemicals. For example, unlike most amine solvents, potassium carbonate is non-volatile, does not degrade in the presence of oxygen, SO_2 and other impurities, and has low corrosion potential. These properties eliminate the cost of wash towers and solvent clean up equipment, eliminate VOC emission potentials, and eliminates the need for corrosion inhibitors. While the heat of reaction is nearly one third that of MEA, capture rates in potassium carbonate are much slower. Indeed, potassium carbonate does not react directly with carbon dioxide in the same way as MEA. Instead, CO_2 is first hydrated with water before the base completes the reaction, as shown in the chemical equations below. While CO_2 hydration is slow in the absence of catalyst, carbonic anhydrase is a very efficient catalyst for this reaction (kcat ~ 10^6/s). Therefore, developing and demonstrating enzyme-catalyzed technology is beneficial to the program to employ non-volatile and non-toxic solvents with potentials to reduce cost of capture.

$$CO_2 + H_2O \leftrightarrow HCO_3^- + H^+ \qquad \text{(catalyst needed)}$$

$$H^+ + B \leftrightarrow BH^+ \qquad \text{(fast)}$$

$$CO_2 + H_2O + B \leftrightarrow HCO_3^- + BH^+ \qquad \text{(overall reaction)}$$

Akermin's proof of concept enzyme delivery system used active enzyme encapsulated in a thin polymer film that was subsequently deposited on the surface of the absorber packing. In this case, the enzyme is immobilized on the packing material. This avoids transferring the enzyme into the high-temperature stripper column where it can potentially become thermally inactivated.

From March through September 2013, Akermin completed approximately 2,800 operational hours on flue gas with minimal decline in the performance of the biocatalyst. Around 1,500 hours were completed with undiluted flue gas (12 percent CO_2) with the remainder on simulated natural gas flue gas (4 percent CO_2). Reliable operation was demonstrated, operating availability being 99 percent relative to flue gas supply.

During this time, operation with the carbonic anhydrase enzymes demonstrated 90 percent CO_2 capture and produced a regenerated CO_2 stream with 99.9 percent purity. Heat stable salt accumulation was negligible. Unlike operation with amine-based solvents, solvent carryover was below detection limits, with less than 1.6 percent per year capacity loss due to heat stable salts. Comparatively, previous MEA testing at the NCCC has demonstrated that up to 0.5 percent of solvent can be lost in a day due to volatility and aerosol formation alone.

Figure 57 presents test data with the immobilized enzyme data compared to data with blanks using the same liquid distributor with 55 tubes and with blanks in a 6-tube distributor. Data presented in Figure 57 were collected at various gas flow rates with a constant liquid-to-gas ratio and constant lean loading. It was shown that a first order plot gives a linear presentation of the CO_2 capture data with varied space-time. Data demonstrated that a seven-fold increase in flue

gas flow rate was possible while maintaining 90 percent CO_2 capture in the same column with enzyme operation and a six-fold increase in the mass transfer coefficient.

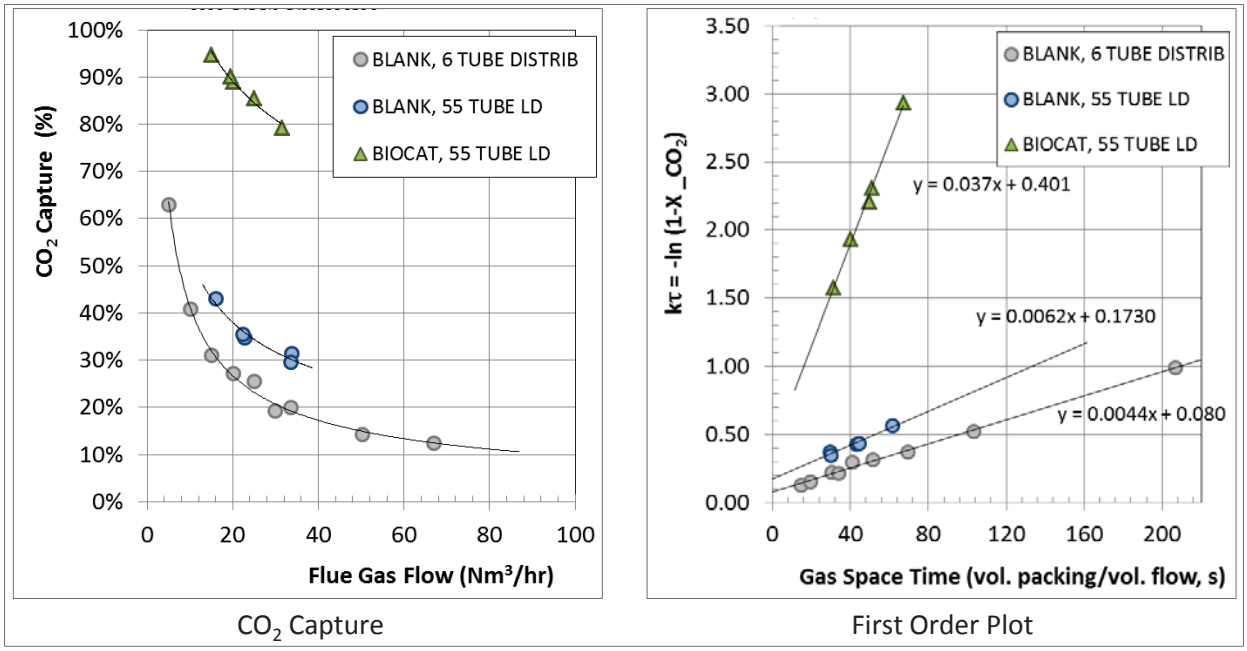

Figure 57. CO_2 Capture and Reaction Kinetics with and without Akermin Enzymes

Beginning in October, Akermin extended operation of the enzyme system, replacing potassium carbonate solvent with a proprietary amine solvent, AKM-24, as indicated in Figure 58. The data represents operation at constant conditions with a gas flow rate of 31.5 Nm^3/hr, a liquid flow rate of 275 L/hr, and lean loading at 0.25 mol/mol, demonstrating stable enzyme performance.

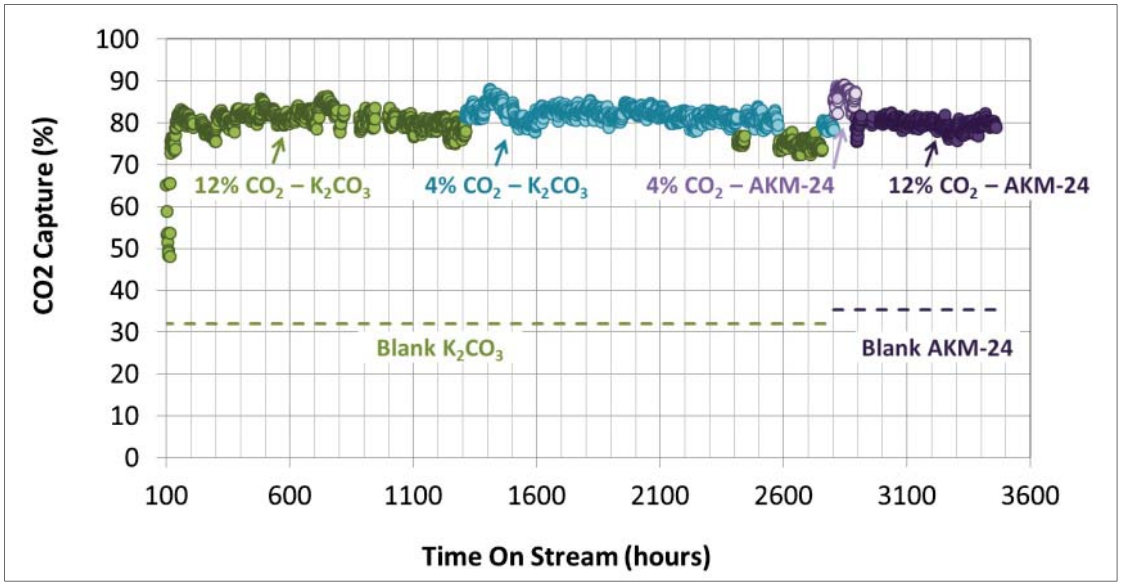

Figure 58. CO_2 Capture over Time at Constant Gas and Liquid Flow Rates and Lean Loading

Approximately 713 hours were achieved with the AKM-24 solvent, including 578 hours with typical flue gas and 135 hours with natural gas-simulated flue gas. The CO_2 capture efficiency was around 80 to 90 percent at design conditions.

In conclusion, Akermin completed a successful test campaign at PC4 with more than 3,500 hours testing the immobilized carbonic anhydrase enzyme-based system. Testing demonstrated:

- More than 2,800 hours on coal flue gas with an average steady performance of about 80 percent CO_2 capture using potassium carbonate solvent
- 700 hours of operation with the AKM-24 solvent, with 80 to 90 percent capture at design conditions and demonstrating stable performance
- Low solvent loss due to essentially zero volatility and also low heat stable salt build up (less than 1.6 percent per year capacity loss due to heat stable salts)
- Aerosol emissions lower than detection limit of 0.8 ppm
- High purity (greater than 99 percent) CO_2 production
- Negligible detectible corrosion rates using 304-stainless steel
- Energy consumption of about 3.5 GJ/ton CO_2 with the Akermin process using potassium carbonate

2.9 Chiyoda Solvent

Chiyoda Corporation, headquartered in Yokohama, Japan, provides services globally in the field of engineering, procurement, and construction for gas processing, refineries and other industrial projects. Chiyoda developed the CT-121 wet FGD process and has built over 60 units worldwide and also licensed the technology to other companies. As part of its business plan, Chiyoda is also supporting development of CO_2 capture technologies and has identified a solvent, T-3, suitable for post-combustion capture applications. In development of the T-3 solvent, testing was conducted in the PSTU.

Prior to testing the T-3 solvent, Chiyoda requested two design modifications to the PSTU absorber and regenerator (see Figure 59):

- Adding piping to recirculate cold-rich solvent back to different levels in the absorber. As the absorption rate for T-3 is slower than for MEA, in once-through operation the solvent leaving the absorber is not fully loaded. Recycling solvent increases rich solvent CO_2 loading, reducing solvent flow to the regenerator for a given capture rate and lowering the heat of regeneration. The recycled flow might also help to flatten the vertical temperature profile in the absorber, which would also improve performance.
- Installing new piping to the regenerator to allow the hot-rich solvent to be introduced at the top of the lower level of packing instead of at the top of the column. This modification was initiated to address the concern about excess solvent carryover from the regenerator. The top bed will be flushed by the condensate return, and this will help suppress solvent carryover.

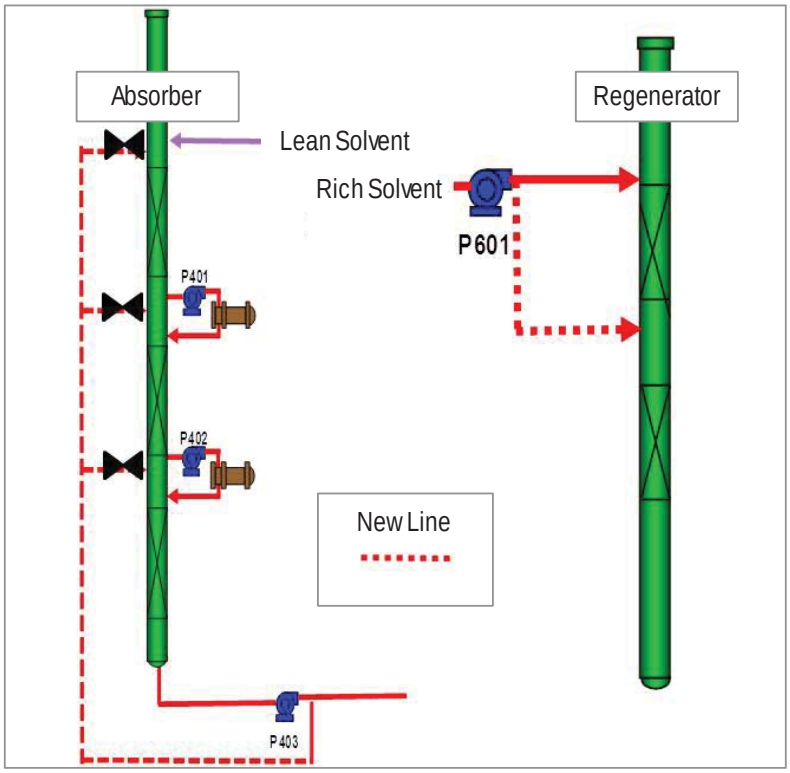

Figure 59. Modifications to PSTU Requested by Chiyoda

The modifications were essentially complete by December 7, 2012, and flue gas was introduced into the absorber on December 14. After several hours of operation, foaming occurred in the wash tower, resulting in a high pressure drop across the packing and carry-over of solvent with the CO_2-depleted flue gas. Occasionally the pressure drop fell but rose again to the previous level. The foam was believed to prevent the wash water from flowing through the packing, and the buildup of water accounted for the increased pressure drop. At a certain water level, the head was sufficient to overcome the resistance offered by the foam and the pressure drop fell. Foaming was not observed in the absorber or regenerator. The plant was shut down, but foaming was seen again during a second test on December 17.

The foaming was unexpected by Chiyoda. The solvent was previously tested for 200 hours in CSIRO's 1-tonne/day (1.1-ton/day) mobile test unit using coal-derived flue gas from the Loy Yang power plant in Victoria, Australia. Australian coal is usually low in sulfur and the plants do not have selective catalytic reduction (SCR) units for NOx control, hence the SO_3 content (not measured) would be expected to be low. Previous testing at the NCCC indicated that SO_3 produces liquid droplets that result in excessive carryover of solvent from the absorber into the wash tower and raises the solvent concentration of the wash water. This would not have been the case in the CSIRO test unit and could explain why foaming did not occur there.

As operation was untenable, Chiyoda agreed to postpone further testing until a means of eliminating the foam was identified. Chiyoda recommended using Shin-Etsu's KS-540 defoaming agent. To test its efficacy and that of other defoaming agents, a test apparatus, shown in Figure 60, was set up in the NCCC on-site laboratory. With the set-up, a known height of water was placed in a clear glass gas-wash bottle and nitrogen bubbled through it using a sintered

glass frit. As indicated in the figure, foaming, which approached 75 mm (3 inches) in height, was formed in a solution of water with 1 wt% Chiyoda solvent. Figure 61 plots foam height versus solvent concentration in water. The concentration of solvent in the PSTU wash water was around 1.2 percent, which corresponds to about 50 mm (2 inches) of foam. If foaming is to be avoided, then the concentration would have to be reduced to levels below this, although the tests do not indicate what the value should be.

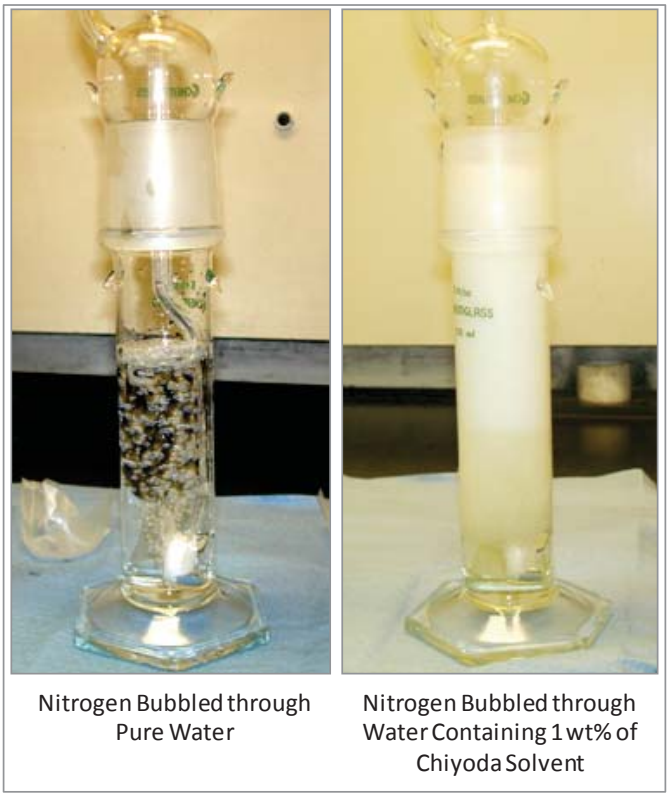

Figure 60. Laboratory Foaming Test Apparatus Used with T-3 Solvent

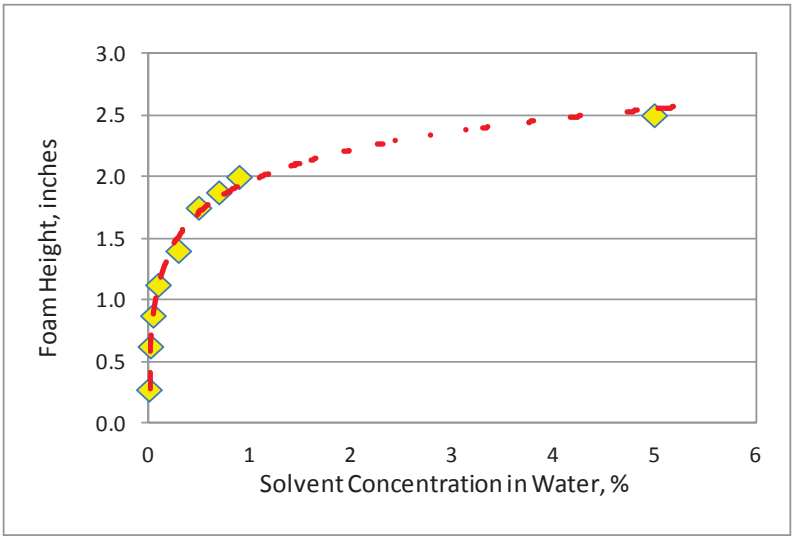

Figure 61. Foam Height vs. T-3 Solvent Concentration in Laboratory Testing

Testing of several defoaming agents showed that Shin-Etsu's KS-540 recommended by Chiyoda was the most effective. The manufacturer recommended using the agent with a concentration of 50 ppmw in the wash water, although the lab tests showed the agent was effective at lower concentrations.

The PSTU restarted on January 7, 2013, and testing was performed with several operating parameters (gas flow rate, wash-water flow rate, and wash-water temperature) around the PSTU wash tower to see if they reduced the foaming tendency. Variation of the operating parameters did not reduce foaming, and a modification to introduce the anti-foam into the wash tower was implemented. After an amount to achieve 50 ppmw was introduced on January 15, the foaming stopped immediately. It was expected that as the wash tower collected condensate and the concentration was reduced that more defoaming agent would have to be added, but no further additions were required.

Once stable operation was established without foaming, the Chiyoda test campaign started on January 17, and parametric tests to determine the optimal operating conditions to maximize the solvent's performance were conducted. Key items evaluated included determining heat of regeneration, optimization of L/G in the absorber, regenerator pressure and reboiler duty, and the temperature profile in the absorber. Testing continued through February, and by the end of the month, 18 of 22 parametric tests were completed with good mass balance closures.

Testing resumed on May 4 following a Gaston Unit 5 outage. For the first test, the CO_2 capture efficiency was lower than expected when compared to similar tests conducted before the outage. The CO_2 loading of the lean solvent leaving the regenerator was higher than previous levels (0.08 mole fraction compared to 0.02), and this was limiting the amount of CO_2 that could be absorbed for a given solvent flow rate. Consequently, the regenerator equipment was closely scrutinized and water was found to be leaking through a faulty valve isolating the reboiler from the regenerator mist eliminator.

Following the repairs, the four remaining parametric tests were completed, after which the 500-hour test commenced at a condition identified by Chiyoda based on the parametric test results. At the end of the steady state period, two additional parametric tests were completed, and the run ended on June 19, achieving over 1,500 hours of testing. Throughout the entire program, samples were taken to monitor solvent degradation and these were all shipped to Chiyoda for analysis. Following the run, the corrosion coupons, of 316L stainless steel and C1010 carbon steel, were removed and sent to the supplier to determine the loss rate of the material. The results showed that the T-3 solvent was significantly less corrosive than MEA.

Discussion of Test Results

The variation in regeneration energy with L/G ratio is presented in Figure 62, which shows the optimum L/G ratio to be around 2.4 L/Nm^3; this value is around 50 percent lower than for MEA. For 90 percent capture, the regeneration energy for T-3 is 2.6-GJ/tonne, around 30 percent lower than the 3.5-GJ/tonne for MEA.

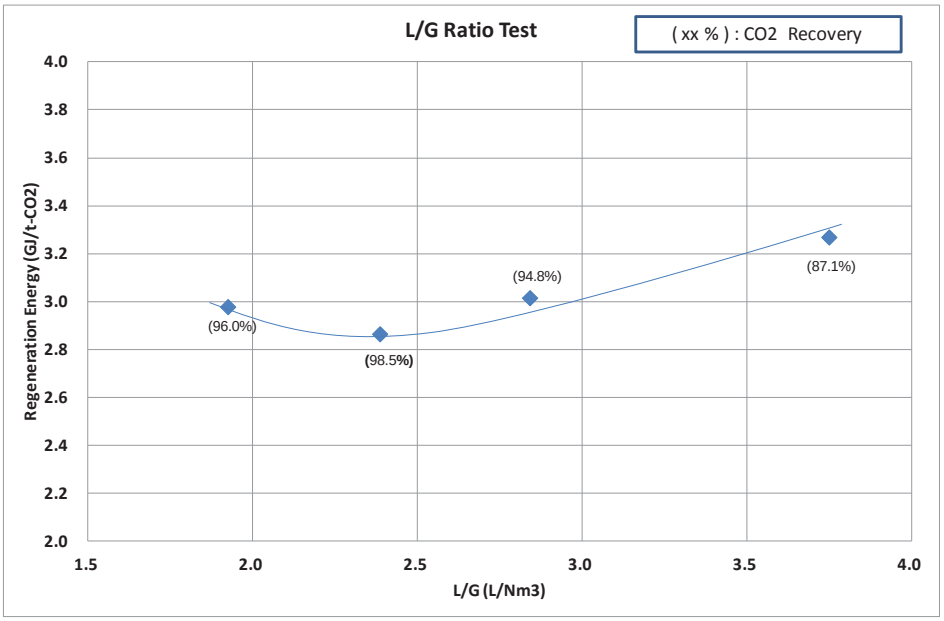

Figure 62. Variation of T-3 Regeneration Energy with Absorber L/G Ratio

The regenerator pressure was varied to understand how CO_2 recovery is influenced by regenerator bottom temperature. The L/G ratio was set at the optimum value of 2.4 L/Nm^3 and the regenerator pressure and steam flow rate were varied. Figure 63 shows that for each regenerator pressure, the CO_2 recovery was highest at the higher bottom temperature. Although there is scatter in the data, CO_2 recovery appears to decrease at higher pressures despite the regenerator bottom temperature increasing. However, the higher pressure lowers the compression ratio required by the CO_2 compressor, and hence the energy consumed and the size of compressor required. The optimal regenerator pressure will be determined by the combined economics of regeneration and CO_2 compression.

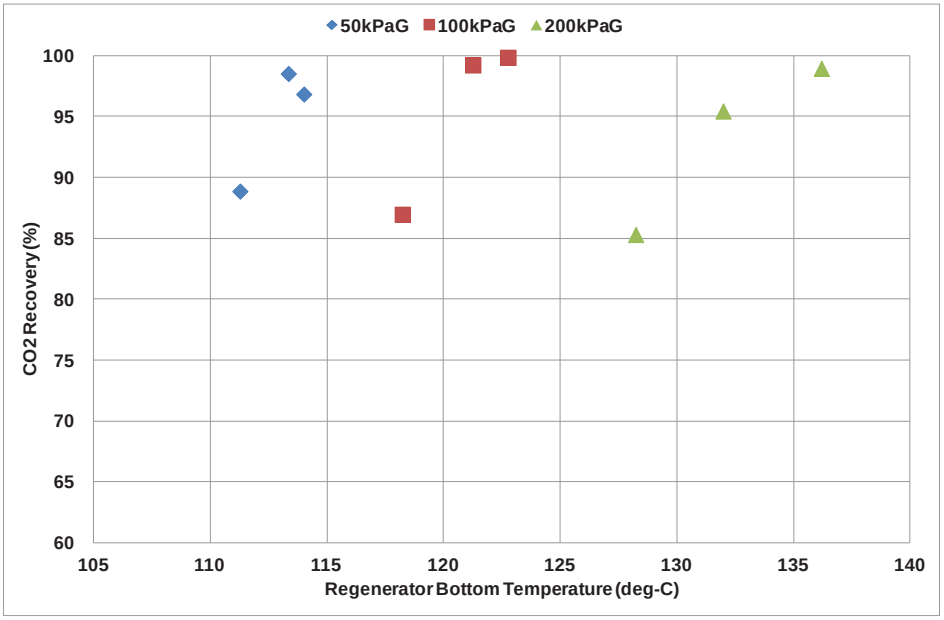

Figure 63. Regenerator Pressure Test

To moderate the absorber temperature profile, intercoolers are available between the first and second, and second and third beds. Lowering the mean solvent temperature in this way increases CO_2 absorption efficiency, increasing CO_2 capture for a given solvent flow rate, and subsequently lowering the regeneration energy. The test was completed at the optimum L/G ratio of 2.4 L/Nm^3. As anticipated, the rich loading leaving the absorber and the CO_2 capture efficiency were both higher with the intercoolers in service (see Figure 64). The absorber temperature profile with and without intercooling is shown in Figure 65.

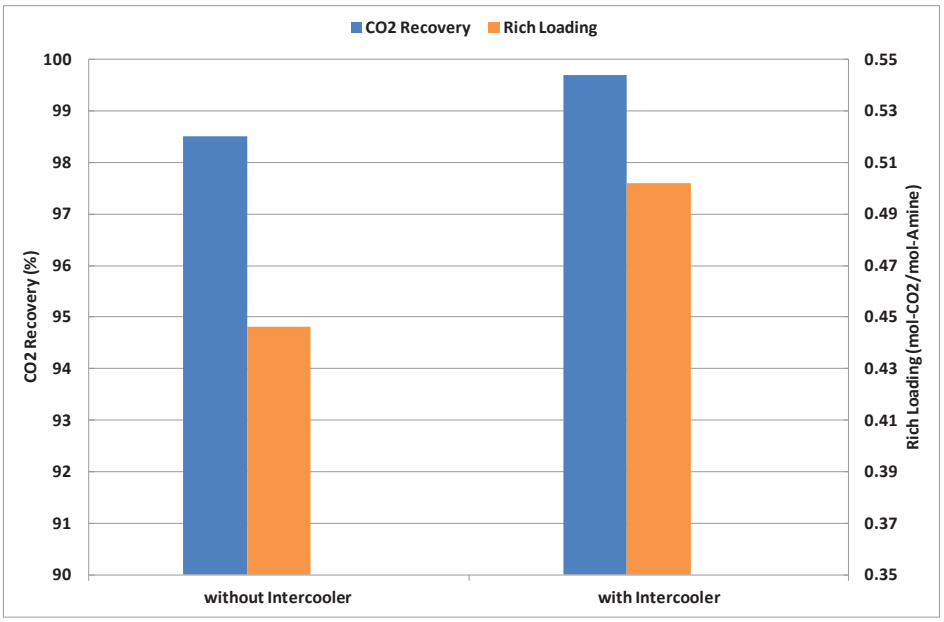

Figure 64. Effect of Intercoolers on Absorber Performance

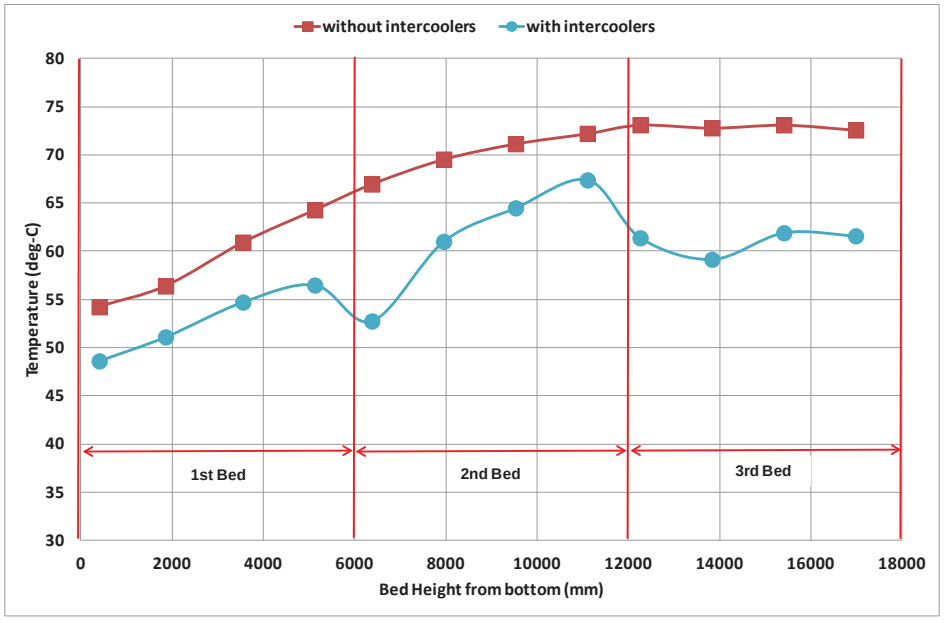

Figure 65. Absorber Temperature Profile with and without Intercooling

Rich solvent circulation tests were completed to increase the rich loading for a given circulation rate. Again, the tests were completed at the optimum L/G ratio of 2.4 L/Nm^3, and two intercoolers were used to moderate the temperature profile. Figure 66 shows how the location at which the recirculated solvent was introduced (above the lower or middle bed) influenced CO_2 recovery and rich loading. Unfortunately, the solvent concentration for Cases B and C with recirculation was around 10 percent lower than for Case A, without recirculation. This might be expected to lower the capture efficiency and loading at approximately 90 percent and 0.40, respectively, but the corresponding values were higher for Case A and B, as demonstrated in the figure. On this basis, it appears that recirculation benefits the performance of T-3.

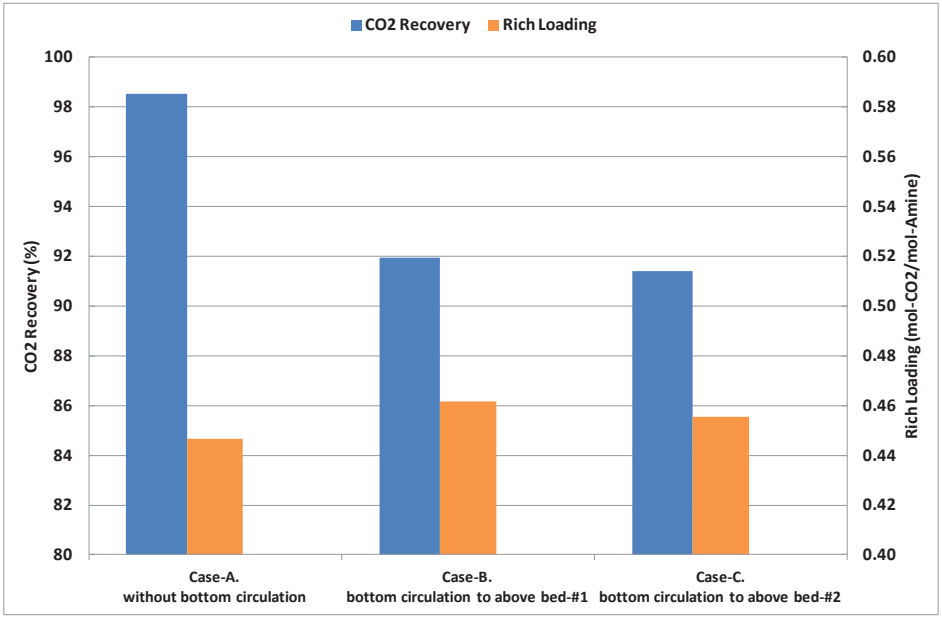

Figure 66. Effect of Recirculating Rich Solvent back to the Absorber

In common with other solvents, losses were higher than expected by Chiyoda based on previous testing. The reason was believed to be because of the SO_3 present in the flue gas promoting the formation of droplets too fine to be removed in the wash tower.

2.10 Cansolv Solvent

As part of its research and development of CO_2 capture processes, Cansolv Technologies conducted extensive testing of its DC-201 solvent in the PSTU in 2012. Testing involved parametric studies, equipment configurations, and solvent additives. In 2013, Cansolv augmented the previous testing with operation using flue gas diluted with air to simulate natural gas-fired operations. Cansolv conducted two additional test campaigns in 2014, the first with DC-103, and the second, a follow-up of natural gas simulation with the DC-201 solvent. The 2014 test results will be reported in later publications.

2.10.1 Solvent Testing in 2012

The piloting campaign duration was three months, from July 24 to October 28, 2012. A total of 1,725 hours of testing was achieved, which represents 80 percent of stable operation over the

period. The test plan was interrupted on three occasions due to E.C. Gaston power plant shut-down or maintenance on the SCR unit and scrubber: from August 15 to August 19; from September 7 to September 17; and on September 27.

Typically, two data points were collected per day, comprising of critical pilot unit parameters, such as temperatures, flows, and pressures, as well as liquid and gas sample analyses. Data collection was initiated after conditions had been stable for at least three hours. Liquid samples consisted of pre-scrubber sump, lean amine, rich amine, reflux, and water-wash recirculation fluids. Mass balance closures between the absorber and the stripper were very good (within 2 percent). The gas flow through the absorber was kept constant at 5,000 lb/hr. The liquid flow rate was varied from 11,000 to 6,800 lb/hr and the steam flow rate from 750 to 1,000 lb/hr, depending on test conditions.

The test objectives included evaluation of the following:

- Approach to equilibrium at various temperatures and L/G ratios (including 1, 2, or 3 absorber beds in service with 0, 1, or 2 intercoolers operating)
- Regeneration energy at various L/G ratios and regeneration temperatures and pressures
- CO_2 capture percentage at various solvent concentrations
- Amine or degradation product concentrations upstream and downstream of the water-wash section as well as in the CO_2 product
- Solvent stability under the oxidative environment, including the effect of SO_2 and NO_2 concentration in the gas
- Corrosion rates
- The effect on CO_2 capture performance at different concentrations of an additive

2.10.1.1 Optimization of Energy vs. L/G Ratio

This part of the test investigated the loading capacity of the solvent in the absorber and its influence on reboiler steam usage. These tests were performed at the same gas flow rate that was used for the evaluation of MEA on the PSTU unit. The amine and steam flows were varied to achieve 90 percent CO_2 capture. Figure 67 gives the results of this first set of experiments. The DC-201 solvent required 40 percent less energy than MEA to achieve the same capture rate using three packing sections in the absorber. The solvent also required 50 percent less circulation (L/G being 4 kg/Nm^3 for MEA and 2 kg/Nm^3 for DC-201).

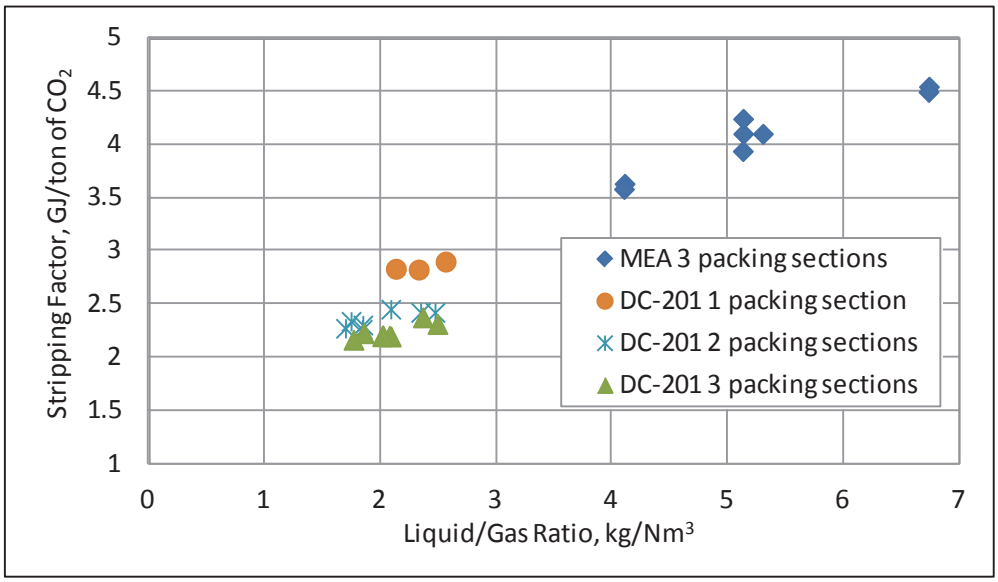

Figure 67. Optimization of Cansolv DC-201 Solvent at Various Absorber Packing Heights

2.10.1.2 Variation of Packing Height

This part of the campaign focused on the effect of absorber packing height on the performance of the capture system. The PSTU is equipped with three packing sections in the absorber, each 20 feet tall. An intercooler is located between each packing section. The solvent is withdrawn from the column at the bottom of one packing section, cooled in a heat exchanger, and returned to the column at the top of the packing section below. Lowering the solvent temperature into the optimal range increases the CO_2 solvent loading.

Three absorber configurations were tested:

- 3 packing sections, 2 intercoolers
- 2 packing sections, 1 intercooler
- 1 packing section, no intercooler

The amine and steam flows were varied to achieve 90 percent CO_2 capture. Results of this set of experiments are shown in Figure 68. The operating conditions (liquid to gas ratio and steam usage per ton of CO_2 captured) were not significantly affected while switching from three to two packing sections. The L/G did not vary, and the stripping factor increased from 2.2 GJ/ton CO_2 to 2.3 GJ/ton CO_2. Under these conditions, the solvent is not kinetically limiting and can reach adequate rich loading.

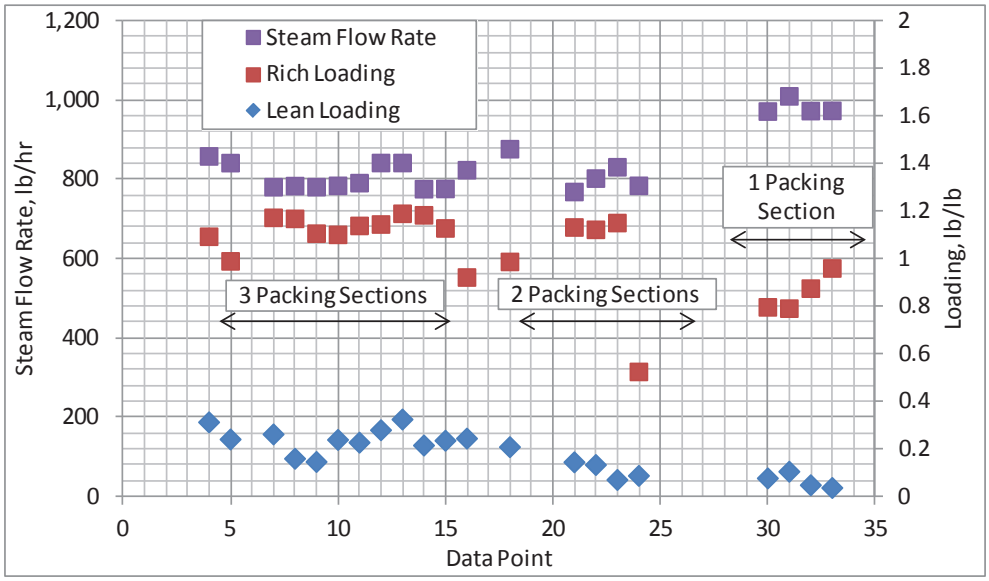

Figure 68. Variation of Steam Flow and Lean and Rich loadings with Absorber Packing Sections

A clearer response can be seen when switching from two to one packing sections. In this case, to maintain 90 percent CO_2 capture, the amine flow had to be increased (L/G going from 2.0 to 2.5 kg/Nm^3), as well as the steam flow. (Stripping factor increased from 2.3 GJ/ton CO_2 to 2.8 GJ/ton CO_2.) With only one packing section, the solvent appeared to be kinetically limiting, and the lower rich loading resulted in a lower lean loading and a higher steam flow rate.

2.10.1.3 Amine Concentration Experiments

During these experiments, the amine concentration in the solvent was varied from 40 to 60 wt% to study the effect on CO_2 capture efficiency and on steam usage (or stripping factor, expressed in GJ/ton CO_2 captured). When the amine concentration in the solvent falls below a given value, the CO_2 capture efficiency decreases due to loss of active amine sites in the solvent. This is shown in Figure 69 where reducing amine concentration from 53 to 40 wt%, reduced CO_2 capture efficiency from about 90 to 84 percent. Similarly, if the amine concentration is increased too much, some limitation in CO_2 mass transfer from the gas to the liquid phases may occur due to the increased viscosity of the solvent. A counter-measure to this loss in performance is to increase reboiler steam flow to lower the lean CO_2 solvent loading and provide extra CO_2 capacity in the absorber. These results are also shown in Figure 69. These tests indicate the following:

- Operational flexibility from 40 to 60 wt% solvent concentration
- Optimum operation with respect to energy consumption between 45 to 55 wt% solvent concentration

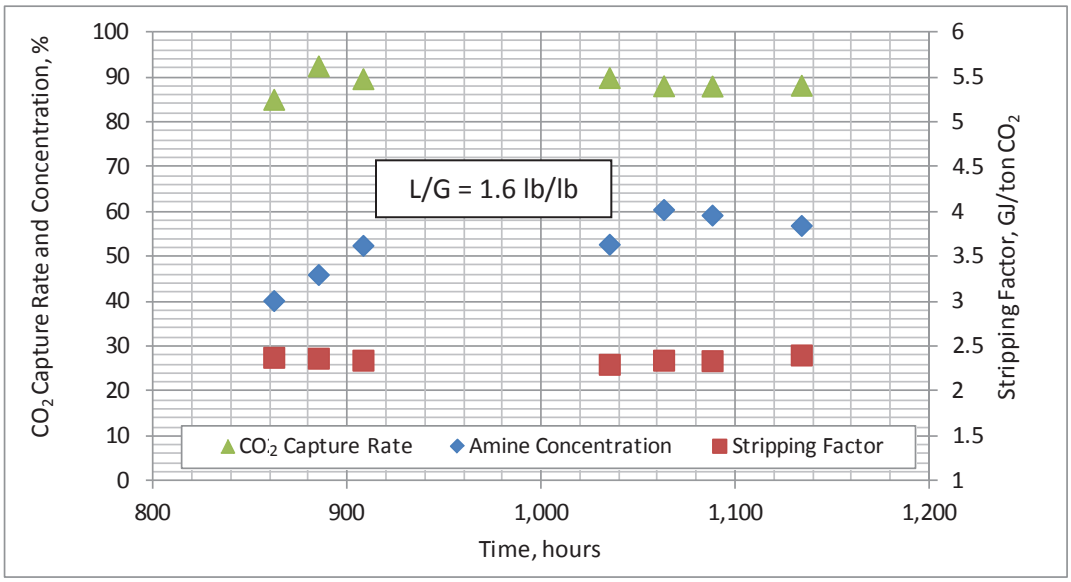

Figure 69. Variation of CO_2 Capture Rate, Amine Concentration, and Stripping Factor

2.10.1.4 Liquid Analysis

Samples from the amine loop, as well as from the pre-scrubber were taken and analyzed for anions, cations, and metals. Figure 70 presents the change of anion concentrations over time in the lean solvent, as analyzed at Cansolv's laboratory in Montreal. Sulfate build-up in the solvent is related to the accumulation of sulfate salts (for example, sodium from the caustic scrubber) although there was also some SO_2 slippage from the pre-scrubber. An average of 1.5 ppmv of SO_2 has been measured in the gas entering the absorber, although this is close to the lower detection limit of the ultraviolet SO_2 analyzer used. In a similar way, the nitrate build-up is related to NO_2 entering the absorber (average measured at 2 ppmv in the gas). No drop in performance was noticed as a result of this contamination.

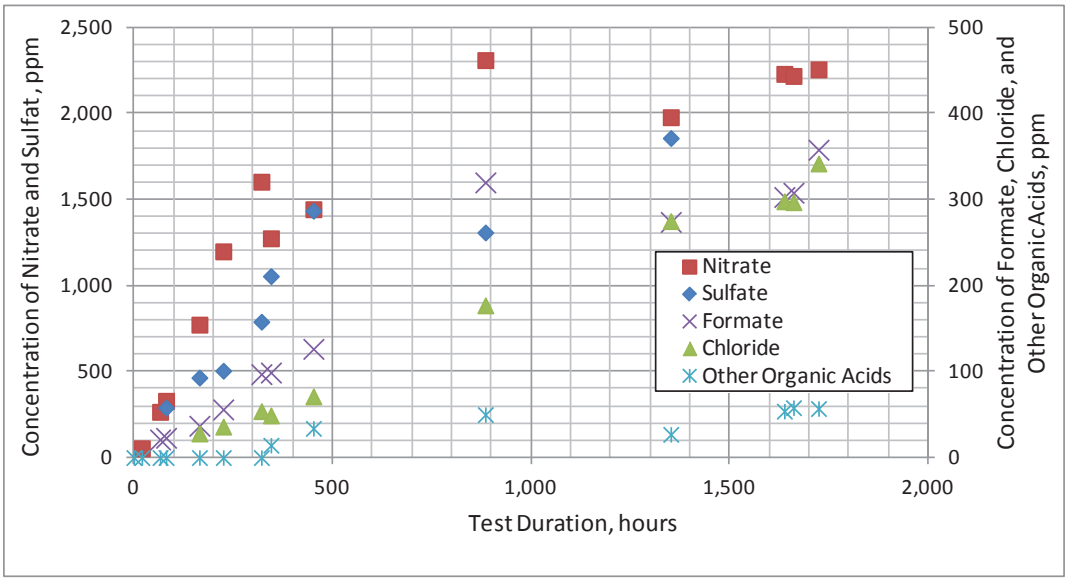

Figure 70. Increase of Anionic Species in Lean Solvent over Time

The main types of reaction involved in the degradation of amine-based solvents are:

- Oxidation of amine or hydroxyl functionalities, leading primarily to low molecular weight organic acids and ammonia
- Formation of heavier molecular weight species by coupling of two amine molecules (The product is still an amine and may have suitable CO_2 absorption properties.)
- Irreversible reaction with SO_2 leading to sulfonated neutral species
- Irreversible reaction with CO_2, leading to the formation of non-alkaline compounds such as oxazolidone, imidazolidone, etc.

The increase in concentrations of formate and acetate gives a primary indication of the degradation rate of the solvent. After three months of testing, the total amount of organic acids was 500 ppmw in solution, which indicates a very low degradation rate of the DC-201 solvent under these conditions. It should be noted that some bleed-and-feed occurred during the test, mainly due to mechanical losses through automated sampling lines.

Analysis for metals was performed by SRI at its Birmingham laboratory. Results are summarized below.

- Metals originating from the flue gas
  - Selenium (2 ppmw in pre-scrubber loop after 1 month of testing)
  - Arsenic (0.4 ppmw)
  - Manganese (2 ppmw)
- Alkyl metals found in the pre-scrubber and the amine loops originating in the caustic and water used in the pre-scrubber
  - Sodium (1.9 wt% in the pre-scrubber and 79 ppmw in the solvent)
  - Calcium (9 ppmw in the pre-scrubber and 3.5 ppmw in the solvent)
- Other metals found relating to the metallurgy of the system
  - Iron (8 ppmw in the pre-scrubber and 1.1 ppmw in the solvent)
  - Nickel (0.22 ppmw in the pre-scrubber and 0.08 ppmw in the solvent)
  - Chromium (0.57 ppmw in the pre-scrubber and 0.07 ppmw in the solvent)

These metals concentrations were much lower than for MEA, and were a good indication of the DC-201 solvent's lower corrosivity. For example, iron was measured at 137 ppmw in MEA (see Table 16), an order of magnitude higher than for DC-201.

Figure 71 plots the concentrations over time of other metals and cations detected in the lean solvent. Aside from the sodium and sulfur levels, no metals were found at sufficient levels to have any impact on the solvent CO_2 capture performance.

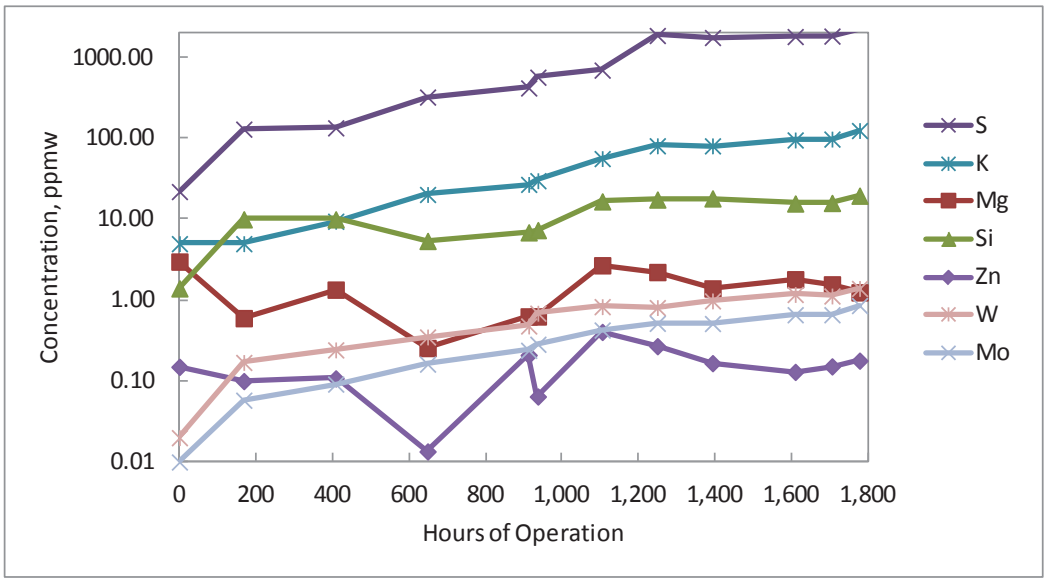

Figure 71. Change in Cations and Metals Concentrations in Lean Cansolv Solvent over Time

2.10.1.5 Gas Sampling

Three emissions surveys were completed at three locations: the CO_2-depleted flue gas streams upstream of the absorber wash tower (outlet of absorber) and downstream of the absorber wash tower, and the CO_2 product gas from the regenerator. Results are presented in Table 29. While analyses for nearly 50 different species were performed, only those with concentrations above the lower detection limit are reported. Acetaldehyde, which typically comes from coal combustion gas, was detected at ppmv levels in the three streams. Formaldehyde, ammonia, and dimethylamine emissions result from the degradation of the solvent. The emissions level leaving the water-wash and in the product CO_2 were found to be low, in the ppmv to the sub-ppmv range. Nitrosamines were also detected, but at the ppbv level.

Table 29. Main Contaminants Found in Gas Streams during Three Sampling Surveys

Contaminant	Abs	Wash 8/16/2012	Regen	Abs	Wash 9/25/2012	Regen	Abs	Wash 10/9/2012	Regen
Acetaldehyde, ppmv	5.51	9.83	5.33	5.22	5.26	4.94	5.7	5.51	5.47
Acrolein, ppmv	0.12	0.0146	0.124	0.069	0.03	0.115	--	--	0.047
Formaldehyde, ppmv	0.066	0.097	0.042	0.035	0.014	0.016	0.13	0.056	0.025
Ammonia, ppmv	0.732	--	--	--	--	--	0.907	0.668	--
THC as Hexane, ppmv	--	0.479	0.941	--	--	--	--	--	0.408
Dimethylamine, ppmv	0.738	0.951	--	0.283	0.432	0.119	1.395	1.024	--
n-Nitrosodiethanolamine, ppbv	--	0.078	0.206	0.041	0.014	--	--	--	--
n-Nitrosodimethylamine, ppbv	52.1	26.7	--	0.718	0.339	0.112	4.081	1.234	0.205

2.10.2 Solvent Testing with Natural Gas Simulation in 2013

Testing commenced on July 11, 2013, and the initial tests varied the liquid-to-gas ratio in the absorber and steam flow rates to the regenerator to optimize operating. Long-term testing was

focused on solvent performance, degradation, and emissions. Cansolv concluded the successful test campaign on October 7, with 1,715 hours of operation with natural gas simulated flue gas.

2.10.2.1 Operation and Results

The CO_2 removal and stripping factor versus total transformation products are shown in Figure 72 and Figure 73, respectively. These parameters were plotted against total transformation products to provide a clear indication of how the solvent performs at different stages of the piloting campaign. Throughout the campaign, overall CO_2 capture performance did not deteriorate significantly as transformation products increased in concentration, since the DC-201 solvent transformation products maintain a certain strong capacity for capturing CO_2. The results in Figure 72 demonstrate no noticeable loss of CO_2 capture performance before a total transformation concentration near the middle of the test.

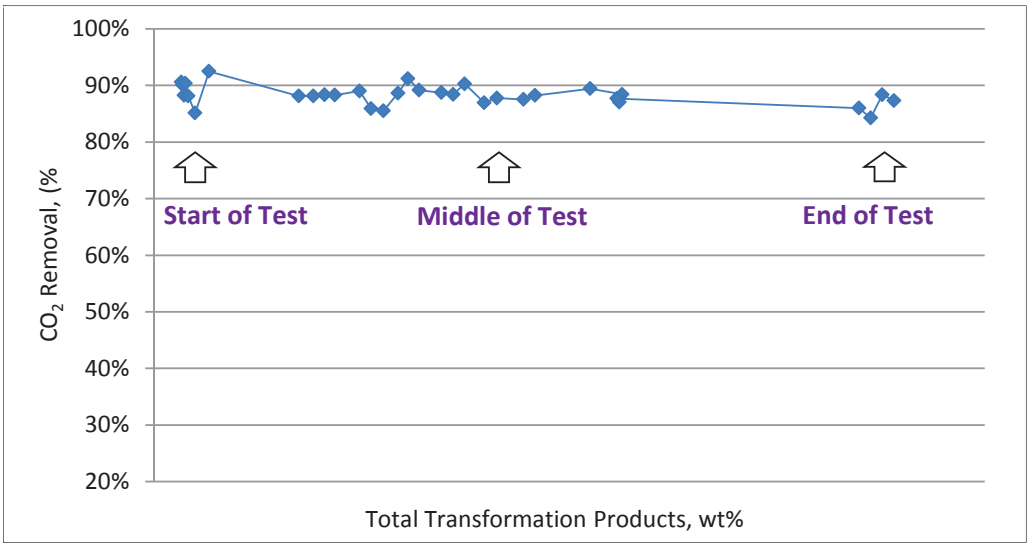

Figure 72. CO_2 Removal over Time for Cansolv Solvent

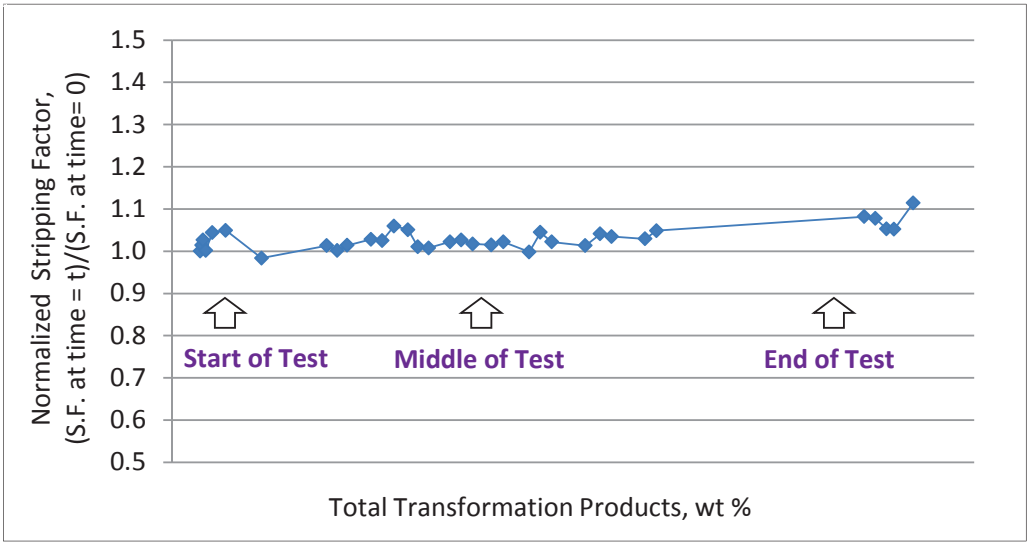

Figure 73. Normalized Stripping Factor over Time for Cansolv Solvent

Similar behavior was observed for the stripping factor, as its performance did not worsen until the later portion of the piloting campaign, as demonstrated in Figure 73. It should be noted that the increase in stripping factor was marginal; the maximum observed was about 10 percent. For commercial applications, the total transformation product concentration will be controlled below the value measured near the halfway point of the test. A thermal reclaimer unit will be used to ensure process performance is not hindered. Also, it is important to note that the results shown for this test were generated in the absence of intercooling or any energy integration options.

Figure 74 plots lean solvent total alkaline concentration versus operational hours. The concentration was determined by titration; therefore, any degradation/transformation products which retain alkalinity were incorporated in the analysis. The results demonstrate that lean solvent total alkaline concentration was controlled near 50 wt%, even as some transformation products formed.

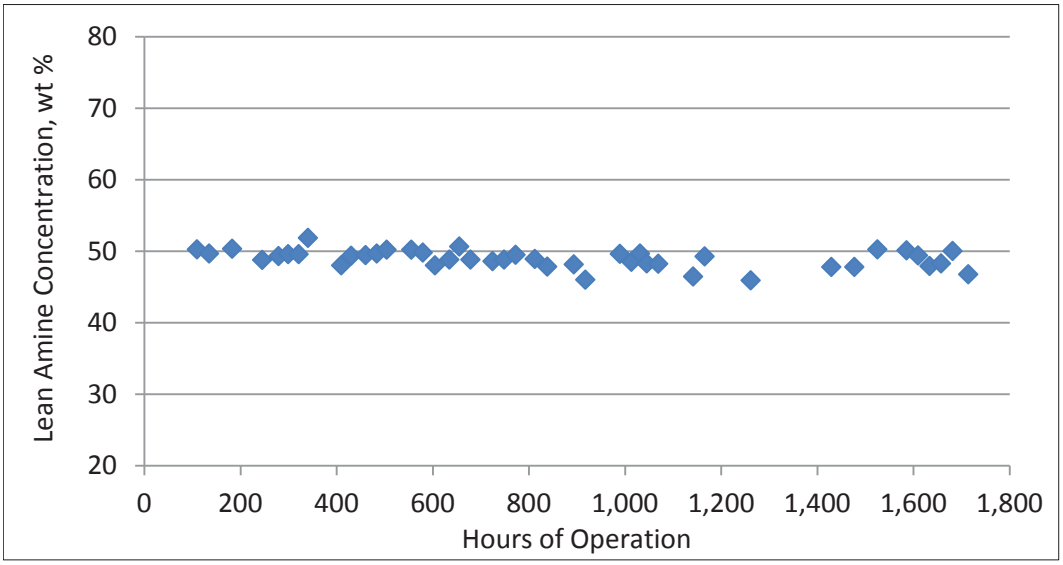

Figure 74. Lean Solvent Total Alkaline Concentration versus Operational Hours for Cansolv Solvent

2.10.2.2 Gas Sampling

Gas sampling was performed using the NCCC impinger train described previously, and the liquid collected was sent to Shell/Cansolv Laboratories for analysis of amine and degradation products. Results of the amine emission surveys performed at NCCC have shown that amine emissions are considerably influenced by the concentration of acid mist (sulfite), particulate, and other flue gas contaminants. To evaluate this phenomenon further, gas emissions tests were conducted with different quality flue gases. Three different flue gas streams were tested:

- Typical coal combustion flue gas
- Simulated natural gas flue gas
- Ambient air

A total of 14 gas sampling tests were performed, and the average results from these tests are summarized in Table 30. The results presented are valid only for the PC4 and cannot be applied

to other pilot or commercial units since the concentration of acid mists and other contaminants such as particulates will vary and will influence amine emission results differently. Also, the results are valid only for the DC-201 solvent; generally, different amines will exhibit different results due to dissimilarities in physical properties. The results demonstrated 33 and 77 times higher emissions compared to the air emission test for simulated natural gas (diluted coal gas) and standard coal flue gas, respectively.

Table 30. Amine Emission Results for Cansolv Solvent Testing

Gas Type	Sulfite Content, ppmv	DC-201 Emission Ratio to Air
Air	0	1
Simulated NG Flue Gas	0.3	33
Typical Coal Combustion Flue Gas	1.3	77

Sampling was also performed on lean solvent over the course of the test campaign to analyze for metals and anions. Figure 75 provides the sampling results for species that accumulated in the solvent over time.

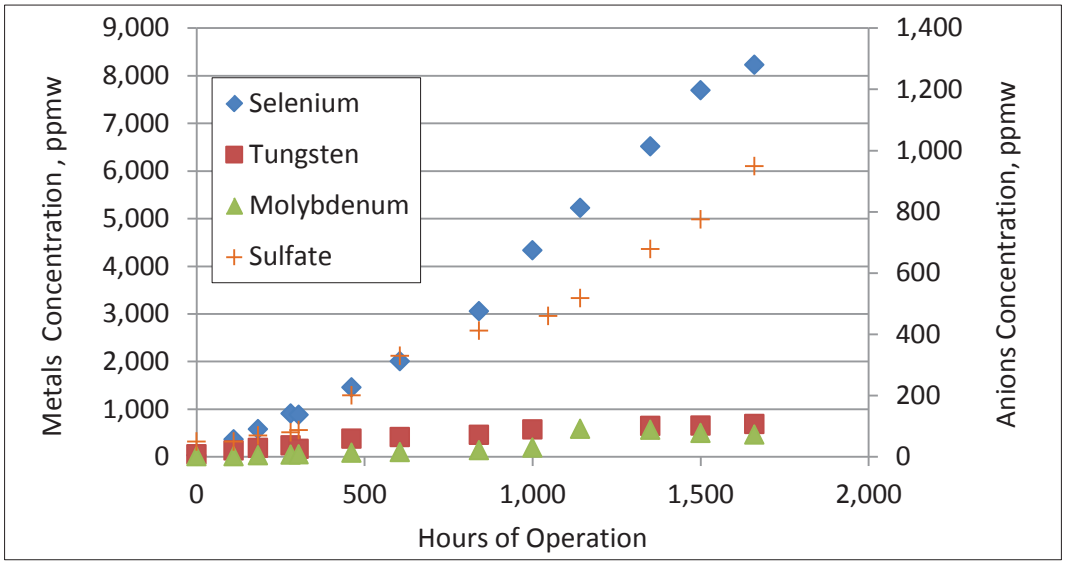

Figure 75. Concentration of Metals and Anions in Lean Cansolv Solvent over Time

2.11 MTR 1-ton/day CO_2 Capture Membrane System

MTR began testing the polymeric Polaris™ membrane system for separating CO_2 from coal-derived flue gas in December 2011, with 9,119 hours of operation achieved during the contract period. The test skid includes two stages of membrane design required for commercial units: cross-flow and countercurrent-sweep membrane modules. The skid processes 250,000 scf/day of desulfurized flue gas, and is designed to capture one ton per day of CO_2 with a capture efficiency of 90 percent. Operational experience with the 1-TPD system has been used to support a scaled-up membrane system to capture 20 TPD of CO_2.

As shown by the process diagram in Figure 76, the 1-TPD system removes CO_2 from flue gas in two steps. The first step uses cross-flow modules with a vacuum on the permeate for CO_2

enrichment, and the second step uses counter-current sweep air to remove additional CO_2 in the feed gas to meet the overall capture target of 90 percent. Before entering membrane modules, the gas is compressed to 20 to 30 psig to generate the necessary pressure ratio for parametric study of membranes installed on the system.

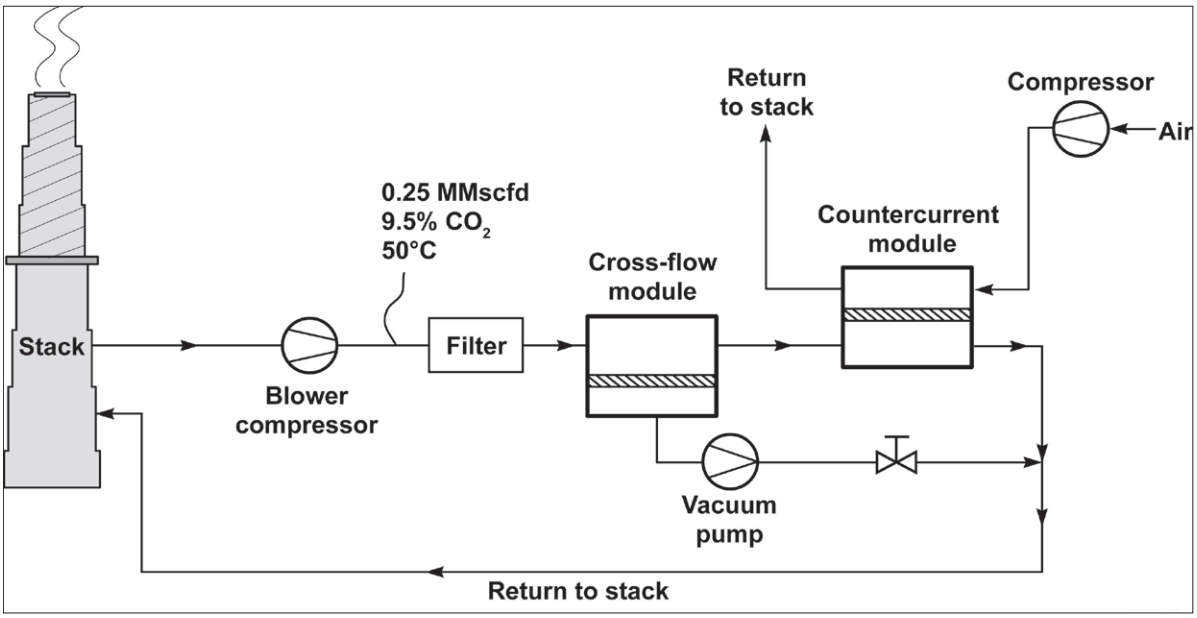

Figure 76. Schematic of MTR Flue Gas Membrane Skid

2.11.1 Operational Results

In 2012, flue gas outages (January to March) and compressor corrosion issues while using the original Atlas Copco dry-screw compressor caused interruptions in the system operation. Most of the continuous system operation was obtained in April to June. Figure 77 shows the real-time CO_2 content during operation from April 19 to June 26 for three gas streams of interest—the feed gas, the CO_2-enriched stream, and the CO_2-depleted stream—and also plots the overall CO_2 capture rate for this period. Air ingress was completely avoided after 300 hours of operation, and the CO_2 content in the feed gas stabilized at about 12 percent. From 300 to 1,000 hours of operation, the two-step membrane operation reduced the CO_2 content to 5 percent in the CO_2-depleted stream, indicating an overall capture rate of approximately 60 percent. The cross-flow modules enriched the CO_2 by a factor of six to eight. With two new sweep modules rotated into the system in early June (after 1,000 hours of operation), the CO_2 content in the CO_2-depleted stream was further reduced to around 3 percent, indicating a CO_2 capture rate of 85 percent.

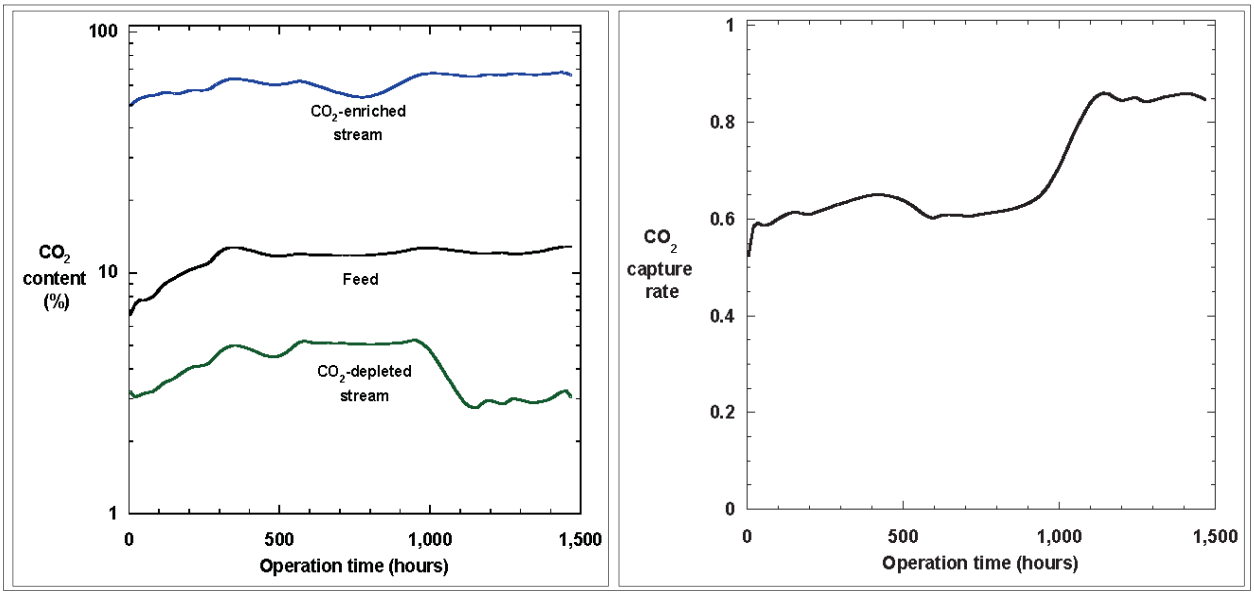

Figure 77. CO_2 Content of Inlet and Outlet Streams and CO_2 Capture Rate during Operation of MTR 1-TPD System from April to June 2012

Two cross-flow modules (one from each vessel) were removed for inspection by MTR. These had been in operation since the beginning of testing in December 2011 through June 2012 and had been exposed to flue gas for almost 1,500 hours with some additional hours on air when flue gas was not available. No particulate was found on either end of the membranes (see Figure 78) or within the membrane envelopes (see Figure 79). The membranes were in excellent condition after about 1,500 hours of operation, suggesting that the pretreatment system worked effectively and prevented fouling of the membranes by flue gas contaminants.

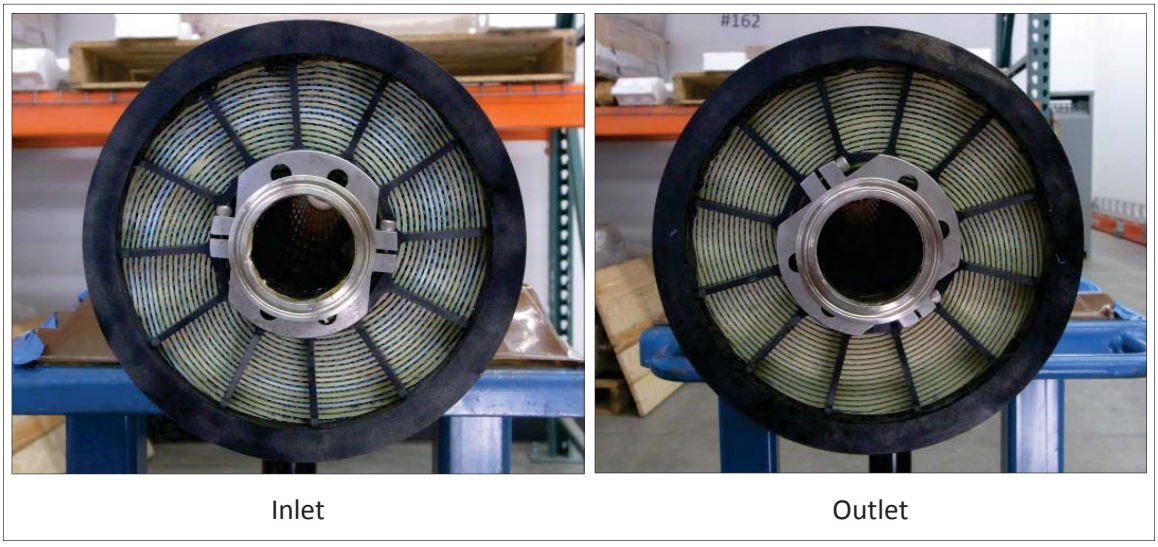

Figure 78. Inspection of MTR Cross-Flow Modules after 1,500 Hours of Operation

Figure 79. Inspection of MTR Membrane Module Sheets and Feed Spacer after 1,500 Hours of Operation

In late 2012, the Atlas Copco feed compressor was replaced with a Gardner Denver Nash liquid ring compressor to improve the overall reliability of the system. During the modification, new cross-flow and sweep modules were rotated into the system. Figure 80 shows the cumulative module performance with respect to CO_2 removal from regular coal-fired flue gas and CO_2 enrichment in the permeate streams for the modules tested between December 14, 2012, and July 11, 2013, and having a cumulative run time of over 1,300 hours. The figure shows the module performance the five periods of continuous operation. These modules again demonstrated stable performance at expected levels of separation, even after remaining idle in the membrane system several times during maintenance and flue gas outages. The fluctuation in module performance was mostly due to ambient temperature variation.

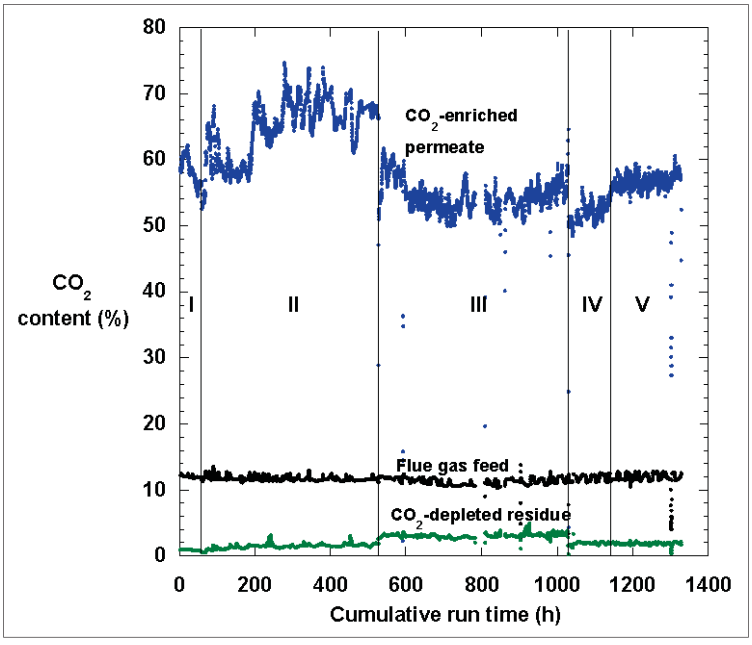

Figure 80. CO_2 Content of Inlet and Outlet Streams during Operation of MTR 1-TPD System from December 2012 to July 2013

MTR performed post-test analyses of the modules that were tested from December 2012 to July 2013. Table 31 lists the pure-gas performance and selectivity of these modules after testing,

relative to their original performance before the test. Both CO_2 permeance and CO_2/N_2 selectivity remained almost unchanged (within the error range of the pure-gas module testing system), even after going through many cycles of system re-start and shutdown and staying idle in the membrane system for over three months during a flue gas outage.

Table 31. Performance of Tested MTR Cross-Flow Modules Relative to Pre-Testing Performance

Module Number	Normalized CO_2 Permeance	Normalized CO_2/N_2 Selectivity
6704	87%	94%
6706	111%	130%

In mid-July 2013, new membrane modules were rotated onto the 1-TPD system for performance validation. The new membranes were fabricated using an optimized method combining multiple processing steps into a single step. This optimized method resulted in reduced fabrication time and labor and materials costs, translating into 15 percent cost savings in module production.

Figure 81 provides a graph of the cumulative module performance with diluted flue gas. Diluting the flue gas with air reduced the CO_2 content of the inlet flue gas from 12 to 4 percent and resulted in a significantly lower CO_2 partial pressure in the feed gas. Separation of CO_2 by membrane technology is primarily driven by the differential in the CO_2 partial pressure. Therefore, without changing the feed gas flow rate and other operating conditions, less CO_2 (percentage-basis and mass-basis) was removed from the feed gas when air-diluted flue gas was used. Nevertheless, the system still achieved excellent performance with more than 80 percent CO_2 capture and an almost 8-fold CO_2 enrichment in the permeate stream. Based on this performance, MTR's model simulations of a full process using CO_2 recycle by sweep projected an increase in the feed CO_2 content from 4 to 15 to 20 percent, resulting in a permeate stream CO_2 concentration of greater than 80 percent (suitable for final purification and compression).

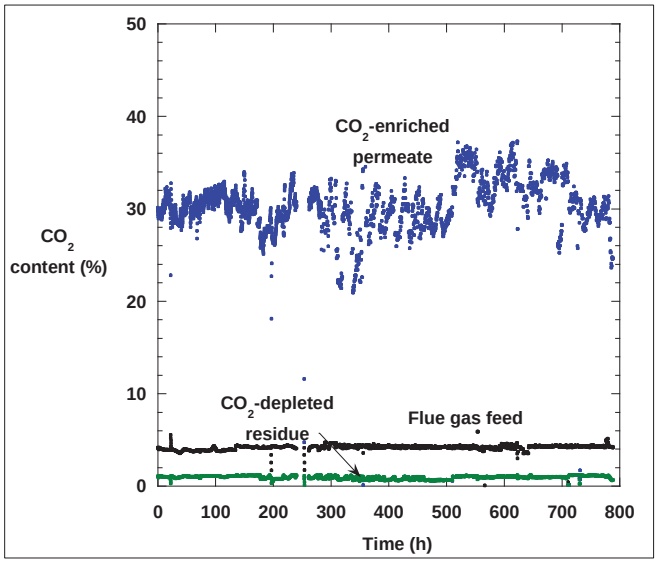

Figure 81. CO_2 Content of Inlet and Outlet Streams of the MTR 1-TPD System during Operation with Diluted Flue Gas in 2013

Testing in 2014 focused on validating the performance improvement of Polaris membranes. The 1-TPD system has two pressure vessels in parallel in the cross-flow step, which allows the testing of up to four cross-flow modules. In January 2014, two new modules made of advanced Polaris membranes were installed in one vessel for validation of performance improvement. Meanwhile, two modules that were tested in 2013 were kept in the other vessel for long-term stability monitoring. Table 32 describes the cross-flow modules being tested in early 2014.

Table 32. Polaris Cross-Flow Modules Tested in the MTR 1-TPD System in Early 2014

Module Number	Membrane Description	Testing Period
6706	Base-Case	I: 12/2012 to 07/2013; II: Since 01/2014
7143	Low-Cost	I: 07/2013 to 10/2013; II: Since 01/2014
7297	Advanced Membrane	I: Since 01/2014
7298	Advanced Membrane	I: Since 01/2014

Figure 82 shows the system performance during operation with typical coal flue gas in 2014. When the system ran at full capacity (during the first 100 hours and after 300 hours in the figure), it captured over 80 percent of the CO_2 from flue gas, and enriched the CO_2 in the permeate stream by a factor of 5.

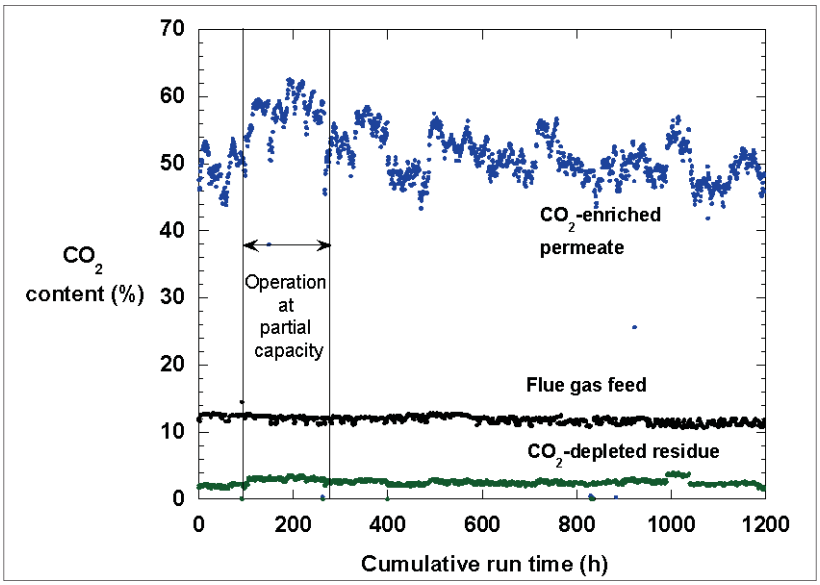

Figure 82. CO_2 Content of Inlet and Outlet Streams of the MTR 1-TPD System during 2014 Operation

The performance data of the 1-TPD system were recorded for the main streams entering and exiting each separation step, with each step having two pressure vessels in parallel. Thus, when the system ran at full capacity, only the average module performance could be obtained. To measure the module performance in each individual pressure vessel, MTR ran the system with only one vessel open in the cross-flow step between about hours 100 and 300. When the capacity of the cross-flow step was reduced to 50 percent, the system was still able to capture over 70 percent of the CO_2. Under this condition, the sweep step worked at higher removal efficiency due to the higher CO_2 content in the feed gas.

The advanced Polaris modules (modules 7297 and 7298) were made from membranes having at least 50 percent higher CO_2 permeance than that of the base-case Polaris membranes. Therefore, the modules were expected to have higher CO_2 removal capacity than the base-case modules that were tested in 2013. This was confirmed by the results plotted in Figure 83. Under similar operating conditions, the advanced module showed 60 percent higher CO_2 removal rate than the base-case module. This translates into 30 percent reduction in the membrane area, and therefore a 30 percent reduction in the membrane system cost required for achieving the same capture rate.

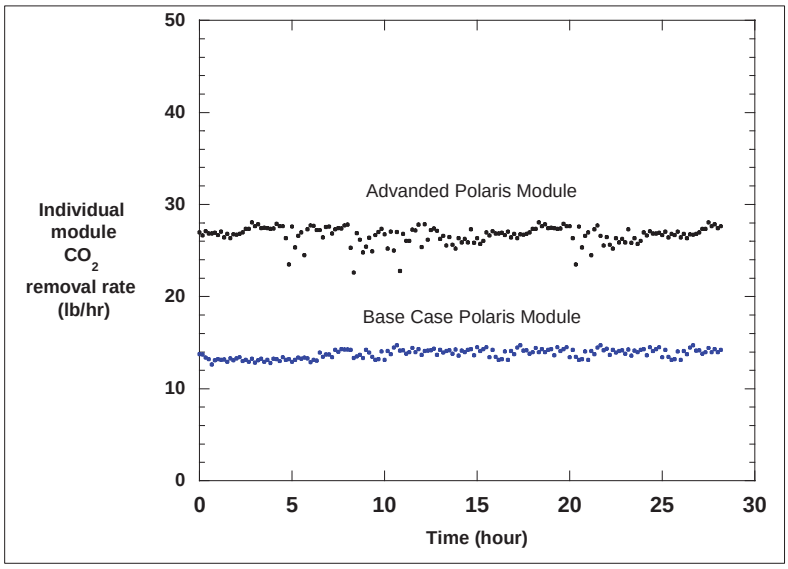

Figure 83. Comparison of CO_2 Removal by Advanced and Base Case Polaris Modules

2.11.2 Lessons Learned

Dry-screw Compressor

Selection of the dry-crew compressor for the 1-TPD system was based on previous operational experience at Cholla Power Plant. The system tested at Cholla in 2010 used an oil-flooded screw compressor that underwent severe corrosion issues caused by water condensation from flue gas. This problem can be avoided with a dry-screw compressor, because it does not use any sealing fluid to generate a high pressure ratio (inlet/outlet), and usually operates at a high temperature (360 to 380°F). In addition, the casing and screw of the Atlas Copco compressor are coated with epoxy to protect the compressor from corrosion due to atmospheric humidity. Early operation experience in 2012 showed that the dry-screw compressor had better resistance to corrosion than the oil-flooded compressor.

However, after three-months of relatively smooth operation, corrosion issues became evident, as rust and black particles were found inside the dry-screw compressor. Figure 84 provides inspection photographs of compressor components after disassembly in August 2012. Evidently, the corrosion–resistant coating degraded with long-term exposure to flue gas, leaving the compressor elements in direct contact with flue gas, and resulting in gradual corrosion. In addition, without the sealing fluid, the compressor has a tight-fit screw-casing design, which reduces the tolerance to particles, dust, and rust. These findings indicated that the dry-screw compressor is not suitable for operation with flue gas.

Figure 84. Inspection of Dry-Screw Compressor Originally Installed on MTR's 1-TPD System

Liquid Ring Compressor

Due to recurring feed compressor issues, MTR replaced the Atlas Copco dry screw compressor with a Gardner Denver Nash liquid ring compressor. Liquid ring compressors are commonly used in the petrochemical industry to handle toxic, corrosive, and explosive gases, and can be purchased with stainless steel internals. With a liquid ring as the sealing media, these compressors have a greater tolerance for solids in the feed. When operating with the liquid ring compressor in 2013, the overall reliability of the 1-TPD system was significantly improved, and no corrosion issues have been found as of this writing.

System Purging during Shutdowns

Following long-term exposure testing of modules conducted during the period in which the compressor was replaced, the modules exhibited low flux and selectivity. Inspections revealed liquid on the membrane surface and within the membrane layers. A reflectance infrared spectrum of the solid residue from the liquid showed similar peaks to that of ammonium bisulfate, suggesting that a majority of the solids present in the module were a mixture of ammonium sulfate/bisulfate (presumably produced upstream in the Gaston Unit 5 SCR). As a result of this finding, MTR implemented a procedure to purge the system with fresh air prior to shutdowns. As indicated by the subsequent test results (e.g., those listed in Table 31), the purging proved effective in preventing fouling and thus extending the membrane service time.

2.12 MTR 20-ton/day CO_2 Capture Membrane System

MTR designed and procured a 1-MWe-scale, 20-TPD CO_2 membrane test skid based on the 1-TPD system test results. In 2014, the system was installed, as shown in Figure 85, and commissioning was completed in preparation for a six-month field test in 2015. The objectives for this DOE-funded project are:

- Optimizing membrane performance and module pressure drop and fouling resistance
- Analyzing system performance, determining optimal power plant integration, and preparing a comparative study of the membrane-based process versus other CO_2 capture technologies
- Determining the impact of recycle air on boiler performance

- Evaluating the membrane potential in an industrial application

Figure 85. MTR 20-Ton/Day Test Unit installed at PC4

2.13 SRI International Sorbent

SRI International, through work funded by the DOE, is developing a novel carbon sorbent process for CO_2 capture. Figure 86 provides micrographs of the sorbent, which features several advantages, including:

- Particles that are about 1 mm, free flowing, and resistant to attrition
- Low cost with a high CO_2 loading of 0.1 to 0.2 kg/kg in the range of 68 to 212°F
- Low heat of reaction, in the range of 25 to 28 kJ/mole of CO_2, and CO_2 is released at atmospheric pressure at temperatures in the range of 176 to 212°F

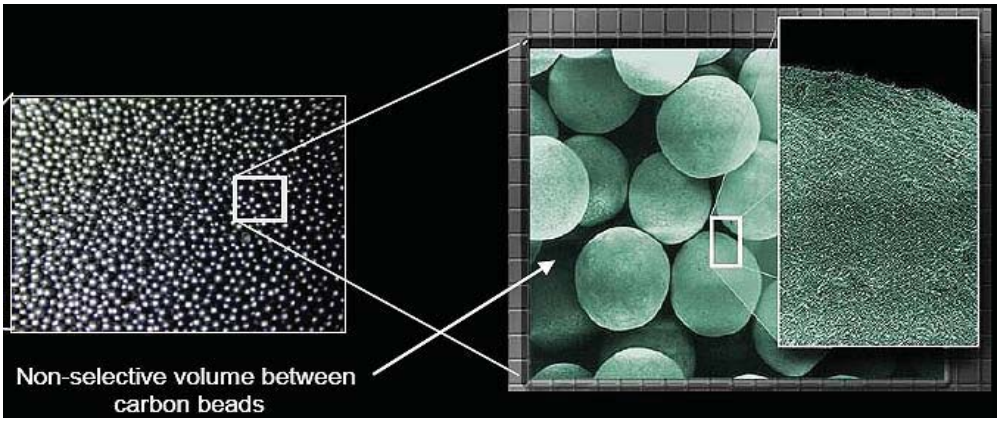

Figure 86. Micrographs of SRI International Sorbent

The SRII sorbent process includes a contactor device of structured packing which distributes the free flowing particles and provides high contact efficiency with the gas stream at a low pressure drop. The vertical design allows the adsorber and regenerator to be incorporated in a single vertical column.

SRII's 40-kWe bench-scale unit operates at near ambient temperature using a falling microbead reactor in which the sorbent granules (microbeads) fall down by gravity counter-current to the flue gas flow. The adsorbed CO_2 is removed by heating the CO_2-loaded sorbent to about 210°F in contact with low-pressure steam. The regenerated sorbent is dehydrated of adsorbed moisture, cooled, and lifted back to the adsorber. The process is designed to produce nearly pure CO_2 from the stripper. The design was tested in a smaller unit at a 3.5 kWe-scale in a small boiler at the University of Toledo for 130 hours, demonstrating CO_2 capture efficiency of 99 percent and producing over 98 percent pure CO_2.

The 40-kWe test skid was commissioned in the fourth quarter of 2013. SRII continued to operate the test skid in 2014 with flue gas to obtain additional data and experience. Following the replacement of a heat exchanger for the dehydrator, SRII performed additional testing of its sorbent process for two weeks with coal-derived flue gas, achieving greater than 90 percent purity in the stripped CO_2 stream with steam regeneration. The operation of the unit indicated certain modifications were necessary for consistent and reliable operation. The test results are summarized below:

- Continuous operation was achieved by using a combination of indirect and direct steam heating of the sorbent in the CO_2 stripper. The indirect heating demonstrated the possibility of heat recovery from the hot dehydrator exhaust.
- A steady flow of 1,200 liters/min flue gas was achieved. The flow was somewhat less than the design flow of 1,800 liters/min. While the target CO_2 capture efficiency was 90 percent, the test results showed that only 70 percent capture was achieved. The lower capture rate was attributed to less than optimal adsorber height.
- The concentration of CO_2 in the stripper outlet was 93 percent. Based on SRII's previous experience, the purity increases with steady state run time when gas flows are optimized.

SRII will continue to optimize system design and will use the PC4 operational data for further scale-up of the process to a 0.5-MWe pilot plant unit.

2.14 DOE Sorbent Unit

DOE designed the C2U to test the CO_2 removal with sorbents composed of amines on a solid substrate. The unit, which utilizes fluidized beds for both absorption and regeneration, was designed and constructed at the National Energy Technology Laboratory. NETL operated the unit for about three years in both circulating and batch modes under a variety of conditions, using two sorbents composed of polyethylenimine on a silica substrate. Testing of the C2U was conducted at the PC4 in 2014. The focus of these tests was to evaluate the accumulation of heavy metals such as selenium on the sorbent. Testing was conducted in circulating and batch modes of operation. Figure 87 shows the C2U as it was installed at the PC4.

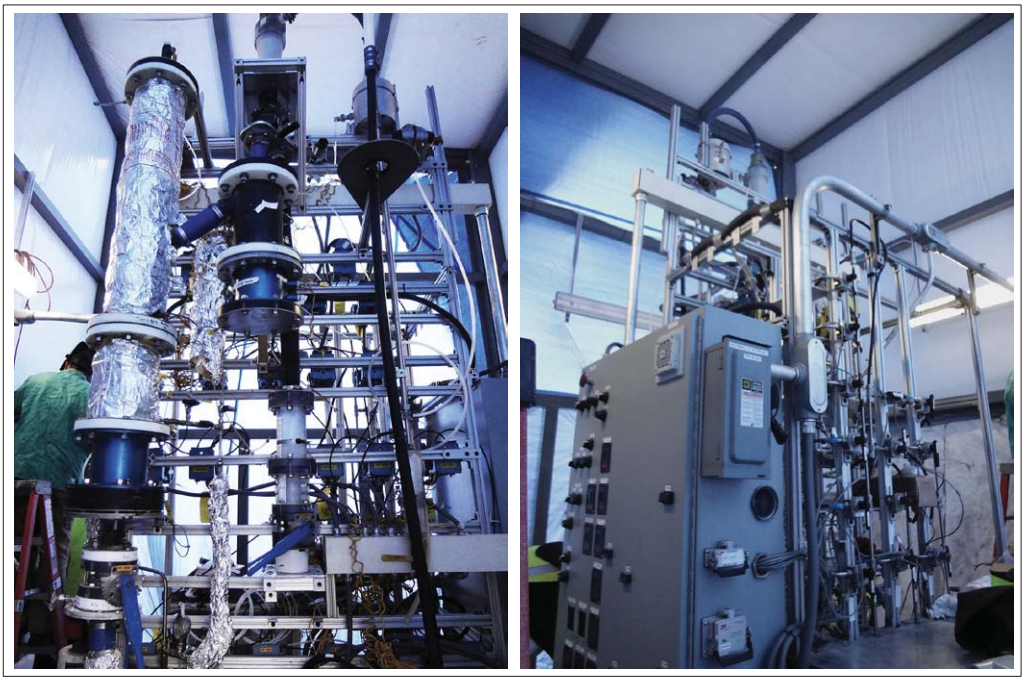

Figure 87. Assembly of the DOE Sorbent Unit

The C2U operated for about 44 hours in circulating mode during the first quarter of 2014. As testing progressed, the CO_2 capture efficiency declined, which was attributed to incomplete sorbent regeneration. Operation resumed in batch mode without regeneration from June through August, with over 346 hours of exposure under simulated natural gas conditions and 282 hours under typical coal-fired conditions. Thermo-Gravimetric Analysis of sorbent samples taken following the circulation tests and the batch tests showed no permanent loss of CO_2 capture capacity.

Analysis of the samples taken before and after testing showed that the trace element concentrations were significantly lower than the hazardous waste standards. Due to the possibility of trace elements being removed from the flue gas upstream of the sorbent, chemical analysis of the inlet flue gas stream is recommended to better gauge trace element accumulation.

2.15 Linde-BASF Solvent and Process

Linde and BASF will demonstrate a 1-MWe CO_2 capture pilot plant processing up to 30 tons CO_2 /day at the PC4. The technology incorporates BASF's novel amine-based process along with Linde's process and engineering innovations, as highlighted in Figure 88. Prior to the design and construction of the plant, the group completed a technical-economic assessment of the process to illustrate the benefits of this DOE-funded project.

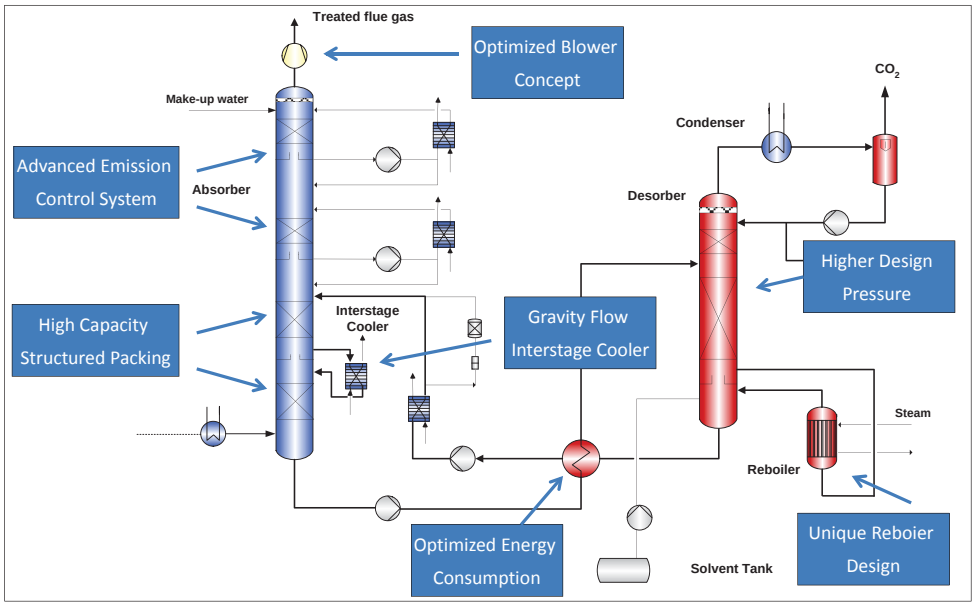

Figure 88. Linde-BASF Process Diagram

Construction and installation of the unit, shown in Figure 89, was completed in 2014. Pre-commissioning activities were completed, and the system was made ready for flue gas operation in 2015. Linde will perform parametric tests to demonstrate the achievement of target performance using data analysis, and will implement long duration tests to demonstrate solvent stability and obtain critical data for scale-up and commercial application.

Figure 89. Installation of the Linde-BASF Pilot Unit

3.0 GASIFICATION

The NCCC gasification process, represented in Figure 90, features the Transport Gasifier, a circulating fluidized bed reactor (see description below in this section). The process includes dry feed systems, syngas coolers, the PCD for hot gas particulate filtration, continuous ash depressurization systems for ash cooling and removal, and a syngas recycle system. Gasification operation, which began in 1999, provides syngas for testing of gasification-related technologies in addition to testing of pre-combustion CO_2 capture technologies. Typical composition of the syngas produced by the NCCC gasifier is given in Table 33. Because of the experimental nature of the NCCC work, the syngas contains a higher concentration of nitrogen than that produced from a commercial Transport gasifier.

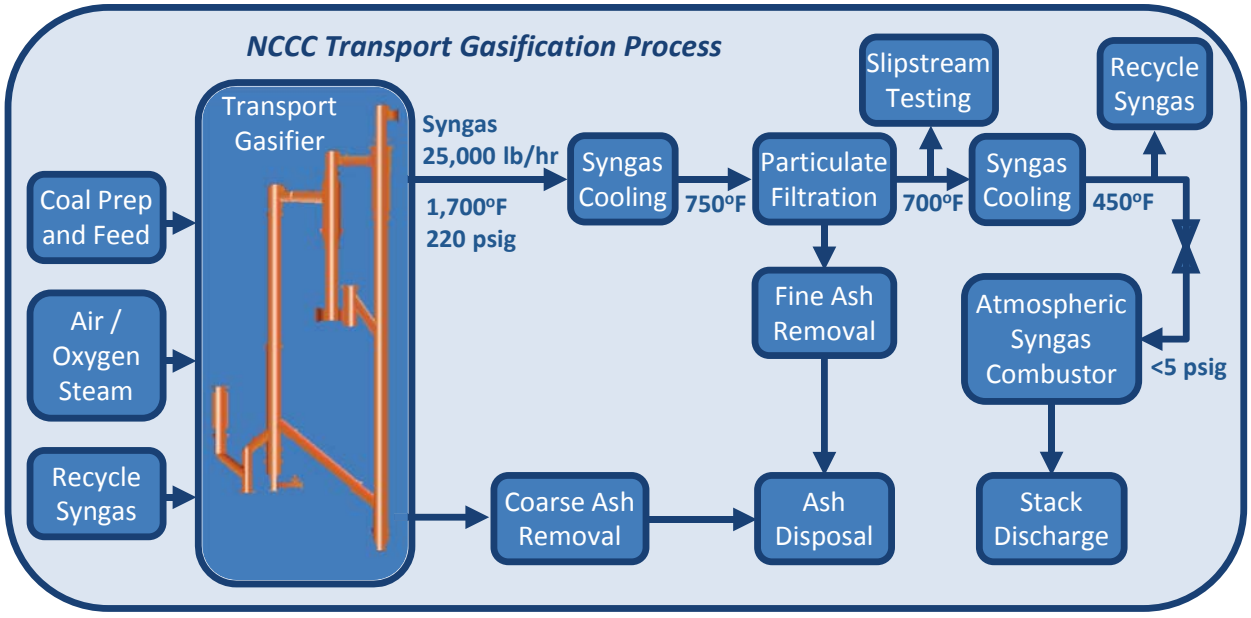

Figure 90. Schematic of NCCC Gasification Process with Operating Conditions

Table 33. Typical Syngas Composition for Air-Blown and Oxygen-Blown Gasification

Syngas Component	Air-Blown	Oxygen-Blown
H_2O, vol%	10	29.9
CO, vol%	8.6	8.2
H_2, vol%	6.9	12.8
CO_2, vol%	8.7	13.5
CH_4, vol%	1.1	1.4
N_2, vol%	64.4	34.1
NH_3, ppm	1,988	2,938

Coal Preparation and Feeding

The coal used as the gasifier feedstock is processed on site. The material is crushed, dried in the fluid bed dryer when necessary, and pulverized to a nominal particle diameter between 250 and

400 microns. Coal is fed to the gasifier using two systems, the original coal feed system and a secondary coal feed system. The original feed system is a lock hopper, horizontal pocket feeder design with a rotary dispenser. The second, developmental PDAC feeder was designed on-site. Like the original feeder, the PDAC system is a lock hopper-based system, but it differs in that it uses conveying gas flow to control the solids feed rate. Coal is fed to the gasifier using one or both feeders at a nominal rate of 4,000 lb/hr.

Transport Gasifier

The Transport Gasifier, shown in Figure 91, is a pressurized, advanced circulating fluidized bed reactor, consisting of a mixing zone, riser, solids separation unit, seal leg, standpipe, and J-leg. The gasifier is equally capable of using air or oxygen as the gasification oxidant. A mixture of air or oxygen with steam is fed into the mixing zone at different elevations and orientations to evenly distribute heat generated from the partial combustion of the circulating solids. The oxygen from the air or pure oxygen feed is completely consumed in this section of the gasifier. The coal is fed at a higher elevation in the mixing zone where the atmosphere is reducing, or oxygen-free. Heat up of the gasifier prior to coal feed is achieved using a direct-fired propane burner.

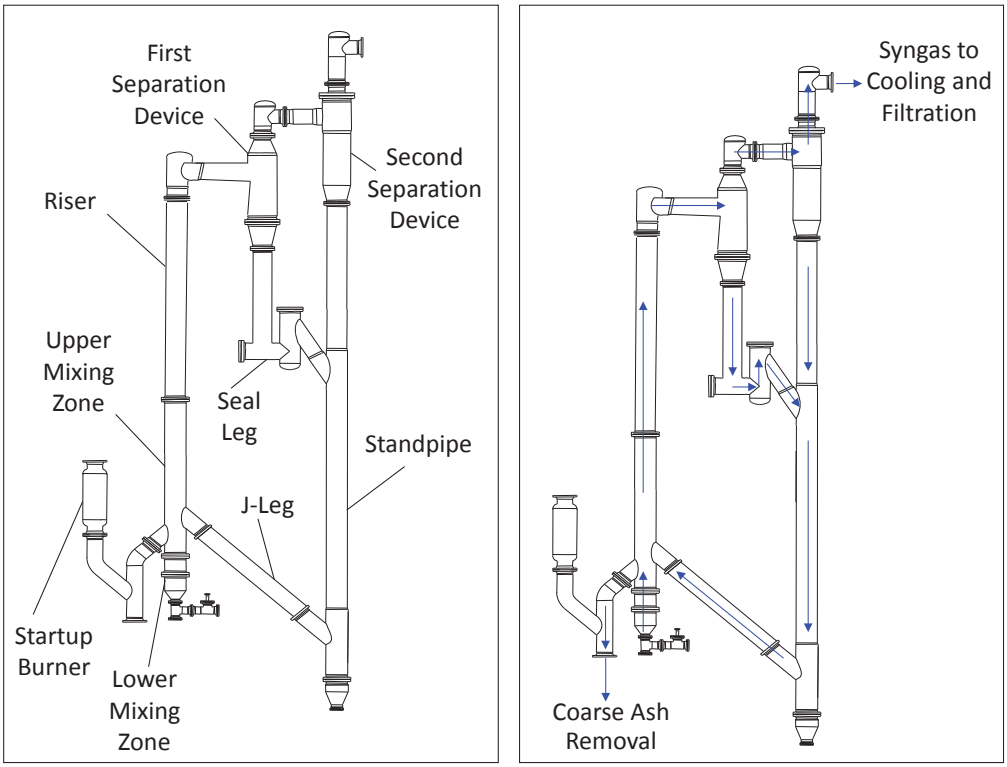

Figure 91. Schematic of NCCC Transport Gasifier

Gasifier Solids Removal

As the coal devolatilizes and chemical reactions occur to generate syngas, the gas and solids move up the riser and enter the solids separation unit. This unit contains two solids separation devices, which use cyclonic action to remove particles. Between the first and second solids separation devices is the seal leg, which prevents backflow of gas. The solids collected by the

separation unit are recycled back to the mixing zone through the standpipe and J-leg. The gasifier solids inventory is controlled by removing gasification ash through the continuous coarse ash depressurization system, which cools and depressurizes the solids. The nominal gasifier operating temperature is 1,800°F, and the gasifier system is designed to have a maximum operating pressure of 294 psig with a thermal capacity of about 41 MBtu/hr.

Particulate Filtration

The syngas exits the gasifier, passes through the primary gas cooler where the gas temperature is reduced to about 750°F, and enters the PCD, where particulate concentrations are reduced from 10,000 to 30,000 ppmw down to less than 0.1 ppmw. The PCD utilizes a tube sheet holding up to 91 filter elements, with failsafe devices located downstream of the elements to stop solids leakage by plugging in the event of element failures. High-pressure nitrogen back-pulsing, typically lasting 0.2 seconds, is used to clean the elements periodically to remove the accumulated gasification ash and control the pressure drop across the tube sheet. The solids fall to the bottom of the PCD and are cooled and removed through the continuous fine ash depressurization system.

Syngas Conditioning Unit

After exiting the PCD, a portion of the syngas, up to 1,500 lb/hr, is fed to the SCU, providing a means to test various pollutant control technologies, including removal of sulfur and mercury compounds, and CO_2 capture. The SCU is also used to test other power technologies such as fuel cells.

Recycle Syngas

The main stream of syngas is then cooled in a secondary gas cooler, which reduces the temperature to about 450°F. Some of this gas may be compressed and sent to the gasifier for aeration to aid solids circulation. The recycle gas compressor is a vertically mounted centrifugal compressor which operates at 500 to 600°F and was designed for a throughput of about 2,000 to 3,000 lb/hr.

Final Syngas Processing

The remaining syngas is reduced to near atmospheric pressure through a pressure control valve. The gas is then sent to the atmospheric syngas combustor, which oxidizes the syngas components. The flue gas from the atmospheric syngas combustor flows to a heat recovery boiler and then is discharged out a stack. A flare is available to combust the syngas in the event of a system trip.

3.1 Gasification Operation

During the contract period, the gasification process operated for about 9,500 hours over 13 test runs, R01 through R13, bringing the total gasification operating experience beginning in 1999 to over 21,080 hours. The gasifier operated in air-blown mode for the majority of testing, with portions of runs R02 and R08 conducted in oxygen-blown mode to support specific technology development. The fuels used included Mississippi lignite from the Red Hills mine and from the Liberty Fuels mine, PRB coal, and raw and torrefied biomass. Table 34 summarizes the gasification runs and the technologies tested.

Table 34. Summary of Gasification Test Runs

Run	Start Date	Duration, hr	Fuel	Developer Technologies Tested
R01	2/09	516	Red Hills Lignite	JM Hg Sorbent; MPT Membrane; WGS
R02	8/09	477 (47 O_2)	PRB	NETL Fuel Cell; WGS Catalyst
R03	11/09	578	PRB, Biomass (200 hr)	MPT & MTR Membranes; WGS Catalyst
R04	4/10	509	Red Hills Lignite, Biomass (109 hr)	JM Hg Sorbent; MPT & MTR Membranes; WGS Catalyst
R05	7/10	1,000	PRB	JM Hg Sorbent; MPT & MTR Membranes; WGS Catalyst; NETL Mass Spectrometer
R06	5/11	1,207	PRB	JM Hg Sorbent; MTR & WPI Membranes; WGS Catalyst
R07	10/11	996	PRB	TDA Sorbent; MPT, MTR, & WPI Membranes; WGS Catalyst
R08	6/12	722 (219 O_2)	PRB, Biomass (219 hr)	CCAT Biomass/O_2-Blown Gasification; WPI, MPT & MTR Membranes; WGS Catalyst
R09	11/12	545	PRB	Stanford TDL; MPT, MTR, WPI, & Eltron Membranes; UA CO_2 Solvent; WGS Catalyst
R10	3/13	827	PRB	JM Hg Sorbent; MPT, MTR, & WPI Membranes; TDA CO_2 Sorbent; WGS Catalyst; UA CO_2 Solvent
R11	8/13	770	Liberty Fuels lignite	MPT, MTR, & WPI Membranes; WGS Catalyst
R12	11/13	516	PRB	MTR & WPI membranes; NETL CO_2 solvent; WGS & COS hydrolysis Catalysts
R13	3/14	839	PRB	JM Hg Sorbent; Stanford TDL; OSU SCL; SRI FT; MTR & WPI Membranes; WGS &COS Hydrolysis Catalysts

3.1.1 Lignite Operation

Operation with lignite during the reporting period utilized Mississippi high moisture lignite from the Red Hills Mine in Choctaw County and from the Liberty Fuels mine in Kemper County. Table 35 lists the properties of these two fuels. For the Liberty Fuels lignite, steady state carbon conversion ranged from 98.2 to 99.9 percent, averaging 98.6 percent.

Table 35. Average Properties of Mississippi Lignite Used in Gasification Runs

Coal Property	Red Hills	Liberty Fuels
As-Received Carbon, wt %	33.0	34.0
As-Received Hydrogen, wt %	2.2	2.3
As-Received Nitrogen, wt %	0.6	0.6
As-Received Sulfur, wt %	0.4	1.0
As-Received Ash, wt %	11.0	8.7
As-Received Oxygen, wt % (by difference)	9.8	7.9
As-Received Volatiles, wt %	24.8	23.4
As-Received Fixed Carbon, wt %	21.0	22.8
As-Received Heating Value, Btu/lb	5,610	5,750
As-Received Moisture Concentration, wt%	41.5	41.8
As-Fed Moisture Concentration, wt%	17.5	17.5
As-Fed Mass Median Diameter, micron	398	396

R01 was the third test run using high moisture Mississippi lignite from the Red Hills Mine, and a major goal of this run was to optimize gasifier operation with this coal. Figure 92 plots the carbon conversion versus gasifier temperature for R01 and the preceding Mississippi lignite test (TC25). The data were taken from steady state operating periods with comparable operating conditions (i.e., approximately the same coal feed rates, pressures, air-to-coal ratios). The figure shows that carbon conversion was not a strong function of temperature, and that high carbon conversions can be achieved at a range of temperatures due to the extremely high fuel reactivity.

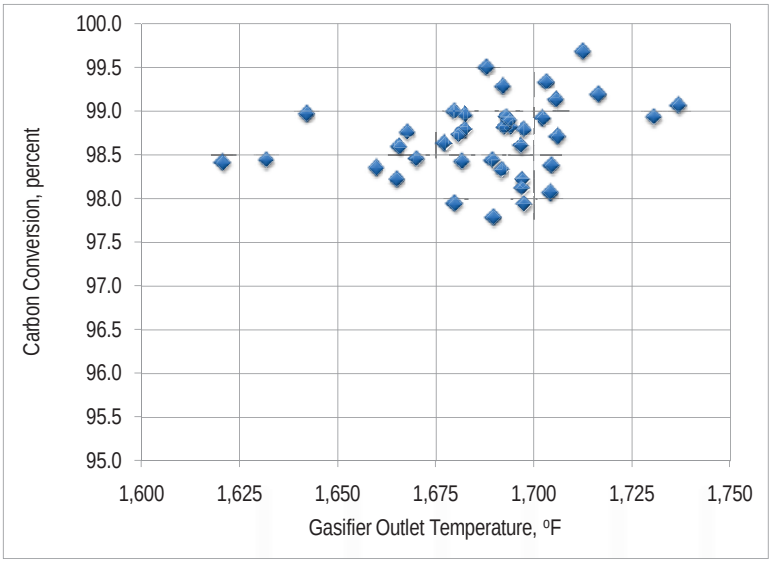

Figure 92. Carbon Conversion versus Gasifier Temperature during Red Hills Lignite Operation

Figure 93 plots the gasifier circulation rate as a function of standpipe level for R01 and previous Mississippi lignite testing. This figure shows some spread of data (particularly at around 200 inH_2O standpipe level) due to other operating factors such as fluidization flow in the standpipe and J-leg. In general, though, the data showed a positive correlation and demonstrated good controllability of the gasifier with this fuel.

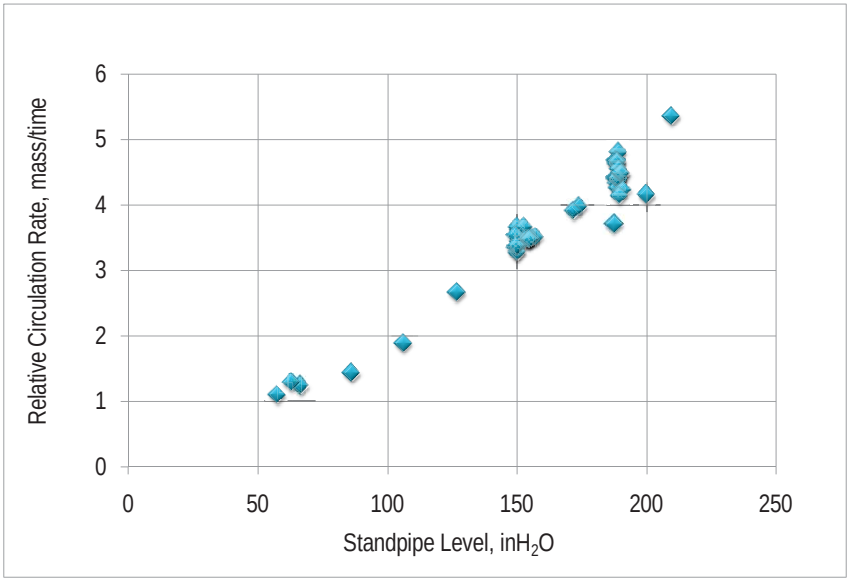

Figure 93. Gasifier Circulation Rate as a Function of Standpipe Level during Red Hills Lignite Operation

Gasifier operation with Liberty Fuels lignite was not significantly different from that with Red Hills lignite. Table 36 provides carbon conversions for the lignite operation.

Table 36. Steady State Carbon Conversions with Lignite Coal

Lignite Source	Average	Minimum	Maximum
Red Hills Mine(R01)	99.1	98.4	99.9
Red Hills Mine (R04)	99.3	97.6	99.9
Liberty Fuels Mine	98.6	98.2	99.9

3.1.2 PRB Operation

The majority of gasification operation at the site has been conducted with PRB coal, comprising a blend from the Southern PRB mines of Jacobs Ranch, Black Thunder, North Antelope/Rochelle, and Antelope. The gasification process and hardware had been optimized using this coal, and operation with PRB provides consistent performance for evaluation of gasification and pre-combustion technologies. During all testing of PRB, gasification yielded high carbon conversions due to the high reactivity of this coal, with run average steady state values ranging from 98.1 to 99.2 percent and maximum steady state values up to 99.9 percent.

Table 37 provides the ranges of the mean values for the coal properties for all PRB test runs.

Table 37. Properties of PRB Coal Used in Gasification Runs

Coal Property	Average
As-Received Carbon, wt%	51.3
As-Received Hydrogen, wt%	3.4
As-Received Nitrogen, wt%	0.8
As-Received Sulfur, wt%	0.3
As-Received Ash, wt%	6.9
AS-Received Oxygen, wt% (by difference)	12.6
As-Received Volatiles, wt%	34.7
As-Received Fixed C, wt%	33.5
As-Received Heating Value, Btu/lb	8,920
As-Received Moisture Concentration, wt%	26.0
As-Fed Moisture Concentration, wt%	20.0
Moisture Content Reduction, %	22.7
As-Fed Mass Median Diameter, microns	396

3.1.3 Biomass Operation during R03 and R04

The NCCC conducted biomass testing to support the DOE goal of development of gasification technologies for the conversion of biomass into clean, sustainable energy and other products. The gasification system operated for the first time co-feeding biomass with PRB coal for 200 hours in run R03. In run R04, biomass was co-fed with lignite coal for 100 hours. The biomass used was in the form of raw wood pellets (see Figure 94), supplied by Green Circle Bio Energy, which were milled and fed to the pressurized gasifier in a dedicated feeder at rates from 500 to 2,500 lb/hr, about 20 weight percent of the total feed rate. Biomass co-feeding during oxygen-blown gasifier operation, conducted in run R08, is discussed separately in Section 3.1.4.

Figure 94. Wood Pellet Biomass Used as Gasification Feedstock in R03 and R04

Pre-Run Biomass Studies

Successful operation with the biomass/coal blend required the NCCC staff to address several challenges associated with feeding and gasifying biomass. First, because biomass is fibrous, it

can be difficult to pressurize and reliably convey. Second, compared to coal, biomass ash can be more prone to agglomerate at gasifier conditions and has the potential to be corrosive. Last, biomass gasification can lead to excess tar formation, which can foul downstream equipment. After assessing the available biomass options, wood pellets were selected for testing because they are currently produced on a commercial scale; the particle size and low moisture content of milled pellets make the material suitable for existing coal mills and feeders in the gasification process; and the low ash and chlorine content reduces the risk of ash agglomeration and corrosion issues.

Preliminary testing completed during 2009 consisted of milling and feeding the biomass at rates from 400 to 3,000 lb/hr in a pressurized off-line system (independent of the gasification process), and showed that reliable feeding could be achieved. Laboratory studies of biomass co-gasification included agglomeration testing, during which blends of biomass and coal ash at varying weight ratios were baked in a muffle furnace at typical gasifier operating temperatures. The baked samples were examined visually, by optical microscopy, and by scanning electron microscopy with energy-dispersive X-ray analysis for signs of agglomeration tendencies. The laboratory testing indicated that the biomass was not prone to agglomeration and was suitable for testing in the gasification process. By adjusting the process parameters according to the preliminary test data, the gasification process operated with reliable feeding and with no evidence of ash agglomeration, corrosion, or excessive tar formation.

3.1.3.1 Biomass Fuel Handling and Feeding

The biomass was milled using the existing roller mill systems. Table 38 lists the R03 and R04 biomass moisture and particle size data before and after milling. A few modifications were made to the mill operational settings for system air flow and mill speed to effect the final particle size distribution. Additionally, system pressure was decreased to raise air flow rates in order to improve material feed from the mill outlet cyclone collector to the pulverized silo. This change was necessary due to the difference in physical properties of biomass relative to coal.

Table 38. Average Biomass Properties before and after Milling

Biomass Property	R03	R04
As-Received Moisture Content, wt %	7	7
As-Fed Moisture Content, wt %	4	4
Moisture Content Reduction, %	43	43
As-Fed Mass Median Diameter, micron	930	830
As-Fed Oversize (>1,180 micron) Content, wt %	38	29
As-Fed Fine (<45 micron) Content, wt %	11	1

While mill system operation was satisfactory, problems occurred during R03 with the dense phase pneumatic conveyor that transfers the processed biomass from the mill system pulverized storage silo to the coal feeder storage silo. The root cause of the transfer problems was a combination of flow restrictions in the discharge piping and insufficient conveying gas supply. During the outage between run R03 and R04, the piping layout was modified to reduce the number of elbows and other areas of unnecessary pressure drop. Additionally, the conveying gas supply to the dense phase feeder was increased and booster gas was added to elbows in the

transfer line. These changes resulted in improved system operation when compared to R03 operation, maintaining solids velocity requirements high enough for consistent transfer of the low density biomass material. While it is recognized that the dense phase conveying is not as well suited for this application as other pneumatic conveying methods (i.e., dilute phase conveying with higher gas to solids ratios), the modifications incorporated provided the most economical path to successful conveying of the biomass at the NCCC.

3.1.3.2 Gasifier and Gas Cooler Operation

Gasifier operation during coal only feeding and during co-feeding of coal and biomass yielded high carbon conversions, as shown in Table 39.

Table 39. Steady State Carbon Conversions with Coal and Biomass Co-Feed in R03 and R04

	Maximum		Minimum		Average	
	R03	R04	R03	R04	R03	R04
Coal Only Carbon Conversion, %	98.7	99.9	97.1	97.6	98.3	99.1
Biomass Co-Feed Carbon Conversion, %	99.6	99.9	98.9	99.3	99.2	99.6

Inspections of gasifier ash samples taken during coal-only feed and during co-feeding periods did not indicate agglomeration (see Figure 95). Additionally, the primary gas cooler performance remained stable, and condensate sampling did not indicate any evidence of tar formation.

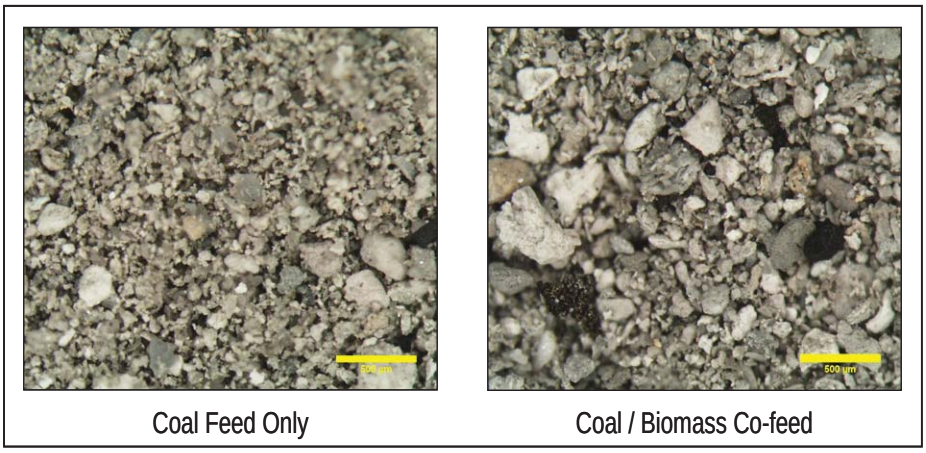

Figure 95. Gasifier Ash Samples during Coal-Only Feed and during Biomass Co-Feed in R04

During the final hours of test run R04, a period of biomass feed only was tested. Primary gas cooler performance began to deteriorate soon after establishing biomass only feed to the gasifier, as the cooler outlet temperature began to rise (evidence of tube fouling). Eventually, this decrease in performance resulted in the end of gasifier operations for R04. Post-run inspections revealed fouling in the primary gas cooler tubes, as shown in Figure 96. Analysis of tube foulant samples indicated the presence of tars but did not reveal any alkali metal content, which can also provide a mechanism for fouling.

Figure 96. Post-R04 Run Inspection of Primary Gas Cooler Tubes

3.1.3.3 Effect of Biomass Co-Gasification on Ash Characteristics

Table 40 lists the characteristics of the ash entering the PCD during gasifier operation with and without biomass co-feeding. Because of the low ash content of the biomass, the addition of biomass reduced the inlet ash concentration with both the PRB coal and the Mississippi lignite. The addition also increased the bulk density and true density of the ash, while reducing the bulk porosity and surface area. The loss on ignition was also reduced, suggesting that the biomass addition improved carbon conversion. There was no significant effect on mean particle size of the ash, as this is controlled primarily by the gasifier solids separation devices.

Table 40. Effect of Biomass Co-Gasification on Ash Characteristics

Gasifier Fuel	Bulk Density, g/cm^3	True Density, g/cm^3	Bulk Porosity, %	Loss on Ignition, %
PRB Coal (R03)	0.25	2.64	90.5	19.2
PRB Coal and Biomass (R03)	0.35	2.74	87.2	9.8
MS Lignite (R04)	0.45	2.62	82.8	10.3
MS Lignite and Biomass (R04)	0.52	2.77	81.1	2.1

Figure 97 shows the effect of biomass addition on the particle-size distribution of ash entering the PCD as measured by Microtrac laser diffraction analysis of the PCD inlet ash samples. The results are presented as a series of differential mass distributions that represent a differentiation of the cumulative mass loading curve. This type of presentation is widely used with fine particle measurements, because the dM/dlogD value reflects the mass concentration of particles in a given size band, and the area under the curve between any two points indicates the mass concentration of particles within that particle size range. As indicated in the figure, the addition of biomass reduced the mass concentration of ash over almost the entire particle size range. With PRB coal, the mass reduction occurred over the range of about 1 to 50 microns. With Mississippi lignite, the reduction was evident over the range of about 0.5 to 30 microns. Little difference is seen in the distributions at the upper end, because those particles are largely removed by solids separation devices in the gasifier.

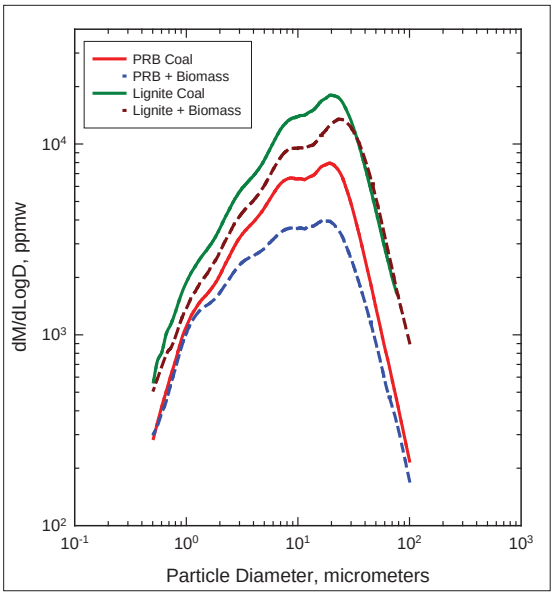

Figure 97. Particle-Size Distributions of Ash Measured at PCD Inlet

Effect of Biomass Addition on Transient Drag

Past studies showed that dustcake drag generally decreases with decreasing ash carbon content indicated by decreasing loss on ignition (LOI). Since the LOI was reduced by the addition of biomass, a commensurate reduction in the dustcake drag was expected. In keeping with previous results, the drag was proportional to the LOI as indicated in Figure 98. The lignite ash has lower drag than that of the PRB due to differences in ash morphology and the slightly larger particle size of the lignite ash resulting in less flow resistance. For both fuels, the lowest drag occurred with coal and biomass co-feeding. Based on these results, the addition of biomass would not adversely affect PCD pressure drop.

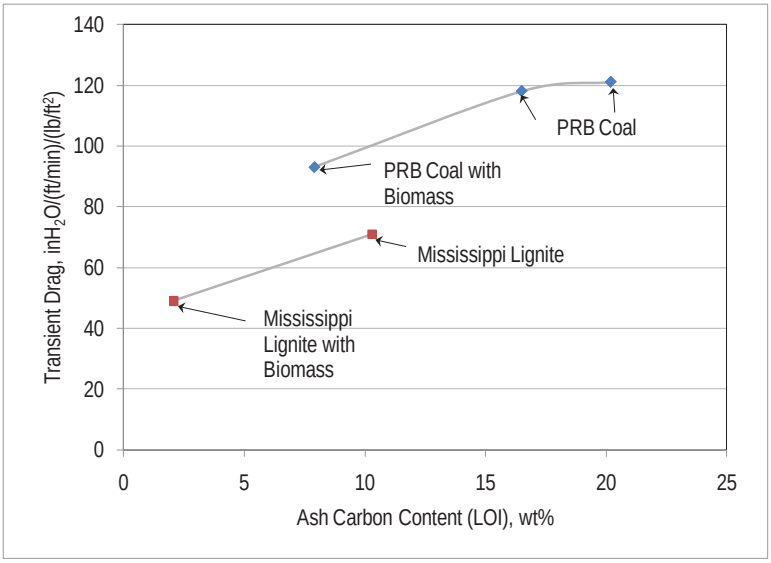

Figure 98. Transient PCD Drag as a Function of Carbon Content

Laboratory Drag Measurements

Figure 99 shows dustcake drag as a function of particle size using the re-suspended ash permeability tester in the on-site laboratory. In these measurements, the ash samples obtained with and without biomass addition are re-suspended in a fluidized bed and passed through various combinations of small cyclones to produce ashes with a range of particle sizes. The ash from the cyclones is collected on a sintered metal plate. Monitoring the flow and pressure drop during the build-up of the dustcake on the sintered plate and weighing the collected cake allows the dustcake drag to be determined as a function of particle size.

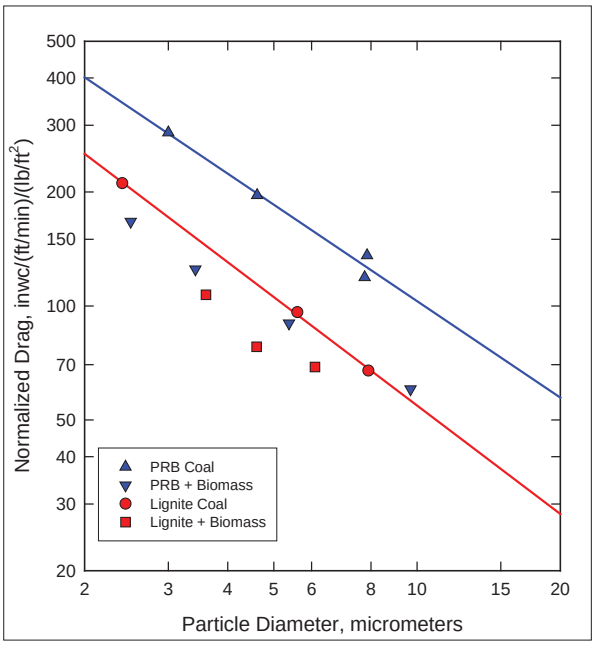

Figure 99. Effect of Biomass Addition on Laboratory Drag Measurements of Ash

As shown in Figure 99, the dust cake drag with both the PRB coal and Mississippi lignite is lower for ashes with biomass addition over the particle size range studied (approximately 2 to 10 microns). This difference is considered to arise primarily from the effect of carbon content shown in Figure 98. From the two figures, it can be concluded that the transient drag of the dust cake is inversely proportional to its mean particle size and proportional to its carbon content, although there is also likely a contribution from other morphological differences.

3.1.4 Biomass Operation in Oxygen-Blown Gasification during R08

During the final portion of the R08 run, 219 hours of oxygen-blown gasification testing were conducted with biomass co-feed on behalf of CCAT. CCAT received funding through the Department of Defense as part of its initiative to develop alternative liquid fuels for U.S. military applications through the utilization of gasification techniques and sustainable fuel sources such as biomass. Previous gasification testing had been conducted by CCAT at the Energy and Environmental Research Center (EERC) of the University of North Dakota utilizing biomass co-feed with coal in the EERC Transport Gasifier. Testing at the NCCC provided an opportunity to validate data collected from testing at the EERC at a larger scale, and extended the biomass operational experience the NCCC obtained previously during the R03 and R04 runs.

3.1.4.1 Test Objectives and Results

The test plan included co-feed testing of both raw and torrefied southern pine biomass pellets with PRB coal at concentrations ranging from 10 to 30 wt% of the total feed to the gasifier. Each test condition was maintained for approximately 24 hours to allow for all required sampling and analysis to be conducted. The objectives for testing were developed jointly by CCAT and NCCC as follows:

- Collect test results and compare with those obtained from the EERC test to determine if operating at a larger scale results in better conversion, higher efficiency, and a syngas quality more suitable for producing liquid fuels
- Achieve the desired coal-biomass mixtures with separate feeding of coal and biomass
- Demonstrate gasification of the coal–biomass mixtures under the test conditions
- Determine carbon conversion and the amount of carbon in the gasifier solids for each test condition
- Demonstrate successful gasifier circulation without forming deposition or agglomeration
- Determine the extent of tars production with the coal/biomass mixtures in the gasifier
- Evaluate hot gas filtration performance at each test condition
- Monitor gasifier operating parameters including solids circulation rate, syngas recirculation rate, and coal/biomass blend

One of the NCCC mill systems was dedicated during the run to processing biomass. The raw biomass pellets, shown in Figure 94, had been previously used as feedstock during the R03 and R04 runs. This was the first gasification operation with torrefied biomass pellets, which are shown in Figure 100. The torrefied pellets had mill operational characteristics similar to PRB coal due to the breakdown of the wood fiber structure by the torrefication process.

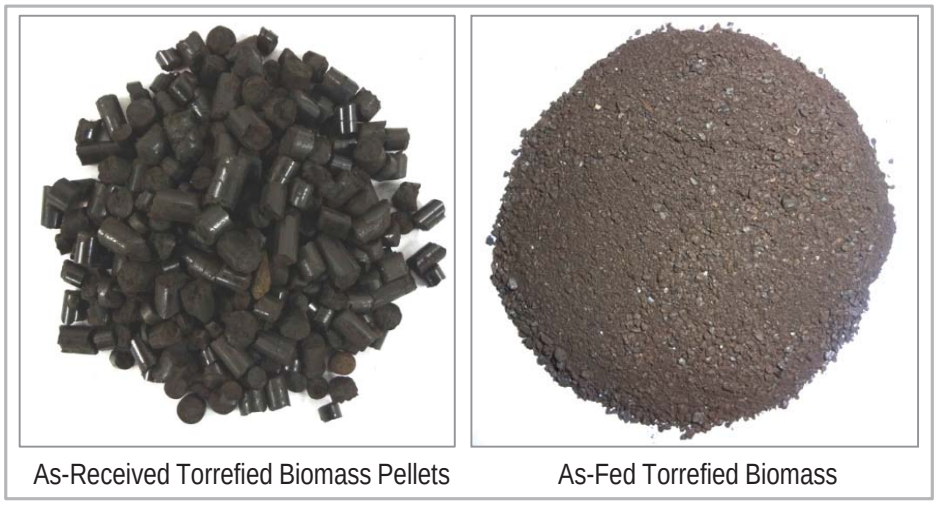

Figure 100. Torrefied Biomass for R08 Co-Feeding

The average particle size distributions for the three feedstocks are shown in Figure 101, with the torrefied biomass more closely following the normal distribution for PRB coal. For the run, a total of 1,600 tons of PRB coal and 41 tons each of torrefied and raw biomass were processed. Table 41 lists the as-received and as-fed properties of the coal and biomass.

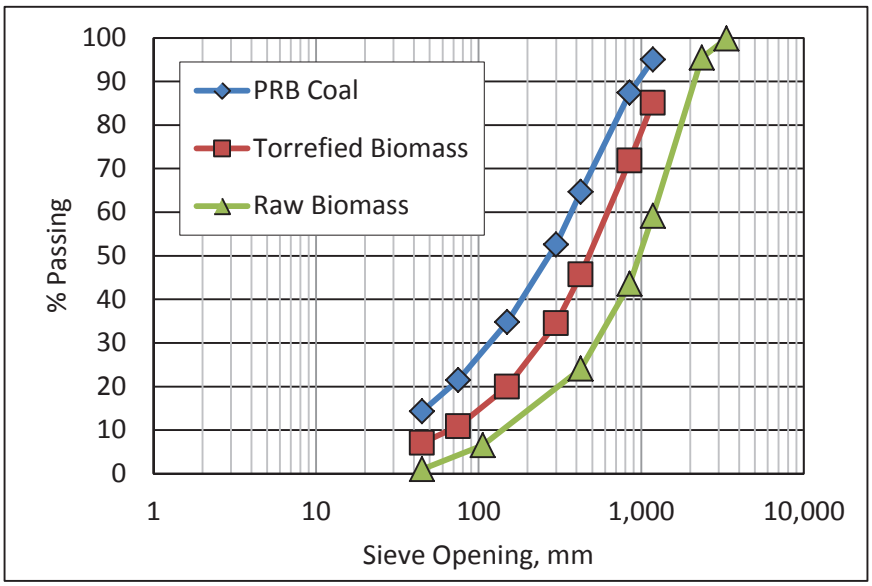

Figure 101. Particle Size Distribution Curves for R08 Gasifier Feedstocks

Table 41. Properties of Coal and Biomass Feedstocks for R08

Property	PRB Coal	Torrefied Biomass	Raw Biomass
As-Received Carbon, wt %	52.1	57.5	48.5
As-Received Hydrogen, wt %	3.5	5.3	5.7
As-Received Nitrogen, wt %	0.9	0.3	0.02
As-Received Sulfur, wt %	0.2	0.01	0.06
As-Received Ash, wt %	6.6	1.8	1.2
As-Received Oxygen, wt % (by difference)	12.1	30.9	38.4
As-Received Volatiles, wt %	42.3	65.3	72.2
As-Received Fixed Carbon, wt %	26.4	28.8	20.3
As-Received Heating Value, Btu/lb	8,960	9,670	8,070
As-Received Moisture Concentration, wt%	25	4.2	6.3
As-Fed Moisture Concentration, wt%	18	7.8	8.0
As-Fed Mass Median Diameter, micron	280	536	990
As-Fed Oversize (>1,180 micron) Content, wt%	5	14.9	40.8
As-Fed Fine (<45 micron) Content, wt%	14	7.1	1.0

The increase in moisture concentration of both forms of biomass after milling operations was unexpected. Two potential causes were longer than planned exposure to ambient moisture before material processing began and lower mill system exhaust gas flow (i.e. higher recycle gas flow) leading to higher relative moisture levels inside the mill system.

After establishing steady gasification operation with PRB feed, torrefied biomass was fed followed by the raw biomass. The actual co-feed percentages for the torrefied biomass were 17, 20, and 29 wt%. Due to the turndown limits of the rotary feeder and the bulk density of the torrefied material, the lowest percentage co-feed was higher than the planned 10 wt%. The actual co-feed percentages for the raw biomass were 12, 20, and 28 wt%. The lower bulk density of the raw biomass allowed for a closer approach to the planned lower co-feed test condition.

Gasifier operating conditions remained stable during all tests and yielded high carbon conversions during both coal-only and biomass co-feed operation, as shown in Table 42. Syngas lower heating values (LHVs) also remained stable during the biomass co-feed periods.

Table 42. Coal and Biomass Co-Feed Operating Parameters

Operating Parameter	PRB Coal Only	Torrefied Biomass Co-Feed			Raw Biomass Co-Feed		
		17 wt%	20 wt%	29 wt%	12 wt%	20 wt%	28 wt%
Gasifier Exit Temp., °F	1,707	1,699	1,698	1,699	1,701	1,708	1,692
Coal Feed Rate, lb/hr	3,607	3,302	3,259	3,201	3,552	3,386	2,784
Biomass Feed Rate, lb/hr	0	652	795	1,288	472	835	1,100
Total Feed Rate, lb/hr	3,607	3,954	4,054	4,489	4,024	4,221	3,884
Oxygen/Fuel Ratio, lb/lb	0.80	0.78	0.76	0.72	0.75	0.71	0.74
Steam/Fuel Ratio, lb/lb	1.20	1.15	1.11	1.02	1.12	1.06	1.18
Carbon Conversion	98.3	98.2	98.4	98.2	98.5	98.0	98.2
Syngas LHV, Btu/scf	97.7	86.7	97.6	110.8	96.7	98.0	95.2

No evidence of agglomeration was observed in the gasifier circulating solids, and the ash removal systems operated without incident. Figure 102 displays the range of ash particle size distributions for both ash discharge systems during the testing.

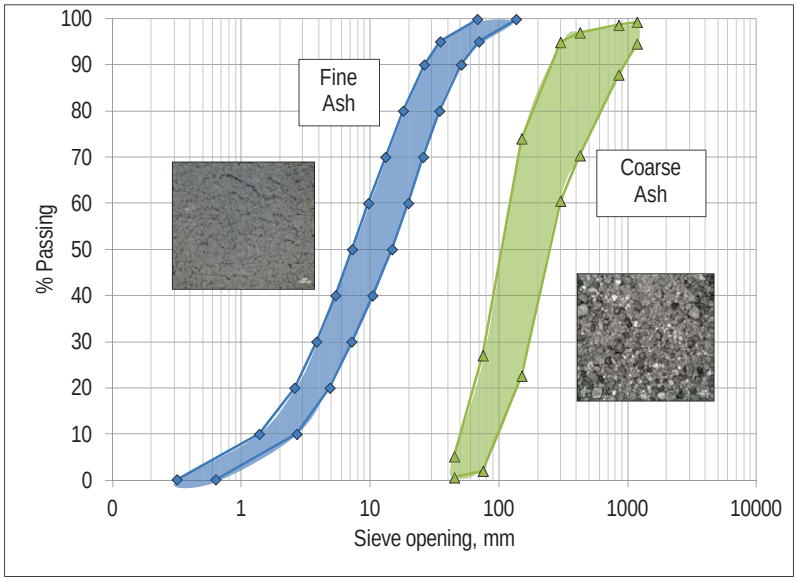

Figure 102. Fine and Coarse Ash Particle Size Distribution Curves for R08 Operation

3.1.4.2 Summary

In summary, performance of the gasification system during the oxygen-blown biomass co-feed testing was stable with no operational problems, and all major test objectives were fulfilled. Very few discernable differences in the operating conditions or quality of the product gas were observed between the test cases performed. Parametric studies on multiple independent operating variables, e.g. steam and oxygen to fuel ratios, are needed to evaluate the effects of biomass type and feed percentage on gasifier outputs relative to their potential use for liquid fuel production. The key conclusions derived from the testing are given below.

- The test plan called for oxygen-blown gasification of PRB coal only and of mixtures of coal with 10, 20, and 30 percent by weight of raw and torrefied pine wood pellets. Actual coal/biomass blends tested contained approximately 12, 20, and 28 wt% raw biomass and 16, 17, 19, 20, and 29 wt% torrefied biomass.
- The hydrogen-to-CO molar ratio of the product gas ranged from 1.34 to 1.70 and was fairly consistent with the various biomass feed fractions. However, relationships between multiple independent operating variables, e.g. steam and oxygen to fuel ratios, are confounded within the matrix making it difficult to ascribe effects to particular variables.
- A mass balance was performed around the gasifier and supporting equipment, with closure greater than 90 percent for all oxygen-blown tests. Carbon conversion ranged from 97.6 to 98.7 percent for all oxygen-blown tests.
- An energy balance was performed around the gasifier using the flows developed from the mass balance, heating value of components, and sensible heat of inputs and outputs. On this basis, energy balance closure ranged from 91 to 103 percent.
- Conversion of feedstocks to product gas was quantified by Cold Gas Efficiency (CGE). The CGE ranged from 59.6 to 69.7 percent for oxygen-blown tests. The CGE appeared to be slightly lower for the raw biomass tests, averaging 61.2 percent compared to torrefied biomass tests averaging 66.8 percent, and 67.8 percent for the coal only case. These results may be attributed to the lower heating value and energy density of raw biomass compared to that of torrefied biomass and coal. However, there is no apparent trend with biomass feed percentage for either feedstock.
- Product gas from feedstock containing torrefied biomass had significantly fewer tars than gas from raw biomass blends. Tar levels increased with higher percentage of biomass for both raw and torrefied feedstock blends. The greatest amount of tars was observed in the 28 percent raw biomass and coal only cases.
- Leaching and pH analyses of both the coarse and fine ash indicate the ash would not be considered hazardous waste for disposal purposes. If the material has suitable characteristics for alternative use, it could be considered a by-product and not a waste.

3.1.5 Automatic Temperature Control of the Gasifier

A new gasifier temperature control scheme utilizing upper and lower mixing zone air flow adjustments was implemented prior to R05. The purpose of this new control scheme was to demonstrate control of gasifier mixing zone temperatures using standard proportional–integral–

derivative controllers to adjust air flow to the different zones while maintaining a constant total air flow to the gasifier. The control scheme was further modified during the run to control gasifier exit temperature by adjusting the gasifier total air flow set point.

Control loop tuning was performed to modify the responsiveness of the controllers to changes in gasifier temperature set point. Since gasifier upper and lower mixing zone temperatures respond rapidly to changes in air feed rate, the temperature controllers were tuned to respond slowly to minimize overshoot. Figure 103 plots the response to a change in temperature set point.

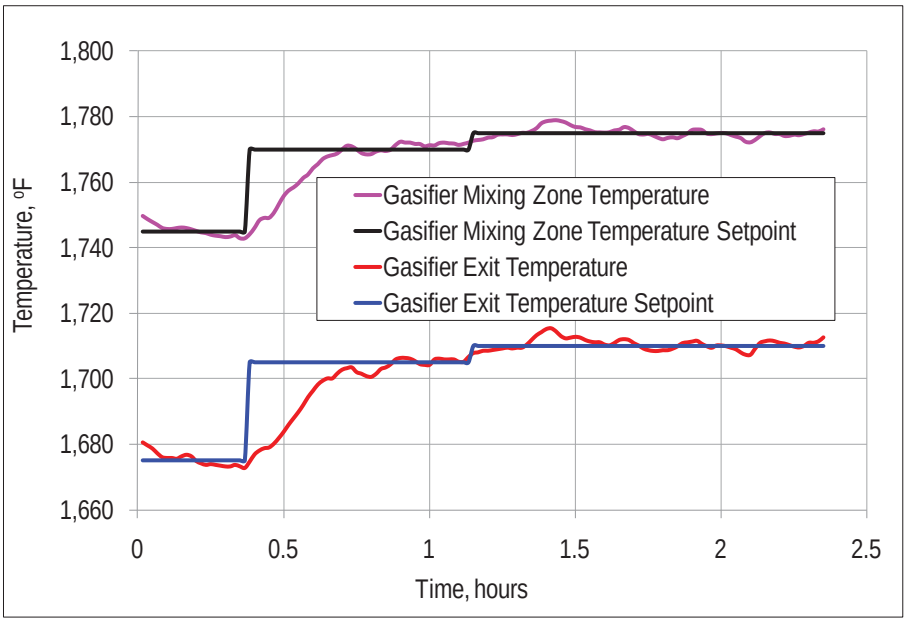

Figure 103. Gasifier Temperature Response to Set Point Change

Additionally, the controllers were optimized to maintain a constant gasifier temperature. Beginning in R06, a more aggressive algorithm was created that accounted for sudden increases and decreases in gasifier temperature resulting from non-steady state operation, such as variations in coal feed rate. Using a rate of change analysis for gasifier temperature, the controller can scale its response by varying the total air flow rate set point more aggressively. After steady state operation has been reached again, the slower tuned controllers take control again. Figure 104 illustrates the improvement in gasifier exit temperature control achieved by these efforts. Gasifier temperature variation was decreased from 5°F achieved during initial control implementation to less than 2 °F during R08 and R09.

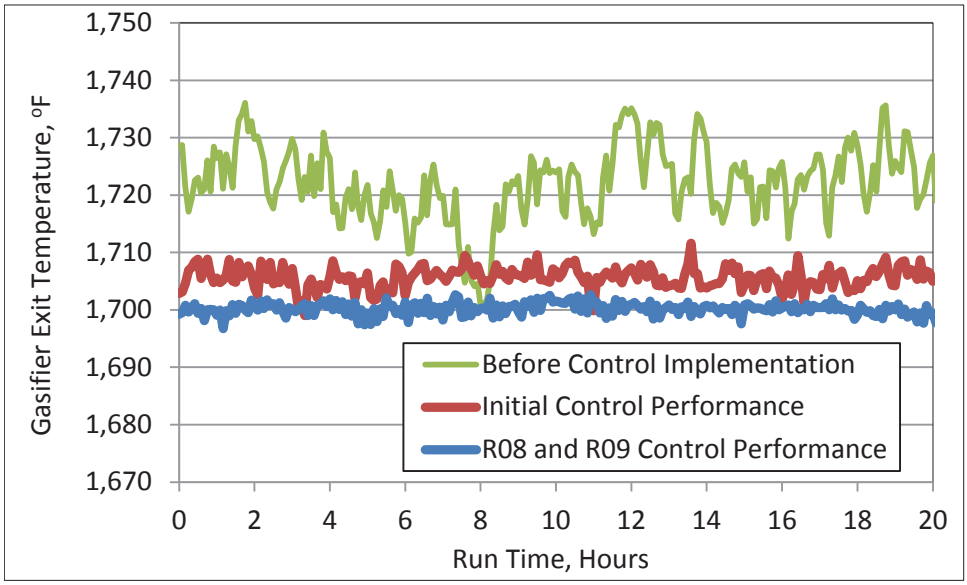

Figure 104. Gasifier Temperature Control during Non-Steady State Operation

In R11, changes in gasifier operating characteristics with the Mississippi lignite as opposed to PRB resulted in larger temperature fluctuations and necessitated additional modifications to the control scheme. Therefore, the gasifier temperature set point was raised, the individual and total air flow controllers were tuned, and the air flow split to the lower and upper mixing zones was modified. Following these changes, the control scheme performance returned to previous levels.

3.2 Coal Feeder Development

The Pressure Decoupled Advanced Coal feeder is a non-mechanical feed control device with no moving parts which combines traditional designs for flow rate control with some of the successful concepts developed on-site for the continuous ash depressurization systems. The driving force for solids flow is a pressure differential, and the solids flow is metered by the nitrogen conveying gas. Although the feeder has operated with high availability since its commissioning and initial operation in 2009, improvements were needed in feed rate steadiness. Several modifications were implemented prior to run R02, and refinements were made in subsequent runs. The resulting feed rate stability improved the overall gasification process performance by providing redundancy in coal feeding and allowing further process control improvements through implementation of automatic gasifier temperature controls discussed in Section 3.1.5.

Physical Configuration Changes

During early operation of the PDAC feeder, high pressure drop had been observed from the bottom of the feeder to the gasifier due to a reduction in diameter of the components and complex geometry. To address this observation, three physical modifications were made to the feeder. First, the original design at the bottom of the feeder was modified to create a smooth transition into the feeder discharge line, eliminating most of the previously observed pressure drop. Second, the discharge line was modified to reduce the number of elbows and make the pipe inner diameter uniform from the feeder to the gasifier further decreasing unnecessary

pressure drop. Finally, the arrangement of nitrogen aeration at the bottom of the feeder was modified to improve the gas distribution; resulting in much improved operability during feeder start-up and low coal feed rate operation.

Control Logic and Instrumentation Changes

Several control logic and instrumentation changes were also implemented to further improve feeder performance. The feeder dispense vessel pressure control was enhanced through both logic changes and tuning in order to maintain vessel pressure constant during lock vessel filling cycles. In addition, a feedback control scheme was implemented that monitors gasifier pressure and triggers the addition or venting of process gas to the feeder in order to maintain a constant pressure differential between the gasifier and the feeder. Together these modifications permitted the controller to maintain a constant coal feed rate by eliminating the impact of upstream and downstream system dynamics. This modification significantly improved steady state feed rate control, as demonstrated by Figure 105, with additional optimization achieved through tuning during subsequent testing. The figure shows the standard deviation of the gasifier outlet temperature during steady state periods for the first on-line testing of PDAC (TC25) and run R02. Because the coal feed rate was steadier in R02, the gasifier temperature variation was lower. Both the maximum and average values of the temperature deviation were more than halved as a result of the modifications.

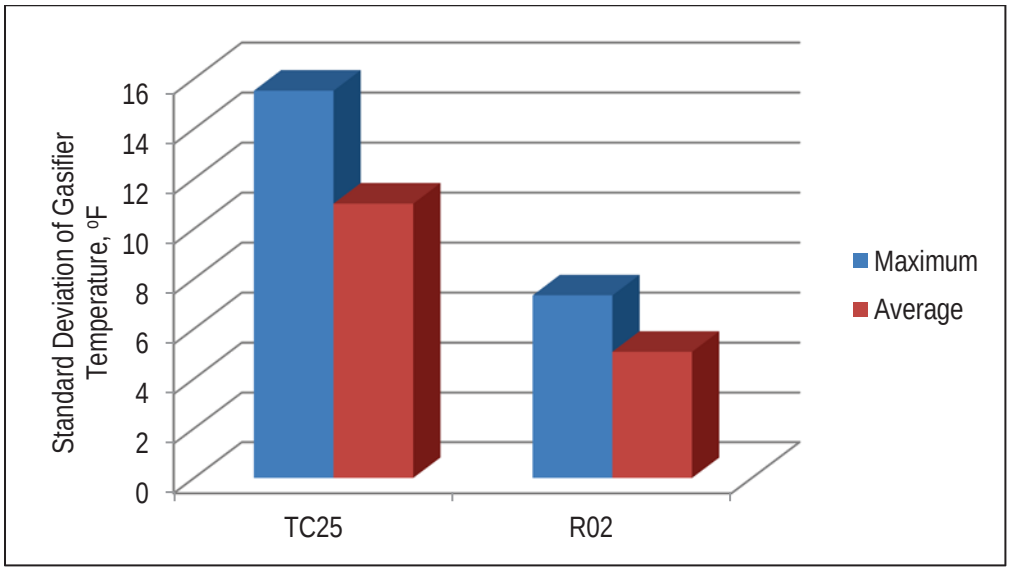

Figure 105. Comparison of Gasifier Temperature Deviation before and after PDAC Feeder Modifications

A coal feed rate trim controller was also designed to detect instantaneous decreases in coal feed rate and respond by automatically increasing nitrogen flow to the feeder to increase coal feed. A new control point utilizing the feeder conveying line differential pressure transmitter, which has been shown to provide a good instantaneous indication of coal feed rate, was included in this modification. While this logic change was originally implemented during R02, further refinement of the control continued through the R07 run, resulting in additional improvement in coal feeder performance. Figure 106 demonstrates the nitrogen flow valve response to the modified controller during R07.

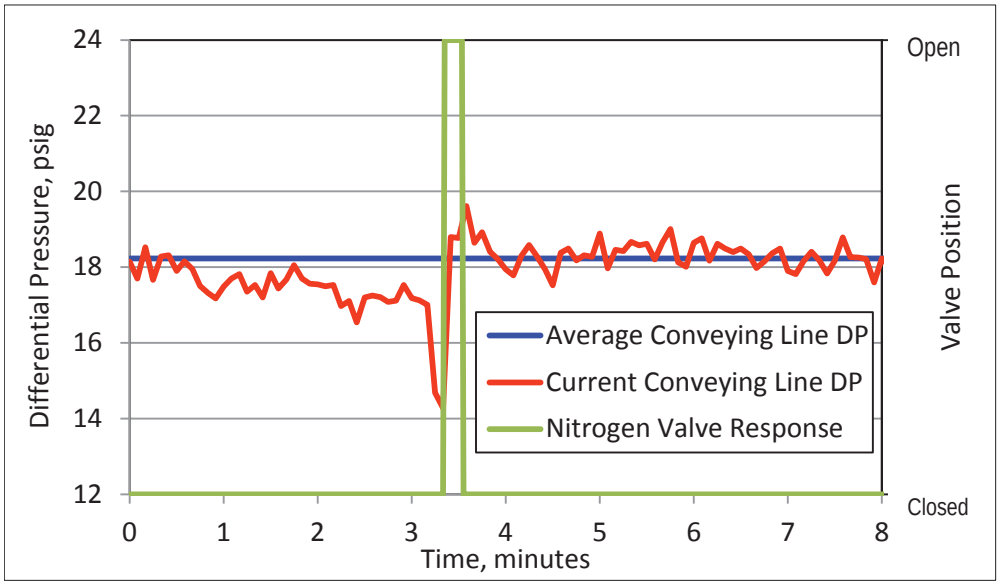

Figure 106. PDAC Feeder Trim Controller Response to Change in Coal Feed Rate

In addition to modifications for improved coal feed rate control to the gasifier, control logic and instrumentation changes were made to improve coal transfer from the feeder atmospheric storage silo to the pressurized dispense vessel. Vibration level probes (discussed in Section 3.3), which were installed on the feeder dispense vessel and lock vessel prior to R02, reliably detected coal level in both vessels and proved a more reliable indication than the capacitance probes used previously. As a result of the increased reliability, the lock vessel filling cycle was optimized to use the level probe indication to end the fill cycle instead of waiting for the timer to cycle. The benefit of this change was especially significant when operating the feeder at higher feed rates where reduction in the pressurization and depressurization cycle time is required.

Control changes were also made to increase the operating level of the feeder atmospheric storage silo. Controlling the silo at a higher level promoted a mass flow regime from the bin, decreasing material segregation that can lead to difficulty in coal transfer to the lock vessel and ultimately coal feed rate fluctuations.

3.3 Sensor Development

3.3.1 Sapphire Thermowell for Gasifier Service

Because gasifier thermocouples are critical for monitoring gasifier performance and for providing control logic input, extensive work at the site has been performed to identify suitable thermowell materials for housing the thermocouples. The primary concern of thermowell performance in the Transport Gasifier is excessive wear of the tip exposed in the gasifier from solids erosion and/or corrosion. Previous studies showed that uncoated HR-160 is the most reliable material of those tested, which included ceramics and other metals such as Hastelloy-X, along with various coatings. Beginning in run R04, evaluation began on a sapphire thermowell supplied by Emerson Process Management and installed in the gasifier riser.

The performance of the sapphire thermowell was compared with an existing HR-160 thermowell installed in the same plane of the gasifier. Both thermowells contained Type-N thermocouples, which have an accuracy of within 0.75 percent. The sapphire thermowell testing showed excellent responsiveness to temperature changes during all testing. The difference between the average steady state temperature indications of the thermocouples averaged about one percent during R04 and averaged about 3.5 percent during R05. While the percent difference between the two temperature indications at the beginning of R05 was close to the expected accuracy for the thermocouple type, the sapphire thermowell indication began to drift low. Further testing in R06 showed a measurement drift of more than 10 percent compared to the reference thermocouple with an HR-160 thermowell.

To prevent damage to the thermowell that may have caused the drift in temperature readings, a new mounting technique was developed based on collaboration with the vendor, which appeared to improve operation with the sapphire thermowell. As the graph in Figure 107 indicates, during R11, the thermocouple with the sapphire thermowell read slightly lower than the reference thermocouple as it had previously, but the difference was consistent and averaged less than one percent. The Rosemount system responded to gasifier changes well, while maintaining mechanical integrity. Further long-term testing is planned.

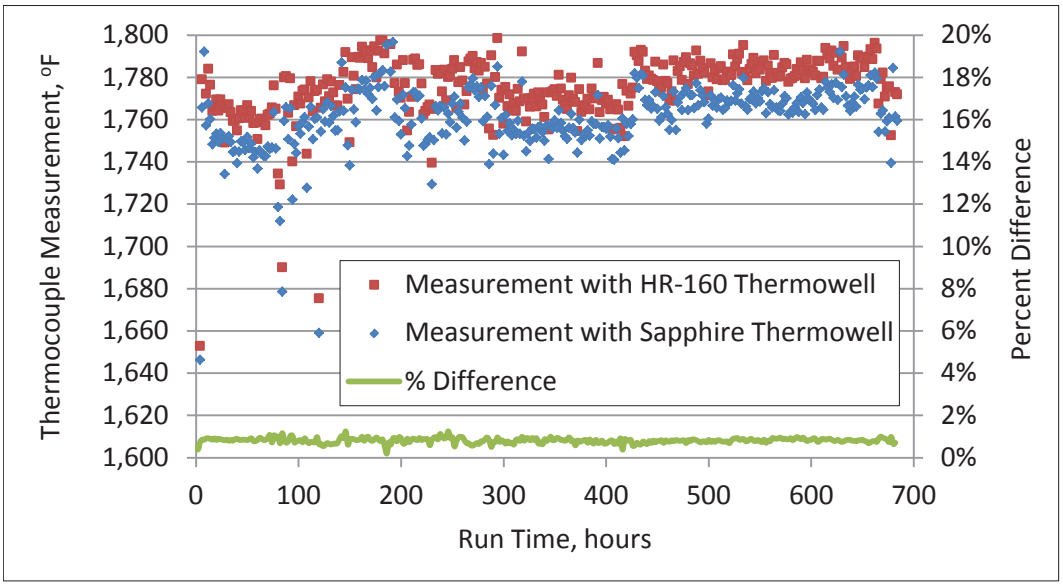

Figure 107. Comparison of Thermocouple Measurements Using Sapphire and HR-160 Thermowells

3.3.2 Dynatrol Vibration Level Probes

Dynatrol Detector level probes supplied by Automation Products, Inc. were installed on the PDAC feeder dispense vessel and lock vessel prior to R02. The new probes replaced capacitance probes that had proved to be unreliable. The vibrating action of the probes prevents them from giving false "covered" indications, unlike the stationary capacitance probes, which often gave covered indications due to dust buildup. To date, no false indications have been observed from the new level probes. The vibration probes have a wide range of material measurement capability, from low density flakes or powders to heavy granules and pellets, and the probes do not require re-calibration in response to variations in feedstock bulk density. Another advantage

of these level probes is that they have a high pressure rating of 1,000 psig, which makes them relevant for applications in commercial IGCC facilities.

The Dynatrol probes proved highly reliable, and will continue to be used in future runs. As a result of the increased reliability of the level probes over the capacitance probes, the lock vessel filling cycle was optimized to use the level probe indication to end the fill cycle instead of waiting for the timer to cycle.

3.3.3 Drexelbrook Point Sensitive Level Probe

Additional level probe technology was tested in the PDAC feeder dispense vessel beginning in R04. A Drexelbrook point sensitive level probe was installed in the top of the dispense vessel to permit control at a high fill level and thus prevent the occurrence of funneling in the vessel. The operating basis of the probe is similar to a capacitance probe but combines a radio frequency signal with circuitry shielding technology to ignore the effects of material buildup on the probe. Initial field calibration of the probe was required using a simple potentiometer adjustment.

Controlling at a higher level helped avoid the development of funnel flow inside the vessel, resulting in a more consistent coal feed rate. After about 6,000 hours of operation, the probe was replaced in-kind due to failure of some electrical components. Otherwise, the Drexelbrook probe has been extremely reliable and will continue to be operated in future runs.

3.3.4 DensFlow Coal Feed Rate Indicator

A coal flow measuring device, the DensFlow meter from SWR Engineering, was installed in the feeder discharge line to the gasifier prior to R04. This device is a non-intrusive technique of measuring solids flow using a patented alternating electromagnetic field. The solids flowing through the device absorb this field energy, and a measurement of density of the material is inferred. Simultaneously, conveying velocity is also calculated by the same sensors. The combination of the two measurements with the cross sectional area of the device yields a mass flow rate of material through the feeder discharge line.

As shown in Figure 108, the new DensFlow meter showed good agreement during the R04 run with the flow rate calculated from the existing weigh cells. However, in subsequent runs, the DensFlow meter consistently indicated flow rates much lower than the rates indicated by the weigh cells. Mass balances supported the accuracy of the weigh cell calculations. The DensFlow meter did prove reliable in indicating instantaneous changes in coal feed rate when compared to conveying line differential pressure readings.

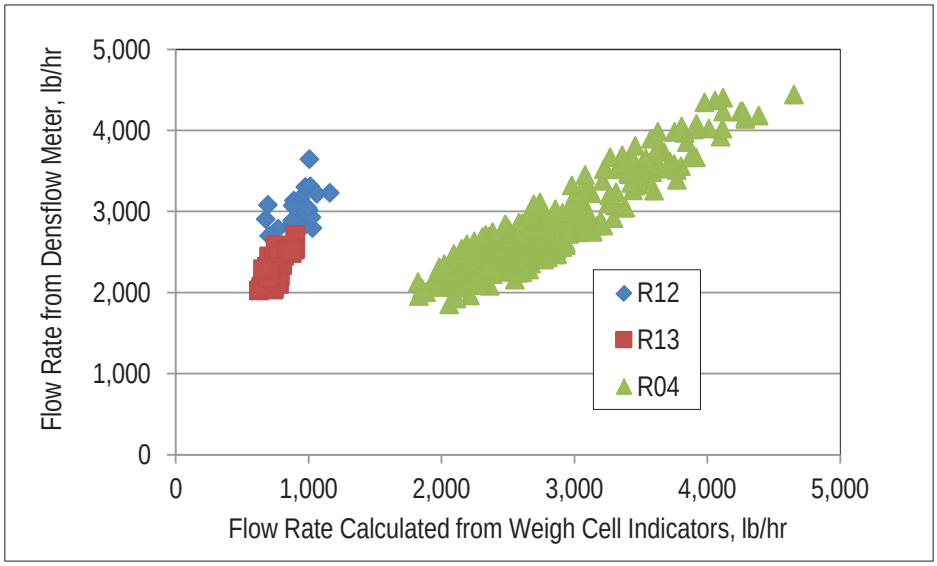

Figure 108. Comparison of Coal Feed Rates from DensFlow Meter and from Weigh Cell Calculation

In collaboration with the DensFlow vendor, several measures were taken to improve the instrument performance, such as re-calibration and off-line testing to establish flow meter operation over a range of coal feed rates and conveying line velocities. These initial efforts were not productive, and additional collaboration is ongoing with the vendor to improve the flow meter performance.

3.4 Hot Gas Filter Elements

Since gasification operation began at the site, hot gas filter elements (candle-type filters) have been used for final particulate removal from the syngas. Extensive testing with ceramic, sintered metal powder, and sintered metal fiber elements has shown that the mass concentration of particulate can be reduced from 10,000 to 30,000 ppmw at the PCD inlet to less than 0.1 ppmw at the outlet. As metal elements proved to be less prone to failure than ceramics, recent testing has focused exclusively on metal materials. Because metals are subject to corrosion, the test program includes long-term evaluation to verify resistance to corrosion sufficient to provide useful service times (at least two years, or about 16,000 hours) for commercial applications.

Table 43 lists the conditions under which the filter elements operate. The elements are cleaned during operation by back-pulsing (reverse flow) with high pressure nitrogen in five-minute intervals to control the tubesheet pressure drop. The PCD collection efficiency is quantified based on isokinetic, in-situ sampling performed at the PCD inlet and outlet. An on-line particulate monitor, the Dust Alert instrument from PCME, is also used for real-time detection of significant particulate loadings at the PCD outlet. Further information on PCD operation and earlier results of filter element evaluation can be found in previously published reports (e.g., PSDF Final Report, available on the web at www.NationalCarbonCaptureCenter.com).

Table 43. Nominal PCD Operating Parameters

Operating Condition	Typical Value
Normalized Dustcake Drag, inH_2O/(ft/min)/(lb/ft^2)	100
Temperature, ^oF (^oC)	750 (400)
Pressure, psig (bar)	200 (14)
Face Velocity, ft/min (cm/s)	3.5 (1.8)
Baseline Pressure Drop, inH_2O (bar)	80 (0.2)
Pressure Drop Rise Rate, inH_2O/min (bar/min)	10 (0.025)
Inlet Loading, ppmw	10,000--30,000
Particulate Mass Median Diameter, micron	10 to 15

Table 44 lists the types of elements tested during the contract period and the maximum number of exposure hours for individual elements of each type.

Table 44. Hot Gas Filter Elements Tested during Contract Period

Filter Material	Supplier/Brand	Maximum Hours of Exposure
Iron Aluminide Sintered Powder	Pall/PSS	16,155
HR-160 Fine Sintered Fiber	Pall/Dynalloy	8,996
HR-160 Coarse Sintered Fiber	Pall/Dynalloy	11,023
High alloy (SR-75) Sintered Powder	Mott	7,501
Coated Alloy Sintered Fiber	Porvair/Sinterflo	7,978
Fecralloy Sintered Fiber	Bekaert	2,960

3.4.1 Collection Efficiency Measurements at Ambient Conditions

As part of the filter element evaluation protocol, all elements are initially screened by measuring their collection efficiencies at ambient conditions in a cold-flow PCD model using ash collected from the NCCC gasification process during test runs. Filter elements with cold-flow collection efficiencies lower than 99.99 percent are excluded from further evaluation in gasification operation. In some cases where collection efficiency was not high enough, the manufacturers incorporated design improvements and subsequently demonstrated efficiency sufficient for installation in the PCD. Cold-flow model collection efficiencies for the elements meeting the collection efficiency criteria and tested in the PCD are given in Table 45.

Table 45. Collection Efficiencies of Individual Filter Elements at Ambient Conditions

Filter Element Type	Filter Condition	Collection Efficiency,%
Pall Iron Aluminide Powder	New	>99.9999
Pall Iron Aluminide Powder	7,700 gasification hours, with pits	>99.9999
Pall Dynalloy HR-160 Coarse Fiber	New	99.9951
Pall Dynalloy HR-160 Coarse Fiber	Used 725 gasification hours	>99.9999
Pall Dynalloy HR-160 Fine Fiber	New	>99.9999
Mott Alloy Powder	New with 3 hours in cold-flow model	>99.9999
Porvair Coated Alloy Fiber	New	99.9938
Porvair Coated Alloy Fiber	New with 3 hours in cold-flow model	99.9980
Bekaert Fecralloy Fiber	New with 4 hours in cold-flow model	99.9975

Results from the cold-flow PCD model showed initial collection efficiencies in excess of 99.9999 percent for all the sintered powder elements, including Iron Aluminide elements with evident corrosion. For the HR-160 sintered fiber elements, the collection efficiency increased with decreasing fiber size, as expected. While the collection efficiencies were lower for the coarser fiber sized elements, they were still high enough initially to meet operational requirements based on commercial turbine particulate limits. Conditioning in the cold-flow model and in the PCD with gasification operation further improved the efficiency of fiber elements.

3.4.2 Post-Operation Pressure Drop Measurements

Following gasification operation, flow test measurements were made on the filter elements to determine the effect of exposure hours on pressure drop and to determine if corrosion was affecting the types of elements installed. Prior to flow tests, free particulate was removed from the elements by operating the PCD back-pulse system for several hours after gasifier shutdown and by air blowing the elements following removal from the PCD.

The pressure drop at a fixed face velocity (3 ft/min) in ambient conditions was measured on each of the filter elements both with the light residual dustcake and after pressure washing with water to remove all particulate. Figure 109 displays the pressure drop measurements plotted as a function of gasification exposure hours following run R12 for the six types of filter elements tested. Because all these elements were installed in the same test campaign, the data were not influenced by differences in dustcake drag or porosity that could otherwise bias the age comparison.

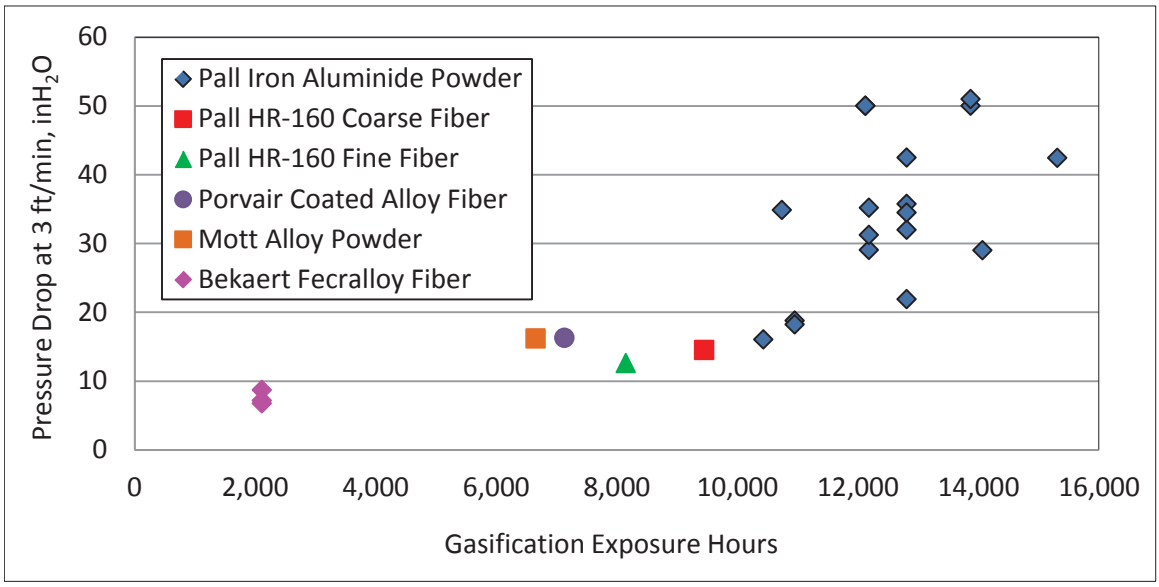

Figure 109. Cold Flow Pressure Drop Measurements for Filter Elements after R12 prior to Cleaning

As demonstrated by Figure 110, washing the elements was effective in reducing the pressure drop to near new values, except for some of the older Iron Aluminide elements. A few of these elements were retired from service.

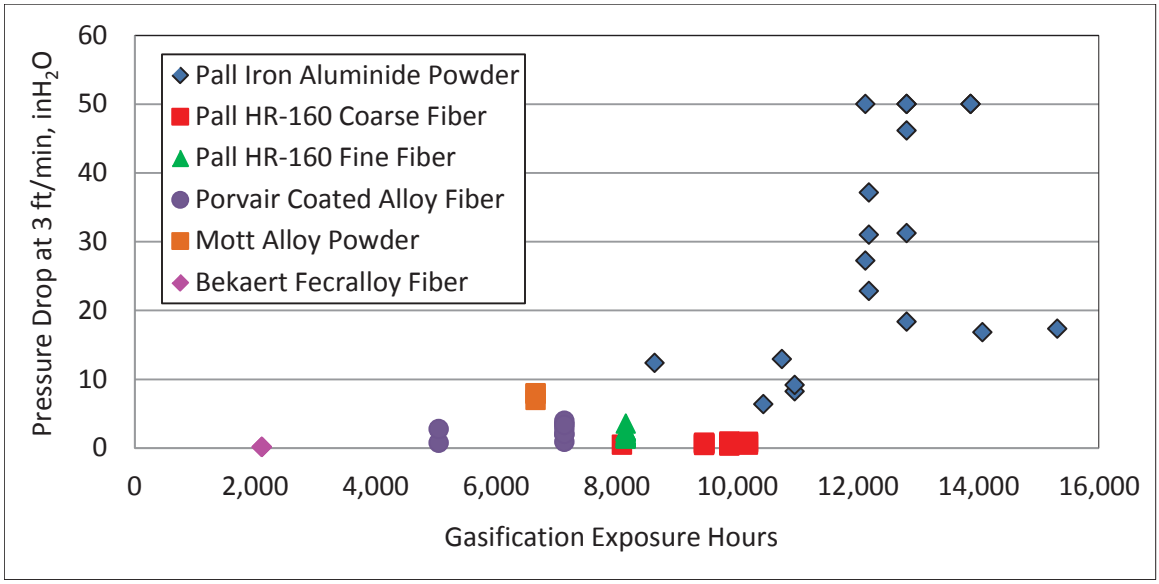

Figure 110. Cold Flow Pressure Drop Measurements for Cleaned Filter Elements after R12

3.4.3 Summary of Filter Element Evaluation

The filter element test program has resulted from collaborative efforts between the NCCC and filter manufactures, and has led to the development of reliable materials for highly efficient syngas particulate removal. Of the six types of elements tested in the contract period, all maintained structural integrity and excellent collection efficiency throughout operation.

Continued testing is planned for these elements to confirm suitability for long-term commercial operation.

Pall Iron Aluminide Sintered Powder Filter Elements

After as much as 16,000 hours of operation, the Iron Aluminide elements consistently demonstrated extremely high filtration efficiency despite the corrosion presumably causing increasing pressure drop, and are considered suitable for commercial applications. The corrosion rate for these elements is expected to be considerably lower in a commercial unit, which would not have as much thermal cycling (compared to a research facility) at conditions promoting degradation of the protective alumina layer. While additional testing is planned, many of the Iron Aluminide elements reaching the 16,000-hour milestone have been retired due to high pressure drop.

Pall HR-160 Sintered Fiber Filter Elements

Testing of the HR-160 coarse fiber elements began in 2001, and collaboration with Pall led to the development of an HR-160 filter media with finer mesh, testing of which began in 2008. The higher collection efficiency of the finer fiber was desired due to indications of particulate breakthrough during back-pulse cleaning. While some corrosion has been noted on both types of elements, they have maintained high collection efficiency and acceptably low pressure drop. Testing of both types of the HR-160 elements will continue for long-term evaluation.

Porvair Coated Fiber Elements

After initial testing of non-coated Fecralloy filter elements in 2007, Porvair modified the filter design and started testing inert-coated elements in 2009. The first gasification test with the coated elements was the only run in which just one type of element was installed in the PCD. With these elements solely in operation, the controllable PCD tubesheet pressure drop and high collection efficiency could be attributed to these elements alone.

Mott Sintered Powder Filter Elements

Testing of the Mott sintered powder of high alloy (SR-75) elements began in 2009. They were developed by Mott with design input on media configuration from NCCC engineers based on operating experience. Mott's material selection was based on test results of coupon material exposure in the PCD.

Bekaert Sintered Fiber Filter Elements

Bekaert developed an element of Fecralloy sintered fiber that was first tested in 2013. Bekaert utilized coupon exposure testing in the PCD and collection efficiency measurements in the NCCC's cold-flow model to refine the filter element design.

3.5 Water-Gas Shift Catalysts

The NCCC performed testing of several different WGS catalysts to establish the optimum operating conditions to support commercial IGCC operation and to evaluate long-term catalyst performance. Water-gas shift catalyst evaluation is completed in one of three pressure vessels shown in Figure 111. The vessels and the lines delivering the syngas are heavily trace heated

and insulated to maintain the required operating temperatures. Some of the key design parameters for the vessels are presented in Table 46.

Figure 111. SCU Reactor Vessels Used for WGS Catalyst Evaluation

Table 46. Design Parameters for WGS Catalyst Reactor Vessels

Design Parameter	Value
Vessel Material of Construction	310 Stainless Steel
Design Pressure, psia	365
Design Temperature, °F	1,000
Height of Parallel Section, inches	48
Internal Diameter, inches	5.2

The syngas at the inlet of the PCD of the gasification process is analyzed using two on-line GCs and an NDIR CO/CO_2 meter, and this information is used as the inlet syngas composition to the WGS vessel. The syngas composition leaving the WGS vessel is provided by gas chromatographs. Syngas moisture content is determined by condensation measurement, as this has proved to be more accurate than using continuous analyzers. The vessel is equipped with inlet flow meters and flow control valves for syngas and for steam. The meters are configured so that they can be checked with a known flow of nitrogen prior to start-up and at intervals during the run.

3.5.1 Evaluation of Steam-to-CO Ratios

Evaluation studies completed at the NCCC show that catalyst vendors generally recommend high steam-to-CO ratios to maximize CO conversion and minimize methane formation. Values as high as 2.6 have been quoted. This is based on requirements by chemical production processes to maximize hydrogen formation (the desired product) and minimize methane formation, a potential contaminant. High steam content also suppresses carbon formation from the cracking of long-chain hydrocarbons. For power plant applications, where the objective may be to capture only 90 percent of the CO_2, incomplete conversion of CO and the production of some methane are acceptable. Moreover, there are little, if any, long-chain hydrocarbons in coal-derived syngas so there is no need for excess steam to suppress carbon formation.

The evaluation studies also indicated that for a 500-MW IGCC plant, a steam-to-CO ratio of 0.1 corresponded to 4 MW of power, so operating with excess steam would have a significant impact upon net power production. For example, if a steam-to-CO ratio of 1.6 was acceptable rather than 2.6, then an additional 40 MW would be available.

To determine the feasibility of operating with steam-to-CO ratios lower than those normally proposed, the NCCC began investigating the performance of WGS catalysts provided by the major suppliers. The terms of the confidentiality agreements signed prevent identification of the catalysts in this report.

Test Procedure

For testing during run R05, 13 pounds of catalyst was installed in the vessel, giving a fixed bed 26-inches deep supported on a 310 stainless steel mesh. The syngas and steam flowed vertically downward through the catalyst. The gas flow rates were held constant during the run to maximize the data collected for a given space velocity. The heat tracing on the line from the header to the vessel was adjusted to achieve an inlet temperature of 540°F to keep the exit temperature below 650°F, above which sintering could occur. The parameter that varied the most was the steam-to-CO ratio. Table 47 lists the test conditions for R05.

Table 47. Water-Gas Shift Catalyst Test Conditions

Test Parameter	Nominal Values
Syngas Flow Rate, lb/hr	50
Steam Flow Rate, lb/hr	0 to 2.0
Operating Pressure, psia	195
Inlet Temperature, °F	540
Superficial Syngas Velocity, ft/s	0.22
Space Velocity, 1/hr	3,240
H_2O/CO Molar Ratio	0.8 to 1.6
Test Duration, hours	780

The mean values for the major syngas components during R05 are given in Table 48 along with the analyzer used to make the determination. Each analyzer has its own error bias which data analysis accentuates when comparing the changes in composition between the inlet and outlet of the reactor.

Table 48. Mean Syngas Compositions at Water-Gas Shift Reactor Inlet and Outlet

	CO	CO_2	H_2	CH_4
Inlet Concentration, vol % (analyzer used)	9.7 (NDIR)	9.7 (NDIR)	7.1 (GC)	1.02 (GC)
Outlet Concentration, vol % (analyzer used)	3.6 (GC)	14.3 (GC)	12.7 (GC)	1.04 (GC)

Figure 112 compares the amounts of CO shifted (delta CO) to the amount of CO_2 formed (delta CO_2) by the WGS reaction. These amounts should be equimolar, one mole of CO being converted to one mole of CO_2 formed, according to the water-gas shift equation:

$$CO + H_2O \leftrightarrow CO_2 + H_2 \quad \text{(water-gas shift equation)}$$

All but one data point fell within 10 percent of perfect agreement, which validated the data quality.

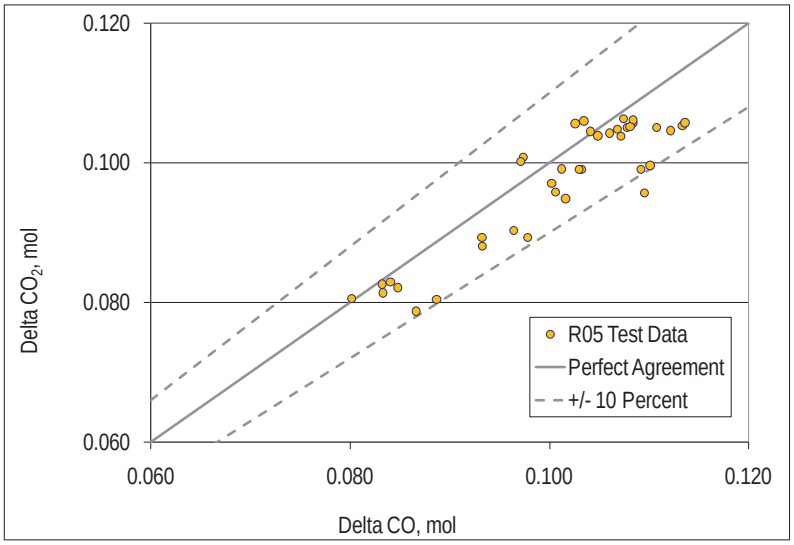

Figure 112. Amount of CO_2 Produced Compared to Amount of CO Shifted

Figure 113 plots the amounts of CO shifted to H_2 by the WGS reaction. The data for hydrogen did not agree as well as that for the carbon dioxide, with the data showing more hydrogen formed than CO consumed. The discrepancy likely arose from small measurement errors. Efforts continue to reduce error as much as possible.

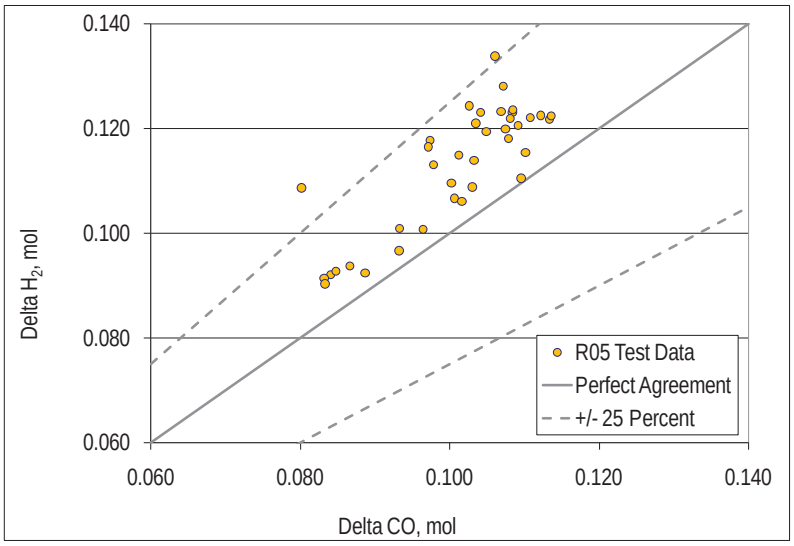

Figure 113. Amount of H_2 Produced Compared to Amount of CO Shifted

Figure 114 presents data showing the measured CO conversion variation with steam-to-CO ratio. Also presented is the equilibrium conversion calculated from information provided by the catalyst vendor. On average, the measured conversions were 70 percent of the equilibrium

values. The trend for both data sets appeared to be asymptotic, with conversions leveling off for molar ratios greater than 1.6.

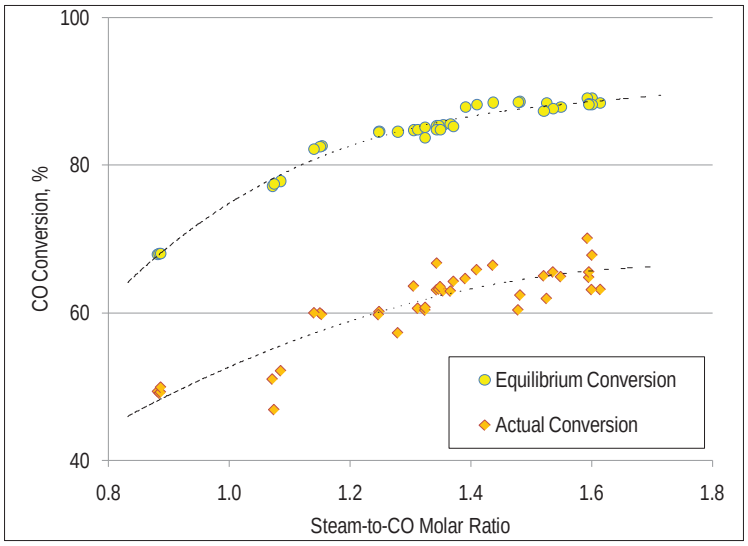

Figure 114. Comparison of Actual and Equilibrium WGS Conversions

The tests showed that sufficiently high CO conversions were achieved at lower than recommended steam-to-CO ratios and that only marginal increases in conversion would be realized for ratios above 1.6. No methane was formed and no carbon was deposited in the reactor. For power generation applications, steam-to-CO ratios lower than those recommended for chemical production applications are acceptable.

3.5.2 Long-Term WGS Catalyst Evaluation

An undisclosed WGS catalyst supplier began testing a catalyst under development in 2011 using coal-derived syngas. Operation with the WGS catalyst included parametric studies and long-term material evaluation. Through R13, the testing had encompassed 3,517 hours of syngas operation, with no significant degradation of the catalyst. Operation was typically conducted at a syngas flow rate of 50 lb/hr, a temperature of 480°F, a pressure of 180 psig, and a steam-to-CO ratio of 1.0 (using only the steam inherent in the syngas). Figure 115 plots the CO conversion achieved for all testing from 2011 through 2013. The steam-to-CO ratio was much higher with Mississippi lignite due to the relatively higher coal moisture, and the CO conversion was correspondingly greater.

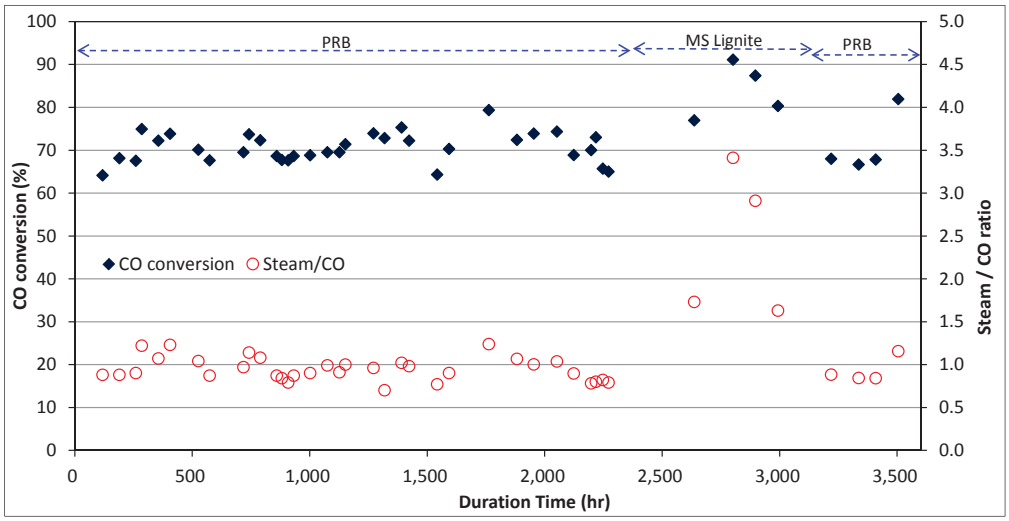

Figure 115. CO Conversion and Steam-to-CO Ratio for WGS Catalyst Testing from 2011 to 2013

Figure 116 provides the results of parametric testing of the WGS catalyst with syngas produced from PRB coal and lignite. In the range tested, the temperature did not significantly affect CO conversion. Lower space velocity achieved by reducing the syngas flow rate to 25 lb/hr increased the conversion to slightly above the estimated equilibrium value.

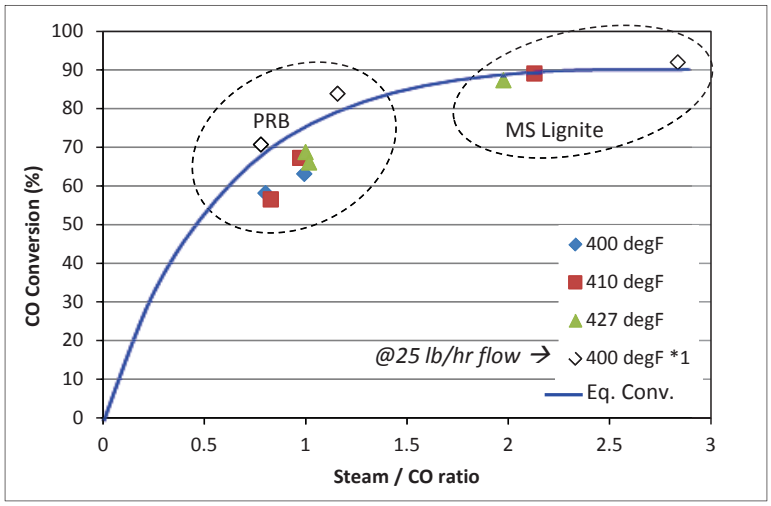

Figure 116. CO Conversion of WGS Catalyst during Parametric Testing

3.6 COS Hydrolysis Catalysts

The catalyst developer which tested the WGS catalyst from 2011 through 2014 also provided a COS hydrolysis catalyst made with a honeycomb configuration, which was tested in R12 for about 400 hours. In R13, the catalyst was operated at a range of temperatures from 480 to 640°F for about 550 hours, and showed the same conversion performance as that in R12.

3.7 Johnson Matthey Mercury Sorbent

In collaboration with the NETL, Johnson Matthey has been developing a palladium-based sorbent to remove mercury and other trace contaminants, such as arsenic and selenium, at high temperature in coal gasification processes. Compared to low-temperature capture by activated carbon, high-temperature capture of these trace elements retains the high thermal efficiency of coal gasification power generation. The sorbent has demonstrated greater than 99 percent capture of mercury, arsenic, and selenium.

Testing at the NCCC began in 2008, with the most recent testing conducted during run R13, for a total of about 3,760 hours. Table 49 lists the test runs and duration for the mercury sorbent. To optimize the sorbent, palladium loadings of 2 wt% and 5 wt% have been tested for performance comparisons. Test conditions for the mercury sorbent are given in Table 50. Initially, the syngas flow rate was limited to about 40 lb/hr. Prior to the R10 run, the NCCC installed a new reactor to accommodate a syngas flow rate of 50 lb/hr.

Table 49. Summary of Johnson Matthey Mercury Sorbent Testing

Run	TC25	R01	R04	R05	R06	R10	R13
Hours Tested	330	170	500	718	1,011	490	540

Table 50. Typical Operating Conditions for the Johnson Matthey Mercury Sorbent

Operating Condition	Typical Values
Syngas Flow Rate	25 to 50 lb/hr
Syngas Condition	Untreated
Temperature	500°F
Pressure	200 psig
Sorbent Quantify, lb	10
Palladium Content, wt%	2 or 5

During the runs, gas samples from the sorbent bed inlet and outlet were collected using a modified EPA Method 29 for trace metal analysis. Analyses were carried out primarily for mercury, arsenic, and selenium. Typical results showed mercury inlet concentrations between 5 and 10 μg/Nm^3 and outlet concentrations for mercury, arsenic, and selenium below detection limits.

Following the runs, the sorbent was removed from the reactor in layers and returned to Johnson Matthey for elemental analyses to determine contaminant penetration levels. Johnson Matthey's sorbent analyses support near-complete absorption of mercury, as the penetration of mercury and other trace metals was limited to the first layers of the sorbent bed.

3.8 NETL Solid Oxide Fuel Cell

Most solid oxide fuel cell testing to date has been performed with natural gas, which is virtually free of contaminants. In 2005, the PSDF exposed the first SOFC (a 1-kW planar cell in support of DOE's Solid State Energy Conversion Alliance) to coal-derived syngas that contained the

various trace elements released during gasification. The final test ran continuously for 70 hours with a constant power output. In a continuation of the development work, DOE has strived to determine the effect of trace species present in coal-derived syngas on SOFC performance. To speed up data collection at a reasonable cost, NETL fabricated a unique multi-cell array (MCA) test skid that can hold as many as twelve small "button" planar SOFCs, each with an active area of 2 cm^2. These are identical in composition and operation to a full-sized cell but at far lower cost. Each button in the array can be different allowing a wide range of variables to be investigated within the same operating period. For example, different electrode materials can be tested at the same current density, or the same electrode materials can be tested under different current densities.

The base plate for the MCA and the assembled array are shown in Figure 117. The twelve buttons are arranged in parallel in four groups of three. The fuel gas is fed from below up the center of a concentric tube and removed down the outer annulus. Air is passed over the upper surface of the buttons and exits through two exhaust channels set in the surface of the array.

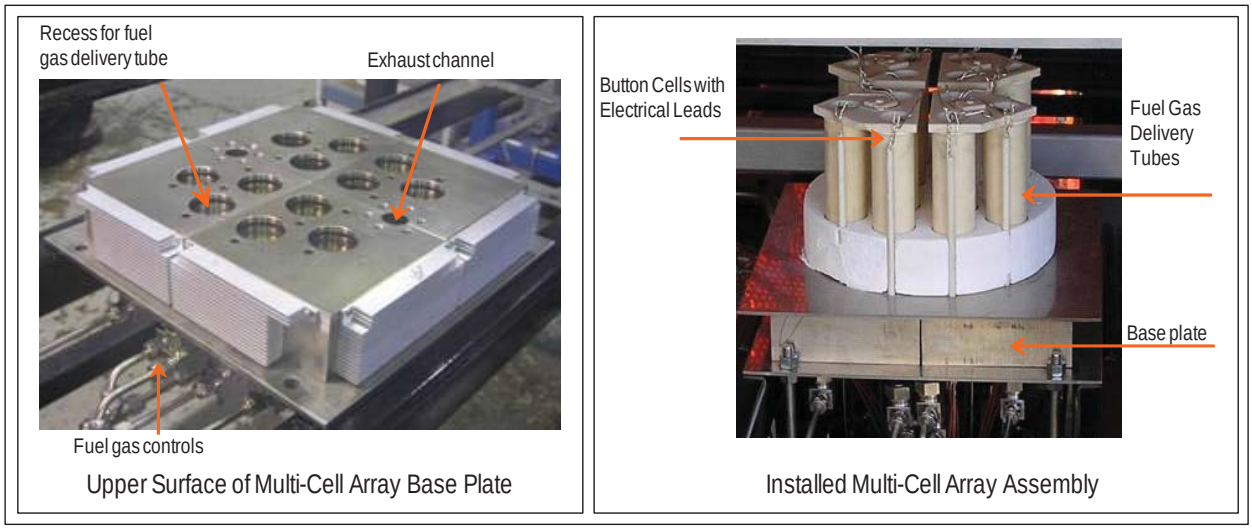

Figure 117. NETL Multi-Cell Array

NETL first began testing of the SOFC MCA on coal-derived syngas at the PSDF in 2008. Several design improvements were identified as a result of this testing, and were implemented and tested at NETL prior to further testing at the NCCC in 2009 during R02.

To achieve uniform performance, each cell was initially fueled with hydrogen and operated at a current density of 250 mA/cm^2 for approximately 24 hours prior to syngas exposure. Under pure hydrogen fuel at this current density, cells uniformly demonstrated power densities in the range of 200 to 225 mW/cm^2, which is typical of this cell construction and gas condition.

The syngas used was desulfurized, having an average H_2S of 3 ppmv. In the 2008 testing, a catalyst was also used to crack the hydrocarbons, but as this pre-treatment step appeared to also remove trace contaminants of interest, it was not employed for R02 testing. Syngas was fed to each cell at around 180 scm, and was enriched with approximately 9 scm of hydrogen. The

syngas temperature was maintained above 400°F to preserve gas-phase trace material content, and no additional water was fed to the system.

Continuous operation on syngas occurred for over 450 hours with ten cells surviving through approximately 350 hours, and eight cells surviving the entire test duration. Losses were typically caused by inadvertent overloading of the cells. For the first 375 hours, the gasifier was operated in air-blown mode, and for the final 75 hours, in oxygen-blown mode. NETL collected more than 4,500 cell-hours of data to support development of gas cleanup systems sufficient for gasifier/fuel cell integration. More than 1 kW of total power was produced.

Upon feeding the hydrogen-enriched syngas, open circuit voltage dropped from above 1.15 V on pure hydrogen to 0.975 V, indicating diminished fuel molecule content (hydrogen, CO, and higher hydrocarbons). Cells were initially loaded to various current densities, with two cells remaining at open circuit voltage to monitor gas composition, three cells set to 125 mA/cm^2, three cells set to 250 mA/cm^2, and four cells set to 375 mA/cm^2. Initial power densities ranged from 95 to 255 mW/cm^2 and deteriorated slightly over the course of the run, which is encouraging as only minimal gas treatment was employed. The power densities achieved were also encouraging given the modest heating value of the syngas.

3.9 NETL Mass Spectrometer

During the 2008 NETL fuel cell testing, NETL operated for the first time its developmental analytical system, a gas chromatography inductively coupled plasma mass spectrometer (GC-ICPMS), for real-time analysis of syngas trace metals. The technique is highly sensitive and able to determine concentrations below one part per billion. Conventional analytical techniques require collection of gas samples over several hours followed by time-consuming analysis. The long sampling interval determines the average composition over the period and does not identify any variations occurring during the interval because of changes in gasifier operation. By incorporating a GC instrument, the new technique allows up to 20 trace elements to be identified simultaneously in a two-minute interval. Shortening the sampling interval allows variation in trace element concentration to be monitored.

While testing the GC-ICPMS analyzer, data were also collected using EPA Method 29. To perform Method 29, the gas sample was bubbled through hydrogen peroxide solution acidified with nitric acid to recover all species of interest including ionic mercury. A second bubbler including potassium permanganate acidified with sulfuric acid was used to remove elemental mercury. (For gasification, all the mercury is expected to be present in elemental form.) The species removed by the solutions were analyzed using conventional ICP MS techniques.

In 2010 (during run R05), the GC-ICPMS was used for the first time in the field to measure mercury concentrations directly during testing of the Johnson Matthey mercury sorbent. Data were collected continuously every 15 minutes. Although measured mercury levels from the GC-ICPMS were higher than those determined by the EPA Method 29, the results demonstrated the potential to gather real-time data and to facilitate control over key parameters. Lessons learned during R05 included the need for additional heat tracing of sampling loops and improved controls for system pressure and syngas flow.

3.10 Ohio State University Syngas Chemical Looping

OSU's SCL process uses countercurrent moving beds and iron-based composite oxygen carriers under reduction-oxidation conditions, converting coal-derived syngas into carbon-free energy carriers for electricity or hydrogen/chemical production. The project is funded by DOE's Advanced Research Projects Agency-Energy, which is providing OSU $5 million for this project. SCL has been successfully demonstrated at bench and sub-pilot scales, and will be tested at the NCCC at a 250-kW pilot scale utilizing up to 900 lb/hr of syngas. Initial commissioning of the SCL pilot unit at the NCCC began in 2013 and continued in 2014.

Start-up activities in run R13 included process heater start-up, solids make-up and discharge sequence and operation check, and solids circulation studies under pressurized and heated operating conditions. Initial reactor heat-up was accomplished using electric heaters installed on the process gas supply lines. Operation of the process with syngas was planned for run R13, but was precluded by issues with the burner.

The solids circulation studies were conducted at ambient pressure and pressures of 30, 60, and 132 psig. In each condition, solids circulation was confirmed using the system pressure balance and particle make-up system. The results indicated reliable reactor system operation with the expected syngas conversion capacity and hydrogen generation. Further, the results showed that the solid circulation rate is controllable within the full range of design conditions. Previous cold model studies at the Particulate Solid Research facility were performed under ambient pressure and temperature. The NCCC circulation studies were successfully performed at elevated and operating pressure for 184 hours without significant issues. Syngas operation of the SCL process is planned following the incorporation of burner modifications.

3.11 Stanford University Tunable Diode Laser

Stanford University's Tunable Diode Laser was designed for real-time analysis of syngas constituents and stream conditions and is considered to be a potential break-through technology for control of advanced gasification systems. During R09, Stanford University's Hanson research group tested the TDL technology with syngas downstream of the PCD. These initial results validated the TDL technology's ability for real-time in-situ monitoring of H_2O, CO_2, and gas temperature in a gasification process. For R13, the TDL was modified to detect syngas CO and CH_4 in addition to temperature and moisture to extend the utility of laser-absorption sensing for gasification processes. The R13 testing validated the earlier results, with meaningful data obtained for all syngas species of interest. The success of the TDL sensor campaigns at the NCCC showed that laser absorption sensing is not only possible in engineering-scale gasifiers, but could be an important new diagnostic tool with the potential for new control strategies in future gasifier utilization and development.

3.11.1 Testing Arrangement

Although the Stanford TDL sensor was applied successfully in university research gasifiers, all previous tests were limited to run times of less than 12 hours, and the sensors could be adjusted by operators during the run. Testing at NCCC offered the first opportunity for measurements in

an engineering-scale system, with the safety and access limitations expected for industrial-scale gasifiers over a duration of several weeks.

Laser absorption is a line-of-sight measurement and requires optical access across the measurement volume. This was a challenge at NCCC where engineering design of optical access in the syngas process piping had not been previously performed. A location was selected 99 feet downstream of the PCD, with the sensor lasers and electronics remotely located in an instrumentation shelter, as illustrated in Figure 118.

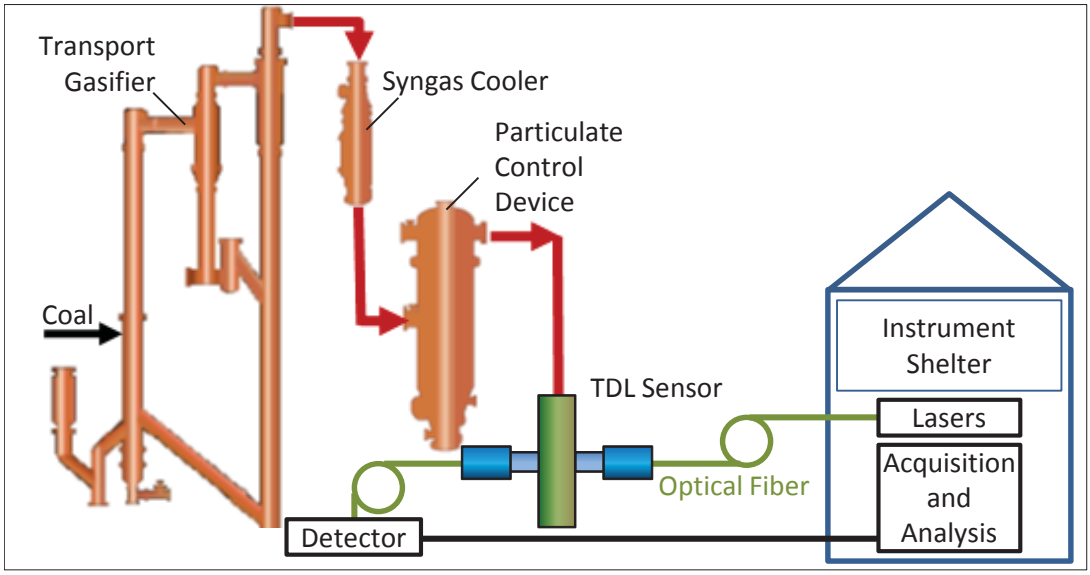

Figure 118. Location of TDL Sensor in NCCC Transport Gasification Process

The installation of windows for laser transmission across the syngas flow required several features to insure no release of syngas in the event of a window failure. Redundant shut-off valves were installed for isolation of syngas from the laser transmitter and receiver. The windows were one-inch thick sapphire, which were mounted onto standard 900-pound ANSI flanges and pressure tested to 1,600 psig at 400°F. A pair of windows was mounted on each side of the syngas flow with a pressure and temperature monitor between each window pair; if the gas between the redundant windows should rise in temperature or pressure, the shutoff valves automatically close on the assumption of a window failure. This optical access design was first used for laser absorption of H_2O during the R09 campaign. For the multi-species measurements conducted during R13, the receiver and transmitter optics were completely redesigned to enable remote optical alignment and detector gain adjustment. The wavelengths needed for CO, CH_4 and CO_2 detection were in the range 2 to 2.3 microns, where telecommunications fiber does not have satisfactory performance, and specialty fiber optics were required.

A modulation strategy, wavelength-modulation spectroscopy, developed at Stanford for measurements of gas temperature and concentration in harsh environments was selected for the TDL sensor to provide sensitive and accurate detection of absorption over a wide dynamic range of optical transmission. The degree of non-absorption losses from phenomena such as beam steering were unknown for this application, and the installation of the optical access produced a long (15 feet) line-of-sight sensor path, producing a long moment arm for angular beam

misalignment from transmitter/detector vibration or beam steering in the syngas. Stanford's modulation strategy has proven highly robust to such effects.

3.11.2 Testing in R09

The demonstration of the Stanford TDL sensor at the NCCC during the R09 test run focused on five areas:

- Design, fabrication, and operation of the sensor while meeting the requirements for safe operation in the syngas process
- Evaluating in-situ syngas TDL measurements with only remote access
- Correlation of in-situ syngas TDL measurements with NCCC analysis equipment
- Comparison of increased time resolution against current sampling-based GC and H_2O measurements
- Reliability of the optical windows to provide safe, stable, long-term operation

The results from the TDL sensor during the R09 test campaign were positive for all of these areas of focus. A prototype sensor for H_2O and gas temperature was designed for optimal performance at the conditions expected for the measurement location (620 to 800^{o}F, 220 to 290 psig, 6 to 10 vol% H_2O, 8-inch path length).

Measurements were conducted during R09 from the beginning (hour 0) until end (hour 630) of the campaign. During the entire test period, the laser transmission was stable and the window performance and optical alignment did not degrade with time or ambient temperature or during gasifier warm-up. There were no leaks or failures in the TDL sensor package. Measurements of H_2O and temperature were made with a time resolution of a few seconds. Sensor performance was evaluated with wide variety of laser scan and modulation parameters. From hours 62 through 97, temperature measurements were suspended and bonus proof-of-concept measurements of CO_2 were conducted. Raw sensor data from the entire campaign was recorded for subsequent optimization of the data analysis procedures. Measurements of moisture content were in good agreement with sampling data although with significantly faster time resolution; temperature measurements also agreed with thermocouple data. Even though successful measurements of moisture and temperature were acquired over the entire campaign (no temperature readings for hours 62 through 97), lessons were learned about optical alignment, optical engineering, and optical transmission for further refinement of sensor performance.

3.11.2.1 Start-up Measurements

The TDL-measured moisture level in the syngas, with a 2-second time resolution as shown in Figure 119 from hour 0 to hour 50. During the first few hours, the sensor successfully tracked ignition of the propane burner used for initial warm-up of the gasifier by the appearance of water vapor combustion product. The stability of the H_2O signal during this period mirrored the stability of the propane burner. Hence, the TDL signal has good potential for rapid feedback to the operator on the stability of the heater. During hour 7, the warm-up period of the gasifier began with a stable propane flame. The moisture content of the syngas steadily increased at the

sampling location downstream of the PCD during warm-up; this variation was expected as the fuel/air ratio of the propane burner was being increased as seen in Figure 119.

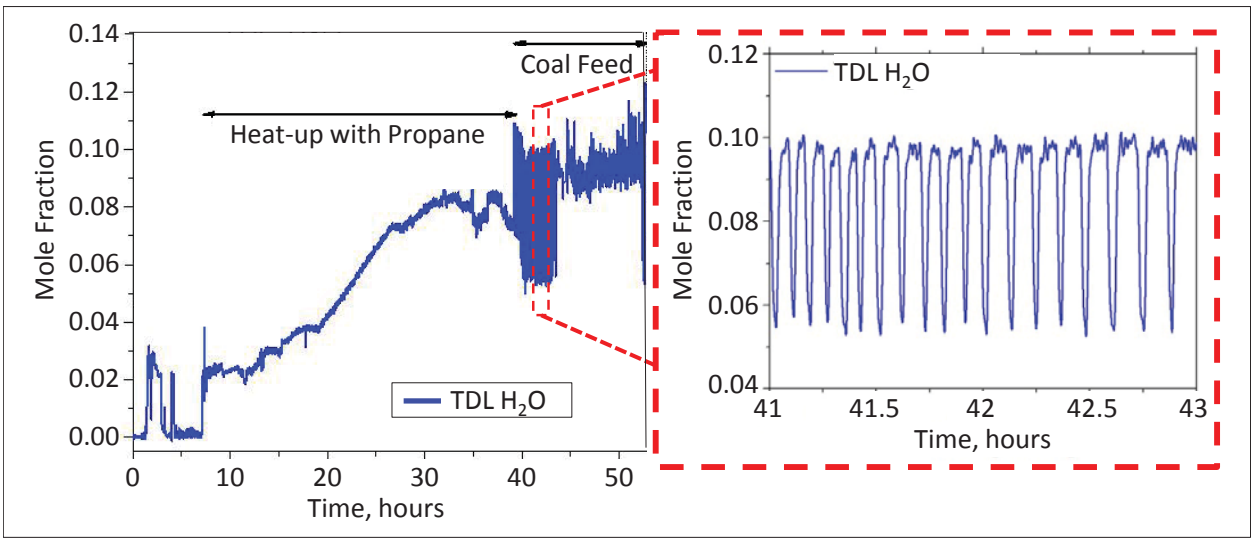

Figure 119. In-Situ Measurements of Flue Gas Moisture during Gasifier Start-Up

The fuel was transitioned to coal (in combustion mode for start-up) at approximately hour 40, and the coal feed rate was pulsed to control the warm-up rate of the gasifier. This transient cycling of the coal fuel is captured in the right panel by the H_2O content variation (with 2-second time resolution) in the flue gases (note that this is not yet syngas as the gasifier is in combustion mode). During this period, propane was terminated at hour 44, and the coal feeding transitioned into gasification mode. This process continued to hour 52 when coal feeding was terminated. This shutdown is also reflected in the TDL measurement of water vapor.

3.11.2.2 Capturing Transients in Operation

Figure 120 presents the syngas moisture level and temperature measurements from the TDL sensor from hours 105.5 to 112; these data are compared to thermocouple data at the PCD outlet and at a location 24 feet downstream of the PCD outlet. The differences between these readings are consistent with the temperature gradient with distance. All three temperatures were stable as a function of time. However, the TDL-measured H_2O content fluctuated with an approximately 10 minute cycle, which correlated with the gasifier temperature also shown in Figure 120. The transients captured in the gasifier temperature were also reflected in the syngas moisture content.

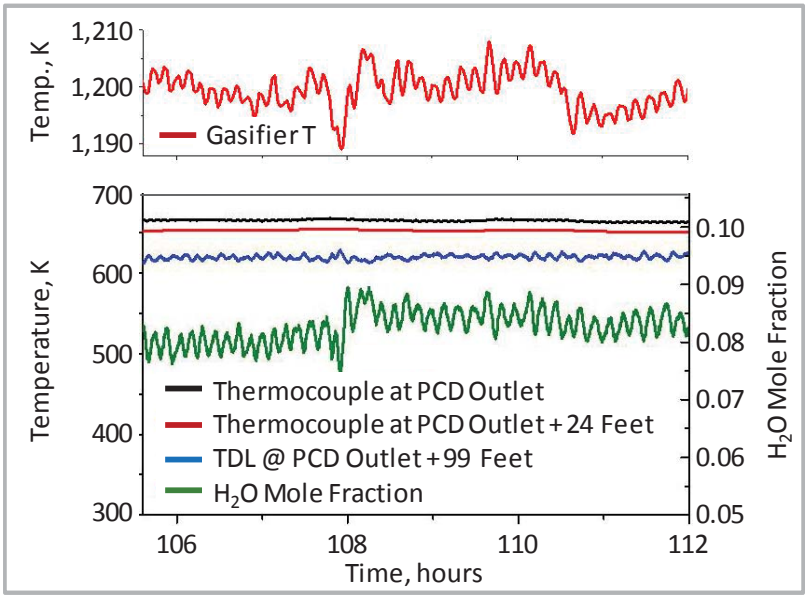

Figure 120. Thermocouple Measurements Compared with TDL Temperature and Syngas H_2O Measurements

Two conclusions drawn from these observations were:

- The syngas H_2O level indicated the transient behavior in the gasifier, demonstrating the feasibility of a gasifier control sensor located downstream of the PCD.
- The stable syngas temperature measured by the TDL sensor reflected the large thermal mass of the gasifier and piping between the gasifier and TDL sensor locations; however, the moisture level measurements were unaffected by this thermal mass, and the high velocity of the syngas flow avoided diffusive mixing.

3.11.2.3 Continuous Monitoring

The TDL sensor collected continuous records of H_2O from hour 140 until hour 575, except for three short periods when the sensor valves were closed as a precaution when gasifier upsets occurred. During the entire period, transmission of the TDL sensor was stable, the windows did not exhibit any indications of fouling, and there were no noticeable effects of variations in temperature. Figure 121 plots the syngas H_2O measurements from the sensor and from condensate samples. These two H_2O measurements methods have similar mean values over the 435-hour record with larger variations in the condensate sampling.

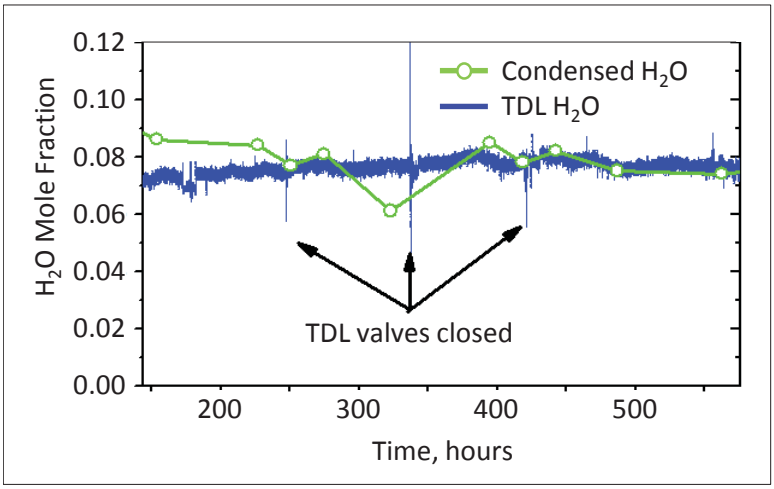

Figure 121. Continuous TDL H_2O Measurements Compared with H_2O Sampling Data

The H_2O mole fraction data of Figure 121 varies with time by approximately ±0.002, which might suggest that the TDL sensor has a ±3 percent statistical uncertainty. However, when the H_2O data are examined on a more expanded time scale, the measured H_2O content has a distinct oscillation suggesting that the sensor is capturing a real variation of H_2O mole fraction. These oscillations in H_2O are strongly correlated with the gasifier temperature, as shown in Figure 122. (Note that the gasifier temperature fluctuations are less than 0.5 percent of the gasifier temperature.) NCCC engineers were able to correlate the variations in the H_2O mole fraction with other data sets: PDAC feeder dispense vessel and discharge line pressure, and PCD back-pulse nitrogen receiver tank pressure. These correlations suggested that the fluctuations in syngas moisture resulted from variations in coal feed rate.

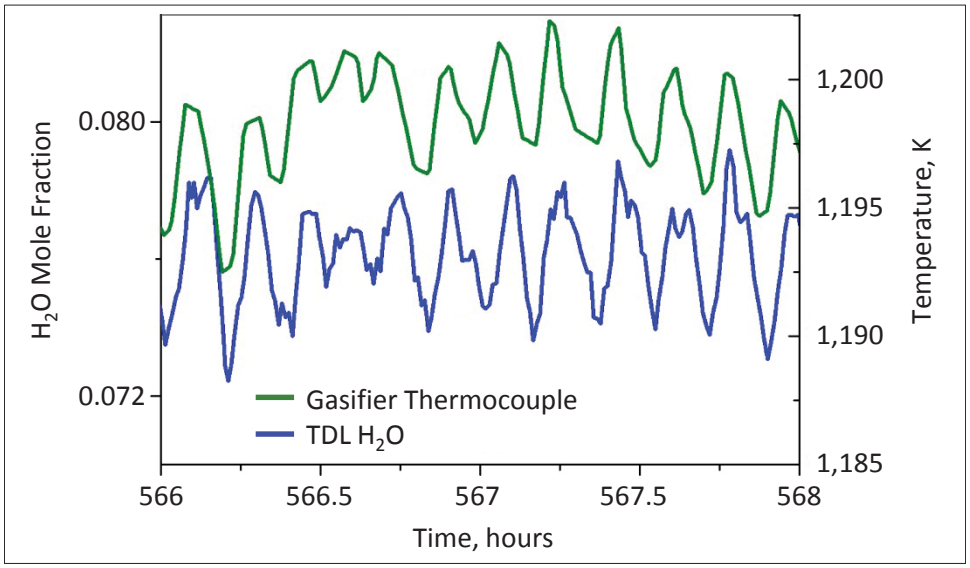

Figure 122. Fluctuations in TDL H_2O Measurements and Gasifier Thermocouple Measurements

Figure 123 demonstrates the nearly perfect correlation of the TDL-measured H_2O mole fraction with the PDAC dispense vessel pressure. As this pressure increases, so does the coal feed rate assuming constant gasifier pressure.

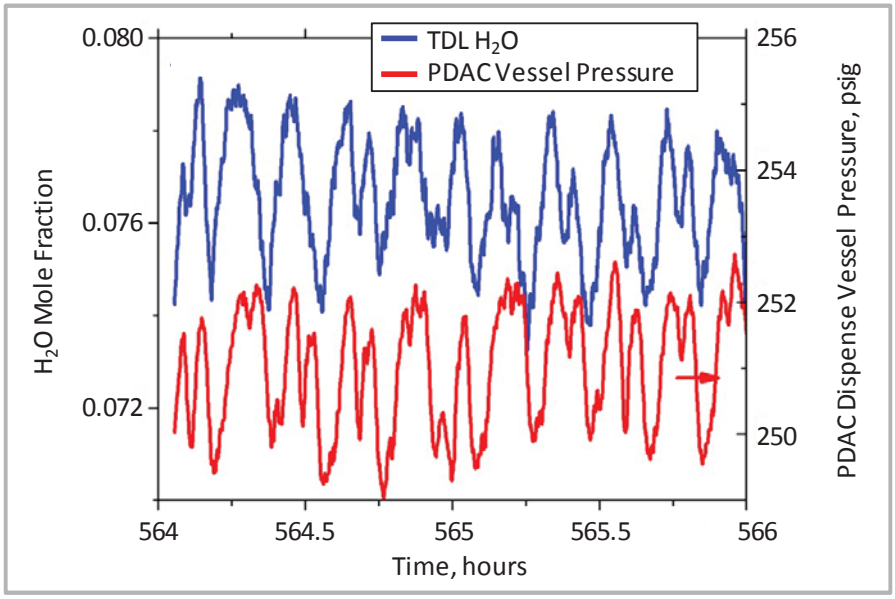

Figure 123. Fluctuations in TDL H_2O Measurements and PDAC Feeder Pressure

Changes in the TDL-measured H_2O mole fraction mirrored changes in the GC measured CO_2, and an example is given in Figure 124 for an event that occurred at approximately hour 420. Note the changes in CO_2 are mirrored in the changes in syngas H_2O. However, the improved time resolution of the TDL sensor provides H_2O mole fraction that captures the variation in the gasifier conditions, and the TDL sensor data is approximately 30 minutes ahead of the GC, illustrating the long time delays from gas sampling, drying, and GC measurement time.

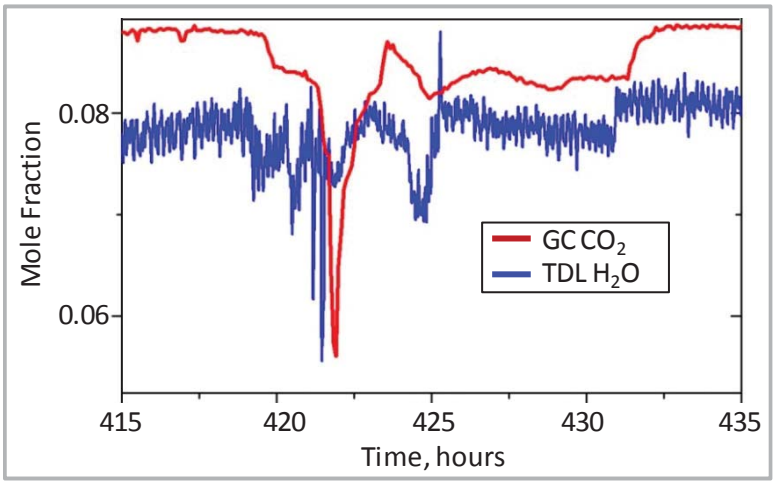

Figure 124. TDL H_2O Measurement and GC CO_2 Measurements during Upset Condition

3.11.2.4 Conclusions from R09 Testing

The optical system was stable over the entire campaign, with no obvious window fouling or loss of alignment due to gasifier or ambient temperature. This optical system was used for monitoring both water vapor content and temperature, the latter based on the ratio of absorption by two water vapor transitions.

One of the water vapor absorption transitions provided temperature-insensitive monitoring of water vapor mole fraction. The H_2O mole fraction was recorded continuously from hour 0 to hour 630, with unattended operation from hour 140 to hour 575. The water mole fraction measurements were in good agreement with liquid water sampling data collected by NCCC. The precision of the H_2O mole fraction measurements appeared to be on the order of one part in a thousand. Variations measured by the TDL sensor in the H_2O mole fraction of the product syngas were on the order of ±2 parts in 80, correlating well with temperature fluctuations in the gasifier of ±2 K and with pressure variations in the coal feed system.

The fraction of transmitted light was less than expected, suggesting that improvements to the optical collection to suppress beam steering could improve sensor performance. Successful unattended operation of the TDL sensor suggests the utility of improving the sensor software for remote (e.g., internet) access to the sensor to assess sensor health and optical alignment. Stanford's first use of remote adjustment of optical alignment was successful, suggesting that remote alignment and sensor operation could be quite feasible for very long-term operation. Stanford's calibration-free, wavelength modulation spectroscopy strategy ensured accurate interpretation of absorption signals even at low light transmission (<0.01 percent). This strategy also suppressed signal variation with changes in the optical transmission. The addition of automatic gain control in the signal processing has the potential for operation over even larger dynamic ranges.

The rapid time-resolution of the TDL sensor allowed it to capture changes in the syngas composition that were not evident in the GC monitor. The TDL sensor also responded to gasifier changes nearly 30 minutes before the GC instrument. The rapid time-resolution suggests that the TDL sensor has promise as a control sensor for the gasifier, even when the TDL sensor is located downstream of the PCD.

3.11.3 TDL Testing in R13

Time-resolved concentration data from all four species, CO, CH_4, CO_2, and H_2O, were successfully collected from the beginning of the test run, as shown in Figure 125. This data shows the transition from combustion-mode operation for gasifier heat up to gasification mode at around 114.3 hours. During the gasifier start-up, the laser transmission was attenuated by more than 99.9 percent by the scattering from particulate in the syngas. Even at the low laser transmission conditions, the sensor was able to simultaneously monitor all four species with sub-second time resolution with signal-to-noise ratios better than 10 on all four species. The figure also illustrates the advantage of the rapid time response of the laser absorption sensor compared to the GC analysis of sampled syngas. Although the mole fractions of the GC and the laser absorption were in good agreement, the GC data was shifted by 20 minutes due to the time delay of flow between sample point and GC measurement.

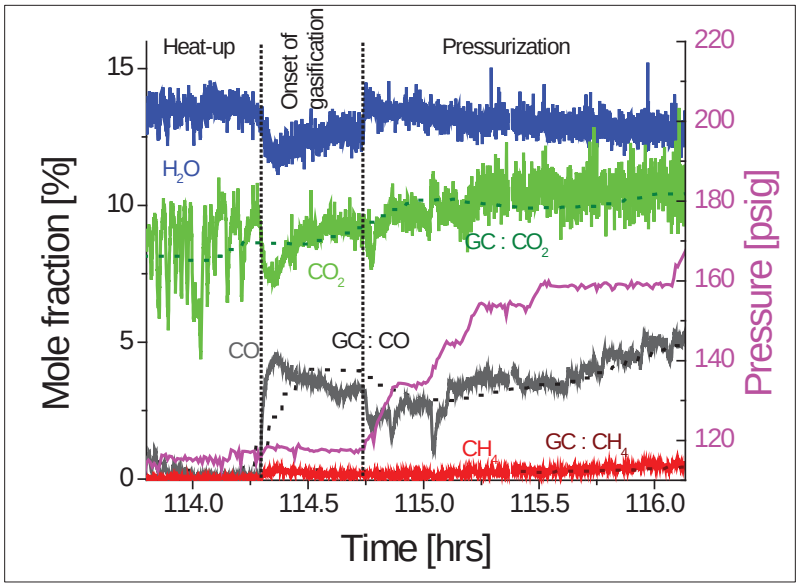

Figure 125. TDL and GC Measurements of Syngas Composition during R13 Start-Up

Figure 126 plots concentration measurements during steady state gasifier operation. The GC data showed steady syngas composition after 121.7 hours; however, the TDL sensor showed there were temporal fluctuations. Concentrations of CO_2 and H_2O showed a positive correlation with temperature, and concentrations of CO and CH_4 showed a negative correlation.

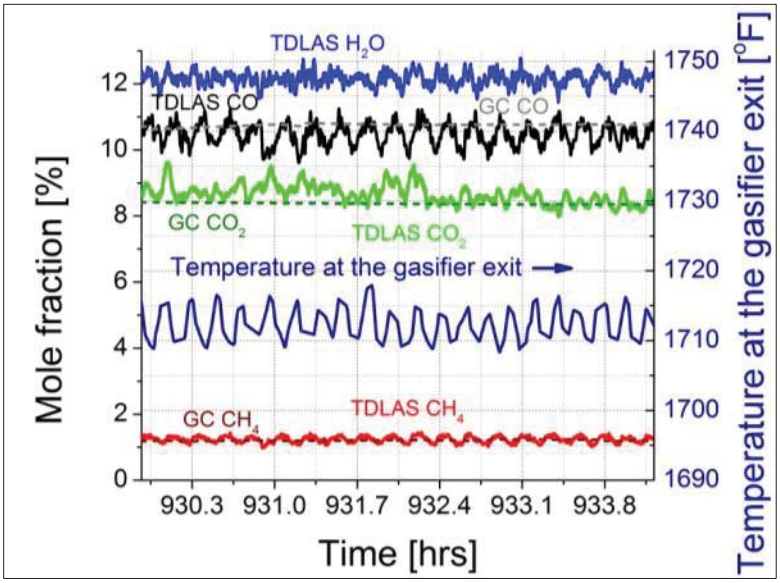

Figure 126. TDL and GC Syngas Composition Measurements during Steady State Gasifier Operation

The test results suggest that the sensor could be used for gasifier control. This work resulted in five significant advancements for laser absorption sensors for practical combustion and gasification applications, which are listed below.

- A novel fiber bundle was developed to combine multiple extended near infrared laser-beams onto a single optical path.

- A normalized, wavelength-scanned wavelength modulation spectroscopy strategy was used for species measurements in dusty syngas with more than 99.9 percent laser transmission losses due to scattering.
- The sensor strategy allowed for sub-second time resolution for simultaneous measurements of four species.
- The prototype sensor demonstrated remotely adjustable detector gain and beam adjustment that enabled alignment optimization that met the safety requirements needed for syngas.
- The optical engineering was sufficiently robust to enable operation without further operator intervention over the entire 54-day measurement campaign.

3.12 SRI Fischer-Tropsch Catalyst

The SRI Fischer-Tropsch catalyst project incorporates a novel approach of FT synthesis that eliminates the conventional product upgrading and refining steps and enhances the ability of coal-to-liquids and coal/biomass-to-liquids processes to compete with petroleum-based processes. SRI's 5-lb/hr bench-scale test skid consists of a FT synthesis reactor system to produce liquid transportation fuels using a selective, wax-free, cobalt FT catalyst provided by Chevron. The first test campaign of this system at the NCCC was conducted during R13 and included system commissioning, catalyst testing with bottle gas, and syngas cleanup testing. Catalyst testing with syngas was not completed due to operational issues. The major accomplishments of the testing are listed below.

- Activated the FT catalyst using pure hydrogen
- Operated the unit for over 60 hours using bottle syngas
- Maintained a hydrogen-to-CO ratio of 1.95 to 2.01 during the bottle gas testing
- Achieved designed conversions and production rates of more than 2 liter/day
- Demonstrated high catalyst hydrocarbon productivity of 0.65 to 0.75 gram (as carbon) per gram of catalyst/hr at 437^{o}F with 34 percent hydrogen, 17 percent CO, and 49 percent nitrogen
- Operated the pumpless thermal siphon heat removal system
- Demonstrated efficient heat removal and nearly isothermal conditions in the two-inch fixed-bed reactor (All previous bench- to pilot-scale studies by others in the field have been limited to a one-inch or less diameter reactor and have not achieved isothermal operation. This was considered by Chevron as the most significant achievement as previous attempts have failed.)
- Successfully ran raw syngas at inlet pressure (175 to 190 psig) and temperature (842 to 1,112^{o}F) for over 24 hours
- With syngas feed, verified that tar does not cause any plugging prior to the tar trap
- Verified syngas compressor operation

3.13 Gasification Process Modifications

Several modifications were made to the gasification process during the contract period to address equipment-related issues. The most significant modification made was the replacement of the gasifier standpipe. During routine inspections of the gasifier in 2009, refractory damage was identified in the standpipe arising from the loss of hot-face refractory. Two places of concern were the intersection of the solids separation unit and standpipe, and the intersection of the J-leg and standpipe.

The refractory in the standpipe and J-leg was the refractory originally installed in the gasifier, and had been in service for 15 years and almost 22,000 hours of operation, experiencing more thermal cycles than would a commercial unit. Figure 127 shows borescope inspection photographs of the standpipe refractory. As seen in the figure, the refractory was in excellent condition following initial operation with the new standpipe in runs R08 and R09. Subsequent inspections showed minimal wear of the gasifier refractory until the post-R13 inspections, which revealed damage in the outlet of the solids separation device. This damage was repaired prior to further operation.

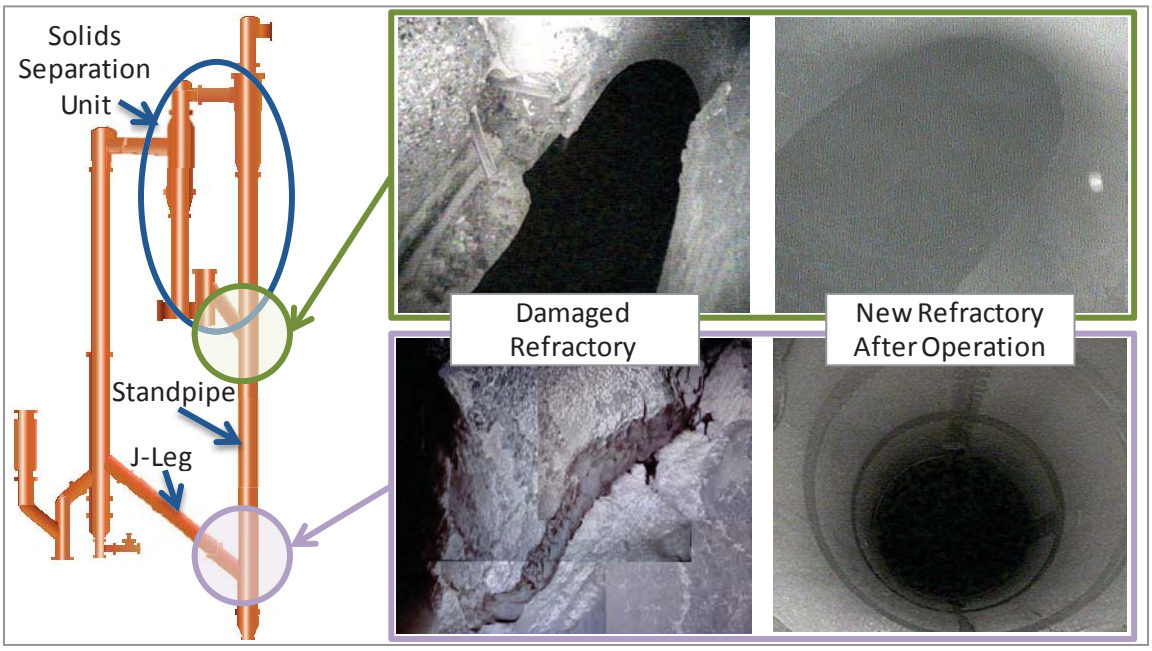

Figure 127. Gasifier Standpipe Refractory before and after Standpipe Replacement

Other modifications made included:

- Repair of a structural weld on the PCD tubesheet
- Implementation of a new pressure letdown device for the Continuous Fine Ash Depressurization system to decrease construction costs of the system
- Replacement of the primary syngas cooler

4.0 PRE-COMBUSTION CO_2 CAPTURE

The NCCC's pre-combustion CO_2 capture program allows evaluation of solvents, sorbents, catalysts, membranes, and other emerging technologies at an appropriate scale with coal-derived syngas produced during gasification runs. The flexibility and scale of the NCCC is well suited to test CO_2 capture and gas cleanup technologies and accelerate their advancement through the component testing and pilot plant stages of development. The NCCC can test multiple projects in parallel with a wide range of test equipment sizes leading up to pre-commercial equipment sufficient to guide the design of demonstration-scale processes.

Pre-combustion facilities include the SCU, which has been in operation since 2004. Figure 128 provides a photograph of the SCU, housing syngas pre-treatment equipment, developer test skids, a dedicated control room and gas analyzer building, and other support equipment. The SCU has undergone almost continuous expansion and upgrading to accommodate testing of new technologies.

Figure 128. Syngas Conditioning Unit

The SCU can test multiple technologies simultaneously at different syngas flow rates up to 1,500 lb/hr and syngas conditions at temperatures up to 700°F. Figure 129 is a schematic of the pre-combustion facilities showing recently tested technologies. A variety of syngas conditioning steps can be implemented to meet developer requirements such as hot gas cleanup, cold gas cleanup, sulfur removal, trace metal removal, WGS, or hydrocarbon treatment. Extensive gas analysis capabilities include nine process and two laboratory GCs, and two NDIR CO_2 analyzers. The instruments run continuously and feature automated sample switching, which increases the number of sample points monitored by single instrument. The SCU also has the capacity for

injection of specialty gases to adjust syngas quality and composition supplied to developers such as augmentation with hydrogen, CO_2, or H_2S. Bottle gases are also used for off-line testing.

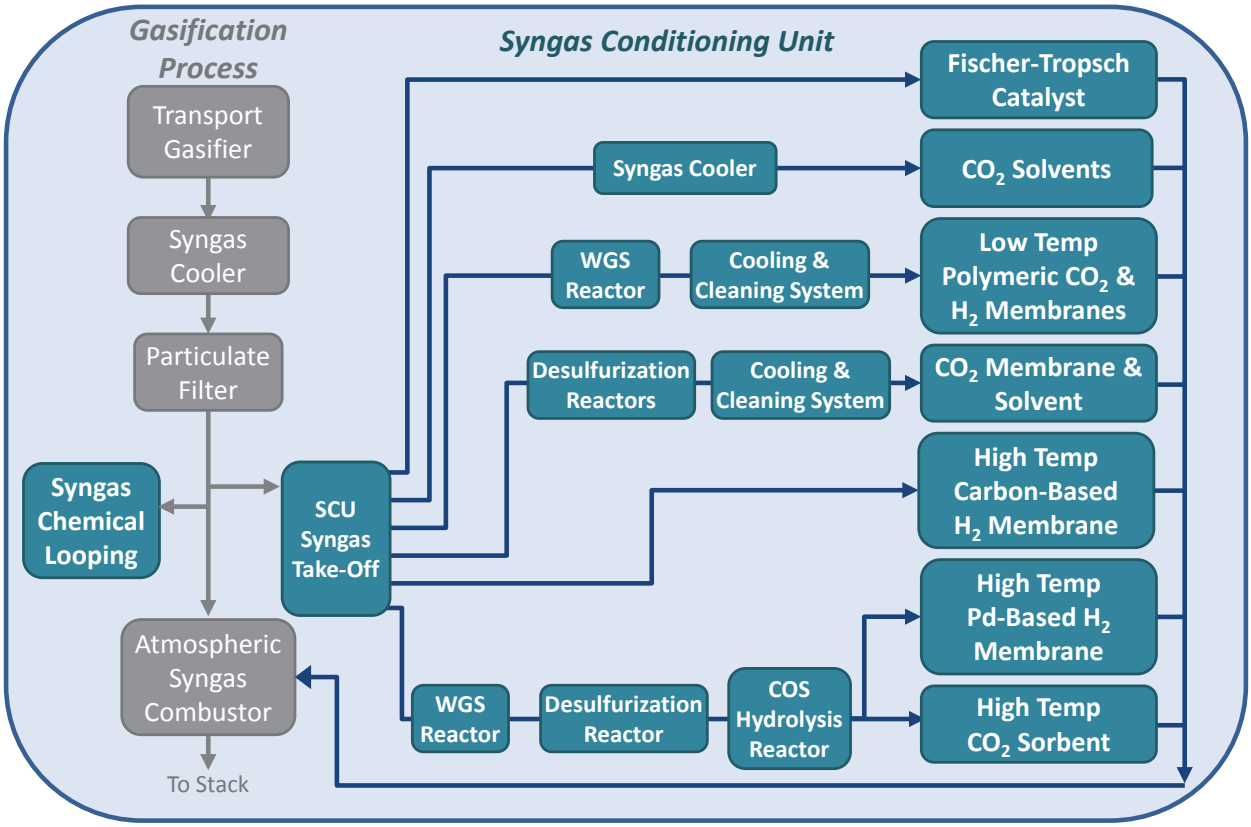

Figure 129. Schematic of Pre-Combustion Facilities with Developer Units

4.1 Media & Process Technology Hydrogen Membrane

Media & Process Technology, a technology innovator specializing in the development of high-performance, low-cost ceramic membranes, first tested its hydrogen-selective Carbon Molecular Sieve membrane at the site in 2008. MPT began evaluation of the CMS technology, as described in Table 51, first with single tubes, then progressing to a pilot bundle containing up to 17 tubes before developing a full-scale tube bundle processing up to 50 lb/hr of syngas. After successfully demonstrating the full-scale CMS in 2012, MPT incorporated WGS functionality into the CMS bundle to produce a catalytic membrane reactor, or CMR. This concept allows the separation of hydrogen simultaneously with its formation.

Table 51. Scales of Membranes Tested by MPT

Scale	Dimensions	Surface Area, m^2	H_2 Throughput, SCFH
Single Tube	0.57 cm OD x 76 cm length	0.009	1.5
Pilot-Scale Bundle	3.8 cm OD x 76 cm length	0.115	19
Full-Scale Bundle	7.6 cm OD x 76 cm length	0.762	128

Table 52 lists the tests conducted by MPT in development of the CMS.

Table 52. Summary of MPT Carbon Molecular Sieve Testing

Run Number	Test Duration, hr	Membrane Configuration Tested
TC25	19	Single tube
R01	100	Single tube
R03	100	10 single tubes
R04	40	10 single tubes
R05	250	14-tube bundle
R07	300	86-tube bundle
R08	100	86-tube bundle
R09	370	86-tube bundle
R10	380	86-tube bundle as CMR
R11	350	86-tube bundle as CMR

4.1.1 Single Tube and Pilot-Scale Membrane Bundle

In early field tests conducted with single-tube membranes and membrane tube bundles, MPT confirmed the process viability of hydrogen separation and the removal of CO_2 and other contaminants from coal-derived syngas without pre-treatment. Highlights of MPT's testing through 2010 are given below.

High Temperature Operation without Syngas Pre-Treatment

During initial testing, syngas fed to the MPT membrane was pretreated with a scrubber to remove hydrocarbons. The pretreatment was successful in allowing steady state permeation at an operating temperature of 350°F. One of the test objectives in 2010 was to eliminate the pre-treatment. During the first test without the prescrubber, in April 2010, the membrane permeate flux decreased by 80 percent compared to previous operation due to fouling on the membrane surface. Increasing the operating temperature from 350 to 450°F eliminated most of the fouling, with the flux reduction only 10 percent less than previous operation.

For the next run in August 2010, MPT modified the test unit to accommodate membrane permeation at 530°F. At this temperature, no permeance reduction was observed, indicating the higher temperature operation was necessary to prevent fouling. Subsequently, the membrane was operated for more than 100 hours continuously at this higher temperature without any degradation in membrane performance and materials. In summary, the 2010 tests demonstrated stable membrane performance and material integrity at this elevated temperature without syngas pretreatment for contaminants removal.

The success of this higher temperature operation confirmed the process feasibility of warm gas separation by membranes and the advantage of no pretreatment for contaminants removal from coal-derived syngas. Moreover, this warm gas temperature is compatible with the operating temperature for water-gas shift reaction using sour gas shift catalysts. Therefore, process intensification via integration of gas clean up, water-gas shift reaction, and hydrogen separation into a single step is technically feasible.

Scale-Up to Multiple Tubes and Tube Bundles

One of the major commercialization barriers associated with the inorganic membranes for high temperature gas separation is the field implementable module/housing/element design, in particular for applications under the coal gasification environment. During the two tests conducted in 2010, MPT methodically scaled up the test membrane unit from the single tube membrane used in the initial tests to multiple tubes and then to a pilot-scale multiple tube bundle. The pilot-scale membrane configuration and housing design employed for these tests proved adequate for the selected operating conditions, i.e., 520 to 570°F and 250 psi for a period of greater than 300 hours, with no leakage detected. The successful demonstration of the pilot-scale bundle during 2010 established an important milestone to justify testing of the full-scale membrane bundle.

Separation Performance

During MPT's testing in 2010 with the multiple single tubes and pilot-scale bundles, the CMS membranes consistently enriched hydrogen to greater than 90 percent purity from 30 to 40 percent in the feed. No membrane degradation in the presence of H_2S was observed.

During testing with single tubes, the product gas consistently contained greater than 98 percent hydrogen with less than 15 ppm H_2S. In the 2010 tests, the removal efficiency of CO_2 and H_2S was lower; the CO_2 content was reduced from 6 to 8 percent in the syngas feed to 2 to 3 percent in the permeate, and the syngas feed concentration of 280 to 350 ppm H_2S was reduced to 20 to 90 ppm in the permeate. Post-run analyses indicated that the membrane peak selectivity occurred at the lower, original design temperature. Following the 2010 tests, MPT optimized the membrane pore structure to improve separation performance at the higher temperature of 530°F.

4.1.2 Full-Scale Membrane Bundle

The full-scale bundle, shown in Figure 130, consists of 86 alumina tubes arranged in a ceramic collar, and is designed for operating temperatures up to 570˚F and transmembrane pressure drops of over 300 psi.

Figure 130. MPT Full-Scale CMS Bundle

MPT's first test with the full-scale CMS was in 2011 during run R07. Operation was conducted with untreated syngas and demonstrated consistent performance and mechanical stability of the bundle and module product.

Demonstration of High Purity Hydrogen with Palladium Membrane Post-Treatment

For the 2011 test run, MPT developed a palladium alloy membrane and installed it downstream of the CMS membrane as a post-treatment for about 10 hours of operation. As a post-treatment, the palladium membrane was exposed to the treated syngas with higher hydrogen content and virtually no sulfur contaminants, which can degrade the palladium. With the CMS permeate fed to the palladium membrane containing 78 to 84 percent hydrogen, the hydrogen content of the final product gas was consistently above 99 percent. Further, no degradation in the performance of the palladium membrane was detected. This study supported the technical feasibility of post-treatment with palladium membranes to produce hydrogen at purity levels required for applications such as fuel cells.

Improvement of Gas Distribution in the Full-Scale CMS Bundle

During the first full-scale CMS bundle test, performance with raw syngas at 480°F and 215 psia was lower than anticipated based on previous tests with single tubes and the pilot module. Hydrogen permeance for the syngas was on average 0.8 $m^3/m^2/hr/bar$, about half the value expected for pure hydrogen. The hydrogen concentration in the permeate was also lower than expected. With around 7 vol% hydrogen in the syngas, the permeate contained about 35 vol% hydrogen compared to 55 vol% in previous tests. With around 40 vol% hydrogen in the syngas, the permeate contained 80 vol % hydrogen compared to 95 vol% or more in previous tests.

In January 2012 at MPT's Pittsburgh laboratory, MPT investigated performance of the full-scale membrane bundle tested during R07. The lab testing indicated considerable discrepancy between the permeance for pure helium and for gas mixtures of He/N_2 or He/Ar. As this discrepancy was not observed for the single-tube and the pilot-scale module testing, the reduced performance was attributed to poor radial distribution of the syngas within the bundle. To improve distribution, baffles similar to those used in shell-and-tube heat exchangers were installed longitudinally to force the syngas to flow across the bundle diameter and so access the interior tubes.

MPT tested a number of baffle arrangements using a 60:40 He/Ar mixture and identified one that raised permeance to about 1.4 $m^3/m^2/hr/bar$, almost 90 percent of the pure helium value. To extend the range of operating pressure and gas flow rates and confirm the improved performance of the bundle prior to testing with syngas in R08, off-line tests on MPT's test skid at the NCCC were completed. The off-line testing was carried out in April 2012 using a 70:30 He/N_2 mixture and achieved permeance values of 1.45 to 1.51 $m^3/m^2/hr/bar$, 95 to 99 percent of the value for pure helium. These results confirmed that the baffle arrangement identified by MPT improved gas distribution within the membrane bundle, enabling it to achieve results similar to those of single tubes. Hence, this baffle arrangement was included in a new membrane module for future testing.

During the subsequent R08 run during 2012, test data confirmed the results obtained from off-line testing, as the hydrogen permeance was within 85 to 90 percent of the pure component value. Further, the product hydrogen purity was in the range of 50 to 55 percent from raw syngas containing about 8 percent hydrogen, far exceeding the 35 to 40 percent hydrogen purity results obtained in earlier tests at NCCC. Overall, the redesigned baffle was able to successfully overcome the feed flow distribution problem experienced during R07 test campaign.

Further testing of the full-scale bundle was conducted in run R09 in 2012, during which the CMS was operated for almost 400 hours, processing 50 lb/hr of raw flue gas at 190 psia and 500°F. For short-duration tests, the syngas hydrogen content was increased to 40 vol% (simulating the syngas produced by a commercial oxygen-blown gasifier), resulting in hydrogen permeate purity of about 95 percent (dry basis). This degree of product enrichment is greater than that achieved for the single tube and pilot-bundle membranes and indicates the improvements made in the quality of the deposited CMS layer.

High permeate moisture levels limited the accuracy of hydrogen permeance determinations, but helium and nitrogen pure-component permeance measurements were made periodically to give an indication of membrane performance stability. The permeance for helium was about 1.1 $m^3/m^2/hr/bar$ and that for nitrogen was about 0.01 $m^3/m^2/hr/bar$; these values were stable throughout the 300-hour continuous test period and corresponded to values obtained from off-line characterization tests for the membrane bundle.

4.1.3 Catalytic Membrane Reactor

After successfully demonstrating the full-scale CMS bundle, MPT incorporated the WGS functionality into the bundle to produce a catalytic membrane reactor. This concept allows the separation of hydrogen simultaneously with its formation. Testing of the CMR was conducted in 2013 during runs R10 and R11.

For R10, MPT tested the catalytic membrane reactor concept by installing WGS catalyst inside the CMS vessel surrounding the membrane bundle. The WGS catalyst had been crushed and sieved to 1,000 to 450 microns and placed into the CMS vessel, completely filling the internal space. Initial testing with the tightly packed catalyst next to the membrane bundles resulted in tube failure. Further testing with the vessel only partially filled with the catalyst, leaving two to three inches of space at the top, was conducted without tube failures.

A total of 380 testing hours was completed during R10. Raw syngas from PRB coal with around 8 vol% moisture was fed at 50 lb/hr with the reactor conditions held at 200 psia and 500°F. No additional steam or hydrogen was added to the syngas. At the conditions tested, approximately 25 percent of the CO was shifted to hydrogen, and the membrane flux remained stable. The CO conversion rate was lower than expected, possibly due to the low H_2O-to-CO ratio.

MPT further evaluated the CMR in run R11, completing 350 hours of operation without any membrane tube failure. On average, CO conversion was 50 percent with the moisture inherent in the syngas, and there was no reduction in membrane permeance. The higher CO conversion was attributed to the higher inherent moisture content in syngas from the lignite coal used in R11 compared to that from the PRB coal used for R10. MPT plans to further develop the CMR in future test runs at the NCCC.

4.2 Membrane Technology & Research CO_2 and Hydrogen Membranes

In 2009, MTR began testing two types of polymeric membranes for pre-combustion applications at the NCCC: a CO_2-selective Polaris™ membrane and a hydrogen-selective Proteus™ membrane. Successful operation led to scale-ups of both membrane types and demonstration of

a membrane-assisted CO_2 liquefaction process. Both CO_2- and hydrogen-selective membranes offer potentially high-efficiency gas separation in various gasification applications. A dual membrane design concept developed by MTR, which combines high-temperature hydrogen-selective membranes for hydrogen recovery and CO_2-selective membranes integrated with a refrigeration unit for CO_2 purification, may offer significant cost and energy savings over conventional acid gas removal for IGCC processes.

MTR scaled up the CO_2 membrane testing from a 50-lb/hr spiral-wound module to an integrated system designed to process 500 lb/hr syngas, equivalent to the syngas output of a 0.15 MWe IGCC power plant. MTR scaled up the hydrogen membrane from a 1-lb/hr stamp cell to spiral-wound modules, first at 10 lb/hr, and later at a 50-lb/hr scale. Figure 131 provides photographs of the equipment used for testing at the 1- to 50-lb/hr scales.

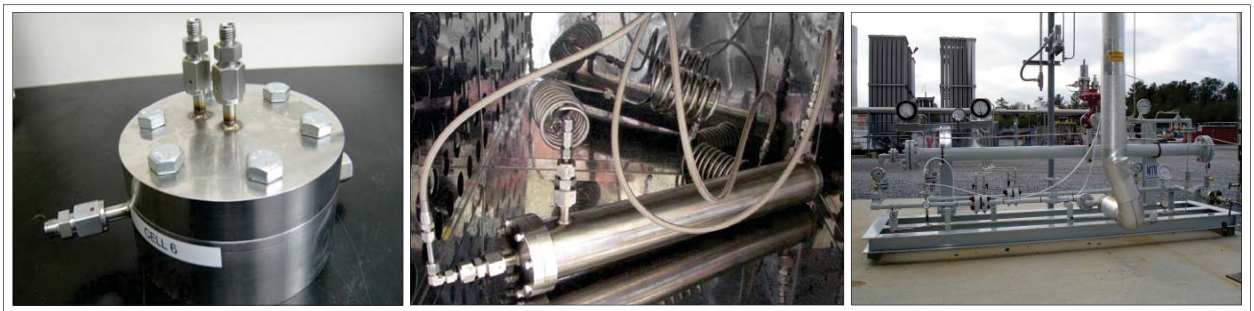

Figure 131. MTR Small-Scale CO_2 and Hydrogen Membrane Test Units

The 500-lb/hr system consists of membrane, compressor, and refrigeration skids, which are shown in Figure 132 as installed at the SCU. This system was designed to test a membrane-assisted CO_2 liquefaction process, which is described in Section 4.2.2.

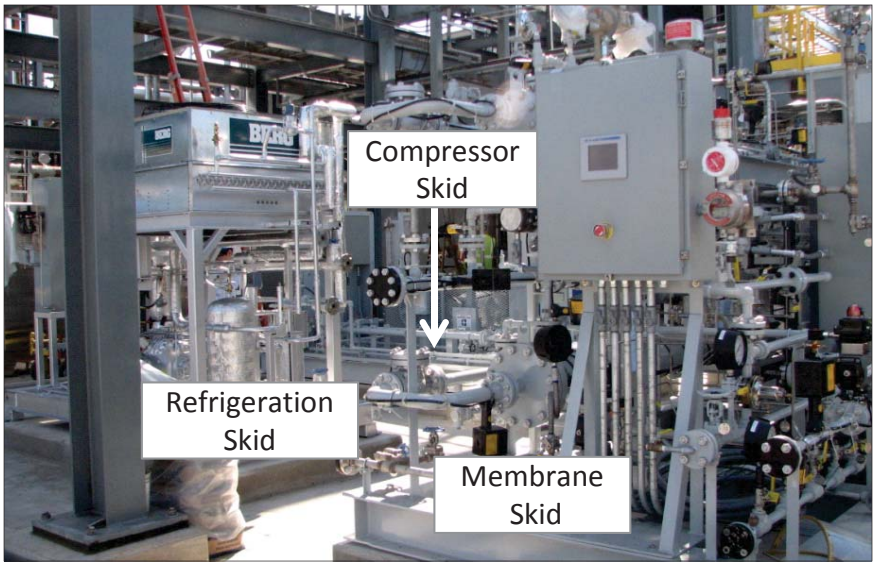

Figure 132. MTR 500 lb/hr Integrated Membrane-Assisted CO_2 Liquefaction Process

4.2.1 Polaris CO_2 Membranes

Initial testing of the Polaris membranes was conducted during run R03 in November 2009, and Polaris modules were tested with the 50-lb/hr skid or with the 500-lb/hr process for all subsequent gasifier campaigns ending with the R11 run in August 2013. Table 53 lists the tests performed with the small-scale unit. This testing utilized shifted syngas treated for hydrocarbon removal, with operating conditions of about 170 psig and near ambient temperatures.

Table 53. Summary of MTR's Polaris Membrane Testing with 50-lb/hr Skid

Run Number	Test Duration, hr	Feed Flow Rate, lb/hr	Membrane Selections Tested and Skid Changes
R03	500	10	Lower flux membrane
R04	500	25	Higher flux membrane
R05	800	25	Improved hydrocarbon removal system; added heat tracing
R06	661	50	Improved hydrocarbon removal system using cooled water
R07	807	50	New membrane configurations; two modules installed in series
R08	288	50	New membrane configurations; two modules installed in series
R09	186	50	New membrane configurations; one module installed
R10	670	50	New membrane configurations; one module installed

During the R03 run, operation included approximately 20 days of continuous operation with a single module, with the feed syngas additionally pre-treated to bring the sulfur content below 10 ppm. The feed temperature fluctuated between 23°F and 77°F during the field test, mainly due to changes in the ambient temperature. Figure 133 shows the CO_2 removal performance of the Polaris membrane module, with CO_2 enrichment from 10 to 12 percent in the feed to 40 to 60 percent in the permeate. The performance was stable during the entire test period, indicating no deterioration of the membrane module after exposure to the shifted, desulfurized syngas.

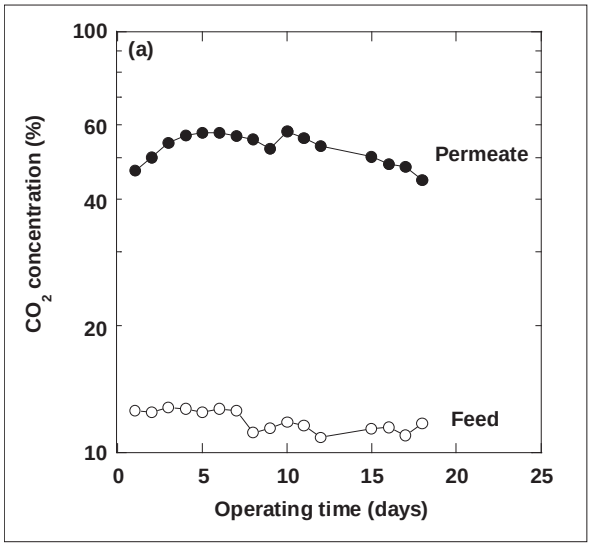

Figure 133. CO_2 Concentration in Feed and Permeate Streams of Polaris Membrane during R03

Figure 134 shows mixed-gas permeance and mixed-gas CO_2/gas selectivity values for the module over time. In general, the Polaris membrane module showed CO_2 permeance of 100 to 300 gpu, CO_2/H_2 selectivity of 6 to 10, CO_2/CO selectivity of 10 to 20, and CO_2/N_2 selectivity of 20 to 50. It should be noted that a relatively low permeance Polaris membrane module was prepared for this test to control the stage-cut in the experiment to less than 15 percent. If a high permeance Polaris module were used with the available syngas feed rate, most of the feed gas would have permeated the module. The important result from this test was that the module performance was stable with time.

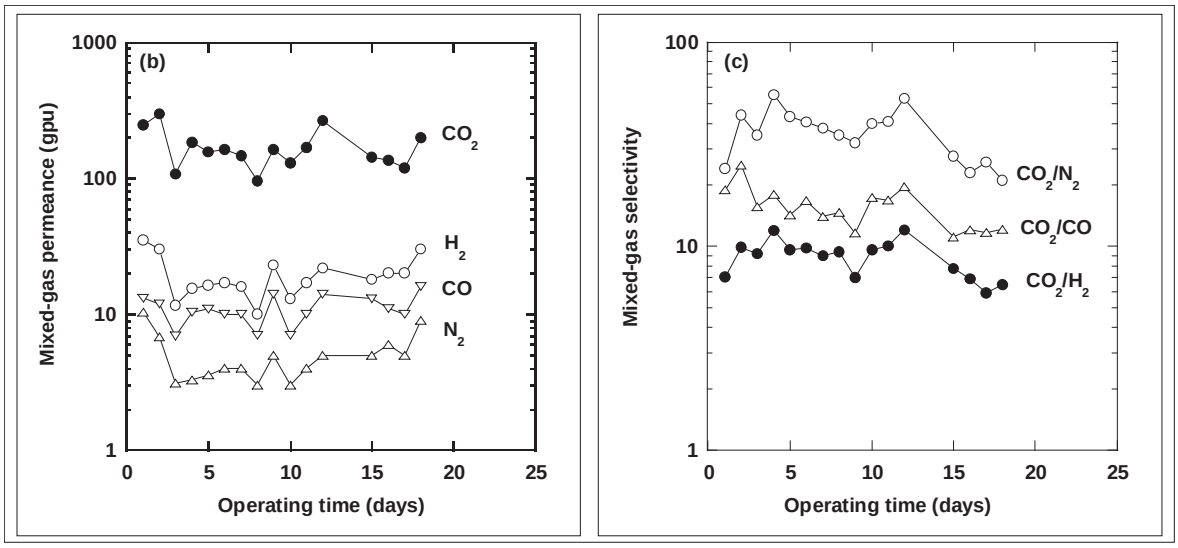

Figure 134. Mixed-Gas Permeance and Selectivity of Polaris Membrane Module during R03

During R06 and subsequent runs, the syngas was not desulfurized prior to entering the membrane skid. Testing with syngas containing H_2S showed that the membrane modules were stable in the presence of H_2S. Figure 135 plots the H_2S/CO_2 selectivity of the module at 90°F over time during R06, with the H_2S content of the feed syngas at about 320 ppm. The membranes showed H_2S/CO_2 selectivity of around 3, consistent with rubbery polymers where separation is determined by the solubility selectivity. H_2S, with a critical temperature of 373 K, is more condensable than CO_2 with a critical temperature of 304 K; therefore, H_2S has higher solubility and permeability than CO_2. Thus, the Polaris membranes also provide one way to co-capture H_2S and CO_2 if desired. Since H_2S is more permeable than CO_2 through Polaris membranes, if 90 percent CO_2 is removed from the syngas, even greater percentages of H_2S will be removed at no additional cost.

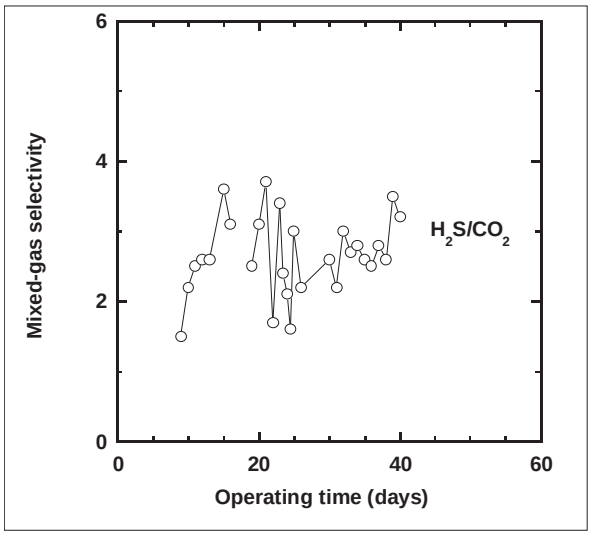

Figure 135. H_2S/CO_2 Selectivity of Polaris Membrane Module during R06

4.2.2 Polaris Membrane-Assisted CO_2 Liquefaction Process

Based on successful pilot-scale module testing, a larger membrane demonstration system for treating 500 lb/hr of syngas was designed, built, and installed at NCCC. This system tested not only the membrane components, but also the overall membrane process for syngas purification and CO_2 liquefaction. The liquefaction of CO_2 is an integral step in CO_2 capture and sequestration from syngas using membrane technology.

Before entering the membrane system, the syngas was pre-treated to reduce the concentration of sulfur compounds (H_2S and COS) to below 1 ppm, sent to a water quench tank and scrubber to remove long-chain hydrocarbons, and then cooled to 50°F. Two zinc oxide beds were used to remove H_2S and COS, avoiding their co-liquefaction in the liquid CO_2 condenser of the membrane system, and the hydrocarbons were removed to prevent build-up and blocking of the valves and piping.

As indicated in the process diagram provided in Figure 136, the system includes two stages of membrane modules for CO_2 separation. The first membrane stage can accommodate one or two 8-inch diameter modules with a membrane area of up to 40 m^2, and the second membrane stage holds one or two 4-inch diameter modules with a membrane area of up to 6 m^2. The system also houses a sulfur polishing reactor and two desiccant dryers for sulfur and moisture removal upstream of the compressor and refrigeration skids, heaters, and control panels. The first-stage membrane permeate is pressurized to about 29 bar in the compressor, and then the compressed gas stream is liquefied in the refrigeration skid which removes the CO_2. Uncondensed gas is fed to the second-stage membrane for further CO_2 separation. The second-stage membrane permeate stream is combined with the first-stage permeate stream, and the combined stream is treated in the sulfur polishing reactor. The overall system captures 70 percent of the CO_2 in the feed as high-pressure, high-density fluid ready for sequestration.

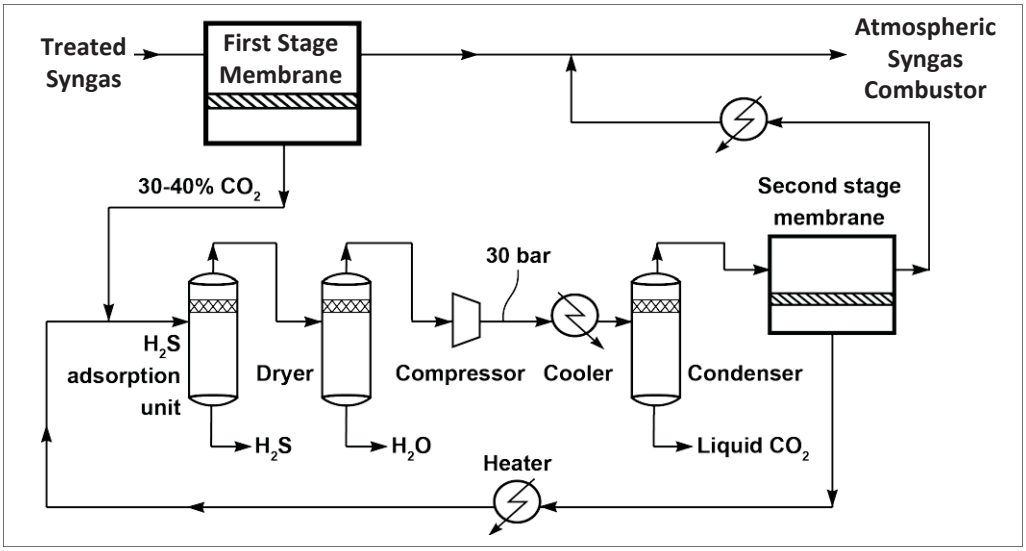

Figure 136. Block Flow Diagram of MTR Polaris Membrane-Assisted CO_2 Liquefaction Process

Table 54 summarizes activities conducted at NCCC using the larger membrane demonstration system.

Table 54. Summary of MTR Test Runs of Large-Scale CO_2 Membrane System

Run Number	Membrane Selections Tested and Changes in CO_2 Liquefaction System
R09	System brought on-line and successfully produced ~15 lb/hr of liquid CO_2 at 30 bar
R10	Polaris membrane stability test; liquid CO_2 successfully produced
R11	Improved Polaris membrane modules; liquid CO_2 production increased to 35-40 lb/hr

During the R10 run in March and April 2013, the first-stage membrane enriched CO_2 from 9 percent in the feed to 33 percent in the permeate. The membrane system successfully produced a liquid CO_2 stream in the condenser at 86°F and 30 bar, containing more than 95 percent CO_2. Figure 137 shows the CO_2 content in the liquid CO_2 stream over time. The fluctuation in the CO_2 content (or the reduction of CO_2 content to less than 80 percent) was presumably due to sporadic, brief shutdowns of the chiller that caused the CO_2 lean gas to flow into the liquid CO_2 stream. The liquid CO_2 production rate was 10 to 15 lb/hr, corresponding to about 30 to 45 percent of the feed CO_2. These results were close to the values expected from process simulations based on measured membrane properties.

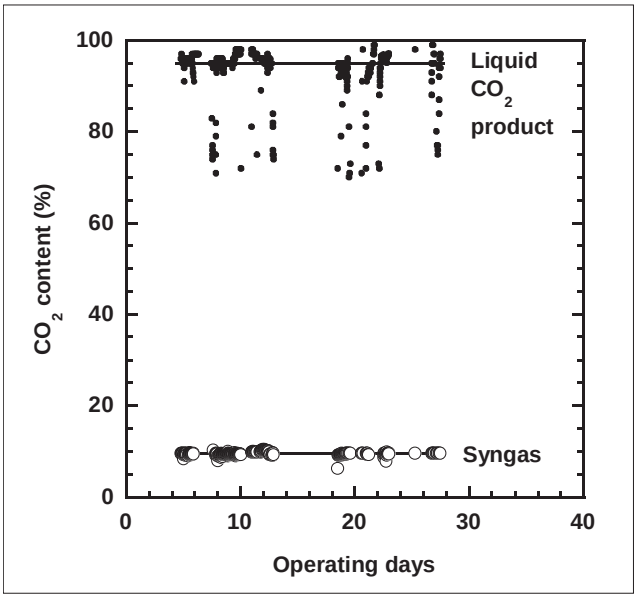

Figure 137. CO_2 Content of Feed and Product Streams of MTR 500 lb/hr Membrane System during R10

Table 55 records several samples of measured liquid CO_2 stream compositions after the system was running at steady state for several hours, and compares these results with the predicted compositions from a commercial process simulator (CHEMCAD 6.3). The liquid streams were at -22°F and 30 bar. In the simulation, the H_2S content in the feed gas entering the condenser was assumed to be 5 ppmv, and the Soave-Redlich-Kwong thermodynamic equation of state was used to describe the phase behavior of the gas mixtures. As shown in the table, the measured and predicted values were fairly close.

Table 55. Measured and Predicted Composition of Liquid CO_2 Stream of MTR 500 lb/hr Membrane System during R10

Component	Measured Compositions of Liquid CO_2 Stream, mol%			Predicted Composition, mol%
	Sample 1	Sample 2	Sample 3	
CO_2	94.36	97.43	99.00	98.52
N_2	3.67	1.34	0.32	1.26
CO	0.54	0.20	0.04	0.18
CH_4	0.09	0.06	0.01	0.03
H_2	0.56	0.19	0.01	0.01
H_2S	0.78	0.78	0.62	0.20

Following the testing described above, minor modifications were made to the demonstration system, including the addition of improved Polaris membrane modules. The system was then operated during the R11 run. The first-stage membrane enriched CO_2 from 11.5 percent in the feed to 40 percent in the permeate, which was higher than the permeate CO_2 content in the R10 run (about 33 percent), due to the improved Polaris membrane modules. The membrane system continuously produced a liquid CO_2 stream in the condenser containing more than 95 percent

CO_2 at -27°F and 27 bar. The liquid CO_2 production rate improved significantly in R11, at 35 to 40 lb/hr, which corresponded to about 60 to 70 percent of the feed CO_2. The run time of the demonstration system was over 400 hours during R11 with no degradation in membrane performance. Figure 138 shows the CO_2 content in the liquid CO_2 stream over time.

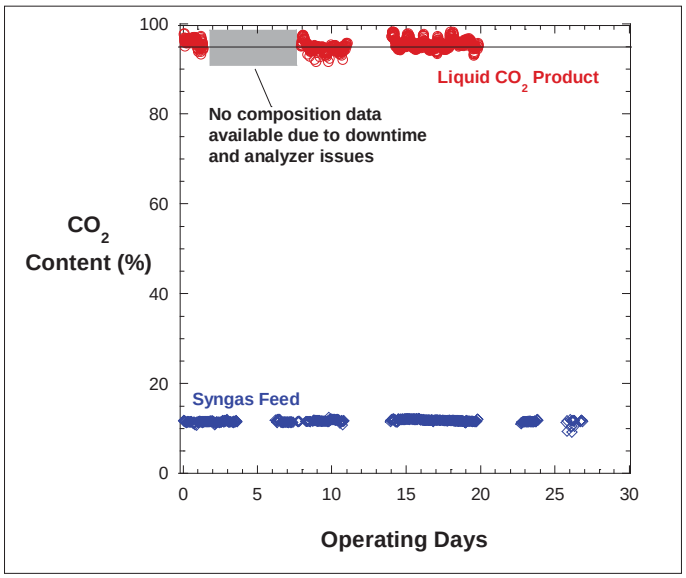

Figure 138. CO_2 Content of Feed and Product Streams of MTR 500 lb/hr Membrane System during R11

The operation of the 500 lb/hr syngas demonstration unit concluded in R11. It successfully demonstrated that an integrated Polaris CO_2 membrane-refrigeration system can reliably produce liquid CO_2 from coal-derived syngas. The successful operation of this system provides a baseline for future optimization and improvement.

4.2.3 Proteus Hydrogen Membranes

Proteus membranes were first tested in run R03, and were tested in all subsequent gasification runs through R13, with the exception of R11, during which modifications were in progress to allow testing of the Proteus membrane in MTR's 50-lb/hr skid. These modifications were made to increase the skid operating temperature, and included the addition of an indirect electric gas heater on the feed line, installation of insulation and heat tracing on the entire skid, and replacing all temperature and pressure gauges with high-temperature-rated equivalents. Table 56 summarizes the Proteus membrane testing achieved through R13.

Table 56. Summary of MTR's Proteus Membrane Testing

Run Number	Test Duration, hours	Feed Flow Rate, lb/hr	Proteus Membrane Testing Scale and Notes
R03	500	1	Membrane stamps; H_2S was removed from syngas
R04	500	1	Improved membrane stamps; syngas contained H_2S
R05	800	1	Improved membrane stamps; syngas contained H_2S
R06	661	10	Membrane stamps and lab-scale modules; syngas contained H_2S.
R07	807	10	Lab-scale modules; syngas contained H_2S
R08	288	1	Improved membrane stamps; syngas contained H_2S
R09	186	1	Improved membrane stamps; syngas contained H_2S
R10	582	1	Improved membrane stamps; syngas contained H_2S
R12	417	50	Semi-commercial membrane modules
R13	529	50	Semi-commercial membrane modules and improved membrane stamps

Figure 139 plots the hydrogen concentrations in the membrane feed and permeate streams during the first testing in run R03. The operating temperature was 275°F, and operating pressure was 130 psig. The Proteus membrane demonstrated a seven-fold enrichment of hydrogen, with hydrogen concentrations ranging from 9 to 11 percent in the feed and 55 to 81 percent in the permeate.

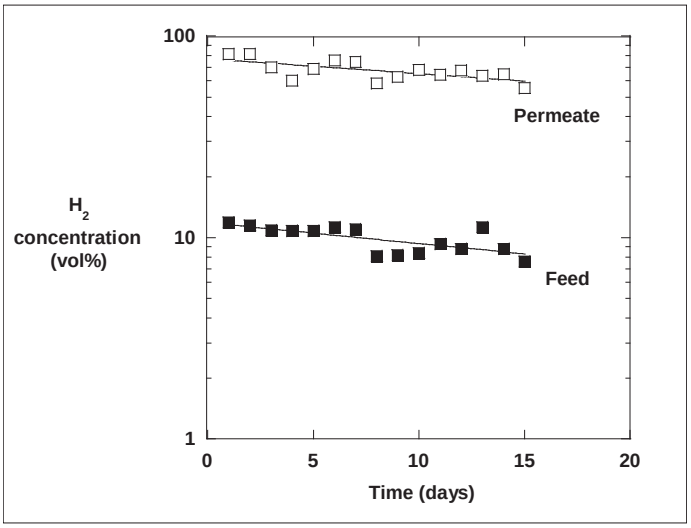

Figure 139. Hydrogen Concentration in Feed and Permeate Streams of Proteus Membrane during R03

Figure 140 shows the mixed-gas hydrogen and CO_2 permeance and the H_2/CO_2 selectivity over time at 275°F during R03. The Proteus membrane stamp showed a hydrogen permeance of about 230 gpu and H_2/CO_2 selectivity averaging about 15. In addition, the membrane performance was stable with time when exposed to the raw syngas at 275°F, indicating the short-term (two-week) robustness of the membrane.

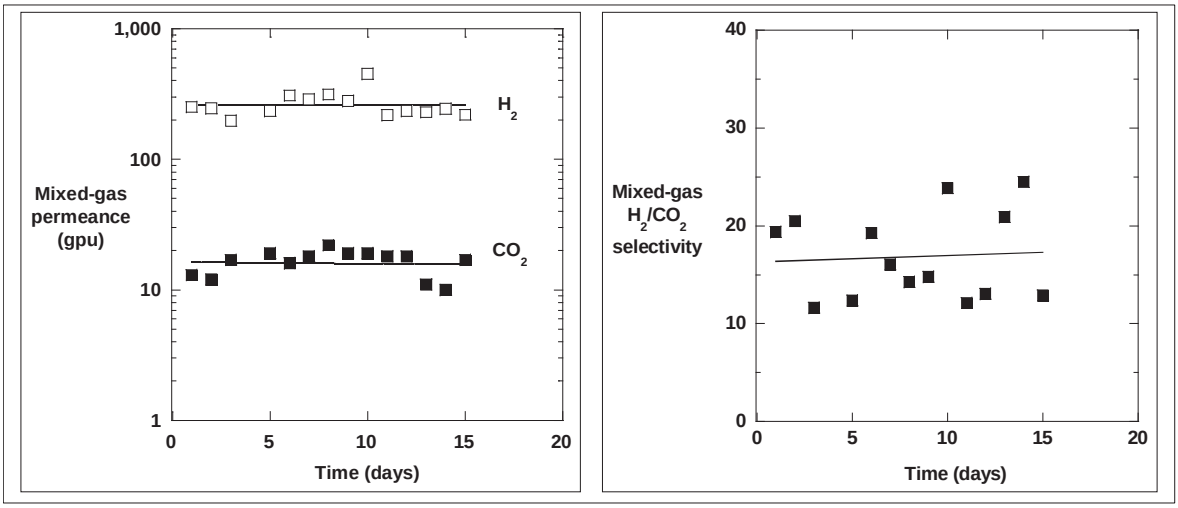

Figure 140. Mixed-Gas Permeance and Selectivity of Proteus Membrane during R03

Stamp tests of improved Proteus membranes continued during the R04 and R05 runs with stable membrane performance and consistent hydrogen enrichment from about 12 percent in the feed syngas to 70 to 80 percent in the permeate stream. The syngas during these runs contained H_2S on a ppm level, and results showed that H_2S did not significantly impact membrane performance.

During the R06 run, both lab-scale Proteus membrane modules and membrane stamps from the scaled-up Proteus membrane production process were tested with syngas containing H_2S and COS. The first two lab-scale modules seemed to develop defects during the high temperature operation at NCCC, indicated by an increase in hydrogen permeance and a decrease in H_2/CO_2 selectivity over time. MTR modified the module configuration and prepared a third lab-scale module, which showed stable and good H_2/CO_2 separation properties for the remaining test period.

A Proteus membrane stamp was tested for four days, and the modified lab-scale module (6373) was then tested for four days. Figure 141 shows the hydrogen concentration in the feed (average of the feed and residue gas) and permeate streams, and Figure 142 provides the mixed-gas permeance and H_2/CO_2 selectivity over the test period. The data indicated hydrogen enrichment up to six- and seven-fold by the membrane stamp and module. The Proteus membrane stamp exhibited good separation properties with hydrogen permeance of 210 gpu and H_2/CO_2 selectivity of 25. The separation properties were similar to those of the earlier field tests in runs R03, R04, and R05. The Proteus module showed hydrogen permeance of 135 gpu and H_2/CO_2 selectivity of 23 at 250°F, in good agreement with the lab test separation performance. Both types of Proteus membranes were stable over the time tested when exposed to the raw syngas containing sulfur components and aromatic hydrocarbons.

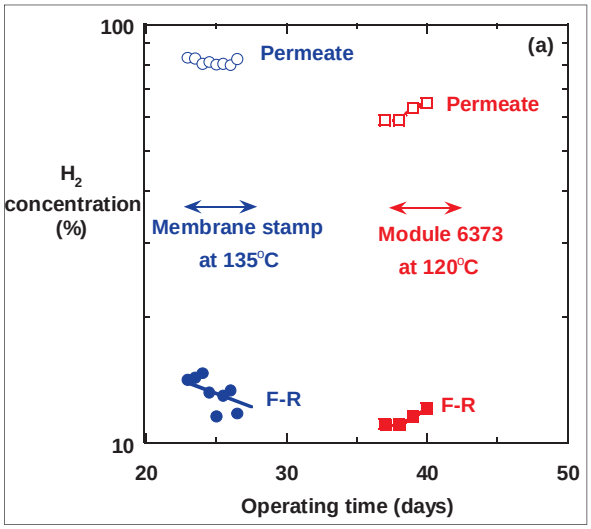

Figure 141. Hydrogen Concentration in Feed and Permeate Streams of Proteus Membrane during R06

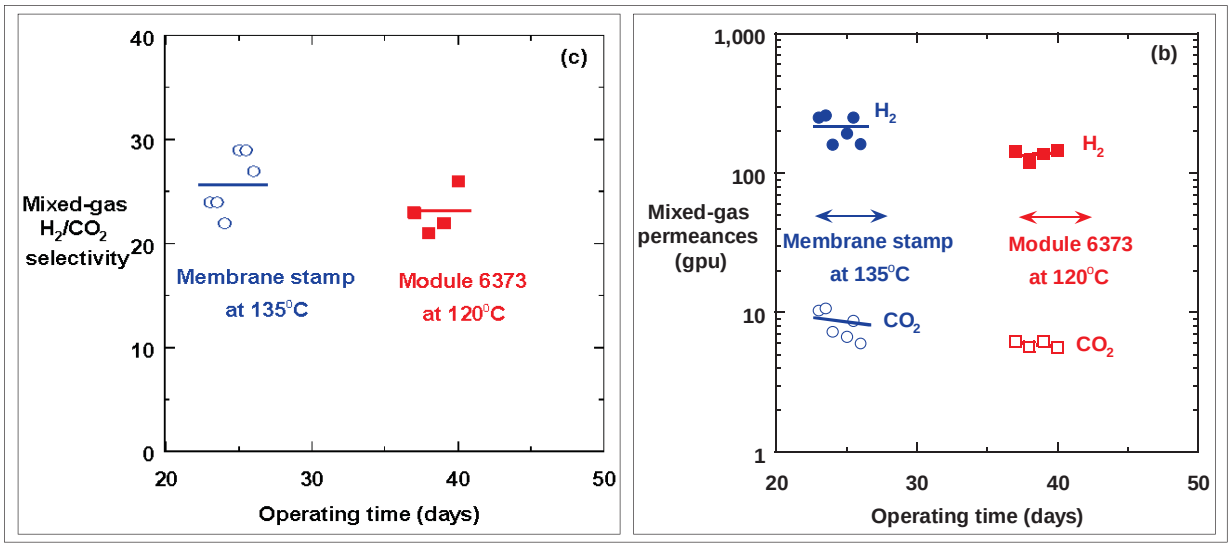

Figure 142. Mixed-Gas H_2/CO_2 Selectivity and Permeance of Proteus Membranes during R06

Based on results obtained during R03 through R07, MTR continued to develop the Proteus membrane for better separation performance and long-term stability. During gasifier runs R08, R09, and R10, new Proteus membrane stamps were evaluated, which had been optimized to achieve higher hydrogen permeance, higher H_2/CO_2 selectivity, and good H_2/H_2S selectivity. Separation performance of the Proteus stamp in R10, at operating conditions of 257°F and 170 psig, is shown in Figure 143. The hydrogen concentration ranged from 7 to 13 percent in the feed and from 65 to 85 percent in the permeate. These results demonstrated a seven-fold enrichment in the hydrogen content.

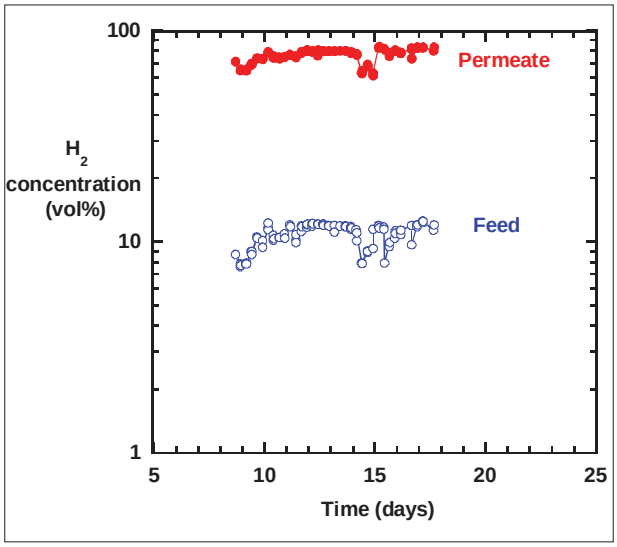

Figure 143. Hydrogen Concentration in Feed and Permeate Streams of Proteus Membrane during R10

Figure 144 provides plots of mixed-gas permeance of H_2, CO_2, and H_2S, as well as the H_2/CO_2 and H_2/H_2S selectivity values during R10. The Proteus membrane stamp showed a hydrogen permeance of around 350 gpu, H_2/CO_2 selectivity around 20, and H_2/H_2S selectivity around 40. These values exceeded those obtained in the earlier runs at NCCC. Moreover, the membrane performance was stable with time when exposed to the raw syngas at 257°F, indicating the short-term (three-week) robustness of the membrane.

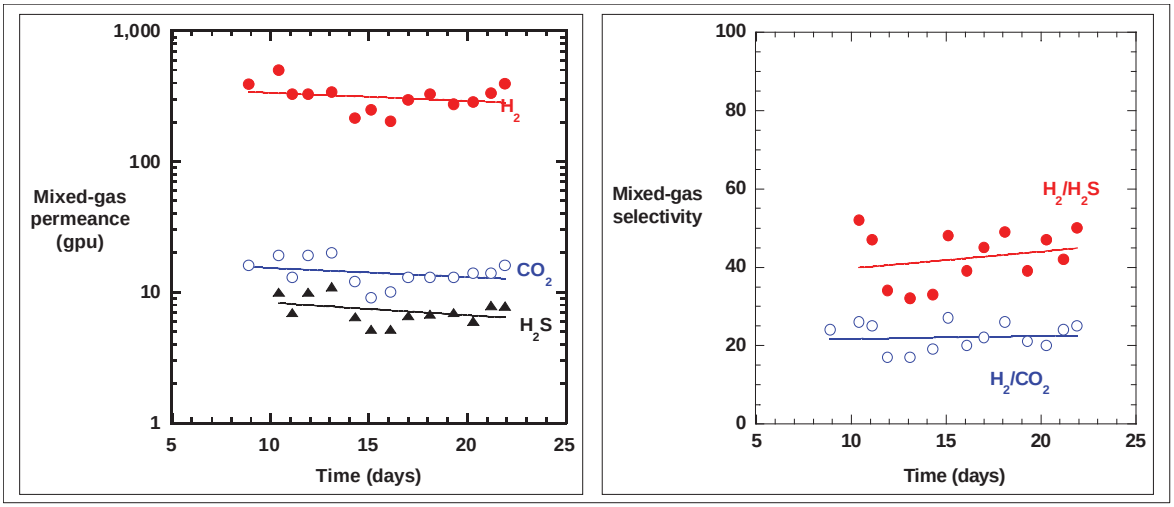

Figure 144. Mixed-Gas H_2/CO_2 Selectivity and Permeance of Proteus Membrane during R10

Based on the improvements made to the Proteus membrane and module development knowledge gained during the run, the Proteus membrane was further scaled up to the semi-commercial membrane module scale. Four-inch Proteus membrane modules were assembled and were first tested on the 50-lb/hr scale during the R12 run. The results from two different four-inch Proteus modules that were tested individually during the gasifier run are shown in Figure 145.

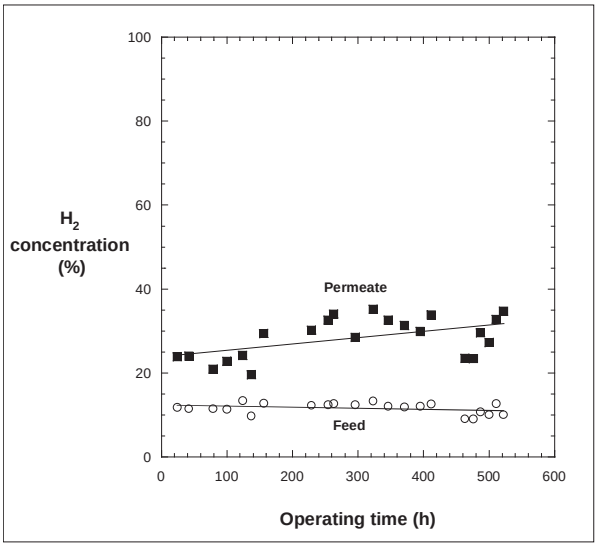

Figure 145. Hydrogen Concentration in Feed and Permeate Streams of Proteus Membrane during R12

While the hydrogen concentration was enriched in the permeate to two to three times the feed concentration, the results were lower than anticipated based on Proteus stamp and small module results from previous gasifier runs conducted at NCCC. Minor nitrogen leaks were evident in both modules, but the main reason for the low module separation performance was poor temperature control on the membrane skid.

Proteus modules operate at elevated temperatures, with optimal performance between 257°F and 302°F. Performance drops at lower operating temperature, particularly below 212°F. The indirect electric heater was able to pre-heat the syngas feed to set points up to 302°F, but insufficient heat tracing on the feed piping and module vessel, combined with non-ideal heat tracing temperature sensor locations, led to poor overall skid temperature control. Between the end of R12 and the start of the R13 run, additional heat tracing was installed, and the location of the heat tracing temperature sensors were moved to ensure better skid temperature control.

Figure 146 shows the hydrogen concentration in the feed and permeate streams of the 50-lb/hr skid for the duration of the R13 run. A single four-inch Proteus membrane module was used for the entire R13 run to measure membrane performance, long-term stability, and the effect of high-temperature syngas conditions on module components (spacers, glue lines, etc.). The module was exposed to temperatures between 212°F and 302°F for the duration of the gasifier run. While the hydrogen concentration was enriched in the permeate by approximately three to four times the feed concentration (an improvement over experimental results from R12), the enrichment was lower than anticipated based on Proteus stamp and small module results from previous runs conducted at NCCC. Analysis of semi-commercial Proteus modules continues to provide insight into further module improvement and development. Future testing plans include continued testing of improved semi-commercial Proteus modules on the 50-lb/hr skid at NCCC.

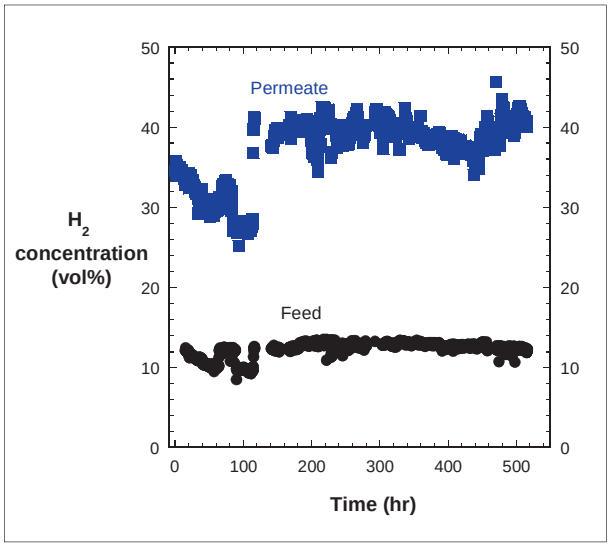

Figure 146. Hydrogen Concentration in Feed and Permeate Streams of Proteus Membrane during R13

In addition to a semi-commercial Proteus module, improved Proteus membrane stamps were also evaluated during R13. This second generation (Gen-2) Proteus membrane is being developed specifically for operation up to 392°F (200°C). Figure 147 shows the hydrogen enrichment of the Gen-2 Proteus membrane. Similar to earlier versions of Proteus, the hydrogen concentration in the permeate was consistently over 80 percent, which represents a seven-fold hydrogen enrichment of the feed for temperatures between 212 and 302°F (100 and 150°C).

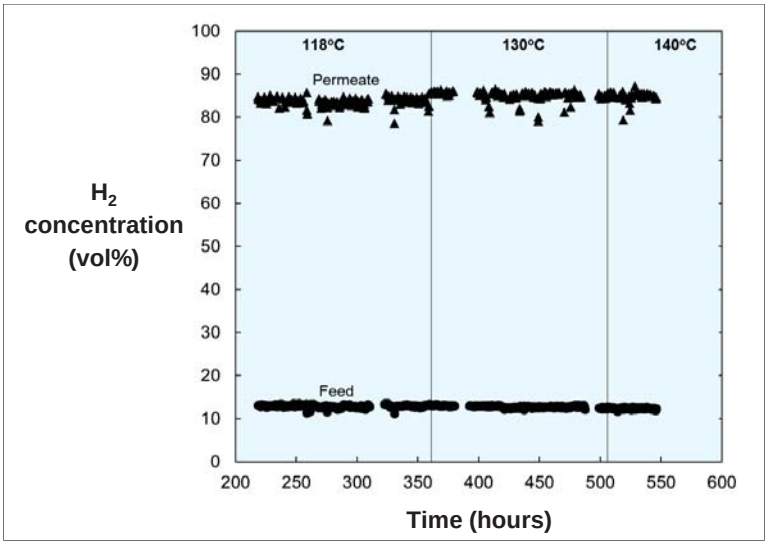

Figure 147. Hydrogen Concentrations of the Gen-2 Proteus Stamp Cells Feed and Permeate Streams during R13

The calculated Gen-2 Proteus stamp H_2/CO_2 and H_2/H_2S selectivities throughout the R13 run are shown in Figure 148. The H_2/CO_2 and H_2/H_2S selectivities were affected minimally by increased temperature and were an improvement over previously reported Proteus stamp selectivity values. The calculated H_2/CO_2 selectivity remained between 30 and 35 for the majority of the test period, and the H_2/H_2S selectivity was typically 50 to 60. The successful

results of the Gen-2 Proteus membrane stamps provide a baseline for future optimization and membrane performance improvement. Future testing of Gen-2 Proteus stamps with syngas at the NCCC is planned.

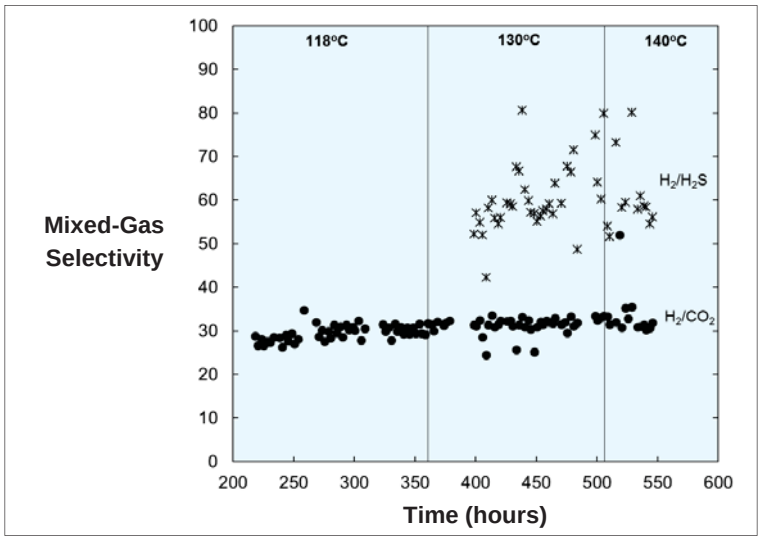

Figure 148. Mixed-Gas Selectivity of H_2/H_2S and H_2/CO_2 of the Gen-2 Proteus Stamps during R13

4.3 Worcester Polytechnic Institute Palladium-Based Hydrogen Membranes

The Center for Inorganic Membrane Studies at WPI has been developing a high temperature palladium-based membrane to separate hydrogen from syngas for power generation. WPI tested 13 palladium and palladium-alloy pilot-scale membranes during eight test runs (runs R06 through R13) at the NCCC. Testing was conducted at 842°F (450°C) using single membrane modules in nitrogen/hydrogen (N_2/H_2) bottle gas mixtures and in syngas. All membranes were fabricated with a porous surface area about 200 cm^2, having a one-inch outer diameter and ten-inch long porous stainless steel seamless tubular supports from Mott Corporation. The total testing time for all 13 membranes was 4,275 hours, representing about a half of a year of operation. Testing achieved 1.4 lb/day of hydrogen production and 99.85 to 99.95 percent hydrogen purity at 842°F and 12.6 bar under actual syngas feed conditions.

Table 57 summarizes the testing completed by WPI and the principal characteristics of the composite palladium (Pd) and palladium-alloy membranes used. The palladium alloys were formulated using gold (Au) and/or platinum (Pt). Two of the membranes tested employed a proprietary protective surface coating. Results are given in the following sections, which are categorized according to membrane composition.

Table 57. Summary of WPI Testing of Palladium and Palladium-Alloy Membranes

Run Number	WPI Run Number and Test Date	Membrane Designation	Composition and Thickness, micron	Testing Time, hr
R06	R06-1 7/11-7/22-2011	MA-129b M-04	13.1(Pd)	250
	R06-2 7/21-8/05-2011	MA-128b M-03	10(Pd)+0.2(Au)	275
	R06-3 8/09-8/20-2011	MA-126b M-01	8.2(Pd)+0.16(Au)	225
R07	R07-1 11/10-11/17-2011	MA-128c M-03b	9.6(Pd)	175
	R07-2 11/22-12/12-2011	MA-137b M-07	8.7(Pd)+0.5(Au)	475
R08	R08-1 6/28-7-26-2012	MA-145b M-08	7-10(Pd)+0.33(Au)+0.1(Pt)	650
R09	R09-1 12/12-12/19-2012	MA-138c M-09	8.5(Pd)+0.35(Au)+0.06(Pt)+ protective coating	175
R10	R10-1 3/21-3/31-2013	MA-142 M-10	9.6(Pd)	225
	R10-2 4/10-4/21-2013	MA-129c	14(Pd)+0.9(Au)	250
R11	R11-1 8/05-8/20-2013	MA-150b	5(Pd)+0.8(Au)+0.9(Pd)	350
R12	R12-1 11/21-12/05-2013	MA-151b	4(Pd)+0.5(Pt)+0.9(Pd)	350
	R12-2 12/07-12/13-2013	MA-158	4.8(Pd)+0.45(Pt)	150
R13	R13-1 3/23-4/18-2014	MA-136b	10.3(Pd)+0.3(Au)+0.09(Pt)+ protective coating	725

4.3.1 Palladium-Gold Membranes

The first category was composed of asymmetric membranes consisting of a layer of palladium and a top layer of gold. Different thicknesses, listed in Table 58, were used for testing the behavior of these membranes. The membrane designated MA-150b contained an additional top layer of palladium.

Table 58. Composition of WPI Palladium-Gold Membranes

Membrane Designation	Layer Thickness, micron	WPI Run Number
MA-126b (M-01)	8.2(Pd) + 0.16(Au)	R06-3
MA-137b (M-07)	8.7(Pd) + 0.5(Au)	R07-2
MA-129c	14(Pd) + 0.9(Au)	R10-2
MA-150b	5(Pd) + 0.8(Au) + 0.9(Pd)	R11-1

Hydrogen Permeance of Pd-Au Membranes

The permeance of Pd-Au membranes was measured during operation with syngas and with N_2/H_2 gas mixtures. Figure 149 plots the initial hydrogen permeance measured at WPI's lab (shown as a single point in yellow), permeance under N_2/H_2 gas mixtures (shown with the series filled in white), and permeance under syngas conditions (shown as a solid-colored series).

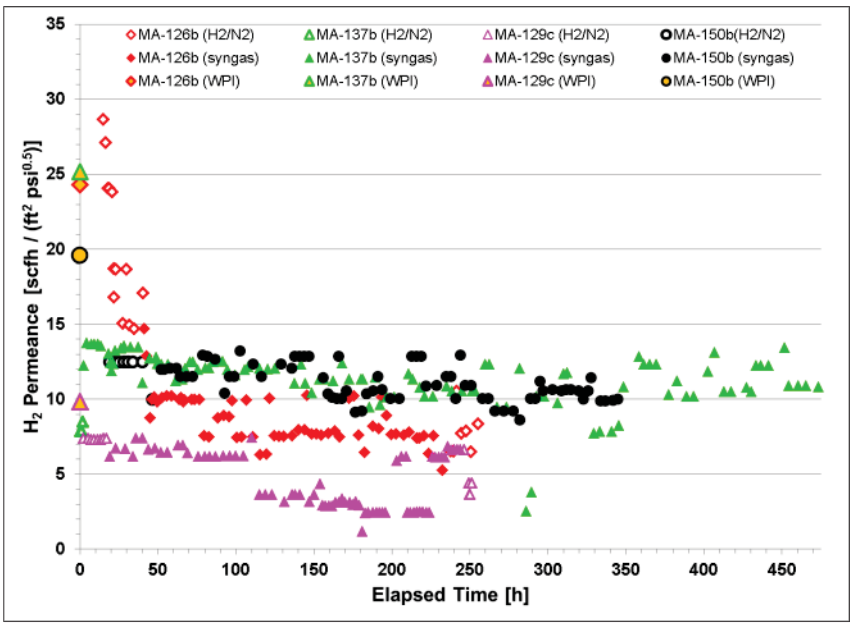

Figure 149. Hydrogen Permeance of WPI Pd-Au Membranes over Time

MA-126b showed an initial flow of around 19 scfh followed by a decrease to 8 scfh after around 10 hours with a further decrease to 6 scfh after 200 hours.

MA-137b showed a stable hydrogen flux of 37 scfh/ft^2 in a N_2/H_2 mixture. After switching to syngas, the flux decreased slowly from 60 to an average value of 50 scfh/ft^2 in 470 hours, producing 1.4 lb/day at the end of the test.

For the MA-129c membrane, the lab-measured hydrogen permeance at 842°F was 11 scfh/ft^2/psi$^{0.5}$ with a hydrogen-to-helium (H_2/He) selectivity greater than 2,700. This Pd-Au membrane was tested for a total of 251 hours at 842°F under N_2/H_2 mixtures and syngas atmospheres. After 40 hours in the N_2/H_2 mixture, the average permeance value was 7.3 scfh/ft^2/psi$^{0.5}$, which corresponded to a 25 percent decrease. Upon syngas introduction, the hydrogen permeance decreased further to 6.2 scfh/ft^2/psi$^{0.5}$, corresponding to a 37 percent decline.

Membrane MA-150b showed a lab-measured hydrogen permeance of 19.6 scfh/ft^2/psi$^{0.5}$ and a H_2/He selectivity higher than 2,207. This Pd-Au membrane was tested initially in N_2/H_2 for about 50 hours at 842°F. The permeance declined immediately, as observed in previous tests. Upon syngas introduction, the permeance was constant and stable for additional 300 hours.

MA-126b experienced a hydrogen permeance decline under the N_2/H_2 mixture feed during the first 20 hours, which suggested that some contaminants were adsorbed from the piping and stripped out with the hot N_2/H_2 mixture. MA-137b appeared to have no drastic initial hydrogen flux decline such as the one observed MA-126b. However, taking into account the permeance measured at the WPI lab before the test at NCCC, MA-137b should have had an initial hydrogen flux of around 80 scfh/ft^2. It is believed that contaminants entrained by the hot plant nitrogen adsorbed quickly on the Pd surface. MA-150b exhibited a similar initial drop in hydrogen permeance as soon as the membrane was switched to a N_2/H_2 mixture and maintained at the same level for 350 hours.

MA-129c operated in syngas with the addition of H_2S at a concentration of up to 10.6 ppm, leading to a reduced hydrogen permeance of 2.6 scfh/ft^2/psi$^{0.5}$. After stopping the H_2S input, the membrane recovered its initial hydrogen permeance of 6.2 scfh/ft^2/psi$^{0.5}$ within 30 minutes.

Conclusions from this testing were that these membranes underwent a fast loss in permeance (from lab-measured values to those obtained during NCCC testing) possibly due to the adsorption of unknown contaminants on the surface; and a gradual decrease in hydrogen permeance occurred in some cases, indicating bulk contamination.

Hydrogen Purity Produced by Pd-Au Membranes

Figure 150 plots measurements of hydrogen purity from the palladium-gold membranes during syngas operation.

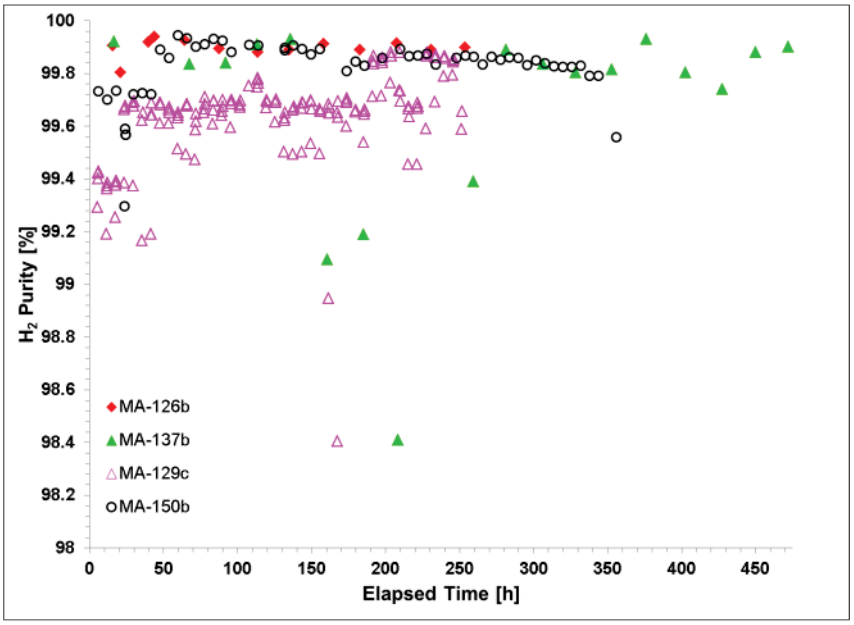

Figure 150. Hydrogen Purity Produced from WPI Pd-Au Membranes during Syngas Operation

The hydrogen purity of the MA-126b membrane was above 99.9 percent during most of the testing. During a post-run inspection, no carbonaceous deposit was observed on the membrane surface. However, the protective coating deposited on the membrane peeled off of the surface and was dark in color, indicating that some carbonaceous matter may have deposited inside. The Pd layer where the coating peeled off appeared very shiny.

Data from membrane MA-129c showed that the H_2S addition had no effect on the hydrogen purity. This experiment showed that the Pd-Au membrane can exhibit long-term stability in syngas.

4.3.2 Palladium-Gold-Platinum Membranes

The composition of Pd-Au-Pt membranes is listed in Table 59. Two of these membranes, MA-136b and MA-138c, were treated with the protective coating.

Table 59. Composition of WPI Palladium-Gold-Platinum Membranes

Membrane Designation	Layer Thickness, micron	WPI Run Number
MA-145b (M-08)	7-10(Pd) + 0.33(Au) + 0.1(Pt)	R08-1
MA-138c (M-09)	8.5(Pd) + 0.35(Au) + 0.06(Pt) + protective coating	R09-1
MA-136b	10.3(Pd) + 0.3(Au) + 0.09(Pt) + protective coating	R13-1

Hydrogen Permeance of Pd-Au-Pt Membranes

Figure 151 provides a graph of the hydrogen permeance of the Pd-Au-Pt membranes. The initial permeance measured at WPI's lab is shown as a single point in yellow, permeance under N_2/H_2 gas mixtures is shown with the series filled in white, and permeance with syngas is shown with a solid-colored series.

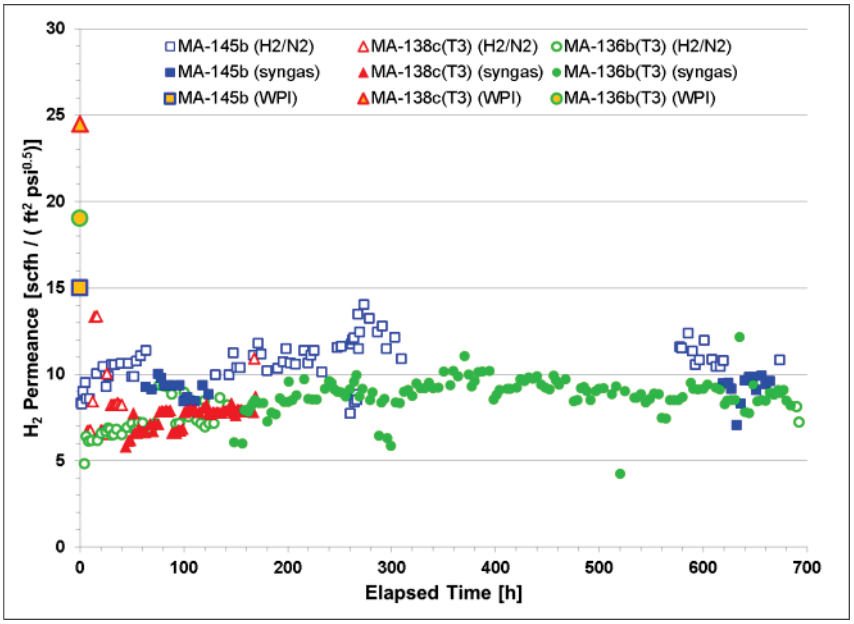

Figure 151. Hydrogen Permeance of WPI Pd-Au-Pt Membranes over Time

For membrane MA-145b, the hydrogen permeance at 842°F measured at WPI was 15 scfh/ft^2/psi$^{0.5}$ with a H_2/He selectivity higher than 1,000. At NCCC, MA-145b was tested for a total time of 460 hours at 842°F in N_2/H_2 and in syngas. The membrane first operated for 50 hours in a N_2/H_2 mixture. The permeance declined between the value previously measured at WPI and the initial value at NCCC. However, it appeared that the permeance partially recovered with time in the N_2/H_2 atmosphere. Upon syngas introduction, the permeance was constant, but a gasifier trip occurred after 60 hours, and a N_2/H_2 mixture was used to preserve the membrane. During the second time the membrane operated in the N_2/H_2 mixture, the permeance again recovered to a value quite close to the one measured at WPI. The recovery of the permeance might have resulted from the Pt addition, yet this hypothesis needed further verification. Due to the long time needed to repair the gasifier, the membrane was cooled down to ambient temperature and remained at atmospheric temperature and pressure for over 200 hours. After the gasifier was repaired, a second test was started. The membrane operated in a N_2/H_2 mixture, and the measured permeance was the same as before the test interruption. The permeance in syngas was stable and very close to the value measured during the first 60 hours in syngas. Unfortunately, a second gasifier trip occurred, and the run was terminated.

Membrane MA-138c, which contained the protective coating, showed an initial lab-measured hydrogen permeance of 25 scfh/ft^2/psi$^{0.5}$ with a H_2/He selectivity higher than 680. The final helium permeance equaled 0.7 sccm/bar with average permeance equal to 3.7 sccm/bar. At NCCC, MA-138c was tested for a total time of 169 hours at 842°F in N_2/H_2 and in syngas. The membrane first operated for 40 hours in a N_2/H_2 mixture. The hydrogen permeance declined from the value previously measured at WPI and the initial value at NCCC. After 40 hours in the N_2/H_2 mixture, the average measured permeance was equal to 8.6 scfh/ft^2/psi$^{0.5}$, which corresponded to a 65 percent decrease. Upon syngas introduction, no significant decrease in the permeance was observed, indicating that permeance inhibition occurred in the N_2/H_2 mixture. The permeance decrease in N_2/H_2 was attributed to the carryover of contaminants from piping. The permeance remained constant in syngas and equaled 9.4 scfh/ft^2/psi$^{0.5}$ after 123 hours in syngas. After syngas exposure, a N_2/H_2 mixture was introduced, and the membrane showed essentially the same permeance. The relatively large decrease in hydrogen permeance (65 percent) was the highest observed and may have been due to plugging of the coating by hydrocarbons.

For the MA-136b membrane, WPI lab measurements indicated a hydrogen permeance at 842°F of 16.4 scfh/ft^2/psi$^{0.5}$ and a final ideal selectivity equal to 732. After testing at the WPI lab, the protective coating was applied. At NCCC, the coated membrane was tested for a total of 718 hours at 842°F in N_2/H_2 mixtures and in syngas. The membrane first operated for 142 hours in a N_2/H_2 mixture. The permeance declined from the value previously measured at WPI, similar to all the previous runs at NCCC with uncoated membranes. After 142 hours in the N_2/H_2 mixture, the average measured permeance value was equal to 7.3 scfh/ft^2/psi$^{0.5}$, which corresponded to a 55 percent decrease, again similar to previous runs at NCCC without using coatings. After the N_2/H_2 operation, syngas was introduced and maintained for 578 hours. During the first 200 hours, the hydrogen permeance slightly increased followed by a sustained average permeance value of 9.0 scfh/ft^2/psi$^{0.5}$ until the end of the test. The lack of sulfur resistance while using the protective coating may have been due to operating conditions.

Hydrogen Purity Produced by Pd-Au-Pt Membranes

Figure 152 provides measurements of hydrogen purity from the Pd-Au-Pt membranes. MA-145b produced hydrogen with a purity higher than 99.8 percent during testing. This new ternary alloy membrane appeared to have been less affected by coking processes, as post-run inspections showed no trace of coking on the membrane surface. Further experiments were conducted to confirm the benefits of Pt addition to the Pd-Au membranes. The hydrogen purity produced by MA-138c was higher in syngas than in the N_2/H_2 mixture due to the fact that hydrogen flux is lower and the nitrogen leak is higher in the N_2/H_2 mixtures. The purity of the hydrogen produced in syngas by MA-138c was constant and as high as 98.8 percent at 842°F and 12.6 bar. MA-136b had a purity greater than 99 percent but had a slight and steady decline throughout the 700-hour test.

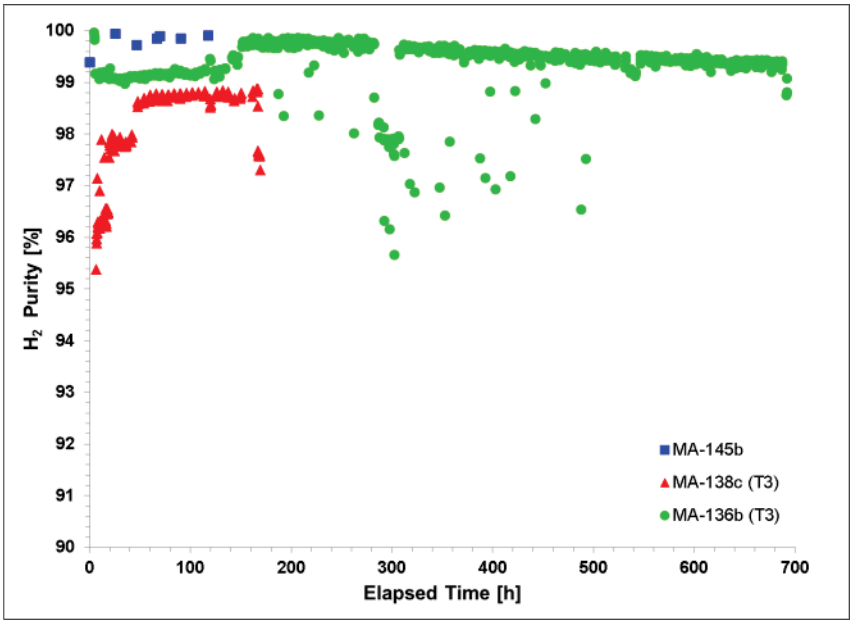

Figure 152. Hydrogen Purity Produced from WPI Pd-Au-Pt Membranes during Syngas Operation

4.3.3 Palladium-Platinum Membranes

Table 60 lists the composition of the two palladium-platinum membranes tested.

Table 60. Composition of WPI Palladium-Platinum Membranes

Membrane Designation	Layer Thickness, micron	WPI Run Number
MA-151b	4(Pd) + 0.5(Pt) + 0.9(Pd)	R12-1
MA-158	4.8(Pd) + 0.45(Pt)	R12-2

Hydrogen Permeance of Pd-Pt membranes

Figure 153 plots the initial hydrogen permeance of Pd-Pt membranes measured at WPI's lab (shown as a single point in yellow), permeance under N_2/H_2 gas mixtures (shown with the series filled in white), and permeance under syngas conditions (shown as a solid-colored series).

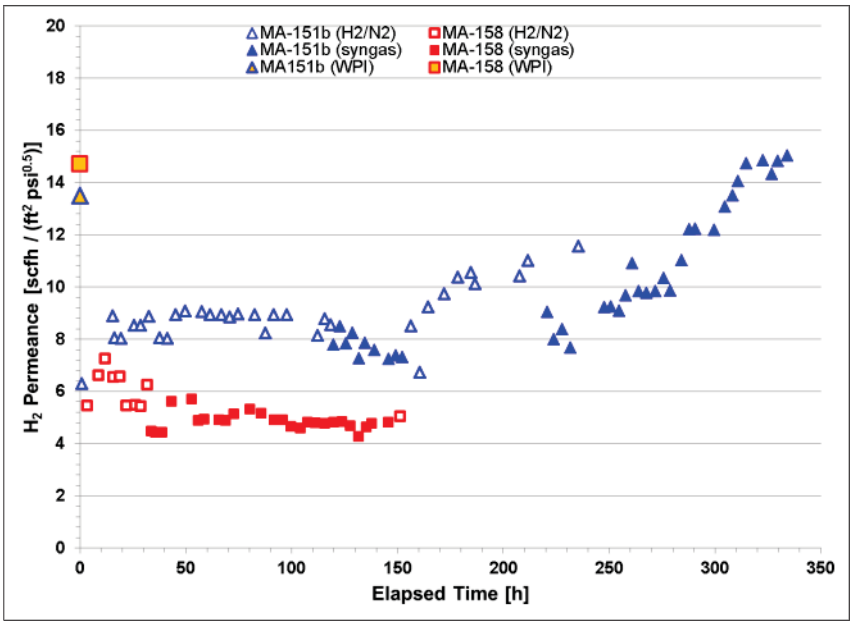

Figure 153. Hydrogen Permeance of WPI Pd-Pt Membranes over Time

Membrane MA-151b is a Pd-Pt-Pd membrane with a high content of platinum close to its surface still having good initial hydrogen permeance characteristics. Lab results showed an initial permeance of 13.5 scfh/ft^2/psi$^{0.5}$ with a H_2/He selectivity of 393. This Pd-Pt-Pd membrane was tested for a total of 350 hours at 842°F in N_2/H_2 mixtures and in syngas. The membrane first operated for 120 hours in a N_2/H_2 mixture. After 120 hours in the N_2/H_2 mixture, the average measured permeance value was equal to 8.6 scfh/ft^2/psi$^{0.5}$, which corresponded to a 36 percent decrease from the value previously measured at WPI's lab. Upon syngas introduction, no significant decrease in the hydrogen permeance was observed, indicating that permeance inhibition occurred in the N_2/H_2 mixture. The permeance of the MA-151b membrane remained constant in syngas after 160 hours. At 160 hours, the flow started to increase abruptly, indicating the opening of pinholes and the loss in selectivity.

For the membrane MA-158, the hydrogen permeance at 842°F measured at WPI's lab was 14.3 scfh/ft^2/psi$^{0.5}$, with the final ideal selectivity equal to 590. At NCCC, MA-158 was tested for a total of 150 hours at 842°F in N_2/H_2 mixtures and in syngas. The membrane first operated for 30 hours in a N_2/H_2 mixture. After 30 hours in the N_2/H_2 mixture, the average measured permeance value was equal to 5.9 scfh/ft^2/psi$^{0.5}$, which corresponded to a 59 percent decrease. The permeance of MA-158 membrane also remained relatively constant in syngas after 150 hours.

Hydrogen Purity Produced by Pd-Pt Membranes

Figure 154 shows the hydrogen purity produced from the Pd-Pt membranes. MA-151b showed an initial hydrogen purity of 98 percent that remained stable for 100 hours of operation with N_2/H_2. After that period, syngas was introduced and held for about 50 hours, and the purity increased to about 99 percent. When N_2/H_2 was introduced again, the purity had a steady drop to 93 percent. When the operating atmosphere was changed again to syngas, the purity initially recovered; however, a decline in purity continued until the end of the test. MA-158 was tested

for a shorter period. Nevertheless, this membrane was more stable and produced higher hydrogen purity than MA-151b. With N_2/H_2, the MA-158 membrane showed a hydrogen purity of 99 percent, and with syngas, the membrane produced hydrogen with a purity of greater than 99.5 percent.

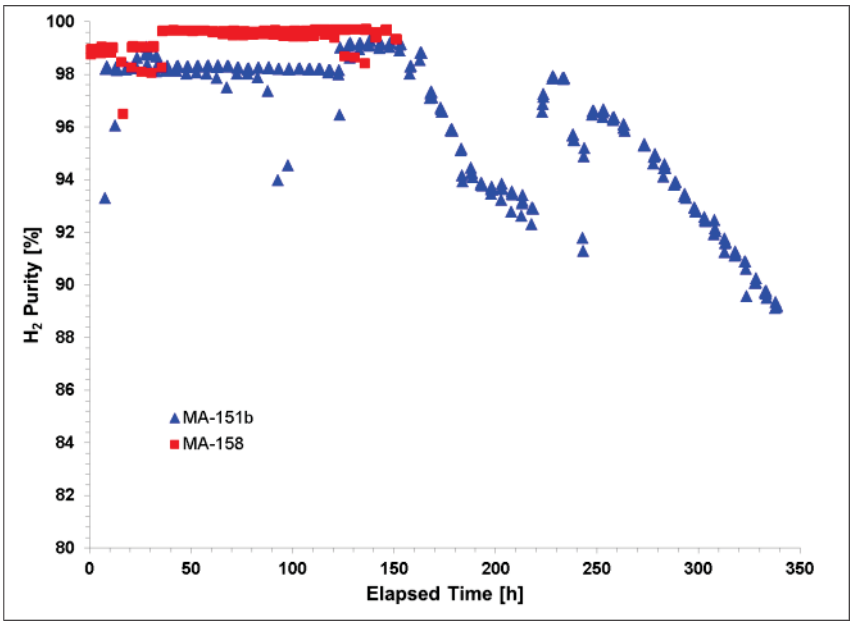

Figure 154. Hydrogen Purity Produced from WPI Pd-Pt Membranes during Syngas Operation

4.3.4 Pure Palladium Membranes

Table 61 provides the composition of the two pure palladium membranes tested.

Table 61. Composition of WPI Pure Palladium Membranes

Membrane Designation	Layer Thickness, micron	WPI Run Number
MA-129b (M-04)	13.1(Pd)	R06-1
MA-142	9.6(Pd)	R10-1

Hydrogen Permeance of Pure Pd Membranes

Figure 155 plots the permeance of the pure palladium membranes tested. The initial hydrogen permeance measured at WPI is shown as a single point in yellow; the permeance during N2/H2 operation is shown with the series filled in with white; and the permeance with syngas is shown with a solid-colored series.

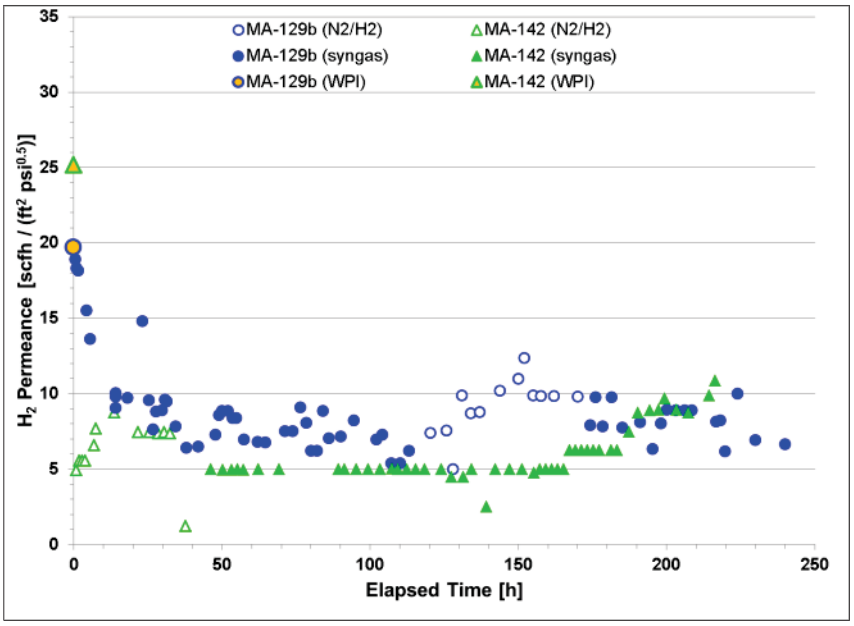

Figure 155. Hydrogen Permeance of Pure Pd Membranes over Time

MA-129b showed an initial hydrogen flow of around 19 scfh in syngas. However, after around 10 hours, the flow rapidly declined to 8 scfh and further down to 6 scfh after 200 hours. The decrease in hydrogen flow was believed to be caused by impurities in the syngas (heavy metals, hydrocarbons, sulfur compounds, etc.). After removal, the surface of the membrane was covered with a thick black layer.

MA-142 had a lab-measured hydrogen permeance at 842°F of 25.2 scfh/ft^2/psi$^{0.5}$ with a H_2/He selectivity higher than 2,500. At NCCC, the membrane first operated for about 40 hours in N_2/H_2. The permeance declined between the value previously measured at WPI and the initial value at NCCC. After 40 hours in the N_2/H_2 mixture, the average measured permeance value was equal to 7.5 scfh/ft^2/psi$^{0.5}$, which corresponded to a 70 percent decrease. Upon syngas introduction, no significant decrease in the hydrogen permeance was observed, indicating that permeance inhibition occurred in the N_2/H_2 mixture. The permeance of the MA-142 membrane remained constant in syngas and equaled 5.0 scfh/ft^2/psi$^{0.5}$ after 120 hours (80 percent decline compared to WPI level). At 120 hours, the flow increased abruptly, indicating the opening of pinholes and the loss in selectivity.

Hydrogen Purity Produced from Pure Pd Membranes

Figure 156 plots the hydrogen purity produced by the two palladium membranes. The hydrogen purity of MA-129b was higher than 99.2 percent at the beginning of the test and declined to 96.8 percent after 240 hours. The H_2 purity of MA-142 produced in syngas was of 99.7 percent at 842°F and 12.6 bar and was constant for 120 hours. The purity decreased dramatically to reach a value of 77.9 percent after 227 hours.

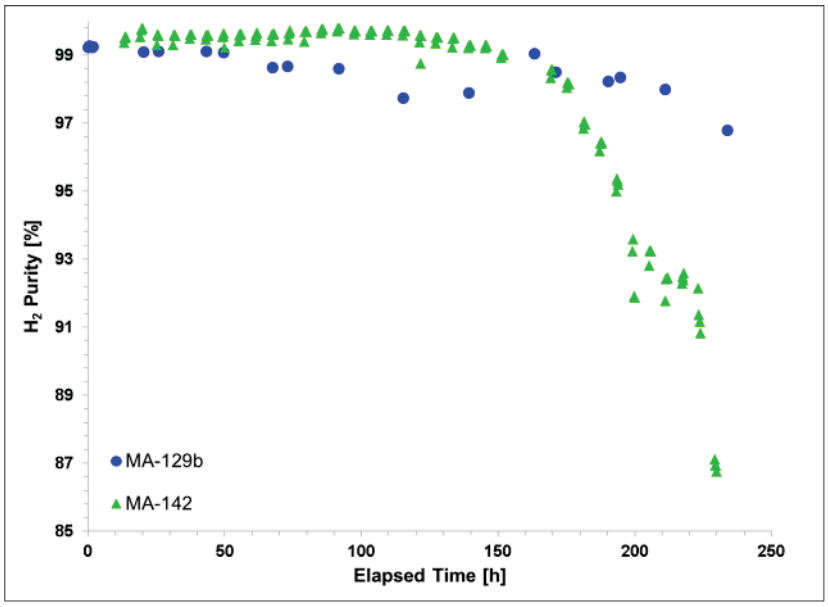

Figure 156. Hydrogen Purity Produced from WPI Pure Pd Membranes during Syngas Operation

4.4 Eltron Research & Development Hydrogen Membrane

Under DOE sponsorship, Eltron Research & Development developed a high-temperature hydrogen transport membrane (HTM) for pre-combustion capture of CO_2. The HTM technology, shown in Figure 157, uses a multi-layer metal alloy tube to separate hydrogen from coal-derived syngas providing high purity hydrogen, and concentrating CO_2 for downstream capture of high pressure carbon suitable for utilization or sequestration. Eltron's membranes can withstand high differential pressures of up to 1,000 psi, allowing for successful integration with advanced, high-pressure coal gasification processes.

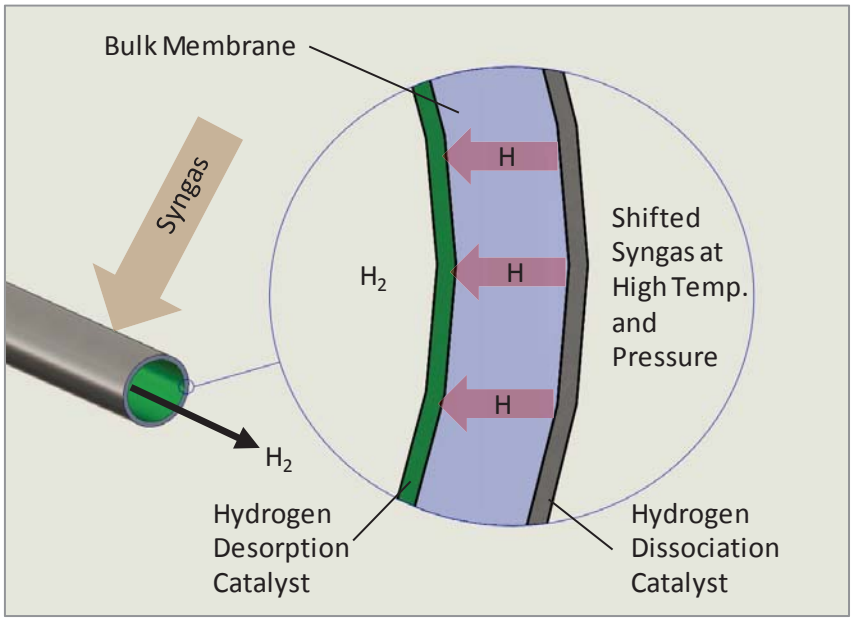

Figure 157. Schematic of Eltron Hydrogen Membrane Tube

The two membrane tubes tested were of 0.5-inch outer diameter (OD), with one tube 8 inches long and the other, 6 inches long. The 8-inch long tube was installed for permeation testing, and the 6-inch long tube was installed for exposure-only testing. Figure 158 shows these two membrane tubes.

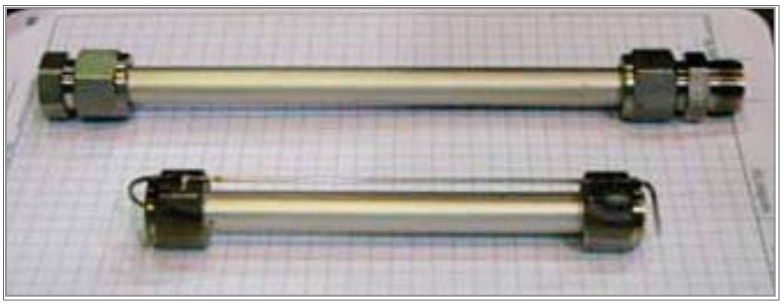

Figure 158. Eltron Membrane Tubes

The membranes were tested at about 640°F for a total of 204 hours during R09, including 183 hours of syngas operation with hydrogen enrichment and 21 hours with bottled hydrogen/nitrogen gases. The system operated with 10 lb/hr shifted and sweetened syngas (less than 1 ppmv sulfur). With hydrogen enrichment, the hydrogen concentration of the syngas reached about 38 to 40 vol% (dry basis). During the testing period, the membrane consistently demonstrated a hydrogen flux of about 20 scfh/ft^2, as shown in Figure 159. The step increase in flux at around 50 hours was the result of replacing a rotameter with a higher resolution one. Hydrogen purity in the permeate stream was greater than 99.87 percent during the entire testing period, which indicated excellent membrane integrity without leakage.

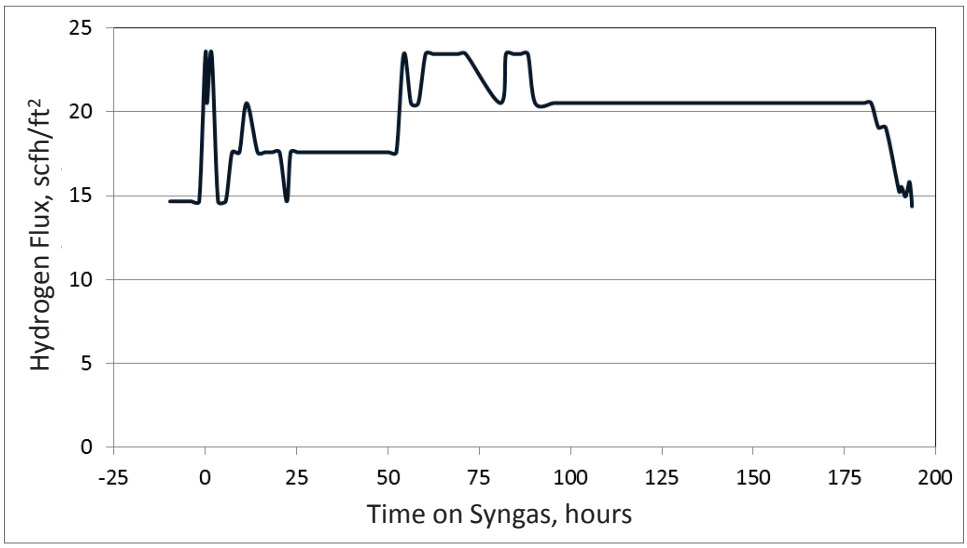

Figure 159. Eltron Membrane Hydrogen Flux during R09 Testing

Eltron's post-run inspection showed the membranes to be in good condition. Through the NCCC testing, previous field testing at two other gasification facilities, and economic and engineering studies, Eltron demonstrated the potential for the HTM technology as a viable alternative to commercially available hydrogen separation and carbon capture processes.

4.5 TDA Research CO_2 Sorbent

Technology developer TDA Research is advancing a sorbent-based pre-combustion CO_2 capture technology to remove more than 90 percent of CO_2 from shifted syngas at relatively low cost. The sorbent is a proprietary carbon-based material modified with surface functional groups to physically adsorb CO_2 from shifted syngas. The CO_2 capture system operates at relatively high temperature (greater than 400°F) and uses four beds to operate based on pressure-swing adsorption and regeneration. Because the sorbent and the CO_2 do not form a true covalent bond, the energy needed to regenerate the sorbent is much lower than that observed for either chemical absorbents or amine-based solvents, and is comparable to that of Selexol. If desired, the sorbent can be regenerated isothermally and CO_2 can be recovered at pressure (about 150 psia), significantly reducing the total energy needed to regenerate the sorbent and to compress the CO_2 for sequestration.

Figure 160 provides views of TDA's demonstration unit, showing (a) the four-bed high temperature PSA-based CO_2 separation sub-assembly; (b) the syngas conditioning sub-assembly; and (c) the unit installed at the NCCC.

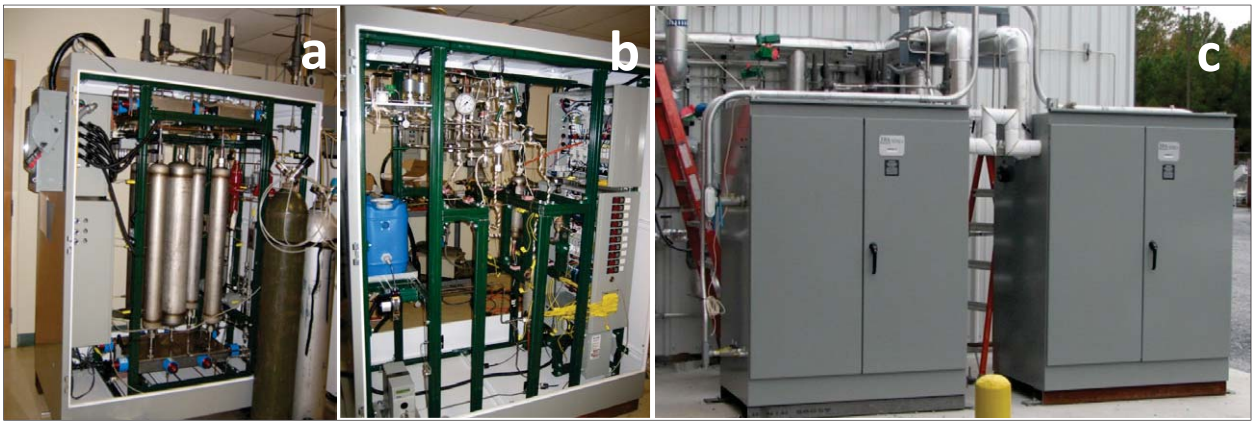

Figure 160. Field Demonstration Unit for TDA Sorbent

As part of the technology development, TDA tested the sorbent system during R07 for 308 hours and over 1,200 adsorption/regeneration cycles, utilizing about 5 lb/hr sweet, shifted syngas. The field testing results showed the pre-combustion capture technology to be fully capable of removing more than 90 percent of CO_2 from the syngas generated by an air-blown Transport Gasifier. The sorbent maintained consistent performance in the field, which closely matched the results in the laboratory using a simulated syngas mixture, suggesting that the potential impurities in the coal-derived syngas gas did not lead to sorbent degradation.

TDA modified the process to combine the WGS reaction and sorbent CO_2 capture in the same reactor for testing in run R10, during which the system operated for 384 hours. The integrated operation of the WGS catalyst and CO_2 sorbent in a single step drives the equilibrium-limited WGS reaction towards hydrogen without the need to add large amounts of steam to the syngas, greatly reducing the cost of carbon capture. In run R10, TDA completed testing using 3.5 lb/hr of untreated syngas, demonstrating CO conversions above 90 percent at steam-to-CO ratios of less than 1.2, while maintaining CO_2 capture above 96 percent.

4.5.1 Sorbent Testing in R07

During the initial field test in R07, the four-bed CO_2 sorbent reactors operated as designed with multiple steps for each cycle, (adsorption, equalization, blow-down/regeneration, and re-pressurization). During these cycle tests, TDA's system successfully removed more than 98 percent CO_2 from the syngas. The sorbent regeneration cycles were carried out at pressures greater than 54 psig, resulting in recovery of CO_2 at pressure.

Figure 161 plots the CO_2 in the syngas product stream compared to the CO_2 in the inlet syngas during the initial start-up of testing. The feed CO_2 concentration was taken from a single measurement since a continuous measurement was not available. Within two hours, the CO_2 levels dropped, leaving only small cyclic CO_2 breakthrough (attributed to a small leakage from one of the sorbent beds, which was driven by incomplete regeneration due to failure in one of the valves). Nevertheless, once the system reached steady state, the average CO_2 removal was over 98 percent.

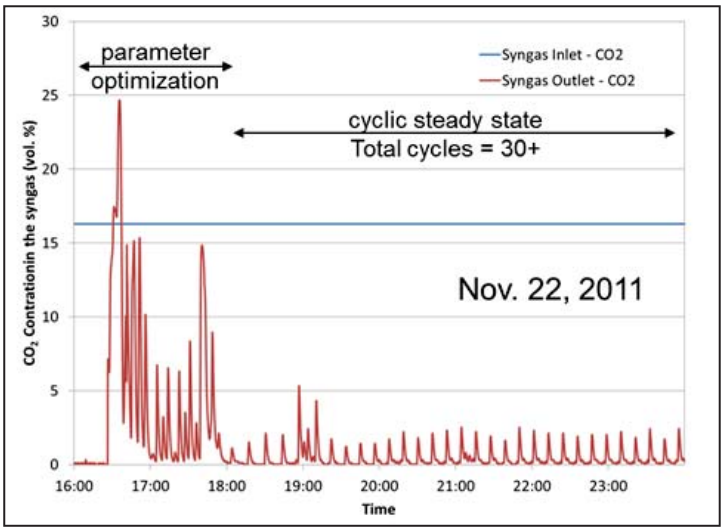

Figure 161. Inlet and Outlet Syngas CO_2 Concentration during Start-Up of TDA Research Sorbent Unit in R07

Figure 162 shows the CO_2 outlet concentration from the test unit both for the treated syngas (red) and for the regeneration off-gas (blue) for approximately 82 cycles. The overall CO_2 capture was greater than 98 percent for this portion of the testing. The CO_2 in the syngas was allowed to breakthrough to 2 percent to ensure the entire bed was being utilized. The CO_2 concentration in the regeneration stream peaked out at 24 percent and was allowed to regenerate until the CO_2 was below 2 percent to ensure that the bed had sufficiently regenerated.

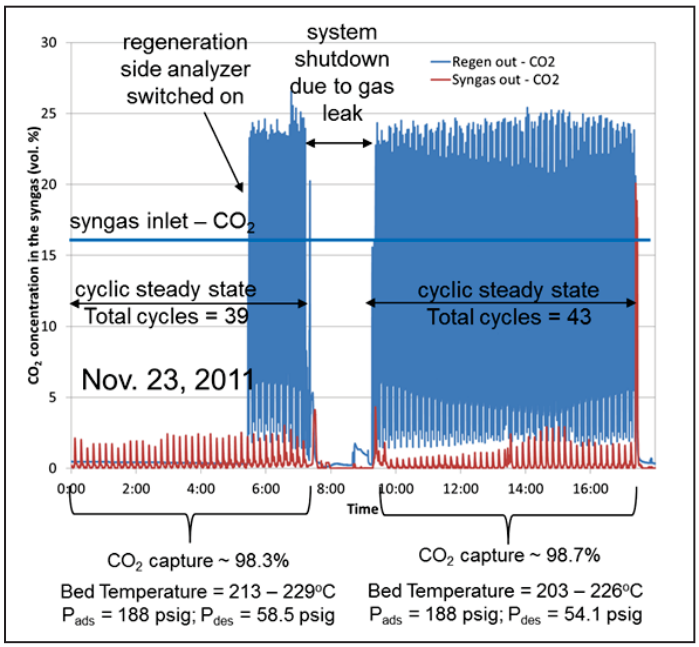

Figure 162. CO_2 Outlet Concentration for Treated and Regenerated Gas Streams of TDA Research CO_2 Sorbent Unit during R07

Once the test unit was operating under steady state conditions, different parameters were changed in order to determine their effect on sorbent performance. One parameter that had a significant impact regarding sorbent capacity was the bed temperature. The average CO_2 capacity (weight of CO_2 adsorbed/weight of sorbent) at the beginning of the field test was slightly lower at 1.2 percent compared to the baseline testing value of 1.6 percent. Lowering the bed temperatures by approximately 20°C increased the capacities to near 1.6 wt%, which matched that of the baseline testing. Figure 163 shows that decreasing the bed temperature 20°C increased the capacity by almost 50 percent without adversely affecting the CO_2 capture rate.

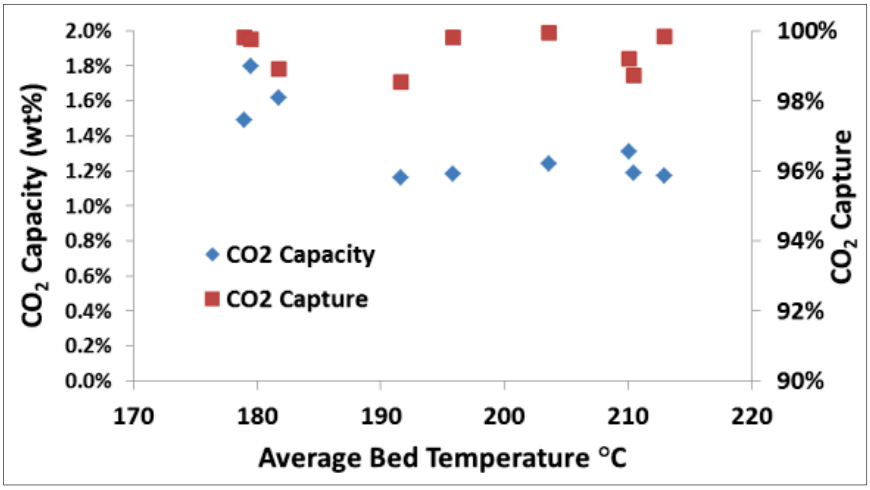

Figure 163. CO_2 Capacity as a Function of Bed Temperature for TDA Research Sorbent during R07

Another operating parameter that was altered was the adsorption time for each bed. While holding all other parameters constant, the adsorption time was varied from 2.7 to 3.05 minutes. Results are given in Figure 164.

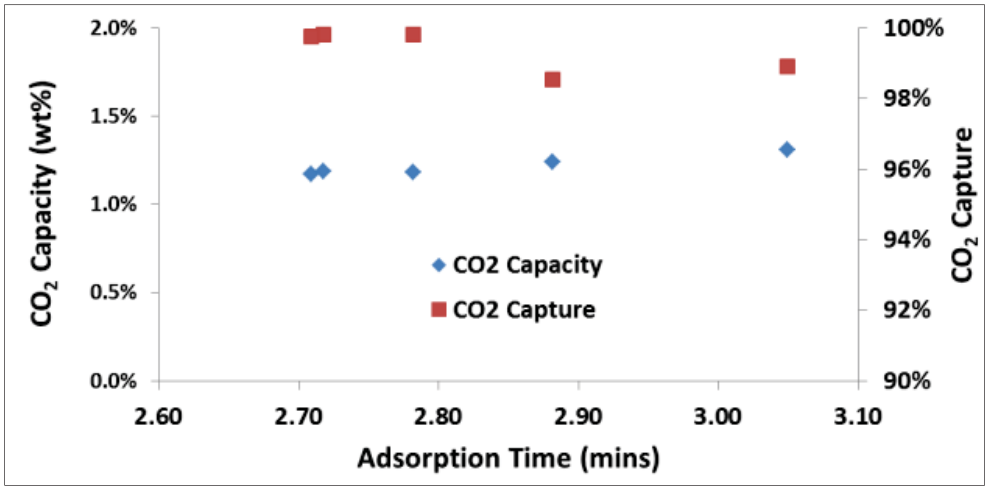

Figure 164. CO_2 Capacity and Removal Efficiency as a Function of Adsorption Time for TDA Research Sorbent during R07

As the adsorption time increased, the capacity also increased, but the CO_2 removal efficiency decreased (as the sorbent was saturated with CO_2, more CO_2 slippage occurred). The CO_2 in the packed bed was adsorbed as a wave traveling through the length of the bed. The increase in adsorption time allowed for this wave to travel farther through the bed, enabling more of the sorbent to be utilized. However, if this wave is allowed to travel too far, the CO_2 leakage will increase. This accounts for the decrease in overall CO_2 capture as the adsorption time increased. Increasing the adsorption time for each bed will decrease the overall size of the sorbent beds while increasing the overall efficiency of the entire system. Longer adsorption times also increase the syngas recovery percentage of system by reducing the number of adsorption and regeneration cycles that a bed must undergo. Therefore, the amount of syngas lost during regeneration is reduced.

Once the testing was completed, the test unit was returned to TDA facilities and the initial baseline tests were repeated to determine if the performance of the sorbent had changed after being exposed to the syngas contaminates and after numerous adsorption cycles. As indicated by Figure 165, the sorbent capacity did not significantly degrade.

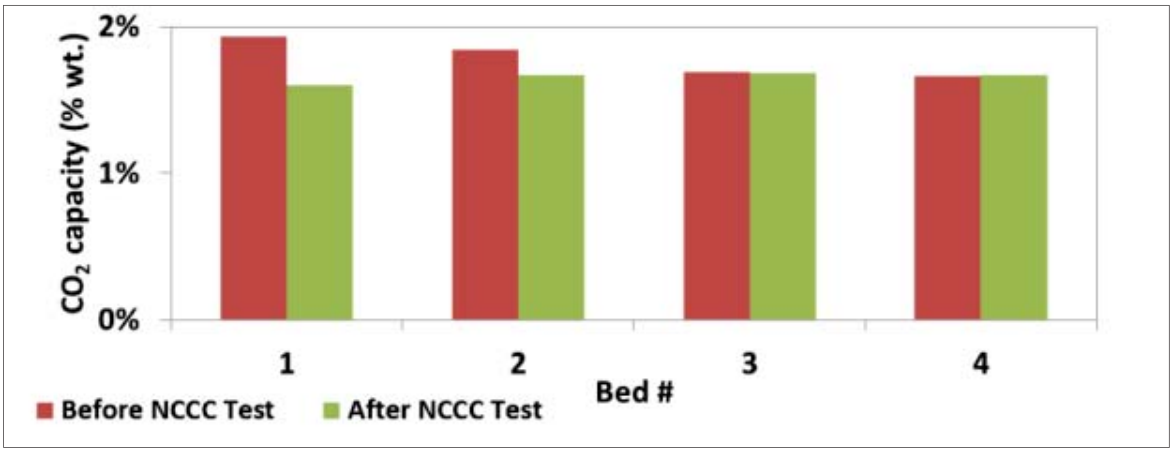

Figure 165. CO_2 Capacity of TDA Research Sorbent before and after R07 Testing

4.5.2 Sorbent Testing in R10 with WGS Functionality

During R10, a series of tests was performed running single bed saturation cycles to determine the sorbent's CO_2 capacity and the CO conversion of the catalyst. Figure 166 graphs the outlet CO_2 and CO content for each bed cycle. The green line represents the amount of CO in the regeneration stream, which is the amount of CO that was picked up by the sorbent and was not converted. To determine the CO conversion for beds 1-3, the CO coming out in the regeneration and CO_2 lean syngas streams were integrated and subtracted from the inlet CO flow rate. The CO_2 sorbent capacity was calculated similarly, with the CO_2 in the outlet integrated and subtracted from the inlet CO_2 and then normalized by the mass of CO_2 adsorbed by the weight of the sorbent. As shown by the graph, the CO in the outlet of beds 1-3 was near zero, while the CO in the outlet of bed 4, which contained no catalyst, reached the inlet CO concentration.

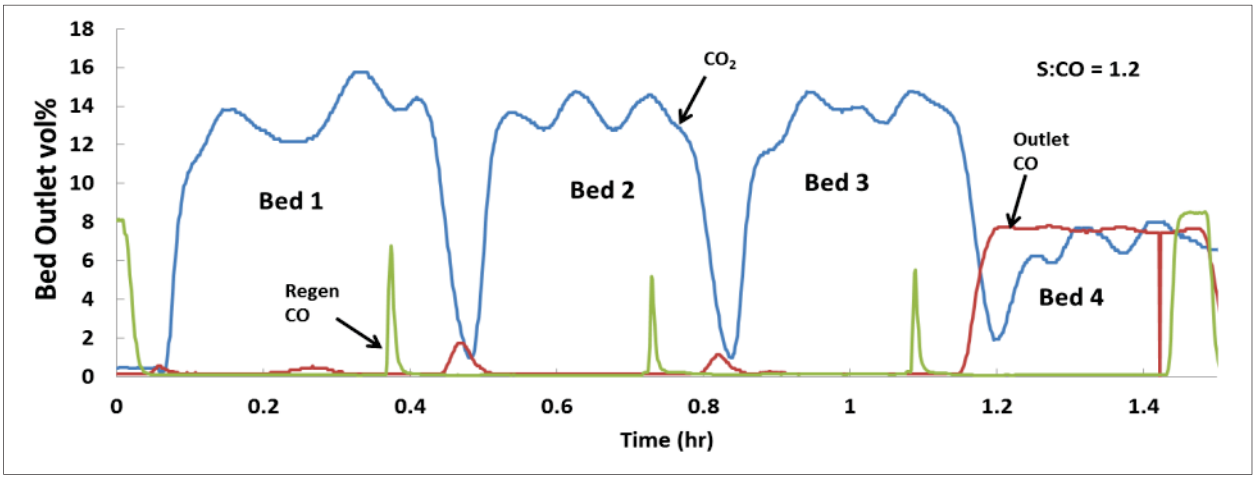

Figure 166. Single Bed Cycle Outlet Gas Composition during TDA Research Sorbent Testing in R10

The CO conversion and weight capacity were averaged for each bed. As shown in Figure 167, the CO conversion at a steam-to-CO ratio of 1.1 was over 5 percent more (96.4 percent compared to 91 percent) than that predicted by the WGS reaction equilibrium at a temperature of 230°C and 200 psig. This shift in equilibrium was most likely due to the closely coupled

removal of the CO_2 product gas, which enabled the reaction to more closely approach completion. That the CO conversion at a steam-to-CO ratio of 1.0 was lower than equilibrium was likely due to the presence of the sorbent section, which occupies the initial 20 percent of the bed at the syngas inlet. Some of the water is picked up at the inlet section (due to the use of nitrogen instead of steam during regeneration, else the bed during a typical cycle will neither pick up nor release water during either adsorption or desorption) and prevents the catalyst section from fully seeing the stoichiometric amount of steam, resulting in lower than equilibrium conversion. There is unreacted CO that is trapped in the voids in this initial sorbent section that can be seen immediately on the regeneration cycle (Figure 166). Adding a small portion of catalyst in this section of the bed may reduce this effect and also increase the conversion at the lower steam-to-CO ratios.

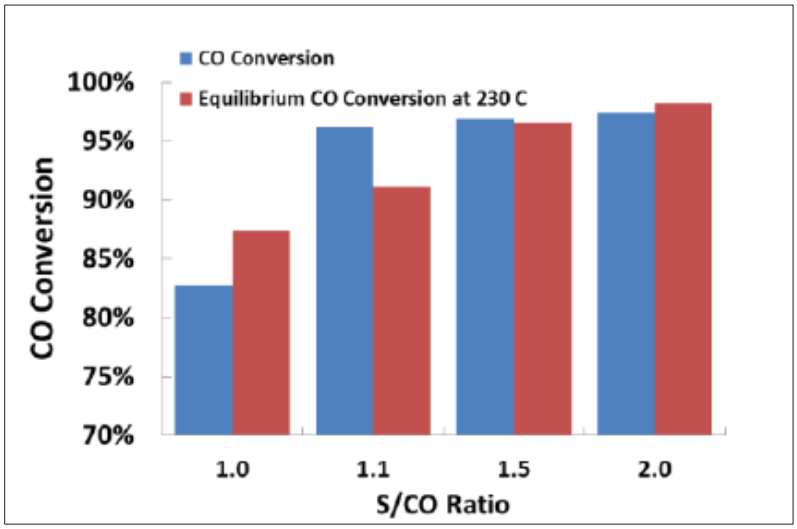

Figure 167. CO Conversion of TDA Research Sorbent and Equilibrium CO Conversion at Various Steam-to-CO Ratios during R10

The CO_2 capacity was calculated at varying steam-to-CO ratios, and the average values are plotted in Figure 168. The capacity of the sorbent was slightly higher in R10 than it was in run R07 at steam-to-CO ratios between 1.0 and 1.5. The increase in CO_2 capacity may have been due to the lower amount of H_2O in the feed stream and subsequent higher CO_2 partial pressure. At a steam-to-CO ratio of 2.0, with the same amount of H_2O in the feed stream as that in R07, the sorbent capacity was lower.

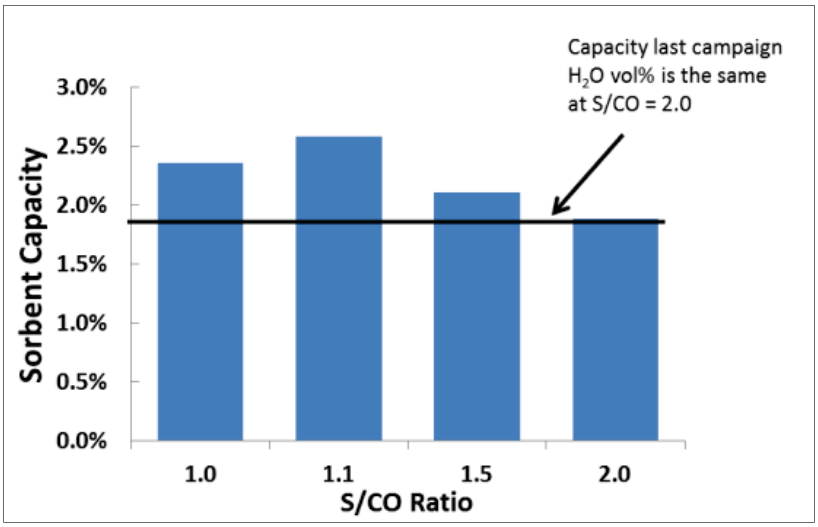

Figure 168. TDA Research Sorbent CO_2 Capacity at Varying Steam-to-CO Ratios during R10

Figure 169 shows the amount of total carbon entering the prototype unit as CO and CO_2 and the amount of carbon exiting the apparatus along with the high pressure syngas. The average overall carbon capture rate for this demonstration test campaign was over 96 percent with an average overall CO conversion of 96.4 percent at an average steam-to-CO ratio of 1.1.

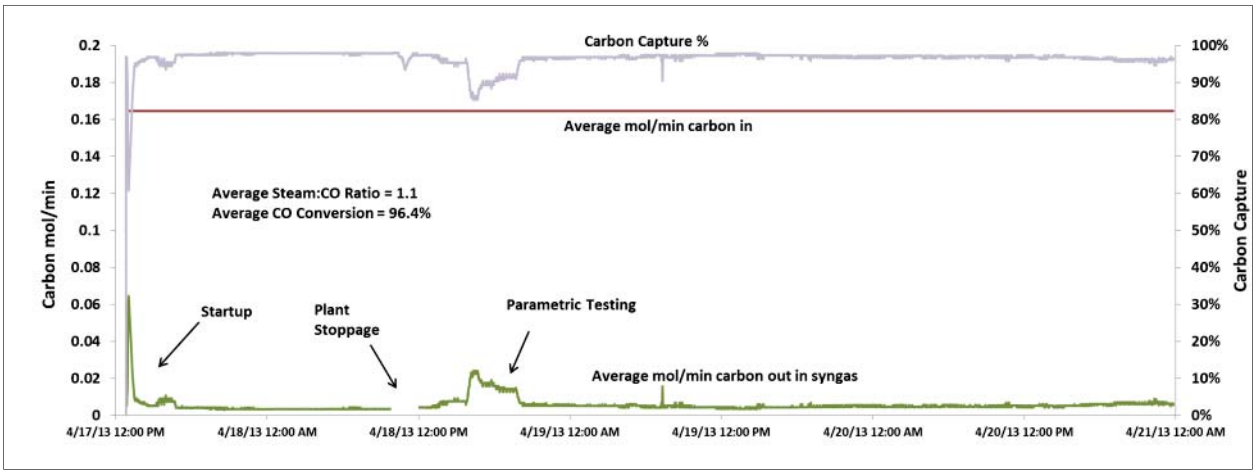

Figure 169. Carbon Capture Rates during a Portion of TDA Research Sorbent Testing during R10

An important observation during these tests was that the bed temperature was higher when the catalyst and sorbent operated together compared to previous testing with only the CO_2 sorbent. Figure 170 shows the temperature rise for the sorbent only case and the combined catalyst and sorbent case. As expected, the temperature increase was much higher when the WGS reaction was combined with the CO_2 removal. The heat effects will be more pronounced with syngas having higher CO/CO_2 content.

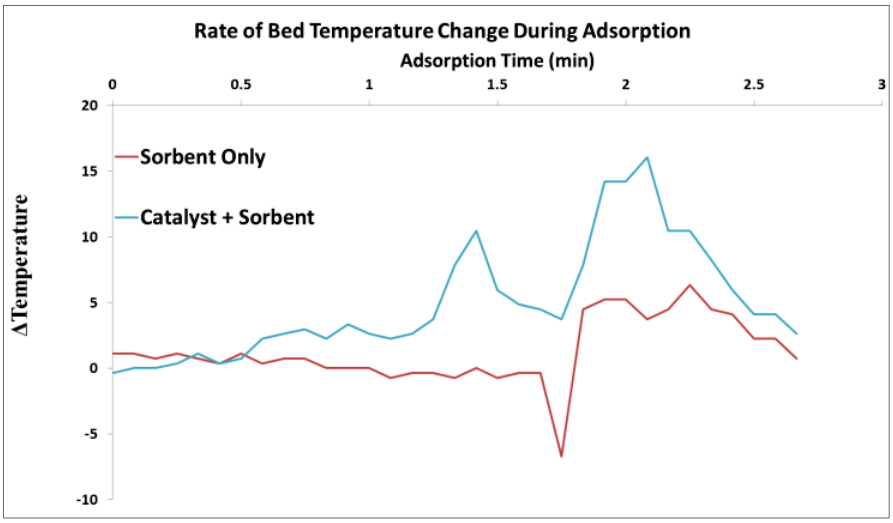

Figure 170. Temperature Difference during Adsorption for Sorbent Only and Mixed Sorbent/Catalyst Bed for TDA Research Sorbent during R10

4.6 Batch Reactor CO_2 Capture Testing

Operation with CO_2 capture solvents has led to the development of accurate sampling methods and the understanding of process chemistry. In establishing a database of solvent characteristics, NCCC researchers have evaluated chemical solvents including ammonia (used to define solvent testing and sampling techniques), the well-established solvent potassium carbonate, and the potentially commercial solvent potassium prolinate. Physical solvents tested include PDMS, the well-documented solvent DEPG, GTA, alkylimidazoles, and hybrid siloxane. In addition to CO_2 absorption characteristics, solvents tested have been evaluated and compared for co-absorption of H_2S, regeneration characteristics, and performance with water addition. Much of the solvent testing has been conducted to support DOE studies at the University of Pittsburgh.

Bench-scale testing of physical and chemical CO_2 solvents is performed using a batch reactor which was manufactured by Parr Instrument Company. The batch reactor and the reactor internals are pictured in Figure 171. A stirrer with a maximum rotational speed of 800 rpm is used to mix the gas and liquid, and a cooling coil and heating jacket are used to control the reaction temperature. Testing can be conducted with up to 10 lb/hr of bottled gases or syngas drawn from the SCU header at around 215 psig. The bottled gases allow absorption to be completed at pressures up to 1,000 psia and so extend the range of data collected. During gasifier operation, raw, unshifted syngas is used for testing. Before entering the reactor, the syngas is cooled to 100°F to remove hydrocarbons and avoid accumulating condensate in the reactor that would dilute the solvents.

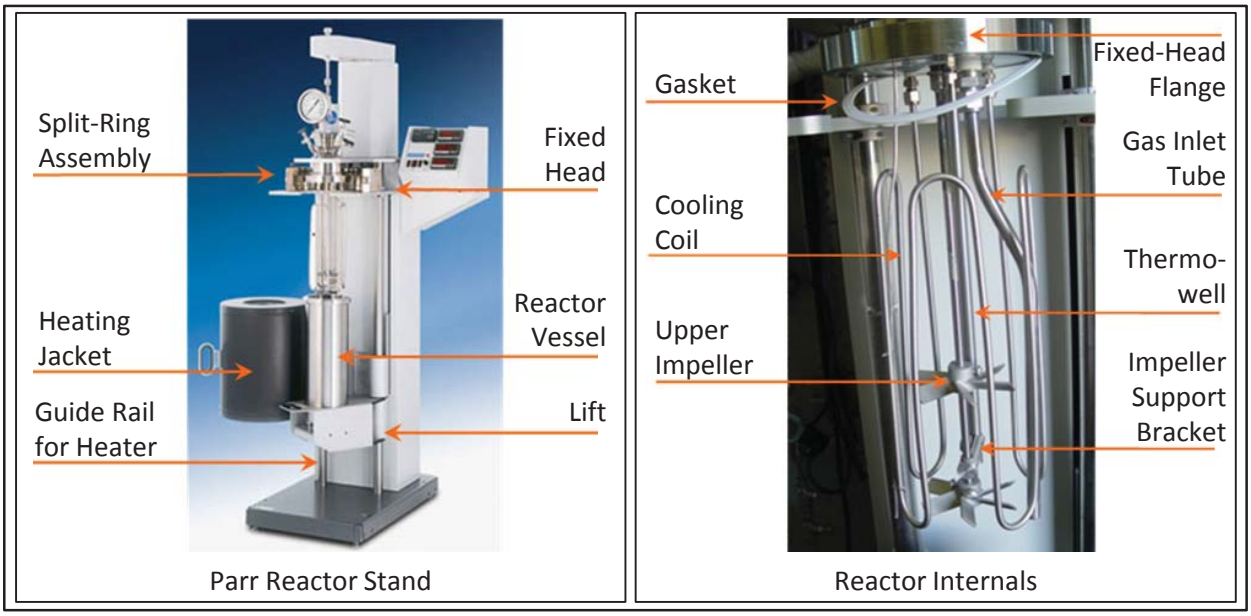

Figure 171. CO_2 Solvent Batch Reactor from Parr Instrument Company

During absorption, the CO_2 lean syngas passes through a back-pressure regulator to be routed back to the atmospheric syngas combustor. During regeneration, the CO_2 released passes through a back-pressure regulator to be routed to a receiving tank. The rate of pressure rise in the tank is used to calculate the rate of CO_2 release. Downstream of each pressure regulator, a gas stream can be extracted and passed to a non-dispersive infrared CO_2 analyzer and a GC for sulfur analysis.

4.6.1 Chemical Solvents

4.6.1.1 Ammonia Compounds

Ammonia can capture CO_2 by two main mechanisms, one involving ammonium carbonate, and the other ammonium carbamate.

The carbonate route involves the following reactions:

$$NH_3 + H_2O + CO_2 \leftrightarrow (NH_4)_2CO_3 \quad (-986 \text{ Btu/lb } CO_2; -24.1 \text{ kcal/g-mol}) \quad \text{Equation 1}$$
$$(NH_4)_2CO_3 + H_2O + CO_2 \leftrightarrow 2NH_4HCO_3 \quad (-260 \text{ Btu/lb } CO_2; -6.36 \text{ kcal/g-mol}) \quad \text{Equation 2}$$

The carbamate route involves the following reactions:

$$2NH_3 + CO_2 \leftrightarrow (NH_3)_2CO_2 \quad (-725 \text{ Btu/lb } CO_2; -17.7 \text{ kcal/g-mol}) \quad \text{Equation 3}$$
$$(NH_3)_2CO_2 + 2H_2O + CO_2 \leftrightarrow 2NH_4HCO_3 \quad (-521 \text{ Btu/lb } CO_2; -12.75 \text{ kcal/g-mol}) \quad \text{Equation 4}$$

If the ammonium bicarbonate (ABC) crystallizes, heat is released, the heat of crystallization being -277 Btu/lb CO_2 (-6.78 kcal/g mol). If the liquor to be regenerated contains crystals, then heat must be applied to dissolve the crystals. If the ABC releases its CO_2 to form carbonate, the heat of reaction (-260 Btu/lb CO_2) is lower than if carbamate is formed (-521 Btu/lb CO_2). Hence, it is important to know the exact chemical route followed. In addition, the formation of

crystals may be beneficial in reducing the heat of regeneration. The crystals can be separated from the liquor, lowering the water content of the ABC-rich liquor sent to the regenerator, thereby lowering the sensible heat requirement. However, this will be offset to some degree by the heat required to dissolve the crystals. A comprehensive model to predict ammonia chemistry is required to resolve these issues.

The thermodynamic software employed for this study was supplied by OLI Systems and is used widely to predict the properties for a range of aqueous solutions. When used to predict the capture of CO_2 using ammonia, the calculations are based on carbamate being the primary product of the reaction. To confirm that this is correct and validate the model, tests were completed in the SCU batch reactor to produce ammonia liquors with a range of compositions. These solutions were analyzed using nuclear magnetic resonance (NMR) spectroscopy.

The NMR technique beams an electromagnetic pulse at the solution and the energy radiated back is influenced by the properties of the molecule's nucleus. A spectral output signal is presented in Figure 172, the frequency shift being a characteristic of the nucleus and the height of the peak being an indication of the amount present. The instrument can be programmed such that the peak value represents the percentage of the species present in solution.

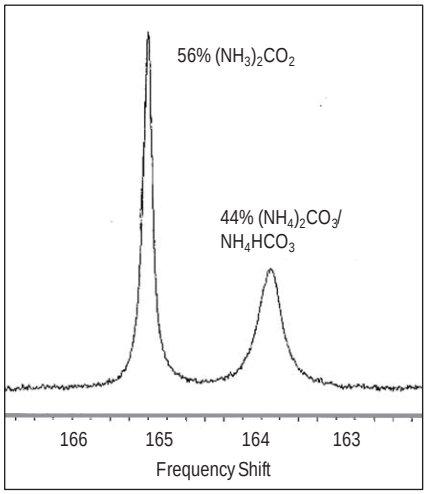

Figure 172. Output Signal from NMR Analyzer

The left-hand peak results only from ammonium carbamate and allows direct determination of this species. The right-hand peak results from a combination of ammonium carbonate and bicarbonate, requiring a means of deducing the proportions of the two species present. Research from the University of Florence showed that the greater the horizontal separation of the two peaks, the greater the bicarbonate content of the left-hand peak. This group then developed a calibration curve using solutions with known carbonate and bicarbonate contents. This calibration curve was used to extract the carbonate and bicarbonate information from the on-site analyses.

Fifteen tests were completed to compare the concentration of ammonium compounds measured by NMR with values predicted by OLI. Figure 173 provides plots of the ammonium carbamate,

ammonium bicarbonate, and the ammonium carbonate concentrations measured by NMR versus those predicted by the OLI program.

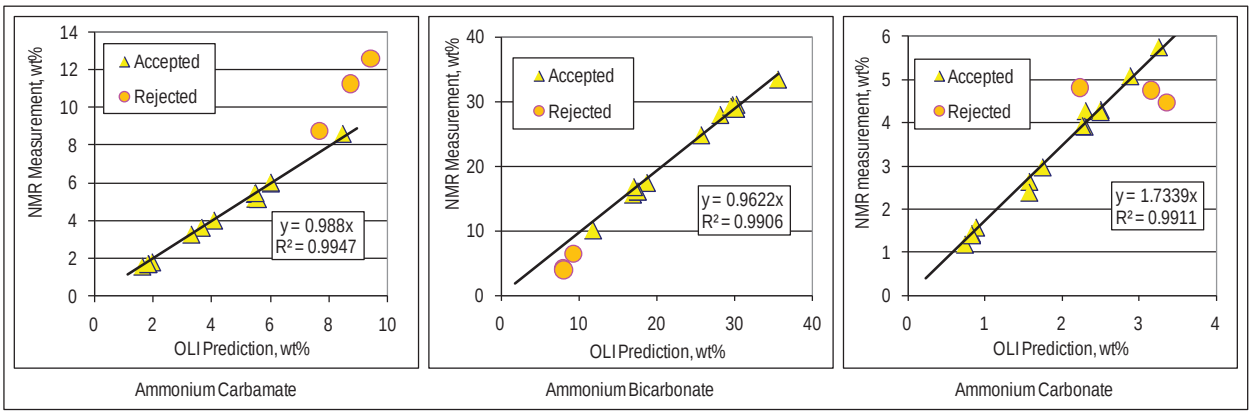

Figure 173. Comparison of Measured and Predicted Concentrations of Ammonia Compounds

As noted in the figure, three data points were rejected from the data set. For ammonium carbamate and ammonium bicarbonate, the slope of almost one indicated good agreement. For ammonium carbonate, the measured values were appreciably higher than the predictions as indicted by the slope being greater than one. The error may have resulted from error in the calibration curve. The ABC results presented in the figure could be slightly over-predicted, giving a slope of less than one.

Adjusting the measured ABC to match the predicted value will increase the amount represented in the right hand peak of the NMR measurement and so the amount of ammonium carbonate measured is reduced. This approach improved the match achieved in the ammonium carbonate plot and lowered the slope to 1.24, but still suggested that the model under-predicts the ammonium carbonate present. It was concluded that the measured ammonium carbamate and ABC were predicted with good accuracy by the OLI model and any error associated with ammonium carbonate was low. This validated the model and allowed its use with confidence for predicting the composition of the ammonia liquor.

The model was also used to predict other performance parameters of interest. Figure 174 presents CO_2 capture data and shows that the model agreed well with the measured values. The perturbation in experimental CO_2 capture efficiency seen around 68 minutes into the test may have been related to the onset of ABC crystal formation after around 64 minutes.

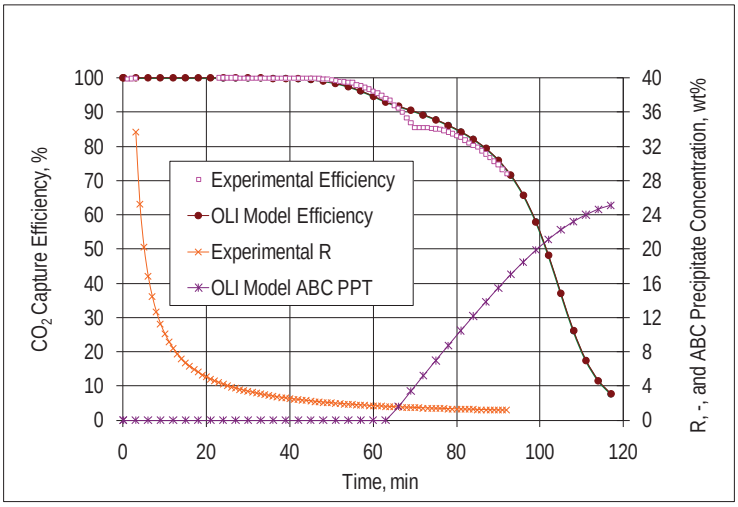

Figure 174. Comparison of Measured and Predicted CO_2 Capture Efficiencies

The "R" value included in Figure 174 represents the ammonia-to-CO_2 molar ratio and fell as the CO_2 content of the liquor increased. When the CO_2 capture efficiency began to decrease after around 50 minutes, R was slightly greater than 2, indicating that the free ammonia was almost depleted. Up to this point, CO_2 capture occurred primarily by the reaction in Equation 3, and carbamate was the primary ammonia compound formed. After this, Equation 4 was the primary CO_2 capture reaction, and the carbamate was converted to bicarbonate. Eventually the saturation concentration was reached, resulting in the formation of ABC crystals after 64 minutes.

Figure 175 presents the concentration of ammonia exiting with the gases leaving the reactor and also shows that the model agreed well with the measured values. Ammonia was released at around 1,000 ppmv at the onset of ABC crystallization even though there was no free ammonia. This was a result of the presence of ammonia anions. The experimental work validated the use of OLI software for predicting ammonia chemistry.

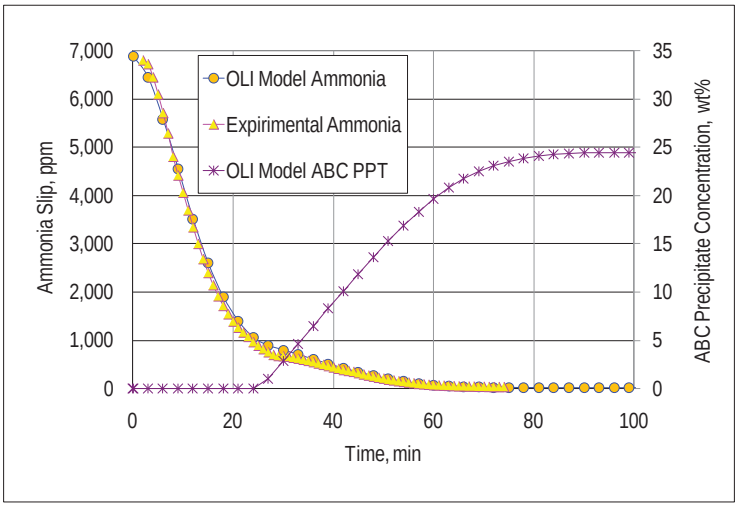

Figure 175. Comparison of Measured and Predicted Ammonia Slip

Modeling Results

Using the properties predicted by the validated OLI model, testing was undertaken to determine how the composition of the liquor leaving the absorber changed as it was heated in the regenerator. The change is presented in Figure 176. This graph shows absolute values for the ammonium bicarbonate crystals and the CO_2 released, and the difference in values for the dissolved species, ammonium bicarbonate, carbamate, and carbonate.

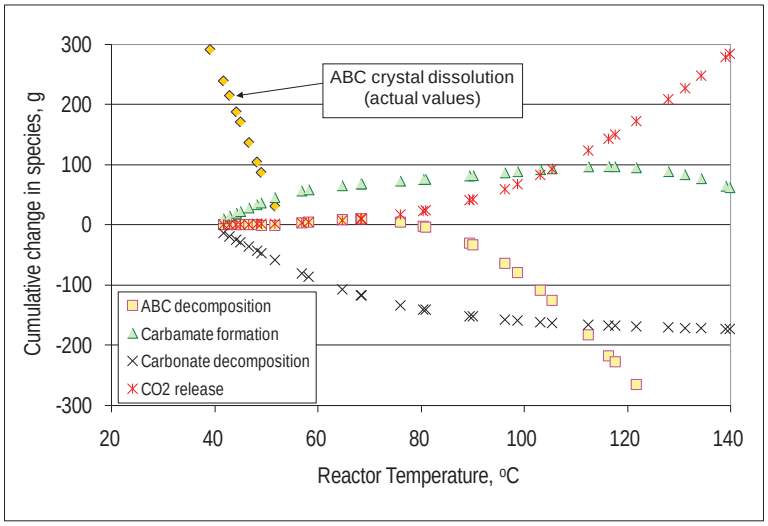

Figure 176. Change in Ammonia Liquor Composition with Reactor Temperature

The model is based on the batch reactor to allow comparison between measured and predicted values. The 40°C (104°F) data represent compositions at the end of an absorption period with 300 g of ammonium bicarbonate crystals in the liquor. As the liquor was heated, the crystals dissolved, and at 53°C (127°F), all the bicarbonate was in solution. At this temperature, 58 g of ammonium carbonate decomposed, forming 47 g of ammonium carbamate according to Equation 5, which is endothermic.

$$(NH_4)_2CO_3 \leftrightarrow (NH_3)_2CO_2 + H_2O \quad (+6.39 \text{ kcal/g-mol};\ +261 \text{ Btu/lb } CO_2) \quad \text{Equation 5}$$

Despite the temperature increase, no ammonium bicarbonate decomposed, and no CO_2 was released. Results suggest that the liquor re-established chemical equilibrium at the new temperature. At around 60°C (140°F), CO_2 release began, but ammonium bicarbonate was being formed and did not start to decompose until the temperature was around 80°C (176°F).

Controlling the absorption temperature at 40°C (104°F) requires additional cooling to remove the heat released when the ammonium bicarbonate crystallizes. When regeneration is required, heat must be added to dissolve the crystals and the temperature raised to above 80°C (176°F) before significant CO_2 is released. Cooling duty and water usage could be reduced if absorption could be carried out effectively closer to 60°C (140°F). This would also reduce the sensible heat required (some of which is recovered using recuperators) to raise the liquor to regeneration temperature.

A possible drawback of operating the absorber at 60°C (140°F) is an increase in ammonia slip in the exiting CO_2-depleted syngas. The ammonia would be scrubbed out using water wash, although this constitutes a system loss.

Raman Spectroscope

The Raman Spectroscope employs a technique that directs a single wavelength laser beam into a solution, and the energy radiated back is influenced by the properties of the molecules present. The scattered light is collected and analyzed, producing a Raman Spectrum. The species associated with the Raman shift are determined experimentally using solutions of known composition. The signal intensity is relative to that of the laser beam.

The results are obtained in real time, unlike the NMR spectroscope, which is used in the laboratory to analyze samples of the solution. Unlike the NMR peaks, the Raman peaks do not give a direct measurement of concentration, and calibration measurements are required. Some researchers have used concentrations measured using NMR to determine the value to be ascribed to the Raman peak, but this is a slow, expensive approach. As the OLI model had been validated, the values predicted by OLI were used to calibrate the Raman output.

A test program was carried out in the SCU batch reactor with a Raman optical head installed in the drain line at the bottom of the vessel. Ammonium hydroxide solution (14-mole percent ammonia) was fed to the reactor, the vessel was pressurized to 300 psia, the stirrer was activated, and the temperature controller was set to 100°F. A known amount of CO_2 was bubbled through the solution after which Raman spectral data were collected. Additional amounts of CO_2 were introduced and further spectral data collected. For each of these data points, the composition of the ammonia compounds present was determined using the OLI software. The measured height of each peak was then matched with the predicted concentration, and a correlation curve developed allowing concentration of a species to be determined from peak height. Good agreement was achieved between measured and predicted values.

The tests were repeated but using 20-mole percent ammonia solution. Figure 177 shows the values predicted by the OLI software compared with values predicted from the Raman peaks using the calibration curve developed from the 14-mole percent ammonia solution. Agreement between the two sets of data was not good, and comparisons of ammonium carbamate and carbonate were similarly poor. More testing and analysis is required to understand how to achieve a correlation that is applicable to all concentrations of ammonia. The incentive for resolving this issue is that the Raman probe with its rapid response could potentially be used to monitor and control a commercial process.

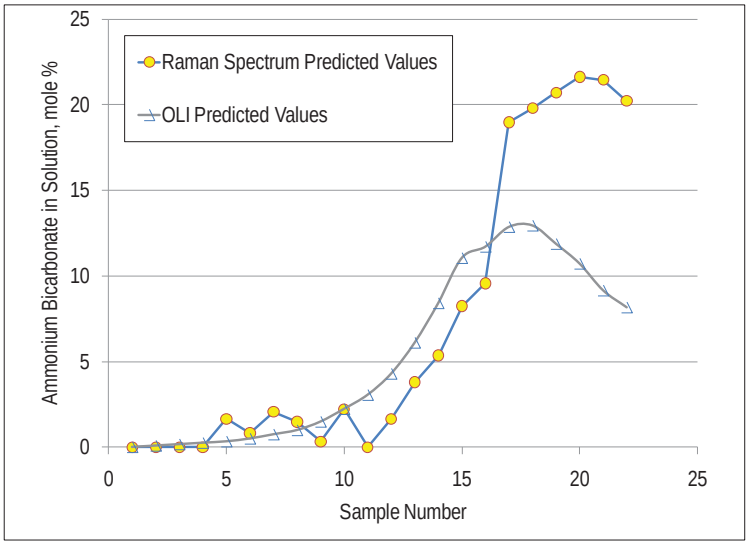

Figure 177. Comparison of Predicted Values for Ammonia Solution

4.6.1.2 Potassium Carbonate and Potassium Prolinate Solvents

To widen the range of chemical solvents under investigation, potassium carbonate and potassium prolinate were tested in the batch reactor and compared with ammonia. Potassium carbonate is an established solvent and is used in the Benfield process for acid gas purification, and amino acids such as proline, are being investigated for post-combustion CO_2 capture. Table 62 lists properties of the two solvents.

Table 62. Properties of Potassium Carbonate and Potassium Prolinate Solvents

Solvent	Molecular Weight, lb/lb-mol	Concentration		Absorption Temperature, °F
		mol%	wt%	
Potassium Carbonate	138	1.7	20	212
Potassium Prolinate	153	5.1	56	102
Ammonium Hydroxide	34	7.6	14	98

Potassium carbonate captures CO_2, forming a bicarbonate, according to Equation 6:

$$K_2CO_3 + CO_2 + H_2O \rightarrow 2KHCO_3 \quad \text{Equation 6}$$

Energy requirements for this process are:

- Heat of reaction: -249 Btu/lb CO_2 (-6.07 kcal/g-mol)
- Heat of crystallization: -395 Btu/lb CO_2 (-9.64 kcal/g-mol)
- Total: -644 Btu/lb CO_2 (-15.71 kcal/g-mol)

As discussed in the previous section, the comparable values for ammonium carbamate/bicarbonate are -521, -277, and -798 Btu/lb CO_2, so the potassium carbonate has lower heats of reaction. This advantage is offset by a lower rate of reaction requiring absorption at a higher temperature (212°F compared to 98°F) for ammonium hydroxide. Additionally, as

$KHCO_3$ has a higher molecular weight, the CO_2 loading is lower than that of ABC. To keep the K_2CO_3 in solution, the concentration is limited to 20 wt%. Together, these characteristics result in a higher solvent flow rate, increasing the heat of regeneration.

Amino acids have several advantageous properties such as low volatility and corrosivity, which offer advantages over amines. Research at the University of Twente in the Netherlands investigating amino acids for post combustion CO_2 capture concluded that L-proline had the highest reaction rate of the amino acid salts in 1-molar aqueous solutions.

Tests were conducted at the NCCC using 5-molar solutions to increase the CO_2 loading. In initial testing, the sodium salt was formed by mixing the proline with sodium hydroxide. CO_2 was bubbled through the solution, and very fine crystals were formed, eventually producing a thick mixture. Similar tests were completed with the potassium salt (using potassium hydroxide), but the final mixture was less viscous, presumably because the potassium salt was more soluble.

Figure 178 compares the CO_2 capture efficiency for the three solvents on molar and mass bases. The performance of the ammonia and potassium carbonate were similar, with the capture efficiency of potassium prolinate falling precipitously after exceeding a molar ratio of 0.5. The CO_2 mass loading for ammonia was shown to be greatly in excess of the other two solvents, with the potassium carbonate having the lowest loading.

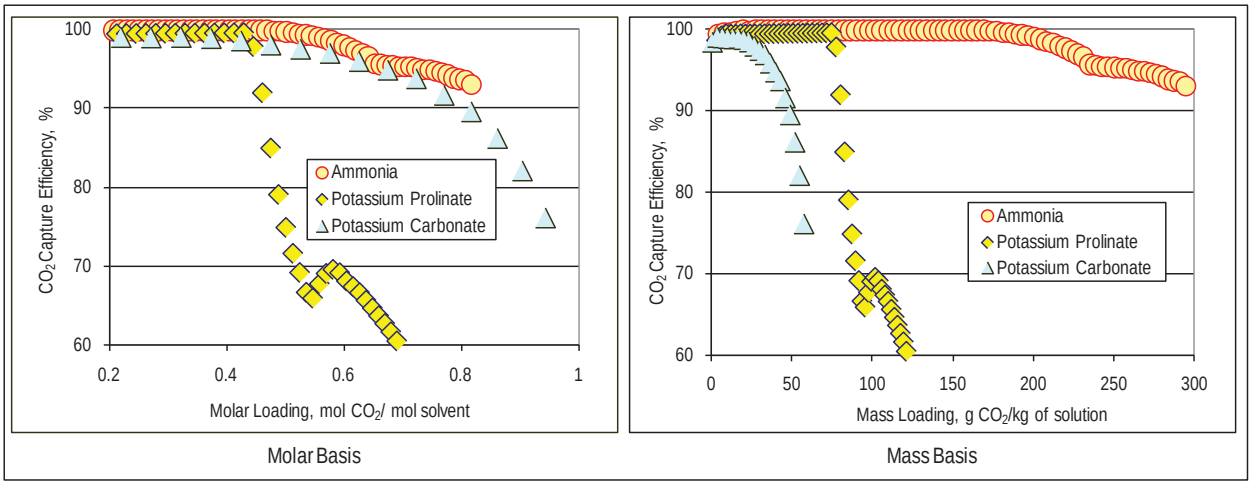

Figure 178. CO_2 Capture Efficiencies for Potassium Prolinate and Potassium Carbonate

Figure 179 graphs the pressure rise in the reactor during heating for each of the three solvents. No CO_2 was vented from the reactor, so all the CO_2 released resulted in pressure increases. The factor "L" represents the molar loading of CO_2, that is, moles of CO_2 per mole of solvent. The higher pressure indicates that the ammonia solution released CO_2 more readily and was regenerated more fully than the two other solutions.

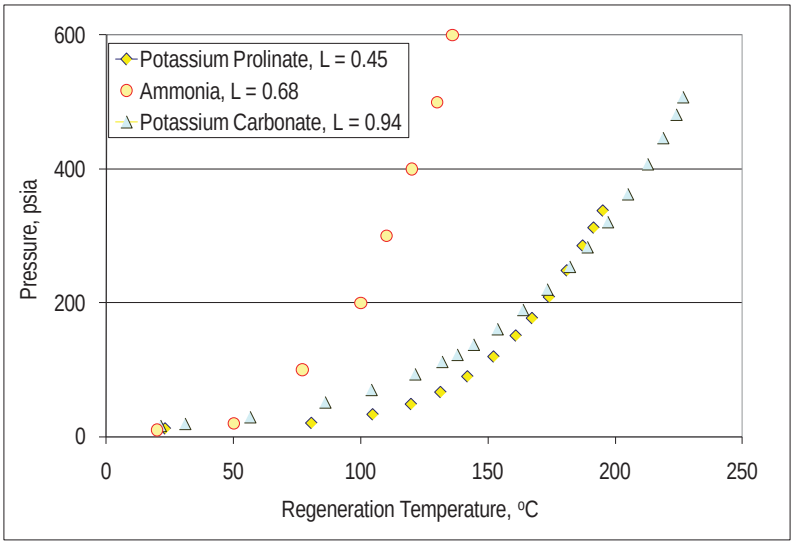

Figure 179. Pressure Increase during Regeneration of Three CO_2 Capture Solvents

4.6.2 Physical Solvents

4.6.2.1 PDMS and DEPG Solvents

PDMS solvent was evaluated in the batch reactor in 2010 at the recommendation of the DOE based on encouraging results obtained in a DOE-sponsored study at the University of Pittsburgh ("CO_2-Philic Oligomers as Alternatives for PEGDME in CO_2 Absorption"). In the study, the PDMS was compared to dimethyl ether of polyethylene glycol (DEPG) and several other oligomeric (consisting of up to five monomers) solvents. The PDMS was identified as one of the two best solvents studied in terms of immiscibility with water, CO_2 capture selectivity, and low viscosity. As DEPG is highly miscible with water, commercial processes must control water buildup, which imposes an energy penalty that could be avoided by the use of a solvent immiscible with water. For example, when DEPG is thermally regenerated to release H_2S, any water present is evaporated, thereby increasing the heat of regeneration.

The PDMS solvent was compared to DEPG in both off-line and on-line tests in the batch reactor in the SCU. The specific gravities and the mean molecular weights of the two solvents are listed in Table 63.

Table 63. Properties of PDMS and DEPG Solvents

Solvent	Molecular Weight	Specific Gravity
PDMS	515	0.87
DEPG	280	0.99

Following initial characterization studies with bottle gases, tests were completed with syngas during R05 to investigate the absorption and regeneration performance of the PDMS and DEPG solvents. Testing consisted of a series of absorption-regeneration cycles. Absorption was carried out at 140°F and 175 psia. Regeneration was achieved either by lowering the pressure

into the range 15 to 88 psia to flash off the absorbed species, or by increasing the temperature up to 300°F to release them thermally.

Figure 180 presents data for DEPG and PDMS showing the variation with time of the CO_2 concentration in the gas stream exiting the reactor during absorption cycles. The initial cycle was completed with fresh solution, which was flash regenerated by lowering pressure to near atmospheric. The minimum CO_2 attained in subsequent absorption cycles was not as low as for the initial cycle, indicating that flashing does not release all the CO_2 absorbed in the previous cycle. The minima showed that DEPG achieved higher absorption efficiencies than PDMS for the initial and subsequent cycles. Also, the CO_2 concentration profile indicated that absorption was maintained for a longer period, allowing DEPG to achieve a higher CO_2 loading level—approximately 1.4 times higher than PDMS based on the area within the concentration profiles.

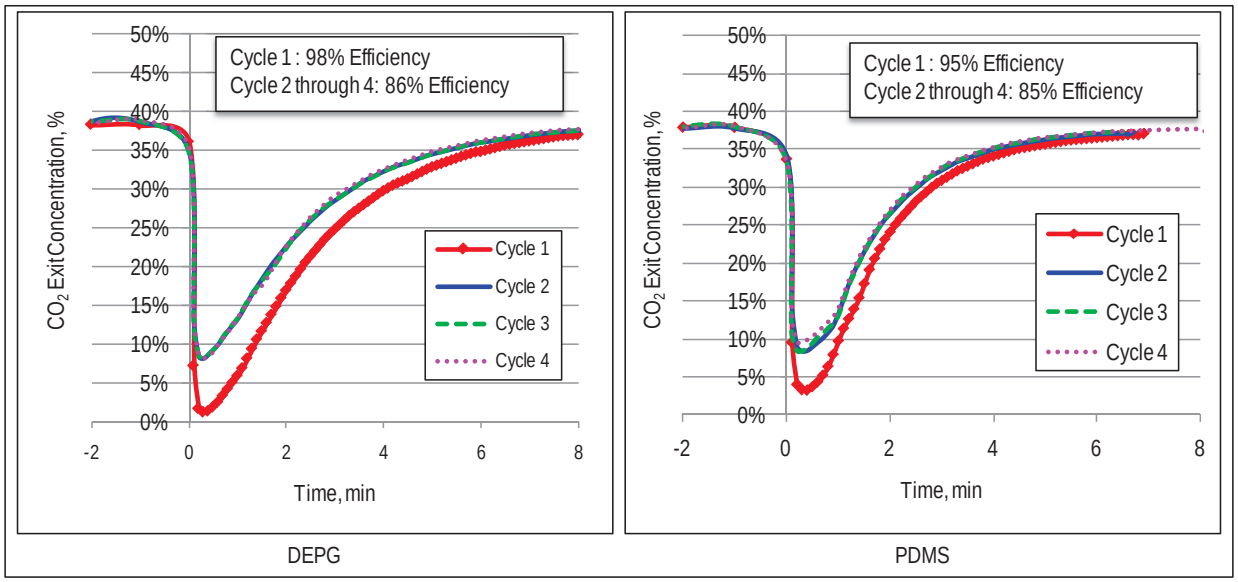

Figure 180. CO_2 Concentration Profile during Absorption Following Flash Regeneration

Figure 181 presents the maximum CO_2 absorption efficiency as a function of the flash pressure used to regenerate the solvent prior to absorption. As flash pressure increased, less CO_2 was released and, as a consequence of the reduced free capacity, CO_2 absorption efficiency fell. Above 40 psia flash pressure, the PDMS appeared to release more CO_2, resulting in higher CO_2 absorption efficiency than for DEPG. At flash pressures below 40 psia, the differences between the DEPG and PDMS were less significant.

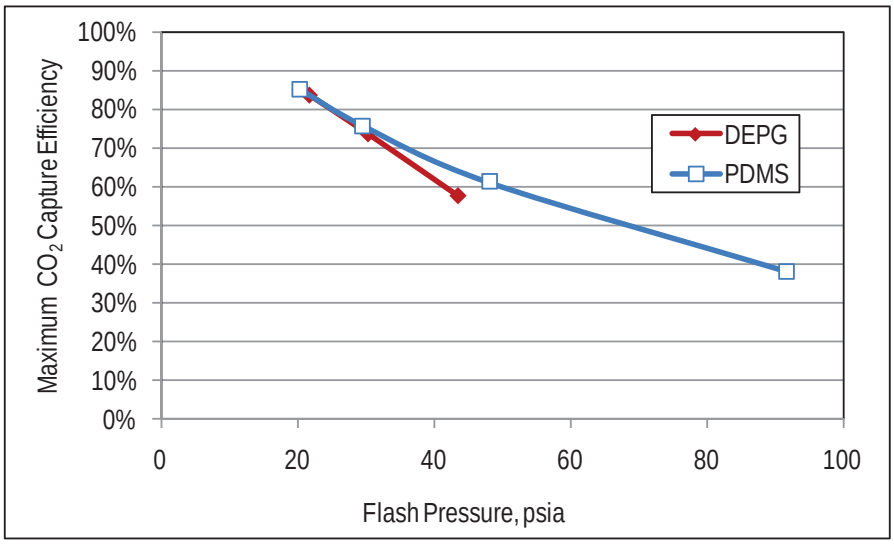

Figure 181. Effectiveness of CO_2 Regeneration at Different Flash Pressures

Figure 182 presents data for the two solvents showing the variation with time of the H_2S concentration in the exiting gas stream during absorption cycles following flash regeneration. Measurement was provided by a batch gas chromatograph that gives a value every three minutes. This accounts for the appearance that the tests start before time zero. The gas sampling sequence was initiated to take a sample around one minute into the run to coincide with the minima identified by CO_2 test results. As for the CO_2 testing, the initial cycle was completed with fresh solution, which was flash regenerated by lowering pressure to near atmospheric.

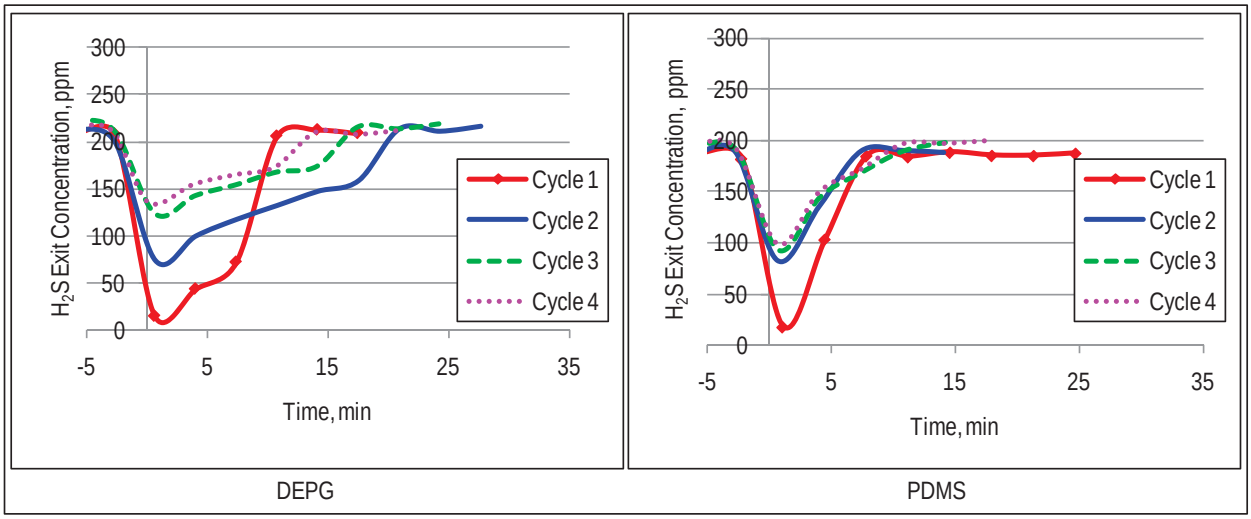

Figure 182. H_2S Concentration Profile during Absorption Following Flash Regeneration

The minimum concentration during the initial absorption cycle was lower for the DEPG than for the PDMS, at 5 and 15 ppmv, respectively. Following the first flash regeneration cycle, the DEPG absorption minimum was still lower—75 ppmv compared to 85 ppmv for PDMS—indicating that the first flash stage was more effective at releasing the H_2S from DEPG. There was some departure from this trend for Cycles 3 and 4 with the DEPG minima values decreasing, indicating that these flash stages were less effective than the first one. The results indicate that

DEPG continued to absorb H_2S and that the sites used later in the test sequence were less amenable to flash regeneration. In contrast, the trends for Cycles 3 and 4 for PDMS were almost the same as for the second cycle, indicating that saturation was reached more rapidly than for DEPG.

Figure 183 plots data for the two solvents showing the variation with time of the H_2S concentration in the exiting gas stream during absorption cycles following thermal regeneration at 302°F. The results show similar H_2S absorption efficiencies for the three cycles indicating that thermal regeneration released all the H_2S from both solvents. The H_2S concentration profiles indicate that absorption was maintained for a longer period with DEPG than with PDMS. From the area within the concentration profiles, the H_2S loading for DEPG is approximately 3.5 times higher than that for PDMS.

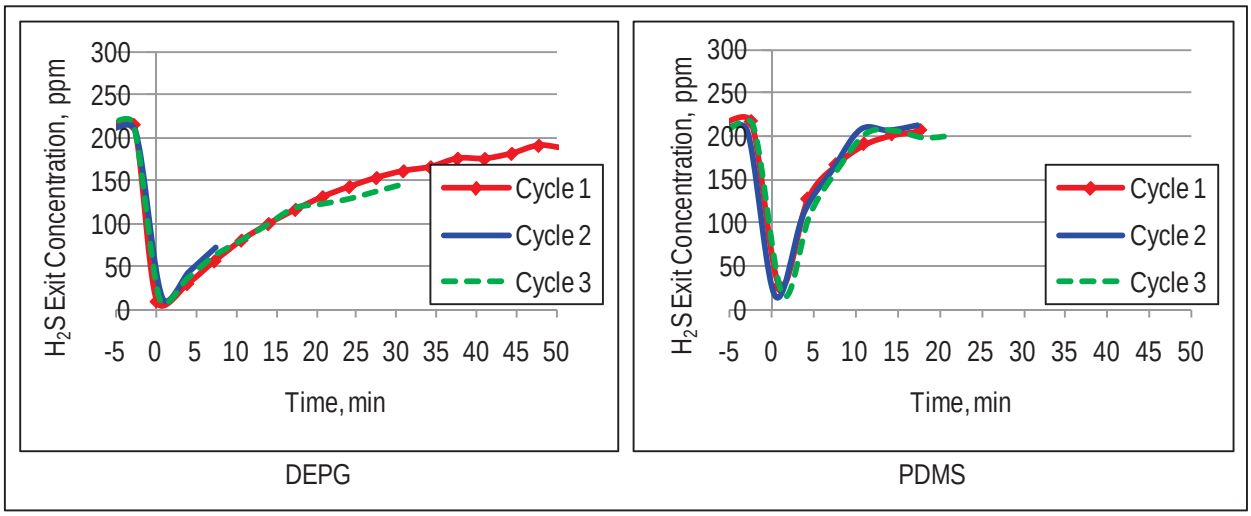

Figure 183. H_2S concentration Profile during Absorption Following Thermal Regeneration

Figure 184 presents the maximum H_2S absorption efficiency as function of the flash pressure used to regenerate the solvent prior to absorption. As flash pressure increased, less H_2S was released, and as a consequence of the reduced free capacity, H_2S absorption efficiency fell. The trend of the data is similar to that of CO_2 presented in Figure 181, but the efficacy of H_2S flash regeneration was lower as indicated by the lower capture efficiency values achieved with H_2S.

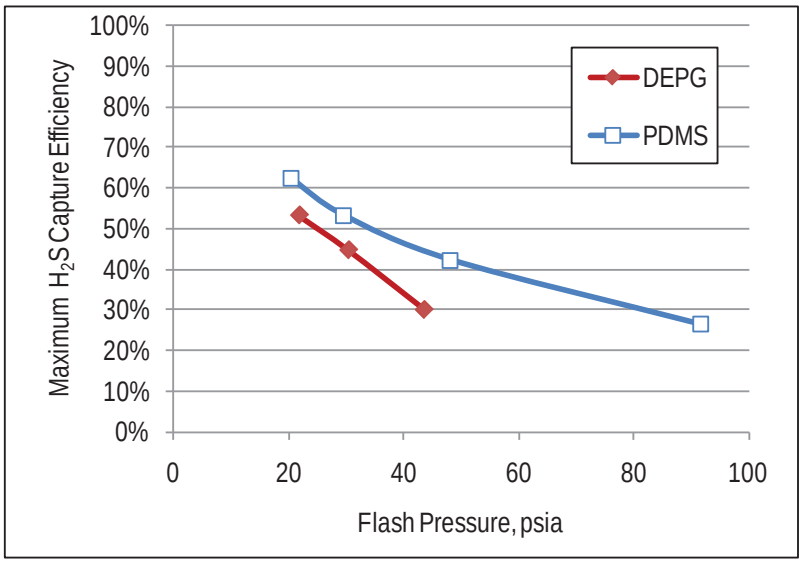

Figure 184. Effectiveness of H_2S Regeneration at Various Flash Pressures

As DEPG has a high affinity for water, some of the regeneration energy required to release H_2S and CO_2 is used to evaporate water and stabilize the solvent moisture content. Since PDMS is immiscible with water, the water can be separated mechanically, eliminating evaporation duty and lowering the heat of regeneration. Ten weight-percent water was added to the solvents to determine the effect of water on CO_2 absorption and regeneration performance. The volume of solvent/water mixture added to the reactor was 4.6 liters to maintain the depth at 10 inches.

Figure 185 presents the moles of CO_2 absorbed in the mixtures. The amount absorbed by the DEPG-water mixture was lower than for DEPG only. The reduction was in the range 15 to 25 percent, more than the straight 10 percent through dilution with water. In contrast, the amount of CO_2 absorbed by the PDMS-water mixture is 5 to 15 percent higher than for PDMS only. With or without water addition, DEPG absorbs more CO_2 than PDMS.

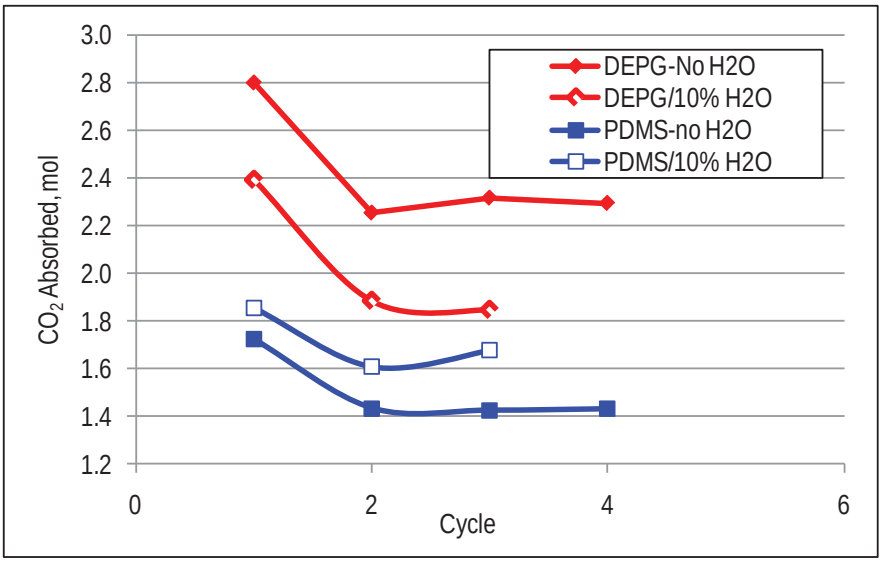

Figure 185. Effect of Water Addition to DEPG and PDMS on CO_2 Absorption

4.6.2.2 Glycerol Triacetate Solvent

NCCC researchers investigated CO_2 capture characteristics of the CO_2 physical solvent glycerol triacetate (GTA), first using bottled gases, and then with syngas during R06. The R06 testing was completed to confirm the initial CO_2 capture results and to evaluate the absorption and regeneration characteristics with H_2S. The GTA solvent was compared to DEPG and PDMS.

Absorption tests with syngas at 160 psig and 104°F were run until the GTA was saturated with both CO_2 and H_2S. Reducing the pressure to atmospheric (flash regeneration) freed almost all the CO_2 and about half of the H_2S. The solution was then heated to temperatures varying from 104 to 237°F to determine the thermal regeneration characteristics of H_2S. The effectiveness of regeneration was determined from the absorption capacity of the GTA during the subsequent runs to saturation. Heating to 212°F freed almost all the H_2S remaining following flash regeneration.

Figure 186 presents some of the CO_2 absorption results collected with the three physical solvents tested at 68°F. In the absence of water, CO_2 capture efficiency with GTA was similar to that with DEPG, and both were superior to capture with PDMS. When 10 percent water was added to the solvents, the performances of GTA and PDMS was unaffected, but that of DEPG deteriorated. Water is immiscible with GTA and PDMS but is soluble in DEPG, and this may account for the difference in performance. System analysis is required to determine if this difference offers any economic advantage.

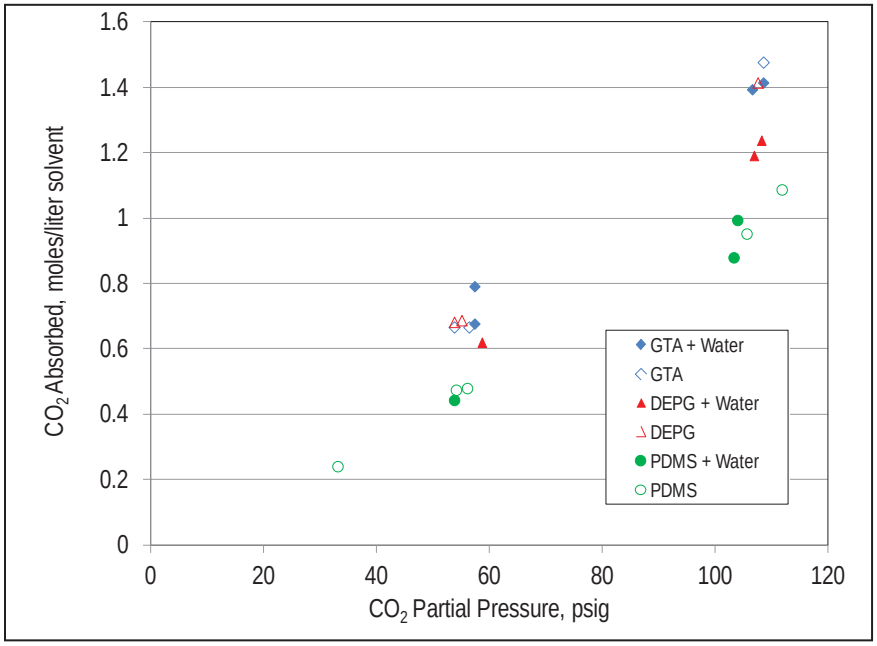

Figure 186. Absorption of CO_2 with and without Water Addition for Three Solvents

4.6.2.3 Alkylimidazole Solvents from the University of Alabama Solvent

The Bara Research group of the University of Alabama (UA) has been researching the use of alkylimidazoles, a group of low volatility and low viscosity liquids, as physical solvents for economical CO_2 separation from processes like IGCC. The NCCC conducted a series of tests on

two solvents, 1-methylimidazole (MEI) and 1,2-dimethylimadizole (DMI), provided by UA to measure CO_2 and H_2S absorption in the SCU batch reactor. These tests included bottled gas mixtures of nitrogen and CO_2 and syngas generated during runs R09 and R10.

Figure 187 plots the absorption of CO_2 from syngas as a function of time at 150 psig for the two UA solvents. The CO_2 in the syngas was supplemented with bottled CO_2 to achieve a partial pressure of about 50 psi. CO_2 was rapidly absorbed, and complete saturation with CO_2 was observed after 10 to 20 minutes. Three curves are shown in Figure 187 that represent used MEI, used MEI plus 20 percent DMI, and fresh MEI plus 20 percent DMI. Fresh solvent did appear to have slightly higher CO_2 capacity than used solvent, but this difference disappeared after a single test.

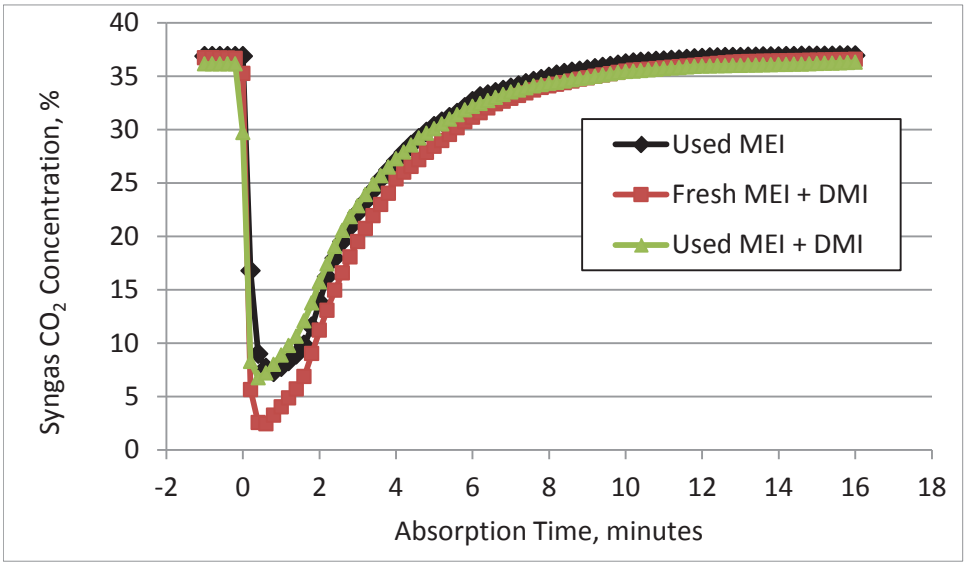

Figure 187. CO_2 Absorption versus Time for UA Solvents

The total CO_2 capacity of the MEI solvent is plotted as a function of CO_2 partial pressure in Figure 188. These measurements were made with bottled gas so that higher partial pressures could be reached. Also shown are the results for the other physical solvents previously tested at the NCCC—DEPG, GTA, and PDMS. The MEI fell in the range of the other solvents.

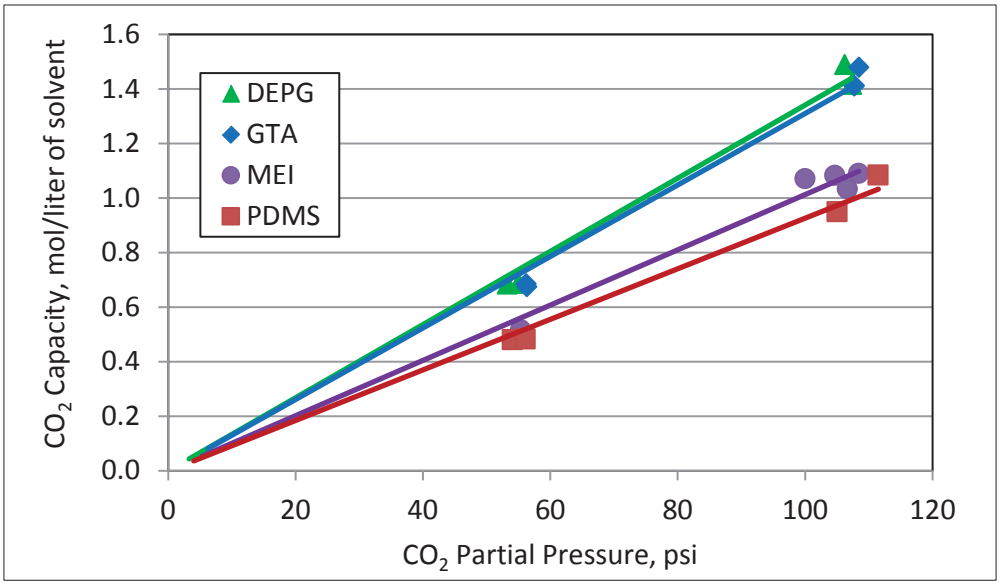

Figure 188. CO_2 Capacity of UA Solvent and Other Physical Solvents

Figure 189 compares the CO_2 capacity measured with syngas to the bottled gas data from the previous figure. Data are shown for 100 percent MEI, for MEI with 10 percent water addition, and with a mixture of 20 percent DMI in MEI. All of the syngas data appeared to be slightly better than the bottled gas curve, but the difference was not significant. For the case with water addition to the MEI, only the quantity of the MEI was used for calculating the amount of solvent. For the mixture of the two solvents, the total amount of both was used. The water diluted the MEI, but did not interfere with CO_2 absorption by the remaining MEI, as some solvent water mixtures have. Addition of 20 percent DMI did not change the CO_2 capacity of the mixture.

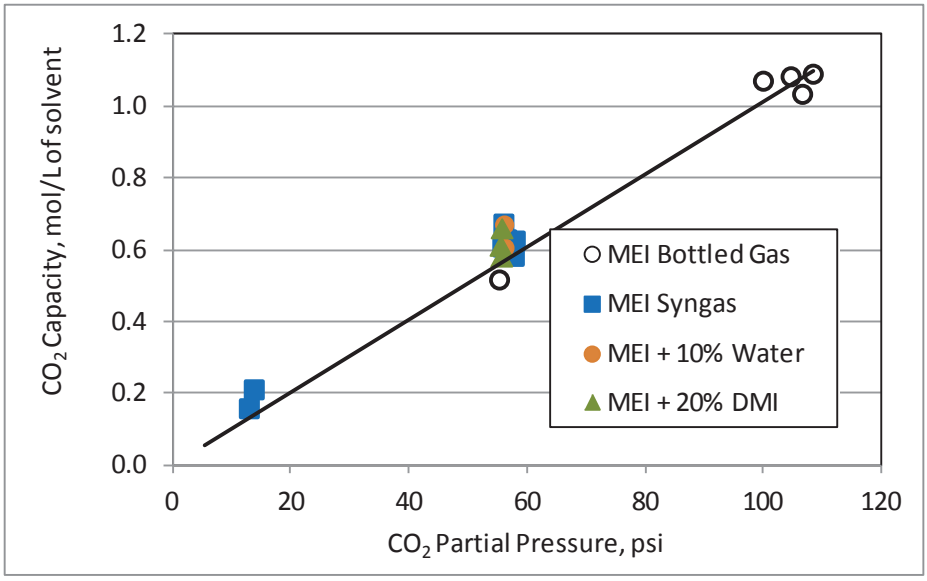

Figure 189. Comparison of Syngas and Bottled Gas Data for UA Solvent

When operating with syngas, the UA solvent also removed H_2S. The fresh undiluted solvent was saturated with CO_2 after about 20 minutes but this did not affect H_2S absorption until after

70 minutes when it too approached saturation. Flash regeneration released all the CO_2 from the sample but was not very effective at removing H_2S. This was indicated by the reduced H_2S absorption achieved in the second run, which reached saturation after 15 minutes. These results suggest that the H_2S reacts chemically and irreversibly with the solvent. The solvent is 99 percent pure, and the reaction may involve the contaminants present.

Variations of the flash technique were tried to improve the H_2S release. For the standard flash regeneration (see Figure 190) the saturated solution was slowly depressurized while being stirred and maintained at absorption temperature. One variant was to release the pressure more rapidly and another was to bubble nitrogen through the depressurized solvent. The only improvement noted was when a regenerated solution was used following a month of storage, but the improvement was not marked.

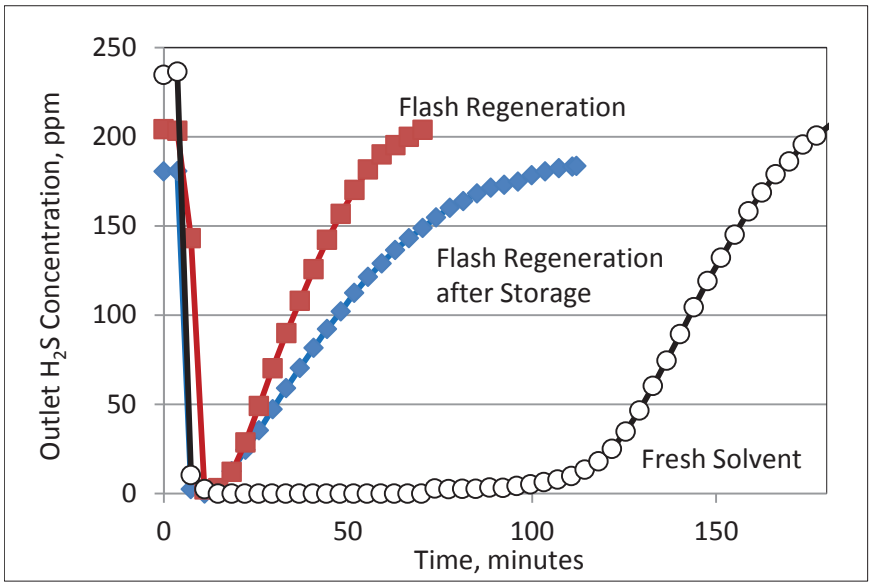

Figure 190. H_2S Concentration of UA Solvents during Regeneration

4.6.2.4 Hybrid Siloxane Solvent

Testing of the hybrid siloxane physical solvent supplied by NETL was conducted in the SCU batch reactor using bottled gases and then with syngas during run R11. The capacity of the solvent was determined at 70°F with 35 percent CO_2 in nitrogen and 165 and 315 psia (CO_2 partial pressure of 50 and 100 psi). The data are plotted in Figure 191 along with data at 70°F for DEPG and PDMS collected in previous test runs. For HSX, the two high points at about 100 psi were measured after the regenerated solvent sat overnight, while the lower one was run immediately after regeneration. This may indicate a slow release of CO_2 similar to that found when testing the University of Alabama solvent.

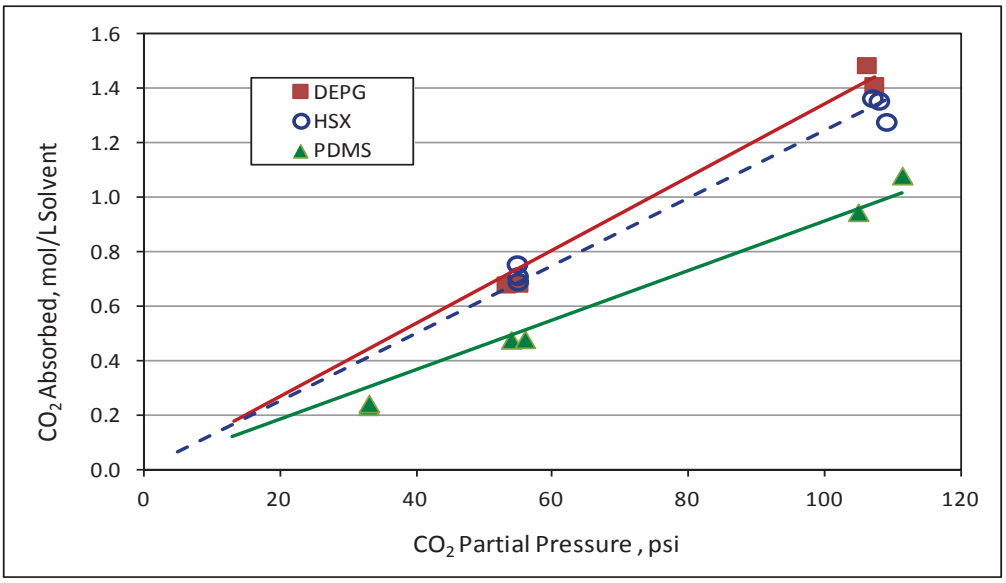

Figure 191. Absorption of CO_2 for Hybrid Siloxane, DEPG, and PDMS Solvents

Operation with the solvent resulted in the formation of a very fine aerosol during absorption, which has not been the case for other solvents tested. Liquid collected in the exit piping indicated that measurable amounts of solvent were carried over during absorption. To desorb the solvent, the pressure was reduced with the stirrer operating. The solvent was then poured into a container to determine solvent losses during the absorption/regeneration process. From the pouring, about one inch of foam was generated on the surface of the solvent, indicating that additional CO_2 was being released.

4.7 Slipstream Unit with Dispersed Bubble Reactor

A slipstream unit was designed to test pre-combustion CO_2 capture with various solvents. The test unit, shown in Figure 192, consists of a Dispersed Bubble Reactor (DBR) with an absorber and a recycle loop (including the standpipe and riser), as well as a regenerator and associated equipment. The DBR is a continuous gas-liquid contacting device designed for high mass transfer rates and CO_2 absorption. Support equipment for the DBR includes a solvent storage area and gas analysis building. Design, procurement, installation, and commissioning were completed in 2009.

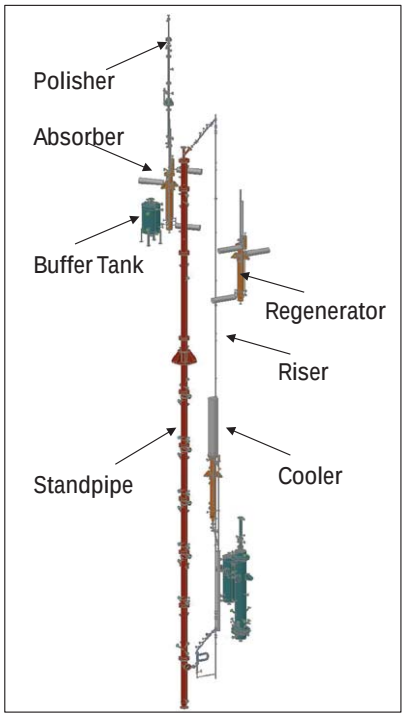

Figure 192. Schematic of Pre-Combustion Slipstream Unit

Table 64 lists the DBR operating conditions. During gasification operation, shifted syngas can be used for capture tests at up to 250 psig. During outages, the DBR can operate with bottle gases (i.e., nitrogen and CO_2) at up to 500 psig absorption pressure to simulate commercially applicable conditions.

Table 64. DBR Operating Parameters

Operating Parameter	Value
Temperature, °F	100 to 135
Pressure (on-line operation), psig	250
Pressure (off-line operation), psig	500
Inlet Gas Flow Rate (on-line operation), lb/hr	250
Inlet Gas Flow Rate (off-line operation), lb/hr	500

The DBR was designed primarily for operation with aqueous ammonia solution. Tests can also be conducted with methyldiethanolamine (MDEA) and dimethyl ether of polyethylene glycol (DEPG) solvents to compare solvent performances, as a large set of commercial operational experience and data are available with these solvents. Depending upon the type of solution or solvent used, the regenerator can operate at low pressure (less than 30 psig with MDEA and DEPG) or at high pressure (500 to 600 psig with aqueous ammonia solution).

DBR Commissioning

The DBR commissioning with water and nitrogen was completed in mid-2009. The DBR operated at pressures between 150 and 450 psig, flow rates ranging from 100 to 800 lb/hr, gas velocities from 3 to 35 ft/s, and water circulation rates up to 6,500 lb/hr. Operation during initial

commissioning demonstrated that the pressure drop across the standpipe cyclone was higher than desired, which resulted in a lower than desired circulation rate. Subsequently, the cyclone inlet insert was removed, and the inlet dimensions were enlarged. Testing of these modifications showed that they were successful in lowering the pressure drop without negatively affecting collection efficiency.

Data from the DBR commissioning tests were analyzed in relation to the pressure drop, gas hold-up, liquid circulation rates, and flow regimes. All these parameters are closely related to the mass transfer and therefore the rate of CO_2 absorption. The brief commissioning tests of the DBR proved the fundamental design concept of the inherent capacity of the gas stream (in a circulating continuous phase environment) to produce a dispersed bubble flow regime leading to a large interface area for gas-liquid contact.

Several parametric tests were performed during the hydrodynamic tests of the DBR absorber. For example, the superficial gas velocity in the riser was varied to evaluate the effect on the measured pressure drop in the riser, calculated frictional pressure drop in the riser and consequently the calculated riser bulk density. As shown in Figure 193, the overall pressure drop in the riser decreased and the frictional pressure drop increased as the superficial gas velocity in the riser was increased. This was consistent with the pressure balance calculations for a circulating system with a fixed liquid level in the standpipe. The resulting decrease in riser density was due to the increase in frictional pressure drop. Tests showed that the riser density remained within an acceptable range to provide sufficient reaction opportunity over the gas flow rate range. The gas hold up rate was calculated for each operating point and was also found to be within the expected values.

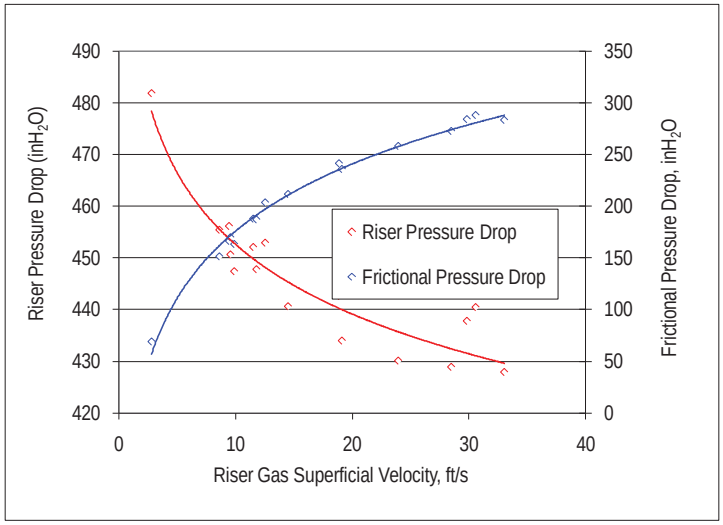

Figure 193. Pressure Drops versus Riser Gas Superficial Velocity during DBR Commissioning

The liquid circulation rate was directly measured by a Coriolis-type mass flow meter. During the initial test, the maximum liquid circulation was about half the predicted liquid circulation rate due to the higher frictional pressure drop in the riser and higher pressure drop in the standpipe cyclone. While the modifications were successful in lowering the pressure drop in the standpipe cyclone and resulted in a modest increase in circulation rate, the maximum liquid circulation rate remained below the original predicted value.

The circulation rate was lower than expected at the higher superficial gas velocities tested. At design conditions, a liquid-to-gas ratio of 20 was reached. At high gas rates, the liquid-to-gas ratio was 3.5, still sufficient for an ammonia-based system but lower than expected due to high frictional pressure drop in the riser. If needed, the circulation rate could be further increased by enlarging the riser diameter or modifying the cyclone. Further testing would be required to confirm that the gas-liquid contact would achieve sufficient mass transfer. With the commissioning data, the gas-liquid transfer area was largely inferred from correlations.

4.8 Pre-Combustion CO_2 Capture Facility Modifications

In addition to installation of technology developer equipment for testing, significant modifications to the SCU were completed to increase capacity and accommodate new testing. Additions made include:

- 1,500 lb/hr syngas supply—An upgrade replacing the 200 lb/hr syngas supply line
- Equipment configuration for independent process operation—Modifications to allow series, parallel, or bypassed operation of all reactor vessels
- Superheated steam header—Addition to support water-gas shift catalyst testing
- 50 lb/hr syngas cooling and cleanup system—An upgraded system to support low-temperature polymeric CO_2/hydrogen membrane testing
- Hydrogen enrichment capability—Establishment of a new syngas supply line with input of bottled hydrogen for high-temperature hydrogen separation membranes testing
- New instrumentation—Additions of flow control, temperature and flow measurements, and pressure control capabilities for improved process control and data quality
- New gas analyzers—Additions of gas analysis equipment for enhanced data acquisition such as new gas chromatographs and moisture probes
- Modifications for hazardous area classification—Upgrades involving various aspects of SCU operation, such as overall layout and instrumentation housing, to ensure safe operation in compliance with OSHA standards for hazardous areas
- Gas analyzer building, control room, and motor control center—Major additions of upgraded buildings with higher capacity
- Syngas cleanup system—Installation of a system with 1,000 lb/hr syngas capacity providing pre-treatments for sulfur and hydrocarbon removal, WGS, and COS hydrolysis
- Hydrogen and CO bottle gas supply system with firewall—Site modifications to accommodate a tube trailer to supply larger amounts of hydrogen, with additional fixed fire protection equipment and a code compliant fire barrier system

Syngas and utilities were installed to support pilot-scale testing at up to 1,000 lb/hr. This new test area is currently occupied by the OSU SCL process.

5.0 TECHNOLOGY ASSESSMENT

5.1 Technology Screening

In collaboration with the DOE, the NCCC developed a technology screening process for identifying technologies to be included in the NCCC test plan. To effectively utilize the NCCC resources and bring the most promising technologies to the market as quickly as possible, the technology screening process identifies superior candidate technologies based on appropriate criteria. In order to avoid overlooking the potential of emerging technologies that are still early in development, the screening process was separated into two pathways: small (lab/bench) scale and large (pilot/engineering) scale. This ensures that the final technology selections form a balanced portfolio that promotes the advancement for both near-term and long-term candidate technologies.

The NCCC maintains a candidate technologies inventory that includes all major developers of relevant technology. The inventory is periodically updated based on emerging data and progress made by each technology developer. Information sources for these updates include DOE review meetings, conferences, and direct communications with vendors and technology developers.

Candidate technologies are evaluated using both quantitative screening criteria (shown Table 65) and qualitative screening criteria related to shared DOE and NCCC objectives and budget considerations. The factors influencing the objectives include cost reduction, fuel flexibility, short-term commercial implementation, and long-term potential. Budget considerations affecting qualitative screening criteria include project funding level, cost of testing, cost of developing, and ease of accommodation.

Table 65. Quantitative Technology Screening Criteria

Ranking Category and Scoring Criteria	Weight Factor
Projected Benefits • Impact on total cost of electricity • Impact on energy consumption • Impact on capital cost • Impact on power plant efficiency • CO_2 emission reduction	60%
Technology Strength • Scientific soundness of concept • Current status of the technology • Simplicity and robustness • Commercialization • Environmental soundness	30%
Organizational Strength • Intellectual property/license of the technology • Capability of further development • Technical and management team	10%

The screening process involves:

- Selection of a technology developer from the candidate technology inventory
- Evaluation of the selected technology developer with due diligence using criteria agreed upon by the DOE/NCCC screening teams
- Establishment of non-disclosure agreements with the selected developer to receive detailed information
- Completion of a technology evaluation report by the NCCC
- Recommendation by the DOE and NCCC screening teams
- Finalization of legal and engineering documentation for the project

5.2 Evaluation of Transport Oxy-combustion Technology

During the reporting period, researchers at the NCCC began investigating the feasibility of TROC technology—coal-fired power production using the Transport Reactor as a pressurized, oxygen-blown fluid bed combustor. Other currently supported oxy-combustion concepts for both pulverized coal boilers and circulating fluidized bed combustors use oxygen mixed with recycled CO_2 as the oxidant for coal combustion. In both concepts, operations are at near atmospheric pressure, and CO_2 from downstream of the combustion system is used to moderate the temperature of the highly exothermic oxy-combustion process. The TROC process, by contrast, uses recycle solids to moderate the combustion temperature and a fluidized-bed solids cooler to maintain the recycle solids temperature. Also, it operates at pressure and has inherently low NOx and SOx emissions without downstream controls.

Following initial screening and detailed studies completed in 2010, two further assessments of the TROC technology were completed in 2011. One study was an update for a previously conducted screening study in 2009 for a 500-MW greenfield TROC as a technology for capturing CO_2 from coal based power plants. This study, "Planning Study of a Greenfield Transport Oxy-Combustion System," updated the greenfield TROC evaluation with knowledge gained in 2010 during a subsequent repowering study. This updated study also compared the economics of the revised TROC greenfield technology to other coal based options for CO_2 capture. The study results indicated that the TROC greenfield case had the lowest levelized cost of electricity of the options considered.

Through past efforts, the NCCC has evaluated TROC technology for both greenfield and repowering applications, comparing TROC with other coal-based technologies for CO_2 capture. A second evaluation, "Economic Comparison of Transport Oxy-Combustion and Natural Gas Combined Cycle with Post Combustion CO2 Capture," extended these past efforts by comparing the economics of TROC to a natural gas combined cycle with CO_2 capture. The results showed that TROC offers a viable economic alternative at capacity factors above 40 percent and an economic benefit at capacity factors above 70 percent.

5.3 Evaluation of Solvent-Based Post-Combustion CO_2 Capture

To assess the progress made in solvent development, NCCC completed an engineering and economic evaluation of PCC plant designs. The five cases studied, listed in Table 66, include a base case with no capture, two cases of capture with MEA, and two cases using the solvent tested at the NCCC with the lowest heat of regeneration (referred to as the advanced solvent). MEA was used as the baseline solvent in keeping with previous work by the DOE; DOE used MEA as the baseline solvent to establish cost and performance estimates against which improvements in post-combustion CO_2 capture technologies could be assessed (Publication DOE/2010/1397, *Cost and Performance Baseline for Fossil Energy Plants*).

Table 66. Five Cases Evaluated in PCC Study

	Solvent	CO_2 Capture, %	CO_2 Emitted, gross basis	
			kg/MWh	lb/MWh
Case 1 (no capture)	-	-	752	1,660
Case 2	MEA	90	86	190
Case 3	MEA	45	453	1,000
Case 4	Advanced	90	86	190
Case 5 (projected)	Advanced	36	500	1,100

5.3.1 Technology Description

The base case for the study (Case 1) is a new-build, pulverized coal plant without CO_2 capture. The unit is designed to meet emissions limits set by the US EPA's New Source Performance Standards and Mercury and Air Toxics Standards. The capital costs are those for an nth-of-kind plant representative of a mature technology and so will be appreciably lower than the first-of-a-kind plants entering service today. The primary design parameters for the plant are summarized below:

- 936-MW gross supercritical, single-reheat coal-fired boiler
- 3,715 psia/1,050°F/1,070°F tandem-compound condensing steam turbine
- 1.1 psia condenser pressure, water cooled via mechanical draft wet cooling tower
- SCR and wet FGD
- Spray dryer absorber (SDA)
- Fabric filter
- Typical southeast USA site
- Costs are in 2012 dollars
- Illinois Basin bituminous coal with 2.5 percent sulfur

As discussed previously in this report, testing of amine-based solvents at the PC4 has resulted in higher than expected solvent carryover from the wash tower, arising from the carryover of fine

droplets whose formation is promoted by the presence of SO_3 in the flue gas. This is formed in the boiler and also in the SCR unit, and levels as high as 5 ppmv have been measured at the inlet to the CO_2 absorber. The combination of an SDA upstream of the wet FGD is expected to lower the SO_3 to below 0.1 ppmv and result in amine carryover falling to acceptable levels.

Four PCC plant design cases were evaluated.

- Case 2 is designed for 90 percent CO_2 capture using MEA as the solvent and consists of two 50-percent CO_2 capture trains treating the complete flue gas stream leaving the power plant.
- Case 3 is designed to achieve CO_2 emissions of 1,000 lb/MWh, per the EPA's March 2012 proposed limit for new plants. One train with 90 percent CO_2 capture is used, with the excess flue gas being sent directly to the stack.
- Case 4 is similar to Case 2, but an advanced solvent is used for CO_2 capture.
- Case 5 is a projection based on the detailed results of the other four cases. As there was insufficient time to complete a detailed study for the EPA's September 2013 proposed limit of 1,100 lb/MWh for new plants, the information determined for the first three cases was adjusted to project thermal and economic performance to meet the new limit using the advanced solvent. As for Case 3, one train with 90-percent CO_2 capture is used.

The primary design parameters for the four capture cases are summarized below:

- A direct contact cooler using dilute caustic soda is used to cool the flue gas, reduce moisture content, and remove all residual SO_2 before entering the absorber. SO_2 reacts with amines forming heat stable salts that cannot be regenerated and so increase solvent make up rates.
- The captured CO_2 is dried and compressed to 2,215 psia. Costs for transportation and storage are not included.
- As the regeneration energy is different for each Case, the steam extraction flow rate for each Case is also different. For each case, the low pressure turbine stages, generator, and condenser are sized for the reduced steam flow. This limits capital cost but means that if steam extraction is reduced, the excess steam cannot be passed to the turbine and boiler load would have to be reduced. This would not be the case for a retrofit application.

Other capture plant features selected (for which alternative options are included in other design studies) are as follows:

- The flue gas fan is placed between the direct contact cooler and the absorber. This location is favored by Fluor who claims it is the location that results in the lowest energy consumption. Other technology suppliers place the fan in alternative locations. The respective merits of these alternative locations need to be evaluated.
    - MHI and Linde place the blower after the absorber wash tower. This may be driven by the need to discharge the CO_2-depleted flue gas to a dry stack.

    - Other developers, including HTC, Hitachi, and Mongstad, place the blower ahead of the direct contact cooler to lower the temperature of the flue gas entering the absorber and improve capture efficiency. This approach is also used on the PSTU.

- The steam for solvent regeneration is extracted from the IP turbine discharge at 162 psia and 878°F. This temperature is too high for direct use in the reboiler and would promote solvent degradation. To recoup some of the low-pressure turbine power loss the steam is expanded through a back-pressure turbine with discharge conditions of around 60 psia and 630°F. Attemperation with boiler feed water is used to achieve the required reboiler steam inlet temperature of 290°F.
    - An alternative approach would be to modify the turbine design to achieve the required pressure and temperature in the IP turbine discharge stream. This may be a more efficient approach given the low stage efficiency of back-pressure turbines. The feasibility of this approach, and the impact on cost and operational flexibility need to be evaluated.
- Two heat integration methods are included in the design to reduce reboiler steam demand.
    - Heat is recovered from the hot-lean solvent in the cross-flow heat exchanger and transferred to the cool-rich solvent, increasing the temperature of the solvent entering the top of the stripper.
    - Heat is transferred indirectly from the hot-lean solvent to solvent drawn from the base of the upper stripping stage and returned to the top of the lower stage. The heat transferred in this loop reduces the heat transferred in the cross-flow exchanger, and by reducing the temperature of the solvent entering the top of the stripper the heat recovered from the overhead condenser duty is reduced.
    - Although not included in this study, for their designs Fluor compresses steam flashed from the hot lean amine and introduces it at the foot of the stripper. It is reported that usage depends on "..relative costs of steam and power…", implying that optimization is for the capture plant only, and not the capture plant integrated with the power plant.
    - This approach also reduces the energy in the hot lean solvent stream passing to the cross flow exchanger and so reduces the temperature of the hot rich solvent passing to the regenerator. In turn, this reduces the heat recovered from the overhead condenser. These interactions illustrate that improvements are not additive and that rigorous modeling is necessary to identify the most cost effective combination of integration measures.
- The condensate from the reboiler contains appreciable energy that can be reused to lower steam demand in the capture and power plants. For this study, heat from the condensate is transferred to the deaerator to reduce steam extraction to the LP feed-water heaters and so increase power from the LP turbine stage. Alternative approaches are possible that need to be evaluated.

- The reboiler condensate could also be flashed similarly to the hot lean solvent, and the two streams combined ahead of vapor compression. This approach would increase boiler feed water make up and this would need to be incorporated in any economic assessment of the approach.

As discussed above, there are a number of alternatives to the flow sheet used for this study. To assist with optimizing the flow sheet and heat integration of the PC and PCC plants, flexible process models are required to determine the most cost effective measures. The NCCC has supported DOE's Carbon Capture Simulation Initiative in its modeling activities by providing steady state and dynamic data collected with MEA.

In over 100 years, without consideration of CO_2 capture, steam cycles have advanced from an efficiency of below 20 percent to over 40 percent with the additional of reheat and progressively higher steam operating temperature and pressure. If CO_2 capture had been a consideration over the 100 years, the power cycle would likely have evolved differently. For example, rather than steam with expansion through a turbine, the working fluid may be CO_2 using a closed-loop Brayton cycle. Study is required to determine the most cost-effective design approach for a power cycle meeting the dual demands of generating power and capturing CO_2.

5.3.2 Results

The capital and operating cost data (including manning levels) used in this study were developed from proprietary Southern Company databases, Southern Company front-end engineering design studies, unit costs for similar equipment, and consulting engineering company cost estimates. Where necessary, equipment costs were scaled using industry-accepted procedures.

The capital costs were those for an n^{th}-of-a-kind plant representative of a mature technology. The error band on the costs is ±30 percent based on the level of engineering work completed. This corresponds to an Association for the Advancement of Cost Engineering International Class 4 estimate with only up to 15 percent of the project definition complete. Since the majority of the equipment is common to all cases, comparative costs are more accurate than the projected error band and are expected to produce a reliable indication of the relative merits of each case.

The performance of the PC plants with PCC using MEA was based on an Aspen Plus simulation developed by NETL. The projected PC plant performance was checked against Southern Company plant data and manufacturer's design data. Projected MEA PCC plant performance was checked against PSTU test data collected at the NCCC.

As physical property data for the advanced solvent were not provided by the developer and are not incorporated in the Aspen database, the simulation approach for MEA could not be used. Instead, performance data collected during testing of the solvent on the PSTU were used. The information included the optimum liquid-to-gas ratio (L/G =1.6) for 90 percent CO_2 capture and the associated heat of regeneration (2.17 GJ/tonne [935 Btu/lb] without heat integration). Mass balances for Case 4 were completed in an Excel spreadsheet and the flow rates were used to adjust the size of the equipment determined more rigorously for Case 2. As discussed earlier, Case 5 was not modeled, and the results presented are based on adjusting data determined more rigorously for the other four cases.

The cost of CO_2 capture is calculated as the difference in cost of electricity for the plant with CO_2 capture and the cost of electricity for the reference plant without CO_2 capture divided by the amount of CO_2 captured per unit of net power.

The following points for 90 percent CO_2 capture were made, illustrating the benefits of the advanced solvent:

- Relative to Case 1, the cost of electricity (COE) with the advanced solvent increased by 50.8 percent and 72 percent with MEA. This 12.2 percent difference stems primarily from the 10.8 percent increase in net output with the advanced solvent (711.1 MW) compared to that with MEA (641.6 MW).
- Relative to Case 1, water makeup with the advanced solvent increased by 32.2 percent and 65.7 percent with MEA. This 20.2 percent reduction stems primarily from the lower heat of reaction of the advanced solvent and the lower solvent circulation rates (resulting from high CO_2 loading) resulting in reduced cooling duty in the absorber (intercoolers) and for the lean solvent trim cooler (downstream of the cross-flow heat exchanger).
- The cost of CO_2 capture with the advanced solvent was 21.8 percent lower than with MEA ($45.3/tonne compared to $57.9/ tonne [$41.1/ton and $52.6/ton], respectively).

Table 67 (capital costs) and Table 68 (thermal and economic performance) present information developed by the study.

Table 67. Capital Costs Breakdown for PCC Study

Costs	Case 1	Case 2	Case 3	Case 4	Case 5
Indirects	291	434	367	410	338
Coal Handling	33	33	33	33	33
Feed Water & Misc. Balance of Plant	88	88	88	88	88
Boiler & Accessories	455	455	455	455	455
Flue Gas Cleanup	275	275	275	275	275
CO_2 Removal & Processing	--	500	266	404	161
Steam Turbine & Piping	168	164	168	168	168
Cooling Water	67	85	76	75	70
Electrical Dist. & Switchyard	60	106	82	106	78
Instrumentation & Controls	30	45	38	45	36
Site, General	69	102	86	102	82
Buildings & Structures	77	114	97	115	92
Freight, Tax, Contingency, and Other	418	620	524	587	485
Total Plant Cost, $million	2,030	3,020	2,552	2,861	2,361

Table 68. Summary of Thermal and Economic Information from the Five Study Cases

	Case 1	Case 2	Case 3	Case 4	Case 5
CO_2 emissions, lb/MWh gross	1,667	193.8	983.5	179.7	1,100
CO_2 captured, tons/hr	-	702.5	351.0	702.5	280.5
Capture efficiency, %	-	90.0	45.0	90.0	35.9
Gross output, MW	936.0	804.8	873.4	868.0	909.1
Net output, MW	856.5	641.6	751.7	711.1	796.5
Net efficiency (HHV), %	37.61	28.17	33.01	31.22	34.97
Net heat rate, Btu/kWh	9,072	12,110	10,340	10,930	9,779
Total plant cost, $million	2,030	3,020	2,552	2,861	2,361
$/kW	2,370	4,707	3,395	4,023	2,964
Fixed O&M. $/kW-yr	36.06	64.16	48.78	56.22	44.17
Variable O&M, $/MWh	4.89	9.97	7.04	9.36	6.67
Cost of electricity, $/MWh [1]					
Fuel	31.8	42.5	36.3	38.3	34.2
O&M	9.7	18.6	13.6	16.9	12.6
Capital	38.5	76.5	55.2	65.4	48.2
TOTAL	80.0	137.6	105.1	120.6	95.0
COE relative to Case 1	1	1.720	1.314	1.508	1.187
Cost of CO_2 capture, $/tonne	-	57.9	59.1	45.3	47.0
$/ton	-	52.6	53.6	41.1	42.6
CO_2 revenue, $ million/yr [2]	-	4.746	2.369	4.746	1.894
$/MWh	-	19.8	8.47	17.9	6.39
COE less CO_2 revenue, $/MWh	-	117.8	96.6	102.7	88.6
COE relative to Case 1	1	1.473	1.207	1.284	1.107
Water makeup, tons/hr	2,016	3,341	2,787	2,665	2,354

(1) 30-year book life, constant 2012 dollars, coal cost $3.50/MBtu, capacity factor 85%

(2) All CO_2 sold at $20/tonne ($18.1/ton)

5.3.3 Potential Improvements

The cost of CO_2 capture for Case 4 comes close to meeting the DOE's Clean Coal Research Program $40/tonne objective for the period 2020 – 2025. To meet this price objective, capacity factor must remain at 85 percent and capture efficiency at 90 percent. Meeting the former requirement will be a challenge if the plant has to cycle because dispatch priority is given to renewable sources, notably wind.

Ways in which the $45.3/tonne value determined by the study might be reduced are discussed below:

- Lower fuel price—A price for coal more competitive than the $3.50/MBtu used in the study might be negotiated. The value for Illinois bituminous coal currently used in EPRI's TAG™ is $2.65/MBtu and would lower the cost of CO_2 capture to $43.5/tonne ($41.1/ton).
- Net power increase—Listed below are some of the measures that might be taken to increase net power output. Some measures may be mutually exclusive, or may reduce efficacy of one another, and modeling is required to identify the most economic combination of measures. Improved modeling capability will help identify the most cost effective approaches.
    - Increase the generating efficiency of the power plant by going to higher steam conditions to lower the coal feed rate per MWh and reduce the amount of CO_2 produced per MWh.
    - Identify how to use the abundant low-grade heat available most economically. This will require a different solvent, or operating the stripper under vacuum to lower the regeneration temperature as is being considered by Akermin. Releasing the CO_2 at low pressure will increase the compression energy thereby at least partially offsetting the thermal benefits.
    - Condensing low-temperature heat recovery from the flue gas provides heat and may reduce SO_3. The heat can be used to reduce boiler feed water steam extraction and increase power generation or dry low-rank fuels and improve boiler efficiency.
    - Design the turbine to produce IP stage extraction steam closer to reboiler conditions, eliminating the back-pressure turbines. Instead of attemperation with boiler feed water, analysis may reveal a more cost effective means to cool the IP steam flow to reboiler inlet conditions.
    - Further solvent improvement: for example, GE's amino-silicone solvent (regeneration at pressure), Carbon Capture Scientific's pressurized stripper, Akermin's enzyme enhanced solvent (all to be tested at NCCC).
    - Design approaches to reduce auxiliary power demand involve: flue gas fan locations; axial flow or centrifugal fans; low pressure drop packing (to be tested by Linde at PC4); and gravity fed rather than pumped intercooler circuits (to be tested by Linde at PC4).
- Reduce capital cost—Alternative equipment designs may lower capital cost and also consume less energy.
    - Replace absorber and stripper with membrane contactors (GTI idea to be tested at NCCC).
    - Flash regeneration replacing stripper design (UT Austin idea to be tested at NCCC).

Despite meeting the $40/tonne objective for CO_2 capture, the increase in the cost of electricity is still significant at around $35/MWh or 45 percent. If the CO_2 could be sold for $20/tonne, which

DOE studies suggest as feasible, then the COE increase would be around $25/MWh or 30 percent.

Case 5, achieving the EPA CO_2 emission limit of 1,100 lb/MWh, has the lowest cost of electricity, $95/MWh, $15/MWh or 20 percent higher than for Case 1 without CO_2 capture. If the CO_2 captured could be sold for $20/tonne then the COE increase would be around $9/MWh or 10 percent.

It is emphasized again that such improvements will not be achieved by first-of-a-kind designs, but only after initial designs have been have been improved thorough manufacturing and operational improvements.

5.3.4 Summary

This study investigated four cases for a PC plant with PCC of CO_2 using two solvents, MEA and the solvent with the lowest heat of regeneration tested at the NCCC.

- For 90 percent CO_2 capture, the COE increase over a plant with no capture, is 72 percent for MEA, which is in keeping with estimates from other studies. The COE increase for the advanced solvent is 51 percent, a significant improvement over MEA but nevertheless still high.
- Ways in which the COE increase might be reduced further are discussed and include improvements to solvents and process equipment, many of which are to be tested at the NCCC.
- Meeting the EPA's proposed CO_2 limit of 1,100 lb/MWh (36 percent capture) results in a COE increase of around 20 percent, and this too can be reduced by improvements to solvents and process equipment.
- The COE increases can be reduced if the CO_2 could be sold to produce a revenue stream. For a representative price of $20/tonne, the COE increase would be reduced to 28 percent and 11 percent, respectively. With solvent and equipment improvements, these values could be reduced further.
- A coal plant with CCS meeting the EPA's proposed CO_2 limit could be competitive provided the CO_2 can be sold and further technological improvements are made. This will only be possible for nth-of-a-kind units once the technology is refined through design, construction, and operational experience.
- Both advanced solvent plant designs, 90 percent and 36 percent capture, come close to meeting the DOE's Clean Coal Research Program $40/tonne objective for the period 2020 – 2025 and could be met with some further improvements to solvents and equipment items.

6.0 CONCLUSIONS AND LESSONS LEARNED

6.1 Post-Combustion CO_2 Capture

6.1.1 PC4 Construction

Design and site preparation for the PC4 began in late 2008, and final construction activities were completed in early 2011. Commissioning of the PSTU was accomplished in March 2011, and testing by technology developers began in mid-year.

Plant upgrades completed in 2014 increased the total PC4 capacity from 12,000 lb/hr of flue gas to about 30,000 lb/hr, allowing simultaneous operation of pilot units. Modifications were also incorporated to simulate natural gas flue gas operations, under which the PC4 operated for 2,500 hours. The NCCC also added the Slipstream Solvent Test Unit, which will allow testing of solvents, such as those in early stages of development, available only in amounts smaller than the 4,000 gallons required for the PSTU.

6.1.2 PSTU Gas and Liquid Analysis

The NCCC developed an impinger train for analysis of amine and degradation products in the flue gas exiting the PSTU absorber. The sample train processes gas that is extracted isokinetically to obtain a representative sample. An ice bath removes both droplets and condensable liquids in an EPA Modified Method 5 (MM5) sample system.

Since startup of the PSTU in 2011, several analyzer changes have been made.

- The performance of a zirconia probe used for oxygen measurements deteriorated more rapidly than expected and had to be replaced more frequently than planned. This deterioration occurred because of the impact with fine water droplets carried over from the direct-contact cooler. Thus, the zirconia probe was replaced with a paramagnetic probe, which performed reliably without replacement at the absorber outlet.
- Initially, capacitance probes were installed to determine the moisture content of the absorber inlet and outlet flue gas streams and the regenerator CO_2 outlet stream. The data collected were inaccurate, so the probes were removed from service. As the gas streams at these three locations are saturated, the moisture content can be calculated using temperature, pressure, and the molecular weight of the gas.
- An FTIR was initially installed at the absorber outlet to monitor ammonia, NO, NO_2, moisture, and amine content of the flue gas. Samples were taken from the wash tower and fed through a 170-foot long heated sample line to the analyzer unit in the on-site laboratory located on the ground floor. The exit flue gas contained a significant number of water droplets that rapidly destroyed the sensor, which operated at around 400ºF (formation of the droplets is promoted by sulfur trioxide (SO_3) present in the flue gas from Plant Gaston). Measures taken to eliminate the droplets were: extracting the sample from the duct using a heated probe and operating the heated line at the maximum temperature to evaporate them; and installing a demister at the inlet to the heated line.

These measures were not successful in protecting the sensor, and so the FTIR was removed from service.

- NO_2 is a precursor in the formation of nitrosamines and also reacts with the amine solvent. To support the investigation of their H3-1 solvent, Hitachi requested that NO_2 meters be installed at the inlet to the absorber. The initial instrument, installed in March 2012, was an NDIR instrument with a catalytic converter. The instrument measures NO, but not NO_2, for a fixed time interval before the sample stream is redirected over the catalyst for a similar time interval to convert the NO_2 to NO and measure the total NOx. The NO_2 is the difference between the two measurements, but as NO is around 95 percent of the total NOx, the calculated value of NO_2 is subject to error. As NO_2 was the most important measurement, NDIR instruments to measure NO and NO_2 specifically were installed at the beginning of 2014.

Liquid sampling is performed using an auto-titration system to determine the solvent concentration and CO_2 loading. The auto-titrator takes a sample automatically every 30 minutes at four locations. Auto-titration analyses of the solvent CO_2 loading are crosschecked using periodic laboratory titrations, carbon mole balance calculations, and the total CO_2 analysis procedure. This technique was developed at the University of Texas and refined at the NCCC, and has been shown to give accurate measurements of the CO_2 loading in various known standard solutions.

6.1.3 MEA Baseline Testing

The process data collected were carefully scrutinized to identify sources of error. No serious flaws were discovered, but a few corrections were made to calculation procedures, resulting in mass balance closures very close to 100 percent for the absorber. The understanding developed and the resolution of data collection issues raises confidence in the ability to provide developers with reliable information when testing their solvents. Achieving good heat balances was complicated by the absence of reliable data for solvent specific heat, which is a function of temperature, MEA concentration, and CO_2 loading.

MEA Carryover

MEA carryover is thought to occur because of the presence of SO_3 aerosol in the flue gas. The aerosol acts as a nucleation site for the formation of droplets into which the MEA diffuses. Many of the droplets are too small to be collected efficiently in the wash tower and thus escape with the CO_2-depleted flue gas. The baseline test data indicated that MEA carryover:

- Increased with SO_3 level—In the moist environment of the absorber, the SO_3 aerosol forms a nucleus for droplet formation, the liquid composition being determined by local water-MEA concentrations. Stack measurements performed by others indicate that 4 ppm of H_2S in flue gas corresponds to about 10^6 particles/cm^3, the majority being 0.1 microns or smaller, so there are abundant sites for droplet formation.
- Decreased with increasing solvent temperature—It is hypothesized that the higher the temperature, the larger the droplets formed and so the easier they are removed in the wash tower.

- Decreased with the upper absorber bed inactive—It is hypothesized that the liquid present on the surface of the structured packing in the upper bed intercepts some of the smaller droplets that would have otherwise passed through the wash tower.
- Decreased with wash water MEA content—The lower the MEA content of the wash water, the lower the equilibrium MEA vapor content of the gas stream.

Total Amine and Degradation Product Carryover

- Almost all the MEA carryover from the plant occurred downstream of the wash tower. As discussed previously, this is because of the SO_3 present in the flue gas. There is essentially no SO_3 present in the regenerator, and MEA carryover was almost negligible.
- Over 97 percent of ammonia produced was carried over from the wash tower, suggesting that oxidation degradation was more pronounced than thermal degradation. Adding an oxidation inhibitor would reduce solvent degradation and so lower ammonia release.
- As ammonia is a degradation by-product, the other degradation products may also be promoted by oxidation. The majority of the formaldehyde and acetaldehyde was carried over from the regenerator, likely due to their lower volatility compared to ammonia.
- Only two nitrosamines were detected: nitrosodimethylamine, which was below 1 ppb, and nitrosodiethanolamine, at about 1 ppb. Neither was detected in the liquid samples.

Metals Accumulation

- The fresh MEA contained about 44 ppbw of RCRA metals (mainly selenium) but the used MEA contained 47,250 ppbw (mainly chromium).
- Chromium was measured at 45,090 ppbw, well in excess of the 5,000 ppbw limit. The majority of the chromium originates from corrosion of the 316L stainless steel. The chromium would be significantly reduced by fabricating the plant from carbon steel, which is standard industrial practice.
- Selenium was measured at 1,950 ppbw, almost twice the 1,000 ppbw limit. The selenium originates mainly from the flue gas. Speciation testing showed that 50 percent of the selenium was selenide, 25 percent selenite, and 25 percent elemental selenium. Selenate, the most toxic form of selenium, was below the detection limit.
- The other metals present above the lower detection limits (LDLs), arsenic (219 ppbw) and barium (265 ppbw) both originate mainly from the flue gas. The variability seen in LDL values is normal, and varies between chemicals and the medium in which they are present.
- For arsenic, 17 percent was present as arsenite and 83 percent as arsenate. Although both are toxic, the former is the most toxic.
- The flue gas content of RCRA metals is very low, but the high level of gas-liquid contact and the chemical environment in the absorber appears effective at removing much of it.
- The solvent process includes a reclaimer to thermally separate the solvent from heat stable salts. It is likely that the accumulating RCRA-listed metals will remain with the

residue, and although this will reduce the quantity of waste, the concentration will be approximately 10 times higher.

Anion Accumulation in Solvent

The anions in the MEA were measured using ion chromatography. The major inorganic anion detected was sulfate, the majority of which likely arises from salts of sodium (pre-scrubber), calcium and magnesium (wet FGD), and potassium and aluminum (coal ash), all cations being detected in used MEA. Some sulfate may also arise from the transmission of SO_2 from the caustic scrubber, but this is thought to be a minor source. The chloride, nitrate, and nitrite originate from the flue gas, and the oxalate and formate are solvent degradation products.

Solvent Metals Removal

While contaminants in the solvent must be limited to prevent operational issues such as foaming, deposition, and sludge formation, one of the greatest concerns is reducing the selenium level, as it infringes the RCRA limit. The initial studies concentrated on the removal of selenium with the effect on the other materials present.

Based on studies of selenium chemistry for water treatment, three different waste water procedures were identified: treatment with copper chloride solution without pH adjustment; treatment with ferric chloride solution with pH adjustment using sulfuric acid; and treatment with ZVI powder with and without pH adjustment.

No precipitation of solids was observed with either copper or ferric chloride, even when a flocculant was added, indicating that there was no removal of selenium or any other metals. It is assumed that the MEA interfered with the precipitating reaction. As MEA is a buffer, a large amount of acid was needed to adjust the pH, and consequently much of the MEA was consumed. From this observation, it was concluded that for a removal process to be successful, it should not require acidification.

For the ZVI tests with acidification for pH adjustment into the range 5 to 6, approximately 75 percent of the selenium in the MEA solution was removed, lowering the concentration from approximately 900 ppbw to 200 ppbw. No other metals were removed. The selenium species in the used solvent were determined twice, first without treatment and then with acidification to reach a pH of 5 to 6. The biggest change was the increase in selenite and corresponding reduction in elemental selenium occurring as a result of acidification. Variation of species with oxygen-reduction potential and pH has been observed by researchers investigating water treatment processes. These are the first known results for aqueous amine solutions.

MEA samples were sent to Texas A&M University to be treated using their proprietary process based on ZVI without acidification. The difference in separation performance compared to the NCCC test results may arise from not using sulfuric acid for pH adjustment. Some of the non-listed metals (calcium, iron, and potassium) increased in concentration, presumably because they are present in the ZVI oxide mixture. Removal efficiency for the ZVI treatment at A&M University were: 96 percent for arsenic; 98 percent for barium; 80 percent for selenium, and 31 percent for chromium.

Three sorbents were tested, but none of these, individually or in combination, removed any of the metals. The MEA was thought to interfere with the separation mechanism.

6.1.4 Aker Clean Carbon Mobile Test Unit

- Round-the-clock operation was achieved at controlled conditions. The extended continuous operation increased understanding of plant and equipment performance and improved the ability to respond to upsets in power plant operation.
- The MTU was designed for northern European operation and was supplied with air-cooled heat exchangers. Summer temperatures in Alabama required the addition of water cooling to some circuits.
- The reclaimer was operated and reduced the concentration of impurities by 80 percent with only minimal loss of solvent.
- The analyses of ammonia and alkyl amines were originally performed by GC-MS after derivatization with benzene sulfonyl chloride. This method has a very high sensitivity of about 1 ug/L for alkyl amines and 1 mg/L for ammonia. However, it was found that sulfamic acid was a poor choice for sampling of ammonia, as sulfamic acid in water solution may hydrolyze to ammonium bisulfate. GC-MS analysis of a blank 0.1-M sulfamic acid sample prepared on site showed indeed an ammonia concentration of 14.5 mg/L, which in fact was comparable to the impinger analysis in this work and would correspond to an ammonia emission of a few ppmv. Hence, sulfamic acid is not applicable for sampling of ammonia. Absorbents like hydrochloric or sulfuric acid should be used in the future.
- With the full anti-mist mode applied, the FTIR reading of MEA concentration in the absorber outlet was less than 1 ppm.
- Net CO_2 loading, defined as the difference between CO_2 rich and lean solvent loadings, was calculated for the executed runs with CCAmine, and a maximum net loading was 2.3 mol CO_2/L solvent, corresponding to a working capacity for the solvent of 10 wt%. The majority of results were, however, in the range between 1.6 and 2.0 mol CO_2/L solvent, corresponding to a working capacity for the solvent between 7 and 9 percent. MEA has a working capacity typically between 5 and 7 wt%.
- Kinetic characteristics for the solvent were assessed based on obtained CO_2 loading in the CO_2 rich solvent. CO_2 loading dropped when approaching and exceeding 90 percent CO_2 capture.
- The pH controlled wash system proved effective at capturing gaseous phase alkaline compounds, i.e. ammonia and alkyl amines. The test results also show low amine emissions achieved with the anti-mist design, and additional reductions may be achieved through further optimization.
- The effect of changing the absorber feed point was investigated, and comparable runs with lower/upper feed points indicate that rich loading decreases by 12 percent when reducing packing height by 39 percent. Specific reboiler duty was not significantly increased.

- Approximately 84 percent of the heat stable salts in the lean amine in the MTU before start of reclaimer operation was removed during the solvent feed period of the reclaiming process.
- There was no net loss of free amine during the reclaiming period, as the free amine concentration in the lean solvent was the same before and after reclaiming. Also, single amine levels were practically unchanged after reclaiming.
- The viscosity was decreased in the lean solvent by reclaiming, while the viscosity in the reclaimer liquid increased significantly during the reclaiming process.
- There is no significant increase in total heat duty during reclaiming. The specific reboiler duty values before and after reclaiming are equal.
- Specific reboiler duty for the CCAmine solvent was shown to be approximately 18 to 20 percent lower than for MEA.

6.1.5 Babcock & Wilcox Solvent

- During the test campaign, a total of approximately 115 test conditions were run. A significant quantity of data was gathered to compare with B&W's process simulation models. In addition to the operating data gathered for process model validation and verification, the test campaign also yielded a great deal of data in other areas of interest, such as corrosion, solvent degradation, and effluent stream characterization.
- Liquid samples were routinely withdrawn using the automated system for the purpose of checking solvent concentration and CO_2 loading. In addition, manual samples were withdrawn at regular intervals to serve as a check to the automatic samples and to further characterize the chemical composition of various process streams. NCCC staff worked with B&W personnel to perform gas-phase to analyze for airborne compounds such as the OptiCap solvent, ammonia, aldehydes, and nitrosamines.
- During the OptiCap test campaign, values in the range of 1,100 to 1,125 BTU/lb CO_2 were achieved at a CO_2 removal efficiency of 90 percent. These results are consistent with both lab- and pilot-scale measurements as well as process simulations, which indicate that further energy savings are possible when using a cross-flow heat exchanger optimized for the OptiCap solvent.
- The highest measured corrosion rate of carbon steel, 17 mpy, was observed in the regenerator where the highest process temperatures existed. Outside of the regenerator, the measured carbon steel corrosion rates were below 10 mpy. However, some instances of mild CO_2 pitting were observed. A detailed analysis of the stainless steel coupons indicated that the highest stainless steel corrosion rate was 5 mpy, also occurring in the regenerator.
- Overall, both the degraded and non-degraded OptiCap solvent solutions provided more corrosion resistance to carbon steel than 30 wt% MEA, which resulted in a five times higher corrosion rate using the same test method and materials.

6.1.6 Hitachi H3-1 Solvent

- Hitachi's H3-1 solvent test campaign at the NCCC was conducted from April 24 through July 16, 2012, including over 1,300 operating hours.
- As the solvent circulation rate increased to 7,000 lb/hr, the CO_2 removal efficiency increased to a maximum value of about 96 percent. As solvent flow rate increased further, CO_2 capture efficiency began to decrease.
- As the solvent flow rate increased, the lean loading also increased because the heat provided (reboiler steam flow held constant) was insufficient to release all the CO_2 from the rich solvent. The net CO_2 loading (rich minus lean loading) at high solvent flow rates decreased significantly, thereby reducing CO_2 removal efficiency.
- For a solvent flow rate of about 7,000 lb/hr where the CO_2 capture was its maximum, the regeneration energy was at its minimum value of approximately 2.4 GJ/ton of CO_2 or 1,030 Btu/lb of CO_2.
- Generally, the CO_2 removal efficiency increased with the reboiler steam flow rate. At the partial load condition when the inlet CO_2 concentration was low, the CO_2 removal efficiency was higher than that of the full load condition.
- As expected, with an increasing number of packed beds, greater CO_2 removal efficiency was achieved. At the operating test conditions with only two packing stages in service, close to 90 percent of the CO_2 was captured. With all three packing stages in operation, CO_2 removal efficiency increased further but with a smaller increment.
- With the intercooler in service, the absorber internal temperature was lower by 10 to 20^{o}F within the packing stages. By lowering the temperature within the absorber, the amount of CO_2 absorbed can be increased without changing the solvent circulation rate or reboiler duty.
- At 2.4 GJ/ton CO_2 or 1,034 Btu/lb CO_2, the regeneration energy required for H3-1 was about 34 percent lower than that for MEA.
- Amine carryover was measured by collecting gas samples at the outlet of the wash tower. Although the extent of carryover was less for H3-1 compared to 30 wt% MEA, the amount of amine carryover for both the solvents was much higher than expected values. This indicates that amine carryover is not only contingent upon the type of solvent, but strongly depends on the design and operation of the absorber and the wash tower.
- As expected, the concentration of the degradation products was very low, in the range of 10 to 15 ppmw, after 1,000 hours of testing.
- For all locations in the PSTU, the electrical resistance probe measurements were nearly constant throughout testing, indicating no significant corrosion.
- Except for selenium, the concentration of metals in the H3-1 solvent was much lower than the RCRA limits.

6.1.7 Akermin Enzymes

Akermin completed a successful test campaign at PC4 with more than 3,500 hours testing the immobilized carbonic anhydrase enzyme-based system. Testing demonstrated:

- More than 2,800 hours on coal flue gas with steady performance of about 80 percent CO_2 capture using potassium carbonate solvent
- 700 hours of operation with the AKM-24 solvent, with 90 percent capture at design conditions
- Low solvent loss due to heat stable salt build up (less than 1.6 percent per year)
- Aerosol emissions lower than detection limit of 0.8 ppm
- High purity (greater than 99 percent) CO_2 production
- Negligible detectible corrosion rates using 304-stainless steel

6.1.8 Chiyoda Solvent

Chiyoda began testing its T-3 solvent in the PSTU in December 2012 and completed testing in June 2013, for about 1,500 hours of operation. Operation with the Chiyoda solvent included 24 test conditions, and mass balances were completed for each condition with 97 percent or higher closures.

- The variation in regeneration energy with L/G ratio showed the optimum L/G ratio to be around 2.4 L/Nm^3; this value is around 50 percent lower than for MEA. For 90 percent capture, the regeneration energy for T-3 is 2.6-GJ/tonne, around 30 percent lower than the 3.5-GJ/tonne for MEA.
- The L/G ratio was set at the optimum value of 2.4 L/Nm^3 and the regenerator pressure and steam flow rate were varied. For each regenerator pressure, the CO_2 recovery was highest at the higher bottom temperature.
- As anticipated, the rich loading leaving the absorber and the CO_2 capture efficiency were both higher with the intercoolers in service.
- Recirculating rich solvent back to the absorber benefits the performance of T-3.
- In common with other solvents, losses were higher than expected by Chiyoda based on previous testing.

6.1.9 Cansolv Technologies Solvent

During the 1,725-hour test campaign in 2012, the Cansolv DC-201 solvent demonstrated:

- The targeted 90 percent CO_2 capture rate
- 50 percent reduction in solvent flow compared to MEA
- 35 percent reduction in energy consumption compared to MEA

- Minimal effect of solvent concentration on performances
- Minimal degradation under oxidative environment, including effect of SO_2 and NO_2
- Low emissions upstream and downstream of water-wash section
- Low corrosion rates

Testing of the Cansolv DC-201 solvent under natural gas flue gas simulated conditions was completed after 1,715 hours of operation in the PSTU. Initial tests varied the liquid-to-gas ratio in the absorber and steam flow rates to the regenerator to identify the operating conditions for the long-term solvent degradation test. Long-term testing was focused on solvent performance, degradation, and emissions. Accomplishments of this testing include:

- Maintained process performance near 90 percent CO_2 removal for the duration of the testing
- Demonstrated a limited influence of transformation product concentration on CO_2 removal
- Demonstrated a maximum increase in overall energy consumption (stripping factor) of about 10 percent without intercooling or energy integration
- Completed solvent emissions testing showing 33 times greater emissions with natural gas simulated flue gas and 77 times greater emissions with typical coal flue gas over emissions with ambient air

6.1.10 MTR Flue Gas Membrane Systems

MTR began testing the polymeric Polaris™ membrane system for separating CO_2 from coal-derived flue gas in December 2011, with 9,119 hours of operation achieved during the contract period.

- From 300 to 1,000 hours of operation, the two-step membrane operation reduced the CO_2 content to 5 percent in the CO_2-depleted stream, indicating an overall capture rate of approximately 60 percent. The cross-flow modules enriched the CO_2 by a factor of six to eight. With two new sweep modules rotated into the system after 1,000 hours of operation, the CO_2 content in the CO_2-depleted stream was further reduced to around 3 percent, indicating a CO_2 capture rate of 85 percent.
- Two cross-flow modules were removed for inspection by MTR. The membranes were in excellent condition after about 1,500 hours of operation, suggesting that the pretreatment system worked effectively and prevented fouling of the membranes by flue gas contaminants.
- MTR performed post-test analyses of the modules that were tested from December 2012 to July 2013. Both CO_2 permeance and CO_2/N_2 selectivity remained almost unchanged (within the error range of the pure-gas module testing system), even after going through many cycles of system re-start and shutdown and staying idle in the membrane system for over three months during a flue gas outage.

- Based on test performance, MTR's model simulations of a full process using CO_2 recycle by sweep projected an increase in the feed CO_2 content from 4 to 15 to 20 percent, resulting in a permeate stream CO_2 concentration of greater than 80 percent, suitable for final purification and compression.
- The advanced Polaris modules were made from membranes having at least 50 percent higher CO_2 permeance than that of the base-case Polaris membranes. Under similar operating conditions, the advanced module showed 60 percent higher CO_2 removal rate than the base-case module. This translates into 30 percent reduction in the membrane area, and therefore a 30 percent reduction in the membrane system cost required for achieving the same capture rate.
- The corrosion–resistant coating on the dry-screw compressor degraded with long-term exposure to flue gas, leaving the compressor elements in direct contact with flue gas, and resulting in gradual corrosion. In addition, without the sealing fluid, the compressor has a tight-fit screw-casing design, which reduces the tolerance to particles, dust, and rust. These findings indicated that the dry-screw compressor is not suitable for operation with flue gas.
- When operating with the liquid ring compressor in 2013, the overall reliability of the 1-TPD system was significantly improved, and no corrosion issues have been found as of this writing.
- MTR implemented a procedure to purge the system with fresh air prior to shutdowns. As indicated by the subsequent test results, the purging proved effective in preventing fouling and thus extending the membrane service time.
- MTR designed and procured a 1-MWe-scale, 20-TPD CO_2 membrane test skid based on the 1-TPD system test results, which will operate in late 2014.

6.1.11 SRI International Sorbent

The SRI International 40-kWe sorbent skid was tested in 2014. Continuous operation was achieved by using a combination of indirect and direct steam heating of the sorbent in the CO_2 stripper. The indirect heating demonstrated the potential for heat recovery from the hot dehydrator exhaust. The performance indicators were lower than expected based on previous testing of SRII's smaller unit at the University of Toledo. While the target CO_2 capture efficiency was 90 percent, the test results showed that only 70 percent capture was reached. The concentration of CO_2 in the stripper outlet was 93 percent, lower than seen previously. Design modifications and process optimization are expected to improve performance and increase the capture rate to the targeted value of 90 percent. SRII will use the operational data for future testing at a 0.5-MWe scale.

6.1.12 DOE Sorbent Unit

The DOE tested its Carbon Capture Unit (C2U) to evaluate CO_2 sorbents composed of amines on a solid substrate. The focus of these tests was exploring the accumulation of heavy metals from flue gas, such as selenium, on the 32D sorbent. Analysis of sorbent samples taken following the

circulation tests and the batch tests showed no permanent loss of CO_2 capture capacity with 400 hours of flue gas exposure. Trace metals analysis was underway.

6.1.13 Linde-BASF Solvent and Process

Linde and BASF will commission a 1-MWe CO_2 capture pilot plant processing up to 30 tons CO_2 /day at the PC4 in late 2014. The technology incorporates BASF's novel amine-based process along with Linde's process and engineering innovations. Linde-BASF completed installation of the unit at the PC4 in 2014, and testing is planned to begin in 2015.

6.2 Gasification

6.2.1 Gasification Operation

During the contract period, the gasification process operated for about 9,500 hours over 13 test runs, bringing the total gasification operating experience to over 21,080 hours. In addition to supporting pre-combustion CO_2 capture processes, gasification operation enabled development of several gasification support processes in-house, and more than 12,000 hours combined of testing of gasification-related technologies by outside developers.

The gasifier operated in air-blown mode for the majority of testing, with portions of runs R02 and R08 conducted in oxygen-blown mode to support specific technology development. The fuels used included Mississippi lignite from the Red Hills mine and from the Liberty Fuels mine, PRB coal, and raw and torrefied biomass.

6.2.2 Coal Feeder Development

Modifications to the developmental Pressure Decoupled Advanced Coal feeder were incrementally made and tested both while feeding coal to the gasifier and while operating in the off-line test system. The modifications resulted in continually improved feed rate control, as demonstrated by more uniform gasifier temperatures. The increased feeder reliability resulted in higher availability of the gasifier and allowed the implementation of automatic gasifier controls.

6.2.3 Sensor Development

Vibration level probes were installed in the PDAC feeder and showed excellent reliability. As a result of the increased reliability, the lock vessel filling cycle was optimized to use the level probe indication to end the fill cycle instead of waiting for the timer to cycle. The benefit of this change was especially significant when operating the feeder at higher feed rates. A point sensitive level probe installed in the top of the feeder dispense vessel permitted control at a higher fill level and thus improved feed rate stability by preventing funneling in the vessel. A new coal feed rate measuring device, the DensFlow coal flow meter, was also installed on the PDAC feeder, although results have shown the need for improvements in accuracy. Collaboration is ongoing with SWR Engineering to improve the coal flow meter performance.

Testing was conducted with a sapphire thermowell in gasifier service, which was modified by the vendor based on early operational results. The ongoing collaboration of the vendor and

NCCC staff resulted in significantly improved performance without the degradation of the sapphire thermowell-housed thermocouple seen in early operation.

6.2.4 Hot Gas Filter Elements

The NCCC supported the development of new hot gas filter elements with efficiency evaluations and syngas operation. The filter element test program has resulted from collaborative efforts between the NCCC and filter manufactures, and has led to the development of reliable materials for highly efficient syngas particulate removal.

The six types of elements tested in the contract period are listed below, with the maximum exposure hours for individual elements of each type.

- Pall Iron Aluminide sintered powder, 16,155 hours
- Pall HR-160 fine sintered fiber, 8,996 hours
- Pall HR-160 coarse sintered fiber, 11,023 hours
- Mott high alloy sintered powder, 7,501 hours
- Porvair coated alloy sintered fiber, 7,978 hours
- Bekaert Fecralloy sintered fiber, 2,960 hours

All the elements maintained structural integrity and excellent collection efficiency throughout operation. Continued testing is planned for these elements to confirm suitability for long-term commercial operation. Long-term evaluations demonstrated excellent filtration performance over an expected two-year commercial service for the most extensively tested elements.

6.2.5 Water-Gas Shift and COS Hydrolysis Catalysts

The NCCC performed testing of several different WGS catalysts to establish the optimum operating conditions to support commercial IGCC operation and to evaluate long-term catalyst performance. Studies to optimize WGS catalyst operation showed that CO conversions adequate to facilitate high CO_2 capture rates can be achieved at lower steam-to-CO molar ratios than those traditionally recommended. Evaluation of the impact of these test results for a commercial 500 MW IGCC power plant showed that the acceptable reduction in steam-to-CO molar ratio (from 2.6 to 1.6) corresponds to a substantial 40 MW increase in net electrical output.

In addition to this study, more than 3,500 hours of testing was achieved with one developmental catalyst, demonstrating long-term stability. The same catalyst developer also provided a COS hydrolysis catalyst made with a honeycomb configuration, which was tested in R12 and R13 for about 950 hours.

6.2.6 Johnson Matthey Mercury Sorbent

The Johnson Matthey mercury sorbent has demonstrated greater than 99 percent capture of mercury, arsenic, and selenium. Testing at the NCCC began in 2008, with the most recent testing conducted during run R13, for a total of about 3,760 hours. To optimize the sorbent,

palladium loadings of 2 wt% and 5 wt% have been tested for performance comparisons. Initially, the syngas flow rate was limited to about 40 lb/hr. Prior to the R10 run, the NCCC installed a new reactor to accommodate a syngas flow rate of 50 lb/hr. Johnson Matthey's sorbent post-run analyses support near-complete absorption of mercury, as the penetration of mercury and other trace metals was limited to the first layers of the sorbent bed.

6.2.7 Ohio State University Syngas Chemical Looping

The OSU SCL pilot-scale process was designed to convert syngas into separated hydrogen and CO_2 streams using a countercurrent moving-bed reducer/oxidizer reactor. The system was constructed and installed, and initial commissioning was conducted. The initial operation identified the need for process modifications, which will be incorporated for future syngas operation.

6.2.8 NETL Solid Oxide Fuel Cell

Operation of the NETL's solid oxide fuel cell multi-cell array demonstrated over 450 hours of continuous operation on partially cleaned syngas. Performance showed remarkable robustness of SOFC materials to trace material exposure as well as acceptable power density given the modest heating value of the supplied syngas.

6.2.9 NETL Mass Spectrometer

During run R05, the GC-ICPMS was used for the first time in the field to measure mercury concentrations directly during testing of the Johnson Matthey mercury sorbent. Data were collected continuously every 15 minutes. Although measured mercury levels from the GC ICPMS were higher than those determined by the EPA Method 29, the results demonstrated the potential to gather real-time data and to facilitate control over key parameters. Lessons learned during R05 included the need for additional heat tracing of sampling loops and improved controls for system pressure and syngas flow.

6.2.10 Stanford University Tunable Diode Laser

Stanford University's Tunable Diode Laser is designed for real-time analysis of syngas constituents and stream conditions and is considered to be a potential break-through technology for control of advanced gasification systems. During R09, Stanford University's Hanson research group tested the TDL technology with syngas downstream of the PCD. These initial results validated the TDL technology's ability for real-time in-situ monitoring of H_2O, CO_2, and gas temperature in a gasification process. For R13, the TDL was modified to detect syngas CO and CH_4 in addition to temperature and moisture to extend the utility of laser-absorption sensing for gasification processes. The R13 testing validated the earlier results, with meaningful data obtained for all syngas species of interest. The success of the TDL sensor campaigns at the NCCC showed that laser absorption sensing is not only possible in engineering-scale gasifiers, but could be an important new diagnostic tool with the potential for new control strategies in future gasifier utilization and development.

6.2.11 SRI Fischer-Tropsch Catalyst

SRI tested a 5-lb/hr bench-scale FT synthesis reactor system to produce liquid transportation fuels using a selective, wax-free, cobalt FT catalyst. Activities completed included system commissioning, catalyst testing with bottle gas, and syngas cleanup testing. The initial operation showed the need to implement system modifications, after which catalyst testing with syngas will be completed.

6.3 Pre-Combustion

6.3.1 Facility Upgrades

To accommodate new projects, the SCU capacity was increased from 200 to 1,500 lb/hr of syngas, and a new gas analyzer building, control room, and motor control center were installed to upgrade the existing facilities. Another major addition was the syngas cleaning system with 1,000-lb/hr syngas capacity providing pre-treatments for sulfur and hydrocarbon removal, WGS, and COS hydrolysis. Additional instrumentation, gas analyzers, superheated steam supply, syngas treatment equipment, and a hydrogen and CO bottle gas supply system with a firewall were also installed. Syngas and utilities were installed to support pilot-scale testing at up to 1,000 lb/hr. This new test area is currently occupied by the OSU SCL process.

6.3.2 MPT CMS Hydrogen Membrane

During multiple field tests conducted at the NCCC, MPT achieved several hundred hours of operation that were focused on hydrogen separation and contaminants removal by the CMS membrane with untreated syngas. Testing progressed from single-tube operation to pilot-scale bundles, and finally, to the full-scale, 86-tube bundle. MPT further advanced the process with development of the CMR. This successful testing demonstrated the technical feasibility MPT's proposed "one-box" process. Results of the testing are listed below.

- Verified the separation performance and material stability of the full-scale CMS bundle—The full-scale bundle was operated with syngas feed rates as high as 600 scfh, pressures greater than 200 psig, and temperatures above 480°F. Over 300 cumulative hours of performance testing was conducted with two bundles with no observed degradation in permeance.
- Demonstrated avoidance of surface contamination by high temperature operation—Testing showed that operation with raw syngas at temperatures around 350°F resulted in deposition of hydrocarbons on the membrane surface and decreased membrane permeance. By operating the membrane at 480°F with raw syngas, MPT verified stable operation with no deposition.
- Developed robust designs for the bundle configuration and housing—The CMS bundle configuration and housing design employed for the tests proved adequate for the selected operating conditions for extended periods of operation. MPT incorporated a baffle design to overcome uneven gas distribution during initial testing of the full-scale bundle, and achieved permeance values near those demonstrated in the lab. The full-scale CMS membranes/bundles/modules developed under this project are ready for future field tests.

- Demonstrated chemical resistance to syngas contaminants—No membrane degradation in the presence of H_2S and other syngas contaminants was observed during the multiple tests conducted, which confirms the chemical stability of the CMS membrane established in MPT's lab evaluation using H_2S as a model contaminant.
- Achieved hydrogen purity greater than 99 percent using a post-treatment membrane—MPT demonstrated the use of a palladium alloy membrane with the CMS permeate as a hydrogen-polishing step. MPT's palladium alloy membrane showed no degradation during the 10-hour feasibility study.
- Validated the performance of the CMS for applications in power generation with carbon capture—Hydrogen purity was enriched to more than 50 percent from the syngas feed containing about 10 percent hydrogen, with more than 60 percent purity expected for a commercial air-blown gasifier. Based on the testing, greater than 94 percent hydrogen purity with as high as 90 percent hydrogen recovery would be expected with syngas containing 40 percent hydrogen from a commercial oxygen-blown gasifier.
- Incorporated WGS functionality with the CMS—During two test runs, MPT operated the CMS with added WGS catalyst to produce a catalytic membrane reactor. Testing achieved up to 50 percent CO conversion, and MPT expects to further develop the CMR in future runs.

6.3.3 MTR CO_2 Membranes

Semi-commercial pilot-scale Polaris membrane modules (containing 1 to 4 m^2 membrane area) showed CO_2/H_2 separation properties similar to those obtained in MTR's laboratory membrane stamp tests. The test also demonstrated the long-term stability of the Polaris modules in a real syngas environment containing up to 320 ppm of H_2S.

The membrane demonstration system processed 500 lb/hr syngas (equivalent to the syngas production of a 0.15 MWe IGCC power plant) containing about 10 percent CO_2, and produced a liquid CO_2 stream containing 95+ percent CO_2. Commercial-scale membrane modules (containing 20 m^2 of membrane area) were used in these tests.

6.3.4 MTR Hydrogen Membranes

Initial Proteus membrane stamp testing with started in November 2009 during the R03 run. Testing was scaled up to lab-scale membrane modules during R06 in July 2011, and pilot-scale demonstration of semi-commercial membrane modules processing 50 lb/hr of syngas began during R12 in November 2013. Results showed the potential of Proteus as a hydrogen-recovery membrane for syngas applications. Future test plans includes continued Proteus module development and testing on a semi-commercial scale and further characterization and optimization of Gen-2 Proteus membranes on syngas at the NCCC.

6.3.5 WPI Hydrogen Membranes

WPI conducted testing to optimize the composition of its palladium-based membranes. The thirteen palladium and palladium alloy membranes were tested at 842°F under syngas conditions

in a single membrane module. The total testing time for all thirteen membranes was 4,275 hours, representing about half a year of commercial operation. The testing demonstrated about 1.4 lb/day of hydrogen production and 99.85 to 99.95 percent hydrogen purity. Based on the testing, WPI has made preparations for scaled-up testing in future runs.

6.3.6 Eltron Research & Development Hydrogen Membrane

Eltron's hydrogen transport membranes were tested at about 640°F for a total of 204 hours during R09, including 183 hours of syngas operation with hydrogen enrichment and 21 hours with bottled hydrogen/nitrogen gases. The system operated with 10 lb/hr shifted and sweetened syngas (less than 1 ppmv sulfur). With hydrogen enrichment, the hydrogen concentration of the syngas reached about 38 to 40 vol% (dry basis). Hydrogen purity in the permeate stream was greater than 99.87 percent during the entire testing period, which indicated excellent membrane integrity without leakage. Post-run inspection showed the membranes to be in good condition.

6.3.7 TDA Research CO_2 Sorbent

TDA tested a CO_2 sorbent system during R07 for 308 hours and over 1,200 adsorption and regeneration cycles, utilizing about 5 lb/hr sweet, shifted syngas. The results showed the pre-combustion capture technology to be fully capable of removing more than 90 percent of CO_2 from the syngas generated by an air-blown Transport Gasifier. The sorbent maintained consistent performance in the field, which closely matched the results in the laboratory using a simulated syngas mixture, suggesting that the potential impurities in the coal-derived syngas gas did not lead to sorbent degradation.

TDA modified the process to combine the WGS reaction and sorbent CO_2 capture in the same reactor for testing in run R10, during which the system operated for 384 hours. The integrated operation of the WGS catalyst and CO_2 sorbent in a single step drives the equilibrium-limited WGS reaction towards hydrogen without the need to add large amounts of steam to the syngas, greatly reducing the cost of carbon capture. In run R10, TDA completed testing using 3.5 lb/hr of untreated syngas, demonstrating CO conversions above 90 percent at steam-to-CO ratios of less than 1.2, while maintaining CO_2 capture above 96 percent.

6.3.8 Batch Reactor CO_2 Capture Testing

Operation with CO_2 capture solvents led to the development of accurate sampling methods and the understanding of process chemistry. In establishing a database of solvent characteristics, NCCC researchers have evaluated chemical solvents including ammonia (used to define solvent testing and sampling techniques), the well-established solvent potassium carbonate, and the potentially commercial solvent potassium prolinate. Physical solvents tested include PDMS, DEPG, GTA, alkylimidazoles, and hybrid siloxane. In addition to CO_2 absorption characteristics, solvents tested have been evaluated and compared for co-absorption of H_2S, regeneration characteristics, and performance with water addition.

- SCU test data showed that with or without water addition, DEPG achieved higher absorption efficiencies than PDMS for initial and subsequent cycles. Also, the CO_2 concentration profile indicated that absorption was maintained for a longer period,

allowing DEPG to achieve a higher loading level. From the area within the concentration profiles, the CO_2 loading for DEPG was approximately 1.4 times higher than that for PDMS.

- The H_2S concentration profiles indicated that absorption was maintained for a longer period with DEPG than with PDMS. From the area within the concentration profiles, the H_2S loading for DEPG is approximately 3.5 times higher than that for PDMS.
- The CO_2 mass loading for ammonia was shown to be greatly in excess of potassium carbonate and potassium prolinate, with the potassium carbonate having the lowest loading.
- In the absence of water, capture efficiency with CO_2 capture solvent GTA was similar to that with DEPG, and both were superior to capture with PDMS. When 10 percent water was added to the solvents, the performances of GTA and PDMS was unaffected, but that of DEPG deteriorated.
- The NCCC conducted a series of tests on two solvents, MEI and DMI, provided by UA to measure CO_2 and H_2S absorption in the SCU batch reactor. Syngas data was collected for MEI and for MEI with added DMI. The CO_2 capacity was in the range of other physical solvents tested previously. Absorption and regeneration tests of the MEI showed that fresh solvent removed much more H_2S than did used solvent. Thermal regeneration at temperatures up to 212°F did not remove H_2S, although various methods of flash regeneration were successful at removing some H_2S. The H_2S absorption appeared to be an irreversible reaction with some component of the solvent.
- The hybrid siloxane physical solvent supplied by exhibited a similar CO_2 loading capacity to DEPG. Operation with the solvent resulted in the formation of a very fine aerosol during absorption, which has not been the case for other solvents tested.

6.4 Technology Assessment

6.4.1 Technology Screening

In collaboration with the DOE, the NCCC developed a technology screening process for identifying technologies to be included in the NCCC test plan. The NCCC maintains a candidate technologies inventory that includes all major developers of relevant technology. Candidate technologies are evaluated using both quantitative screening criteria and qualitative screening criteria related to shared DOE and NCCC objectives and budget considerations.

6.4.2 Evaluation of Transport Oxy-Combustion Technology

Studies were completed to evaluate the technical and economic aspects of TROC technology. These efforts allowed refinement of the process flow sheet and investigation of potential applications of this technology. The studies conclude that in both retrofit and greenfield applications, TROC is a scalable, economically competitive, near-zero emissions option for generating coal-fired power where CO_2 capture is required. A comparison of TROC with pulverized coal plants with CO_2 capture indicated that the TROC greenfield case had the lowest levelized cost of electricity. A comparison of TROC with natural gas combined cycle showed

that TROC offers a viable economic alternative at capacity factors above 40 percent and an economic benefit at capacity factors above 70 percent.

6.4.3 Evaluation of Solvent-Based Post-Combustion CO_2 Capture

To assess the progress made in post-combustion CO_2 capture solvent development, an engineering and economic evaluation of PCC plant designs was completed. This study investigated four cases for a PC plant with PCC of CO_2 using two solvents: MEA and the solvent with the lowest heat of regeneration tested at the NCCC. Conclusions were:

- For 90 percent CO_2 capture, the COE increase over a plant with no capture, is 72 percent for MEA, which is in keeping with estimates from other studies. The COE increase for the advanced solvent is 51 percent, a significant improvement over MEA but nevertheless still high.
- Ways in which the COE increase might be reduced further are discussed and include improvements to solvents and process equipment, many of which are to be tested at the NCCC.
- Meeting the EPA's proposed CO_2 limit of 1,100 lb/MWh (36 percent capture) results in a COE increase of around 20 percent, and this too can be reduced by improvements to solvents and process equipment.
- The COE increases can be reduced if the CO_2 could be sold to produce a revenue stream. For a representative price of $20/tonne, the COE increase would be reduced to 28 percent and 11 percent, respectively. With solvent and equipment improvements, these values could be reduced further.
- A coal plant with CCS meeting the EPA's proposed CO_2 limit could be competitive provided the CO_2 can be sold and further technological improvements are made. This will only be possible for nth-of-a-kind units once the technology is refined through design, construction, and operational experience.
- Both advanced solvent plant designs, 90 percent and 36 percent capture, come close to meeting the DOE's Clean Coal Research Program $40/tonne objective for the period 2020 – 2025 and could be met with some further improvements to solvents and equipment items.